Moduli Spaces of Riemann Surfaces – Homology Computations and Homology Operations

Felix Jonathan Boes
Born 18th November 1988 in Solingen

Anna Hermann
Born 11th April 1990 in Neuwied

12th September 2014
Last update: 16th March 2015

Master's Thesis Mathematics

Advisor: Prof. Dr. Carl-Friedrich Bödigheimer

Mathematisches Institut

Mathematisch-Naturwissenschaftliche Fakultät der

Rheinischen Friedrich-Wilhelms-Universität Bonn

Contents

1. Introduction **7**

1.1. A Survey on the Stable and Unstable (Co-)Homology 7
1.2. Our Results in the Unstable Case 11
1.3. The Rational Homology of the Moduli Spaces in Short Form 16
1.4. Organization of our Thesis 17

2. Cellular Models **19**

2.1. Introduction 19
2.2. The Bundle $\mathfrak{H}^m_{g,n}[(r_1,\ldots,r_n)]$ 22
2.3. The Parallel Slit Complex 26
2.3.1. Cells in Homogeneous Notation 28
2.3.2. Cells in Inhomogeneous Notation 30
2.3.3. Vertical and Horizontal Faces 31
2.3.4. The Parallel Slit Complex 33
2.4. The Bundle $\mathfrak{H}^\bullet_g(m,n)$ 34
2.5. The Radial Slit Complex 37
2.5.1. Radial Cells in Homogeneous Notation 39
2.5.2. Radial Cells in Inhomogeneous Notation 41
2.5.3. Faces 43
2.5.4. The Radial Slit Complex 43
2.6. The Orientation System 44
2.7. Comparison of the Parallel and Radial Models 48
2.7.1. Parallelization 48
2.7.2. Radialization 51
2.8. The Ehrenfried Complex 54
2.8.1. Construction of the Ehrenfried Complex 54
2.8.2. Some Useful Properties 57
2.9. The Dual Ehrenfried Complex 58
2.9.1. The Coface Operator via Coboundary Traces 60
2.9.2. The Dual of κ 65
2.9.3. The dual Ehrenfried complex of $\mathfrak{M}^0_{1,1}$. 66
2.9.4. Classification of the Cells of the Ehrenfried Complex 68

3. Cluster Spectral Sequence **73**

3.1. The Cluster-Filtration on $\mathbb{P}_{\bullet,\bullet}$ and $\mathbb{E}_\bullet$ 73
3.2. The Cluster Spectral Sequence for $\mathbb{P}_{\bullet,\bullet}$ and $\mathbb{E}_\bullet$ 75
3.3. The Cluster Spectral Sequence in Terms of Matrices 76

4. Homology Operations **77**
4.1. Operations on $\mathfrak{Par}_1$ by Patching Slit Pictures . . . 77
4.1.1. The Action of $\tilde{C}^2(\mathbb{C})$ on $\mathfrak{Par}_1$ in Detail . . . 80
4.1.2. Formulas for Q_0, Q_1 and R_1 . . . 82
4.2. Operations for Parallel Slit Domains on Several Levels . . . 84
4.2.1. The Glueing Construction . . . 85
4.2.2. The Operation $\mu_*^{\uparrow\uparrow}$ . . . 87
4.2.3. The Operation $\mu_*^{\uparrow\downarrow}$ . . . 88
4.2.4. The Operation μ_*^{cs} . . . 89
4.3. Operations on $\mathfrak{Par}$ via Bundles . . . 92
4.3.1. The Operation T via the Dual Ehrenfried Complex . . . 95
4.4. The Operation α . . . 98
4.5. Radial Multiplication . . . 100
4.6. Composition of Radial Slit Pictures . . . 104
4.7. Rotation of Radial Slit Pictures . . . 108
4.8. Correlation of Parallel and Radial Homology Operations . . . 109
4.8.1. Placing Parallel Slit Pictures into Annuli via Operads . . . 109
4.8.2. $\mathfrak{Par}$ as a Module over $\mathfrak{Rad}$ . . . 112
4.8.3. Formulas . . . 114

5. On the Computational Complexity **119**
5.1. An Estimation of the Number of Cells of $\mathbb{E}(h, m; 1)$ . . . 119
5.2. Comparison of Computational Approaches . . . 122

6. The Software Project **125**
6.1. Runtime and Memory Improvements . . . 126
6.2. The Library Libhomology . . . 128
6.2.1. The Class ChainComplex . . . 128
6.2.2. The Type CoefficientT . . . 129
6.2.2.1. Obligatory Operations for CoefficientT . . . 129
6.2.2.2. Coefficients in the Rationals and the Integers Mod m . . . 130
6.2.3. The Type MatrixT . . . 130
6.2.3.1. Existing Template Classes . . . 130
6.2.3.2. Requirements on MatrixT . . . 131
6.2.3.3. Optional Requirements on MatrixT . . . 131
6.2.4. Special Implementations of MatrixField . . . 131
6.2.4.1. MatrixField for Coefficients in $\mathbb{F}_2$ . . . 131
6.2.4.2. MatrixField for the Cluster Spectral Sequence . . . 132
6.2.5. The Type DiagonalizerT . . . 133
6.2.6. The Class DiagonalizerField . . . 134
6.2.6.1. Overview and Usage of DiagonalizerField . . . 134
6.2.6.2. Implementation Details . . . 135
6.2.7. The Type HomologyT . . . 136
6.2.7.1. Essential Members . . . 137
6.2.7.2. The Class HomologyDummy . . . 137
6.2.7.3. The Class HomologyField . . . 137

6.2.8. Serialization . . . 138
6.2.8.1. Storable Types . . . 138
6.3. The Program Kappa . . . 140
6.3.1. The Tool `compute_css` . . . 140
6.3.1.1. Usage . . . 141
6.3.1.2. Implementation Details . . . 142
6.3.2. The Class Tuple . . . 143
6.3.2.1. Data Members . . . 144
6.3.2.2. Class Methods To Get Started . . . 145
6.3.2.3. Basic Properties of a Tuple . . . 146
6.3.2.4. The Horizontal Face Operator . . . 148
6.3.2.5. The Orientation Sign . . . 149
6.3.2.6. Preparations for the Map κ . . . 150
6.3.3. The Class ClusterSpectralSequence . . . 150
6.3.3.1. CSSBasis . . . 151
6.3.3.2. Data Members . . . 152
6.3.3.3. Generating Bases . . . 152
6.3.3.4. Generating Differentials . . . 154
6.3.3.5. More Member Functions . . . 155
6.4. Remarks on Compiling . . . 155
6.4.1. Installing the Required Software . . . 155
6.4.2. Building the Projects . . . 156
6.4.3. More Remarks . . . 156
6.5. Results . . . 156
6.5.1. The Parallel Case . . . 157
6.5.1.1. Genus $g = 0$ and Punctures $m = 0, \ldots, 6$ . . . 157
6.5.1.2. Genus $g = 1$ and Punctures $m = 0, \ldots, 6$ . . . 161
6.5.1.3. Genus $g = 2$ and Punctures $m = 0, 1$ . . . 169
6.5.1.4. Genus $g = 3$ and Punctures $m = 0, 1$ . . . 173
6.5.2. The Radial Case . . . 177
6.5.2.1. Genus $g = 0$ and Punctures $m = 1, \ldots, 6$ . . . 177
6.5.2.2. Genus $g = 1$ and Punctures $m = 1, \ldots, 6$ . . . 184
6.5.2.3. Genus $g = 2$ and Punctures $m = 1, \ldots, 4$ . . . 193
6.5.2.4. Genus $g = 3$ and Punctures $m = 1$ . . . 199

Appendix **203**
A. The Symmetric Groups $\mathfrak{S}^{\Delta}$ as Semisimplicial Set . . . 203
B. A Brief Review on Factorable Groups . . . 205

Symbol Index **207**

Index **215**

Bibliography **217**

1. Introduction

In this thesis, we study two families of moduli spaces:
(1) the moduli spaces $\mathfrak{M}_{g,n}^m$ of Riemann surfaces of genus $g \geq 0$ with $m \geq 0$ (permutable) punctures and $n \geq 1$ boundary curves and
(2) the moduli spaces $\mathfrak{M}_g^\bullet(m,n)$ of Riemann surfaces of genus $g \geq 0$ with $n \geq 1$ incoming and $m \geq 1$ outgoing boundary curves (the moduli space of cobordisms) and with an extra marked point on each of the boundary incoming curves.

The latter are important for string topology or conformal field theories; the former (but for $n = m = 0$) are the classical moduli space from algebraic geometry or complex analysis. For our techniques to work, we always need $n \geq 1$ in case (1) and $n, m \geq 1$ in case (2).

Under these assumptions of non-empty boundary, the moduli spaces $\mathfrak{M}_{g,n}^m$ and $\mathfrak{M}_g^\bullet(m,n)$ are manifolds of dimension $6g - 6 + 2m + 4n$ respectively $6g - 6 + 3m + 3n$. They are orientable for $m < 2$. Moreover, they are homotopy equivalent to the classifying spaces $B\Gamma_{g,n}^m$ respectively $B\Gamma_g^\bullet(m,n)$ of the mapping class groups $\Gamma_{g,n}^m$ respectively $\Gamma_g^\bullet(m,n)$.

In this introduction, we review the stable and unstable (co-)homology of the moduli spaces and present our results. At the end, we explain the organization of our thesis.

1.1. A Survey on the Stable and Unstable (Co-)Homology

First of all, we recall the definition of the mapping class group. Consider the space $\mathrm{Diff}_{g,n}^m$ of orientation-preserving diffeomorphisms on a surface of genus g, leaving its n boundary curves pointwise fixed while permuting m selected points. Paths in $\mathrm{Diff}_{g,n}^m$ are isotopies and $\Gamma_{g,n}^m = \pi_0(\mathrm{Diff}_{g,n}^m)$ is the group of path components. Analogously, the mapping class group $\Gamma_g^\bullet(m,n)$ is the group of path components of the space of diffeomorphisms on a surface of genus g leaving the n incoming boundary curves pointwise fixed while permuting the outgoing m boundary curves. The group structure is induced by the composition of diffeomorphisms. The mapping class groups $\Gamma_{g,n}^m$ and $\Gamma_g^\bullet(m,n)$ are known to be isomorphic.

Stable (Co-)Homology We begin with a revision of the stable cohomology of $\Gamma_{g,n} = \Gamma_{g,n}^0$. Glueing a pair of pants along one or two boundary curves of a given oriented surface induces a group homomorphism $\varphi_g \colon \Gamma_{g,n} \longrightarrow \Gamma_{g,n+1}$, respectively $\psi_g \colon \Gamma_{g,n+1} \longrightarrow \Gamma_{g+1,n}$ on the mapping class groups, by extending the diffeomorphisms in question via the identity. If the surface has exactly one boundary curve, glueing in a disc induces a homomorphism $\vartheta \colon \Gamma_{g,1} \longrightarrow \Gamma_{g,0}$. Due to [Har85], the mapping class groups $\Gamma_{g,n}$ with $n \geq 1$ are homologically stable. Including several improvements concerning the degree of stabilization we have

Theorem (Harer)**.** *Let $g \geq 0$ and $n \geq 1$. The induced map*

$$\varphi_* \colon H_*(\Gamma_{g,n}; \mathbb{Z}) \longrightarrow H_*(\Gamma_{g,n+1}; \mathbb{Z})$$

is an injection for all $*$ *and an isomorphism for* $* \leq \frac{2}{3}g$*. The induced map*

$$\psi_*\colon H_*(\Gamma_{g,n+1};\mathbb{Z}) \longrightarrow H_*(\Gamma_{g+1,n};\mathbb{Z})$$

is a surjection for $* \leq \frac{2}{3}g + \frac{1}{3}$ *and an isomorphism for* $* \leq \frac{2}{3}g - \frac{2}{3}$*. The induced map*

$$\vartheta_*\colon H_*(\Gamma_{g,1};\mathbb{Z}) \longrightarrow H_*(\Gamma_{g,0};\mathbb{Z})$$

is a surjection for $* \leq \frac{2}{3}g + 1$ *and an isomorphism for* $* \leq \frac{2}{3}g$*.*

A proof including the mentioned improvements can be found in [Wah12].

The composition $\psi_g\varphi_g\colon \Gamma_{g,1} \longrightarrow \Gamma_{g+1,1}$ is injective and $\Gamma_{\infty,1} = \cup_{g=1}^{\infty}\Gamma_{g,1}$ is the stable mapping class group. We obviously obtain $\varinjlim H_*(\Gamma_{g,1};\mathbb{Z}) \cong H_*(\Gamma_{\infty,1})$.

Theorem (Mumford's Conjecture (Madsen–Weiss [MW07]))**.** *The rational cohomology of the stable mapping class group is a polynomial algebra*

$$H^*(\Gamma_{\infty,1};\mathbb{Q}) \cong \mathbb{Q}[\kappa_1, \kappa_2, \ldots]$$

in the Mumford–Morita–Miller classes κ_i *living in degree* $2i$*.*

Unstable Homology In contrast to the stable picture, very little is known about the unstable one, i.e., the homology or cohomology of single moduli spaces. Note that for a class in degree say 2 to be stable, we have to go to $g \geq 4$.

Before reviewing $\mathfrak{M}_{g,n}^m$, consider the moduli space $\widetilde{\mathfrak{M}}_{g,n}^m$ of Riemann surfaces of genus g where both the boundary curves and punctures are pointwise fixed. For single degrees $* = 1, 2, 3$, there are results known for almost all g. Based on the works of Mumford [Mum67] and Powell [Pow78] the first integral homology is known to be

$$H_1(\widetilde{\mathfrak{M}}_{g,n}^m;\mathbb{Z}) \cong \begin{cases} \mathbb{Z}/10 & g = 2 \\ 0 & g \geq 3 \end{cases}.$$

A proof of this version can be found in Korkmaz–Stipsicz [KS03]. Moreover, [KS03] improves a theorem by Harer [Har91, Theorem 0.a]:

$$H_2(\widetilde{\mathfrak{M}}_{g,n}^m;\mathbb{Z}) \cong \mathbb{Z}^{m+1} \qquad \text{for} \qquad g \geq 4\,.$$

The third rational homology vanishes due to [Har91, Theorem 0.b]:

$$H_3(\mathfrak{M}_{g,n}^0;\mathbb{Q}) = 0 \qquad \text{for} \qquad g \geq 6\,.$$

In case of no punctures but permutable boundary, the first integral homology is known due to Korkmaz–McCarthy [KM00, Theorem 3.12]. Denoting the corresponding moduli space by $\mathfrak{M}_{g,(n)}^0$ they show

$$H_1(\mathfrak{M}_{g,(n)}^0;\mathbb{Z}) \cong \begin{cases} \mathbb{Z}/12 & g = 1, n = 0, 1 \\ \mathbb{Z}/12 \oplus \mathbb{Z}/2 & g = 1, n \geq 2 \\ \mathbb{Z}/10 & g = 2, n = 0, 1 \\ \mathbb{Z}/10 \oplus \mathbb{Z}/2 & g = 2, n \geq 2 \\ 0 & g = 3, n = 0, 1 \\ \mathbb{Z}/2 & g = 3, n \geq 2 \end{cases}.$$

In this thesis we study the moduli space $\mathfrak{M}^m_{g,n}$. For $g = 0$ and $n = 1$, the integral homology of the moduli space $\mathfrak{M}^m_{0,1}$ coincides with the well-known group homology of the braid group on m strings. Besides that, there are some scattered computations for low g and n.

Slit models In [Böd90a] Bödigheimer provides the space of parallel slit domains $\mathfrak{Par}^m_{g,n}$, which is homeomorphic to an affine bundle over $\mathfrak{M}^m_{g,n}$ via the Hilbert uniformization. It is a manifold and an open subspace of a finite semi-multisimplicial space P making it possible (1) to compute the homology of the moduli spaces via Poincaré duality and (2) to define an operad structure by the action of the little cubes operad on the family of moduli spacess $\mathfrak{M}^m_{g,n}$; this induces an action of the Dyer-Lashof algebra on their homology. Exploiting this model, Ehrenfried could completly compute the integral homology for $g = 2$ and $n = 1$, compare [Ehr97]. This is, up to date and apart from $g = 0$ and $g = 1$, the only moduli space whose integral homology is known. His result is reproduced in the following tabl.

$$H_*(\mathfrak{M}^0_{2,1};\mathbb{Z}) \cong \begin{cases} \mathbb{Z} & *=0 \\ \mathbb{Z}/10 & *=1 \\ \mathbb{Z}/2 & *=2 \\ \mathbb{Z}\oplus\mathbb{Z}/2 & *=3 \\ \mathbb{Z}/6 & *=4 \\ 0 & *\geq 5 \end{cases}$$

Later, Godin obtained the same results with different methods, compare [God07]. For $g = 3$ and $m = 1$, Wang computed the p-torsion for many primes in [Wan11]. We will describe her results in detail, see below.

We mentioned above a complex P with a subcomplex P' such that $P - P' = \mathfrak{Par}$. The double complex associated with P admits an explicit combinatorial decribtion. However, the number of cells prevents (even computer-aided) calculations exceeding $h = 5$ where $h = 2g - 2 + m + 2n$. To demonstrate this, we list the number of cells in bidegree (p, q) for $g = 1$ and $m = 3$ (see Figure 1.1). Due to [Vis10], the vertical homology of (P, P') is

$q=5$	640	12425	74610	202825	278600	189000	50400
$q=4$	800	18500	122700	357280	516880	365400	100800
$q=3$	240	7425	57375	185220	289380	217350	63000
$q=2$	10	650	6800	26600	47740	39900	12600
$q=1$	0	0	35	315	910	1050	420
	$p=4$	$p=5$	$p=6$	$p=7$	$p=8$	$p=9$	$p=10$

Figure 1.1.: The number of cells of the bicomplex for $\mathfrak{M}^3_{1,1}$.

always concentrated in its top row being of degree $q = h$. The resulting chain complex, called Ehrenfried complex, is considerably smaller, compare Figure 1.2. These insights make it possible to perform several computations for $h \leq 6$. In [Wan11], Wang computes the elementary divisors modulo p^{k_p} of the differentials in this Ehrenfried complex for $p^{k_p} = 2^6$,

70	700	2520	4480	4270	2100	420
$p=4$	$p=5$	$p=6$	$p=7$	$p=8$	$p=9$	$p=10$

Figure 1.2.: The number of cells of the Ehrenfried complex for $\mathfrak{M}^3_{1,1}$.

3^4, 5^3, 7^2, 11^2, 13^2, 17, 19 and 23. Observe that there might be undetected p-torsion of the form $\mathbb{Z}/p^k\mathbb{Z}$ in case (1) p a prime greater then 23 and $k \geq 1$ or (2) p a prime at most 23 and $k > k_p$. Besides $H_0(\mathfrak{M}^m_{g,n};\mathbb{Z}) = \mathbb{Z}$, we have $H_1(\mathfrak{M}^0_{3,1};\mathbb{Z}) = 0$ due to [Pow78] and $H_2(\mathfrak{M}^0_{3,1};\mathbb{Z}) = \mathbb{Z} \oplus \mathbb{Z}/2\mathbb{Z}$ due to [Sak12]. For $2g + m = 6$ and $n = 1$, the remaining free summands where unkown until this point in time. Using a new spectral sequene, we provide the free parts by computing the rational homology. This, in turn, allows for $g = 3$ and $n = 1$ to conclude, that Wang had indeed discovered all p-torsion for $p \leq 23$.

Theorem (Bödigheimer, Powell, Sakasai, Wang, B., H.)**.** *Let $k_2 = 6$, $k_3 = 4$, $k_5 = 3$, $k_7 = k_{11} = k_{13} = 2$, $k_{17} = k_{19} = k_{23} = 1$ and $k_p = 0$ for $p > 23$ prime. The integral homology of the moduli spaces $\mathfrak{M}^0_{3,1}$, $\mathfrak{M}^2_{2,1}$ or $\mathfrak{M}^6_{1,1}$ is given by the following tables, where $\boxed{\cdots}$ denotes in the first case possible p-torsion for primes $p > 23$, and in the other two cases possible p-torsion of the form $\mathbb{Z}/p^k\mathbb{Z}$ for p any prime and $k > k_p$.*
The integral homology of the moduli space $\mathfrak{M}^0_{3,1}$ is

$$H_*(\mathfrak{M}^0_{3,1};\mathbb{Z}) \cong \begin{cases} \mathbb{Z} & *=0 \\ 0 & *=1 \\ \mathbb{Z}\oplus\mathbb{Z}/2 & *=2 \\ \mathbb{Z}\oplus\mathbb{Z}/2\oplus\mathbb{Z}/3\oplus\mathbb{Z}/4\oplus\mathbb{Z}/7\oplus\boxed{\cdots} & *=3 \\ (\mathbb{Z}/2)^2\oplus(\mathbb{Z}/3)^2\oplus\boxed{\cdots} & *=4 \\ \mathbb{Z}\oplus\mathbb{Z}/2\oplus\mathbb{Z}/3\oplus\boxed{\cdots} & *=5 \\ \mathbb{Z}\oplus(\mathbb{Z}/2)^3\oplus\boxed{\cdots} & *=6 \\ \mathbb{Z}/2\oplus\boxed{\cdots} & *=7 \\ 0\oplus\boxed{\cdots} & *=8 \\ \mathbb{Z}\oplus\boxed{\cdots} & *=9 \\ 0 & *\geq 10 \end{cases}.$$

The integral homology of $\mathfrak{M}^2_{2,1}$ is

$$H_*(\mathfrak{M}^2_{2,1};\mathbb{Z}) \cong \begin{cases} \mathbb{Z} & *=0 \\ (\mathbb{Z}/2)^2\oplus\mathbb{Z}/5\oplus\boxed{\cdots} & *=1 \\ \mathbb{Z}\oplus(\mathbb{Z}/2)^2\oplus\boxed{\cdots} & *=2 \\ \mathbb{Z}^3\oplus(\mathbb{Z}/2)^4\oplus\boxed{\cdots} & *=3 \\ \mathbb{Z}\oplus(\mathbb{Z}/2)^5\oplus(\mathbb{Z}/3)^3\oplus\boxed{\cdots} & *=4 \\ \mathbb{Z}^2\oplus(\mathbb{Z}/2)^4\oplus\mathbb{Z}/3\oplus\boxed{\cdots} & *=5 \\ \mathbb{Z}^2\oplus(\mathbb{Z}/2)^3\oplus\boxed{\cdots} & *=6 \\ \mathbb{Z}/2\oplus\boxed{\cdots} & *=7 \\ 0 & *\geq 8 \end{cases}.$$

The integral homology of $\mathfrak{M}_{1,1}^4$ *is*

$$H_*(\mathfrak{M}_{1,1}^4;\mathbb{Z}) \cong \begin{cases} \mathbb{Z} & *=0 \\ \mathbb{Z}\oplus\mathbb{Z}/2\oplus\boxed{\cdots} & *=1 \\ (\mathbb{Z}/2)^3\oplus\boxed{\cdots} & *=2 \\ \mathbb{Z}^2\oplus(\mathbb{Z}/2)^3\oplus\boxed{\cdots} & *=3 \\ \mathbb{Z}^3\oplus(\mathbb{Z}/2)^2\oplus\boxed{\cdots} & *=4 \\ \mathbb{Z}^2\oplus\mathbb{Z}/2\oplus\boxed{\cdots} & *=5 \\ \mathbb{Z}\oplus\boxed{\cdots} & *=6 \\ 0 & *\geq 7 \end{cases}.$$

One might conjecture that the undetermined torsion $\boxed{\cdots}$ is trivial in all cases.

In [Meh11], Mehner provides a computer program that computes the integral and $\mathbb{F}_2$ homology of single moduli spaces for $n=1$, $g\leq 2$. Moreover, he implements simplicial versions of the Dyer-Lashof operations introduced in [Böd90b] and obtaines some of the generators of the respectively homology via operations.

1.2. Our Results in the Unstable Case

In our thesis, we obtain several new results. In this section, we discuss the most important ones.

We review Bödigheimer's models introduced in [Böd90a] and [Böd06]. We discuss the first model, the space of parallel slit domains $\mathfrak{Par}_{g,n}^m[(r_1,\ldots,r_n)]$ sitting in the semi-multisimplicial parallel slit complex (P,P'). As before, we dissect a given surface using the flow lines of distinguished potential functions with exactly n poles $\mathcal{Q}=(Q_1,\ldots,Q_n)$. Here we permit poles of arbitrary order $r_1,\ldots,r_n\geq 1$ and obtain a parallel slit domain on $r=r_1+\ldots+r_n$ planes. The second model is the space of radial slit domains $\mathfrak{Rad}_g(m,n)$ sitting in the radial slit complex (R,R'). These models are manifolds. Moreover, they are homotopy equivalent to moduli space $\mathfrak{Par}_{g,n}^m[(r_1,\ldots,r_n)]\simeq\mathfrak{M}_{g,n}^m$ respectively $\mathfrak{Rad}_g(m,n)\simeq\mathfrak{M}_g^\bullet(m,n)$. For both models, we construct the associated Ehrenfried complex $\mathbb{E}$ and show that (1) the theorem of Bödigheimer (that the Hilbert uniformization provides a homeomorphism) as well as the theorem of Visy (that the vertical homology of the corresponding double complex is concentrated in degree h) hold for both the parallel slit complex with arbitrary n and $r=r_1+\ldots+r_n$ and the radial slit complex. The following diagram shows the schematic picture of our approach. The homology of the moduli spaces is determined with the help of several models and the lower line represents both the parallel and radial models.

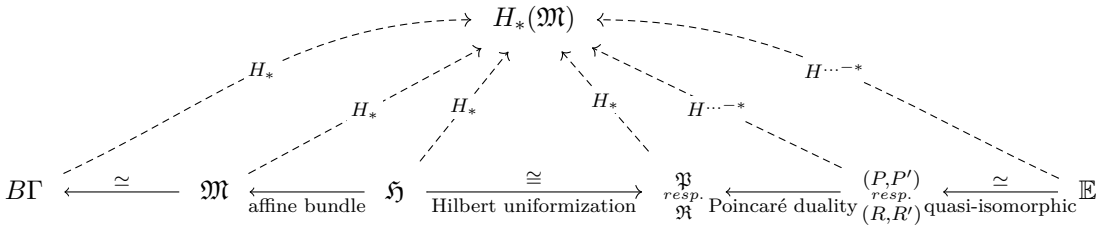

All in all we have:

Theorem (Bödigheimer, Visy, B., H.)**.** *The parallel slit complex respectively the radial slit complex is a relative manifold of dimension* $6g-6+3m+3n+3r$ *respectively* $6g-6+3m+4n$*. The Ehrenfried complex is a quasi-isomorphic direct summand*[1] *of* P/P' *respectively* R/R'*. In particular*

$$H_*(\mathfrak{M}^m_{g,n};\mathbb{Z}) \cong H^{3h-*}(P,P';\mathcal{O}) \cong H^{2h-*}(\mathbb{E};\mathcal{O})$$

where $h = 2g-2+m+n+r$ *and* $\mathcal{O}$ *are the orientation coefficients respectively*

$$H_*(\mathfrak{M}^\bullet_g(m,n);\mathbb{Z}) \cong H^{3h+n-*}(R,R';\mathcal{O}) \cong H^{2h+n-*}(\mathbb{E};\mathcal{O})$$

where $h = 2g-2+m+n$ *and* $\mathcal{O}$ *are the orientation coefficients.*

In [Böd14], Bödigheimer introduces a filtration of the bicomplex $\mathbb{P} = P/P'$ respectively R/R'. It is, roughly speaking, given by the number of components of the critical graph associated with the gradient flow of the given potential function. It induces a filtration of the Ehrenfried complex.

Proposition (Bödigheimer)**.** *There are two first quadrant spectral sequences*

$$E^0_{k,c}(\mathbb{P}) = \bigoplus_{p+q=k} [F_c\mathbb{P}_{p,q}/F_{c-1}\mathbb{P}_{p,q}] \Rightarrow H_{k+c}(\mathbb{P}_{\bullet,\bullet})$$

and

$$E^0_{p,c}(\mathbb{E}) = F_c\mathbb{E}_p/F_{c-1}\mathbb{E}_p \Rightarrow H_{p+c}(\mathbb{E}_\bullet)\,.$$

Both spectral sequences collapse at the second page.

Implementing the spectral sequence for the Ehrenfried complex in a software project we compute the rational and some $\mathbb{F}_p$ homology of certain moduli spaces with $h \leq 8$. A short form of the rational results can be found in Section 1.3 and the complete description is presented in Section 6.5. In particular, we confirm the rational version of Wang's conjecture.

Theorem (Bödigheimer, B., H.)**.** *The rational homology of the moduli space of Riemann surfaces of genus three with one boundary component is*

$H_p(\mathfrak{M}^0_{3,1};\mathbb{Q})$										
$p=0$	$p=1$	$p=2$	$p=3$	$p=4$	$p=5$	$p=6$	$p=7$	$p=8$	$p=9$	$p\geq 10$
$\mathbb{Q}$	0	$\mathbb{Q}$	$\mathbb{Q}$	0	$\mathbb{Q}$	$\mathbb{Q}$	0	0	$\mathbb{Q}$	0

The rational homology of the moduli space of Riemann surfaces of genus two with one boundary component and two permutable punctures is

$H_p(\mathfrak{M}^2_{2,1};\mathbb{Q})$								
$p=0$	$p=1$	$p=2$	$p=3$	$p=4$	$p=5$	$p=6$	$p=7$	$p\geq 8$
$\mathbb{Q}$	0	$\mathbb{Q}$	$\mathbb{Q}^3$	$\mathbb{Q}$	$\mathbb{Q}^2$	$\mathbb{Q}^2$	0	0

[1] To be precise, the Ehrenfried complex is, up to a shift in the homological degree, identified with a direct summand. The inclusion induces an isomorphism in homology.

The rational homology of the moduli space of Riemann surfaces of genus one with one boundary component and four permutable punctures is

$H_p(\mathfrak{M}^4_{1,1};\mathbb{Q})$							
$p=0$	$p=1$	$p=2$	$p=3$	$p=4$	$p=5$	$p=6$	$p\geq 7$
$\mathbb{Q}$	$\mathbb{Q}$	0	$\mathbb{Q}^2$	$\mathbb{Q}^3$	$\mathbb{Q}^2$	$\mathbb{Q}$	0

.

Most of the well-known homology operations on the moduli spaces were constructed via the bicomplexes (see below). In order to realize them in terms of the dual Ehrenfried complex, we provide an explicit formula for the coboundary operator via so-called coboundary traces:

Proposition (B., H.)**.** *The coboundary of a cell $\Sigma \in \mathbb{E}$ of degree p is*

$$\partial^*_{\mathbb{E}}(\Sigma) = \sum_{i=1}^{p} (-1)^i \sum_{a \in T_i(\Sigma)} \kappa^*(a.\Sigma)\,.$$

Using this formula, we discuss some of the well-known homology operations. Moreover, we classify the cells of a given Ehrenfried complex.

Proposition (B., H.)**.** *Every cell in the Ehrenfried complex $\mathbb{E}$ is uniquely obtained as an expansion of a thin cell in $\mathbb{E}$.*

Bödigheimer's models have a strong connection to configuration spaces. Roughly speaking, a parallel slit domain $L \in \mathfrak{Par}^m_{g,n}[(r_1,\ldots,r_n)]$ consists of $r = r_1 + \ldots + r_n$ copies of the complex plane with finitely many slits removed, each slit running from some point horizontally to the left all the way to infinity. There is a pairing of the slits, subject to several conditions. It is reasonable to think that the pairing enables us to jump through a given slit to end up at its partner. The description of a radial slit domain $L \in \mathfrak{Rad}_g(m,n)$ is similar. Here we consider paired slits on an annulus each running from some point radially to the outer boundary. There are various geometric flavoured constructions.

Proposition (Bödigheimer)**.** *For every $g \geq 0$, $n \geq 1$, $m \geq 1$ and partition $(r_1,\ldots,r_n)$ of $r = r_1 + \ldots + r_n$, there are continous maps*

$$par\colon \mathfrak{Rad}_g(m,n) \longrightarrow \mathfrak{Par}^m_{g,n}[(r_1,\ldots,r_n)]$$

and

$$rad\colon \mathfrak{Par}^m_{g,n}[(r_1,\ldots,r_n)] \longrightarrow \mathfrak{Rad}_g(m,n)\,.$$

The maps are indicated in the following by Figures 1.3 and 1.4.

We discuss several homology operations. One family of operations is induced by the action of little cubes operads, namely the ordered configuration spaces with respect to the complex plane $\tilde{C}^k(\mathbb{C})$ or the annulus $\tilde{C}^k(\mathbb{A})$, compare [Böd90b] and [Böd06]. We propose a generalization of the well-known operations on $\mathfrak{Par}^m_{g,n}[(1,\ldots,1)]$ to $\mathfrak{Par}^m_{g,n}[(r_1,\ldots,r_n)]$ for an arbitrary partition $(r_1,\ldots,r_n)$. There are many generalizations which are all covered by our glueing construction. Roughly speaking, one has to decide how two surfaces, corresponding to given parallel slit domains L_1 and L_2, are glued along parts of their boundary and one has to declare an enumeration of the resulting boundaries.

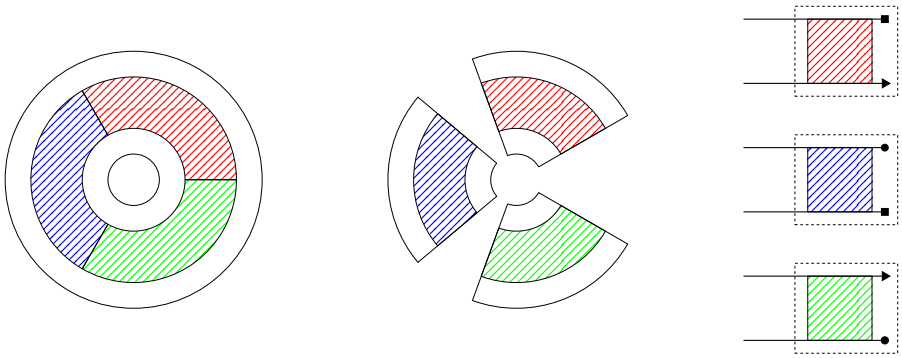

Figure 1.3.: The parallelization map with $n = 1$ and $r = 3$.

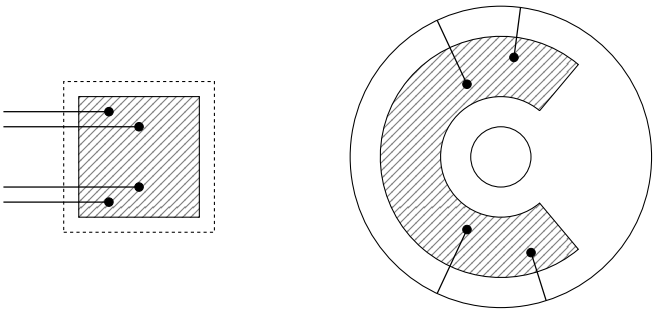

Figure 1.4.: The radialization map.

Definition (B., H.)**.** The **combinatorial type** G which specifies the glueing construction **depends on** the parameters

$$\mathfrak{P}(G) = (g_1, g_2, n_1, n_2, m_1, m_2, (r_1^{(1)}, \ldots, r_{n_1}^{(1)}), (r_1^{(2)}, \ldots, r_{n_2}^{(2)}))$$

and **consists of** the following two data.

(i) A partial, non-empty matching of the planes of the parallel slit domains in $\mathfrak{Par}_{g_1,n_1}^{m_1}(r_1^{(1)}, \ldots, r_{n_1}^{(1)})$ and $\mathfrak{Par}_{g_2,n_2}^{m_2}(r_1^{(2)}, \ldots, r_{n_2}^{(2)})$.

The size of the matching is denoted by $s(G)$. The glueing construction defines a surface of genus $g(G)$ with $m(G) = m_1 + m_2$ punctures and $n(G)$ (yet unordered) boundary curves each consisting of several planes.

(ii) A partial enumeration of the planes such that each boundary curve belongs to exactly one selected planes.

The corresponding ordered configuration is $(r_1^{(G)}, \ldots, r_{n(G)}^{(G)})$. The **set of combinatorial types** that specify a glueing construction is denoted by $\mathcal{G}$.

Proposition (Bödigheimer)**.** *For every combinatorial type $G \in \mathcal{G}$ with parameters*

$$\mathfrak{P}(G) = (g_1, g_2, n_1, n_2, m_1, m_2, (r_1^{(1)}, \ldots, r_{n_1}^{(1)}), (r_1^{(2)}, \ldots, r_{n_2}^{(2)}))$$

there are homology operations induced by the action of the little cubes operad

$$(\tilde{\vartheta}_G)_*\colon H_i(\tilde{C}^2(\mathbb{C}))^{\oplus s(G)} \otimes H_j(\mathfrak{Par}^{m_1}_{g_1,n_1}(r_1^{(1)},\dots,r_{n_1}^{(1)})) \otimes H_k(\mathfrak{Par}^{m_2}_{g_2,n_2}(r_1^{(2)},\dots,r_{n_2}^{(2)})) \longrightarrow$$
$$H_{i+j+k}(\mathfrak{Par}^{m(G)}_{g(G),n(G)}(r_1^{(G)},\dots,r_{n(G)}^{(G)}))\,.$$

In addition to the parallelization and radialization map mentioned above, we have the following propositions relating the space of parallel slit domains to the space of radial slit domains.

Proposition (Bödigheimer)**.** *The action of the little cubes operad on the space of parallel slit domains extends to an operation*

$$\begin{array}{ccc} \tilde{C}^k(\mathbb{A}) \times \mathfrak{Par}^{m_1}_{g_1,1} \times \cdots \times \mathfrak{Par}^{m_k}_{g_k,1} & \xrightarrow{\tilde{\vartheta}} & \mathfrak{Rad}_{\tilde{g}}(\tilde{m}+1,1) \\ \iota \times id \big\uparrow & & \big\uparrow rad \\ \tilde{C}^k(\mathbb{C}) \times \mathfrak{Par}^{m_1}_{g_1,1} \times \cdots \times \mathfrak{Par}^{m_k}_{g_k,1} & \xrightarrow{\tilde{\vartheta}} & \mathfrak{Par}^{\tilde{m}}_{\tilde{g},1} \end{array}\,,$$

where $\tilde{g} = \sum_{i=1}^k g_i$ *and* $\tilde{m} = \sum_{i=1}^k m_i$.

Proposition (Bödigheimer)**.** *Let* $n \geq 1$ *and* $\mathfrak{Par}_n = \coprod_{g,m} \mathfrak{Par}^m_{g,n}[(1,\dots,1)]$ *and* $\mathfrak{Rad}_n = \coprod_{g,m} \mathfrak{Rad}_g(m,n)$*. There is a right module structure*

$$H_*(\mathfrak{Rad}_n) \otimes H_*(\mathfrak{Par}_n) \longrightarrow H_*(\mathfrak{Rad}_n)$$

induced by an action of the little cubes operad.

Proposition (Bödigheimer)**.** *There is a composition operation*

$$\odot\colon \mathfrak{M}^{\bullet\bullet}_g(l,m) \times \mathfrak{M}^{\bullet\bullet}_{g'}(m,n) \longrightarrow \mathfrak{M}^{\bullet\bullet}_{\tilde{g}}(l,n)\,, (F,F') \longmapsto F \odot F'\,,$$

where $\tilde{g} = g + g' + m - 1$.

Besides operations which are induced by the action of little cubes operads, we generalize the operations discussed in [Meh11] to arbitrary n and $(r_1,\dots,r_n)$, present the radial multipliciation

$$\multimap\!\!\bullet\!\!\multimap\colon \mathfrak{Rad}_g(m,n) \times \mathfrak{Rad}_{g'}(m',n) \longrightarrow \mathfrak{Rad}_{\tilde{g}}(m+m',n)\,,$$

with $\tilde{g} = g + g' + n - 1$ and introduce $\alpha\colon \mathfrak{M}^m_{g,n} \longrightarrow \mathfrak{M}^{m+n}_{g,n}$ inducing a split injective map in homology

$$\alpha_*\colon H_*(\mathfrak{M}^m_{g,n}) \longrightarrow H_*(\mathfrak{M}^{m+n}_{g,n})\,.$$

Rotating radial slit domains simultaneously induces the operation of degree one

$$rot\colon H_i(\mathfrak{Rad}_g(m,n)) \longrightarrow H_{i+1}(\mathfrak{Rad}_g(m,n))$$

with $rot^2 = 0$. Eventually, we present formulas relating some of the operations.

Furthermore, we provide an ongoing, extendable software project consisting of about 4500 lines of code. It was used to compute the homology of the moduli spaces for $h \leq 8$ and the first author plans to implement the known operations in order to relate the found generators. In addition, there are upcoming master students under the supervision of Bödigheimer who will implement further features of both the Ehrenfried complex and its corresponding bicomplex.

A deeper study of the cluster spectral sequence, the relations of generators via homology operations and the interdependencies of these operations outline an ongoing research project.

1.3. The Rational Homology of the Moduli Spaces in Short Form

In this section, we present a short form of our computations with coefficients in the rationals. Some of the results were already known, compare the discussion above. We include them anyways. The number of boundary components is always $n = 1$. All cluster spectral sequences with coefficients in $\mathbb{Q}$ and $\mathbb{F}_2$ are found in Section 6.5.

The case $g = 0$: The moduli space $\mathfrak{M}^m_{0,1}$ is the classifying space of the braid group on m strings. Its homology is understood. We have

$$H_*(\mathfrak{M}^m_{0,1};\mathbb{Q}) = \begin{cases} \mathbb{Q} & * = 0 \\ \mathbb{Q} & * = 1 \text{ and } m \geq 2 \\ 0 & else \end{cases}$$

The case $g = 1$: For $m = 0, 1, 2, 3, 4, 5$, the rational homology of $\mathfrak{M}^m_{1,1}$ is given by the following tables.

$H_p(\mathfrak{M}^0_{1,1};\mathbb{Q})$		
$p = 0$	$p = 1$	$p \geq 3$
$\mathbb{Q}$	$\mathbb{Q}$	0

$H_p(\mathfrak{M}^1_{1,1};\mathbb{Q})$		
$p = 0$	$p = 1$	$p \geq 3$
$\mathbb{Q}$	$\mathbb{Q}$	0

$H_p(\mathfrak{M}^2_{1,1};\mathbb{Q})$		
$p = 0$	$p = 1$	$p \geq 3$
$\mathbb{Q}$	$\mathbb{Q}$	0

$H_p(\mathfrak{M}^3_{1,1};\mathbb{Q})$						
$p = 0$	$p = 1$	$p = 2$	$p = 3$	$p = 4$	$p = 5$	$p \geq 6$
$\mathbb{Q}$	$\mathbb{Q}$	0	$\mathbb{Q}$	$\mathbb{Q}$	$\mathbb{Q}^2$	0

$H_p(\mathfrak{M}^4_{1,1};\mathbb{Q})$							
$p=0$	$p=1$	$p=2$	$p=3$	$p=4$	$p=5$	$p=6$	$p\geq 7$
$\mathbb{Q}$	$\mathbb{Q}$	0	$\mathbb{Q}^2$	$\mathbb{Q}^3$	$\mathbb{Q}^2$	$\mathbb{Q}$	0

$H_p(\mathfrak{M}^5_{1,1};\mathbb{Q})$									
$p=0$	$p=1$	$p=2$	$p=3$	$p=4$	$p=5$	$p=6$	$p=7$	$p=8$	$p\geq 9$
$\mathbb{Q}$	?	?	?	?	?	?	$\mathbb{Q}^4$	$\mathbb{Q}^2$	0

The case $g=2$: For $m=0,1,2$, the rational homology of $\mathfrak{M}^m_{2,1}$ is given by the following tables.

$H_p(\mathfrak{M}^0_{2,1};\mathbb{Q})$				
$p=0$	$p=1$	$p=2$	$p=3$	$p\geq 4$
$\mathbb{Q}$	0	0	$\mathbb{Q}$	0

$H_p(\mathfrak{M}^1_{2,1};\mathbb{Q})$							
$p=0$	$p=1$	$p=2$	$p=3$	$p=4$	$p=5$	$p=6$	$p\geq 7$
$\mathbb{Q}$	0	$\mathbb{Q}$	$\mathbb{Q}^2$	0	$\mathbb{Q}$	$\mathbb{Q}$	0

$H_p(\mathfrak{M}^2_{2,1};\mathbb{Q})$							
$p=0$	$p=1$	$p=2$	$p=3$	$p=4$	$p=5$	$p=6$	$p\geq 7$
$\mathbb{Q}$	0	$\mathbb{Q}$	$\mathbb{Q}^3$	$\mathbb{Q}$	$\mathbb{Q}^2$	$\mathbb{Q}^2$	0

The case $g=3$: The rational homology of $\mathfrak{M}^0_{3,1}$ is given by the following table.

$H_p(\mathfrak{M}^0_{3,1};\mathbb{Q})$										
$p=0$	$p=1$	$p=2$	$p=3$	$p=4$	$p=5$	$p=6$	$p=7$	$p=8$	$p=9$	$p\geq 10$
$\mathbb{Q}$	0	$\mathbb{Q}$	$\mathbb{Q}$	0	$\mathbb{Q}$	$\mathbb{Q}$	0	0	$\mathbb{Q}$	0

1.4. Organization of our Thesis

Let us sketch the organization of the content of this thesis. The **first chapter** is this introduction.

The **second chapter** provides a detailed description of our models. Section 2.1 serves as an overview of our approach. The details are carried out in the subsequent Sections 2.2-2.8. Having this done, one has all ingredients to make sense of the following diagram.

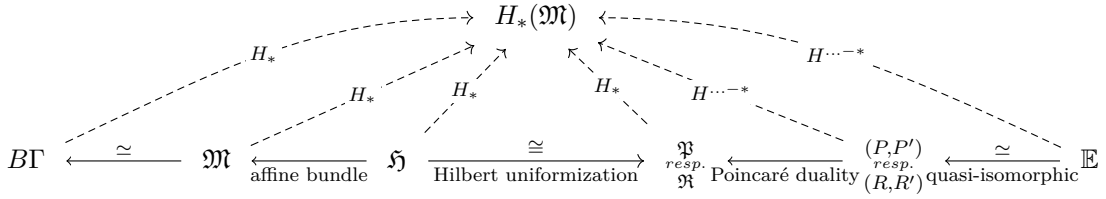

The rightmost model is the Ehrenfried complex. It is a finite chain complex and its differentials admits an explicit description. The homology of the moduli spaces is computed via its dual. In Section 2.9, we provide an explicit formula for its coboundary operator. Hereby, we begin with an explanation of our geometric intuition in order to make the upcoming definitions, statements and proofs straightforward.

The **third chapter** is a brief introduction to the cluster spectral sequence. We introduce the cluster filtration of the bicomplex and the Ehrenfried complex and show that the associated spectral sequences collapse at the second page.

The **fourth chapter** covers various homology operations. Sections 4.1-4.6 describe operations defined either for $\mathfrak{Par}$ or $\mathfrak{Rad}$. Operations and formulas relating $\mathfrak{Par}$ and $\mathfrak{Rad}$ are discussed in Section 4.8. In Section 4.1, we review well-known operations on $\mathfrak{Par}$ via little cubes operads and propose a generalization in Section 4.2. Operations on $\mathfrak{Par}$ which are induced by bundle maps are discussed in Section 4.3. In Section 4.4, we present the operations α. The radial multiplication is treated in Section 4.5 and the composition of two radial slit domains is reviewed in Section 4.6. The rotation of radial slit domains in introduced in Section 4.7.

The **fifth chapter** is a brief analysis of the computational complexity of homology calculations via the Ehrenfried complex. We compute the number of its cells and discuss nearby algorithms used to derive homological data.

The **sixth chapter** provides the documentation of our software project and lists all cluster spectral sequences we computed.

The **Appendix** reviews possibly unkown notation.

Acknowledgements

First and foremost, we thank Professor Bödigheimer for endless hours of inspiring discussions and guidance during the completion of our Master's Thesis. We thank Professor Vygen from the Insititute for Discrete Mathematics and Professor Griebel from the Institute for Numerical Simulation for the opportunity to run our computer program on their highly efficient machines. Furthermore, we thank a lot of people for proof-reading or for their support with carrying out our computer program: Linus Boes, Mathias Gerdes, Christian Hemminghaus, Johannes Holke, Nils Hoppmann, David Hornshaw, Philipp Ochsendorf, Emanuel Reinecke, Max Schmidt, Jannik Silvanus, Raffael Stenzel and Peter Zaspel. Our deepest thank goes to our families who supported us warmly during our studies.

Online Version

A PDF version of this thesis and the computer program can found at

`http://felixboes.de`.

2. Cellular Models

2.1. Introduction

As mentioned above, we are interested in two families of moduli spaces. The first family consits of the moduli spaces $\mathfrak{M}^m_{g,n}$ parametrizing Riemann surfaces of genus $g \geq 0$ with $n \geq 1$ boundary curves and $m \geq 0$ permutable punctures. The second one is composed of moduli spaces $\mathfrak{M}^\bullet_g(m,n)$ parametrizing Riemann surfaces of genus $g \geq 0$ with $m \geq 1$ permutable outgoing boundary curves and $n \geq 1$ incoming boundary curves, where on each incoming curve a point is marked. Let us review Bödigheimer's models for these moduli spaces. All details as well as valuable pictures are found in [Böd90a], [Böd90b] and [Böd06].

In order to obtain a good semi-multisimplicial model $\mathfrak{Par}^m_{g,n}[(r_1,\ldots,r_n)]$ for $\mathfrak{M}^m_{g,n}$, we replace every boundary curve by a point with a non-zero tangent vector attached. Thus $\mathfrak{M}^m_{g,n}$ is the moduli space of conformal equivalence classes $[F,\mathcal{P},\mathcal{Q},\mathcal{X}]$, where F is a Riemann surface of genus g with a set of punctures $\mathcal{P}=\{P_1,\ldots,P_m\}$ and with (enumerated) points $\mathcal{Q}=(Q_1,\ldots,Q_n)$ at which (non-vanishing) tangent vectors $\mathcal{X}=(X_1,\ldots,X_n)$ are attached. The moduli space $\mathfrak{M}^m_{g,n}$ is the quotient of the contractible Teichmüller space by the action of the corresponding mapping class group $\Gamma^m_{g,n}$. Under the assumption $n \geq 1$, the action of $\Gamma^m_{g,n}$ is free so that $\mathfrak{M}^m_{g,n}$ is a manifold of dimension $6g-6+2m+4n$. In this section, we do not elaborate on the advantages of the above mentioned model $\mathfrak{Par}^m_{g,n}[(r_1,\ldots,r_n)]$, but state that it is primarily used to translate the Dyer-Lashof operations defined on configuration spaces into those defined on the moduli spaces, see Chapter 4. In what follows, we fix a moduli space $\mathfrak{M}^m_{g,n}$ and an ordered partition $(r_1,\ldots,r_n)$ of $r=r_1+\ldots+r_n$ with $r_j \geq 1$ for every j.

In Section 2.2, we introduce the bundle $\mathfrak{H}^m_{g,n}[(r_1,\ldots,r_n)]$ over $\mathfrak{M}^m_{g,n}$. The fibre over a point $[F,\mathcal{P},\mathcal{Q},\mathcal{X}]$ consists of certain meromorphic 1-forms and a fixed number of integration constants. It is an open half-space of a real affine space. Thus the bundle map is a homotopy equivalence. Note that for each partition $(r_1,\ldots,r_n)$ we have such a bundle with fibre dimension depending on $(r_1,\ldots,r_n)$. The fibre over $[F,\mathcal{P},\mathcal{Q},\mathcal{X}]$ parametrizes all harmonic functions u of predescribed behavior, namely with poles of order r_j at the points Q_j in the direction of X_j and logarithmic sinks at the punctures P_i. Such functions are called potential functions.

The critical gradient flow lines of a given potential function u (along decreasing values of u) that leave the critical points of u (to either run into another critical point, into a sink P_j or into a pole Q_j) define the critical graph $\mathcal{K}_0$ on F. Dissecting F along its critical graph $\mathcal{K}_0$, we obtain r open and contractible sub-surfaces $F_1,\ldots,F_r$ which we call basins. On each basin F_j, the harmonic function u is the real part of a holomorphic function w_j, unique up to an integration constant.

Each function w_j maps the basin F_j injectively onto an open domain in $\mathbb{C}$. Its image is obviously the entire plane $\mathbb{C}=\mathbb{C}_j$ with finitely many slits removed, each slit running from some point horizontally to the left all the way to infinity. They are commonly called parallel

slit domains. The slits arise from the (piecewise) cuts along the critical flow lines. Observe that right and left banks of such a flow line are now (piecewise) left respectively right banks of possibly different slits on possibly differrent planes. Encoding this information allows us to re-glue the surface F. We define the space $\mathfrak{Par}^m_{g,n}[(r_1,\dots,r_n)]$ of these parallel slit domains as a subspace of a finite, semi-multisimplicial space P, namely as the complement of the (geometric realization of) the subcomplex of degenerate surfaces P'. The reason for P beeing not multisimplicial is a direct consequence of the fact that the occuring symmetric groups define a semisimplicial set $\mathfrak{S}^\Delta$ together with pseudo degeneracy maps satisfying all but one simplicial identity (compare Appendix A).

Summing up, we have a homeomorphism

$$\mathcal{H}\colon \mathfrak{H}^m_{g,n}[(r_1,\dots,r_n)] \longrightarrow \mathfrak{Par}^m_{g,n}[(r_1,\dots,r_n)]\,,$$

called Hilbert uniformization. The pair (P,P') is a relative manifold $\mathfrak{Par}^m_{g,n}[(r_1,\dots,r_n)] = P-P'$, orientable for $m<2$ and of dimension $3h$ with $h=2g+m+n+r-2$. In particular, the homology of $\mathfrak{Par}^m_{g,n}[(r_1,\dots,r_n)]$ is given by Poincaré duality

$$H_*(\mathfrak{M}^m_{g,n};\mathbb{Z}) = H_*(\mathfrak{Par}^m_{g,n}[(r_1,\dots,r_n)];\mathbb{Z}) \cong H^{3h-*}(P,P';\mathcal{O})$$

with $\mathcal{O}$ the orientation coefficients. The bicomplex of (P,P') is called parallel slit complex and admits a purely combinatorial description treated in Section 2.3.

Turning to the second family of moduli spaces $\mathfrak{M}^\bullet_g(m,n)$, we consider marked conformal equivalence classes of Riemann surfaces with genus $g\geq 0$ and two kinds of boundary cuves. There are $m\geq 1$ permutable outgoing boundary curves $C^+_1,\dots,C^+_m$ and $n\geq 1$ incoming boundary curves $C^-_1,\dots,C^-_n$, each of which has a marked point $P_i\in C^-_i$. Thus, a point in the moduli space $\mathfrak{M}^\bullet_g(m,n)$ is represented by the data $[F,\mathcal{C}^+,\mathcal{C}^-,\mathcal{P}]$, where $\mathcal{C}^+ = C^+_1\cup\ldots\cup C^+_m$ respectively $\mathcal{C}^- = C^-_1\cup\ldots\cup C^-_n$ denotes the entire outer respectively inner boundary, while $\mathcal{P}=(P_1,\dots,P_n)$ is the (enumerated) set of marked points on the n inner boundary curves. Thereby, a conformal homeomorphism $h\colon F\longrightarrow F'$ between such surfaces is called marked if each P_i is mapped to P'_i, and the dot in the definition of $\mathfrak{M}^\bullet_g(m,n)$ refers to this marking.

Analogously to the previous statements, the moduli space $\mathfrak{M}^\bullet_g(m,n)$ is a quotient of the contractible Teichmüller space under the action of the corresponding mapping class group $\Gamma^\bullet_g(m,n)$. Excluding the case $g=0$, $m=n=1$, the action of $\Gamma^\bullet_g(m,n)$ is free. Consequently, $\mathfrak{M}^\bullet_g(m,n)$ is a manifold of dimension $\dim(\mathfrak{M}^\bullet_g(m,n)) = 6g-6+3m+4n$ and a classifying space $B\Gamma^\bullet_g(m,n)$ for the mapping class group $\Gamma^\bullet_g(m,n)$.

We proceed the same way as in the parallel case: In Section 2.4, we describe a homotopy equivalent bundle $\mathfrak{H}^\bullet_g(m,n)$ over $\mathfrak{M}^\bullet_g(m,n)$. In Section 2.5, we introduce the space $\mathfrak{Rad}_g(m,n)$ of radial slit configurations homeomorphic to $\mathfrak{H}^\bullet_g(m,n)$, which allows us to actually perform homology calculations.

The bundle $\mathfrak{H}^\bullet_g(m,n)$ is constructed similarly as above: Over a point $[F,\mathcal{C}^+,\mathcal{C}^-,\mathcal{P}]\in \mathfrak{M}^\bullet_g(m,n)$, an element of the fibre consists of the data $[F,\mathcal{C}^+,\mathcal{C}^-,\mathcal{P},w]$ with $w=(u,v_1,\dots,v_n)$. By this, $u\colon F\longrightarrow\overline{\mathbb{R}}$ is a certain harmonic potential function, and v_k are certain locally defined harmonic conjugates of u on the components, called basins as well, of the complement of the unstable critical gradient flow. The functions u and v_k are used to map the basins $F_1,\dots,F_n$ of F into n annuli $\mathbb{A}_1,\dots,\mathbb{A}_n\subset\mathbb{C}$ with outer radius equals 1. This process can be reversed. Since the critical flow lines define segments on the annuli that can be

glued together again, the surface F can be re-built from the image of F on the annuli. The points in the space $\mathfrak{Rad}_g(m,n)$ of radial slit domains consist of these annuli together with the information neccessary to encode the glueing. We define $\mathfrak{Rad}_g(m,n)$ in a simplicial way such that $\mathfrak{Rad}_g(m,n) = R - R'$ is the geometric realization of the complement of a subcomplex R' of the semi-multisimplicial complex R.

The pair (R, R') is a relative manifold of dimension $3h+n$ with $h = 2g-2+m+n$, which is orientable for $m < 2$. Altogether, we can express the homology of $\mathfrak{M}_g^\bullet(m,n)$ via Poincaré duality by

$$H_*(\mathfrak{M}_g^\bullet(m,n);\mathbb{Z}) = H_*(\mathfrak{Rad}_g(m,n);\mathbb{Z}) \cong H^{3h+n-*}(R,R';\mathcal{O})\,,$$

where $\mathcal{O}$ denotes the orientation coefficients. In both Sections 2.3 and 2.5, we give a description of the cells of the bicomplexes P and R, followed by the explanation of the vertical and horizontal faces, yielding the boundary operators. In Section 2.6, we define the orientation system $\mathcal{O}$ for the bicomplexes P and R.

We are left to determine the (co)homology of the finite bicomplex (P, P') respectively (R, R'). Both complexes have a close connection to the study of the homology of normed groups and in particular the symmetric groups. To see this, let G be a group with a norm N. The bar complex $B_\bullet(G)$ can be filtered by extending the norm for an element $(g_q \mid \ldots \mid g_1)$ by $N(g_q|\ldots|g_1) = N(g_q) + \ldots + N(g_1)$. In [Vis10], the spectral sequence $\mathcal{N}[G]$ associated with this norm fltration on $B_\bullet(G)$ is studied for a family of groups called factorable (c.f. Appendix B). These are normed groups with a certain normal form for its elements in a given set of generators whose word length norm is N. The symmetric groups with all transpositions as generators are examples of factorable groups. Other examples are more general Coxeter groups. The main result in [Vis10] states that for a factorable group, the first page of the above spectral sequence is concentrated in a single diagonal. Thus the homology of G is the homology of this diagonal. It turns out that the p^{th} column of our bicomplex (P, P') respectively (R, R') is a direct summand of the h^{th} column of $\mathcal{N}^0[\mathfrak{S}_p]$, where q is the homological degree of both sides. It follows that the columns of our bicomplex have their homology concentrated in the degree $q = h$, so the first page of the spectral sequence of the double complex is concentrated in a single row which is by definition the Ehrenfried complex $\mathbb{E}$ associated with (P, P') respectively (R, R').

In Section 2.8, we adapt the known methods to show that $\mathbb{E}$ is a quasi-isomorphic direct summand of $(P, P')^*$ respectively $(R, R')^*$, which was already formulated and proven for the parallel case with $n = 1$ and $r = 1$ the trivial partition.

In Section 2.9, we give an explicit description of the dual Ehrenfried complex: We elaborate our geometric insights on the behavior of the horizontal coface operator, in order to introduce the notion of i^{th} coboundary traces. We then define a canonical bijection between the set of i^{th} coboundary traces and the set of i^{th} cofaces. The coface of a top dimensional cell Σ corresponding to a given coboundary trace a will be called $a.\Sigma$. In Proposition 2.9.8, we provide the formula

$$\partial^*_{\mathbb{E}}(\Sigma) = \sum_{i=1}^{p-1}(-1)^i \sum_{a \in T_i(\Sigma)} \kappa^*(a.\Sigma)\,,$$

which enables us to define the homology operations described in [Böd90b] and [Böd14] via the dual Ehrenfried complex in Chapter 4. Another benefit of this definition is the

classification of the cells of the Ehrenfried complex (c.f. Proposition 2.9.26). Roughly speaking, there are a few distinguished cells of low degree which we call thin. An arbitrary cell is uniquely obtained from such a thin cell by glueing in a certain number of stripes. The geometric meaning and the precise statements are presented in Subsection 2.9.4.

2.2. The Bundle $\mathfrak{H}^m_{g,n}[(r_1,\ldots,r_n)]$

We start off with the construction of the bundle $\mathfrak{H}^m_{g,n}[(r_1,\ldots,r_n)]$ for a fixed moduli space $\mathfrak{M}^m_{g,n}$ and an ordered partition $(r_1,\ldots,r_n)$ of $r = r_1+\ldots+r_n$. Consider a point $[F,\mathcal{P},\mathcal{Q},\mathcal{X}]$ in the moduli space $\mathfrak{M}^m_{g,n}$. For positive real numbers $B^-_1,\ldots,B^-_m$ and $B^+_1,\ldots,B^+_n$ that satisfy the residue equation $\sum_{i=1}^m B^-_i - \sum_{j=1}^n B^+_j = 0$, and complex numbers a_{jk} where $j = 1,\ldots,n$ while $k = 1,\ldots,r_j-1$, there is a **potential function** $u\colon F \longrightarrow \overline{\mathbb{R}}$, i.e.

(i) $u|_{F-(\mathcal{P}\cup\mathcal{Q})}$ is harmonic;

(ii) in a chart domain V_i around P_i with coordinates $z = x+\sqrt{-1}\cdot y$ such that $z(P_i)=0$

$$u(z) = B^-_i \log|z| + \phi_i \qquad \text{with} \qquad \phi_i\colon V_i \longrightarrow \mathbb{R} \text{ harmonic;}$$

(iii) in a chart domain W_j around Q_j with coordinates $z = x+\sqrt{-1}\cdot y$ such that $z(Q_j)=0$ and $(T_{Q_j}z)(X_j) = \frac{\partial}{\partial x} \in T_0\mathbb{C}$

$$u(z) = \Re\left(\frac{1}{z^{r_j}} + \sum_{k=1}^{r_j-1}\frac{a_{jk}}{z^k}\right) - B^+_j \log|z| + \psi_j \qquad \text{with} \qquad \psi_j\colon W_j \longrightarrow \mathbb{R} \text{ harmonic}\,.$$

Such a potential function is unique up to an additive constant D_0, i.e. it is uniquely defined by one real, $n+m-1$ positive and $r-n$ complex parameters. A proof of this classical result can be found in many sources, for example [Koc91]. The condition $\sum_{i=1}^m B^-_i - \sum_{j=1}^n B^+_j = 0$ is imposed by the Residue Theorem (the complex differential ∂u is a meromorphic 1-form, so the sum of its residues vanishes).

Following [Böd90a, Section 3.2], we use the flow of $-\operatorname{grad}_u$, the gradient field of steepest descent of a potential function u, in order to construct the (directed) critical graph $\mathcal{K}_0 \subset F$. This may be seen as a 1-skeleton of F. Before going on, let us look at two very simple examples. In Figure 2.1 we sketch the flow lines of the harmonic function $\Re(z) = x$ and Figure 2.2 pictures the flow lines of $\Re(z^2) = x^2 - y^2$. Geometrically speaking, the conditions on the potential function u are as follows. At every point Q_j, the dominating term is the pole $\Re(\frac{1}{z^{r_j}})$ whereas the terms $\Re(\frac{a_{jk}}{z^k})$ for $k = r_j-1,\ldots,1$ and the logarithmic term $B^+_j\log|z|$ have no influence on the qualitative picture. In Figures 2.1 or 2.2, the chart around infinity pictures the stream lines near a pole of order $r_j = 1$ or $r_j = 2$. At a point P_j the gradient flow has a sink as pictured in Figure 2.3. The coefficients B^-_i respectively B^+_j indicate the magnitude of the logarithmic sink respectively source. Following the stream lines, one will end up either in one of the singularities $\mathcal{P}\cup\mathcal{Q}$ or in a critical point of u. At a critical point, u has the form $\Re(z^k)$ for some $k \geq 2$. The critical graph of u consists of all critical flow lines that start in such critical points. A point $S \in F$ at which grad_u vanishes is called **stagnation point** and we denote the **set of stagnation points** by $\mathcal{S}$ — they are

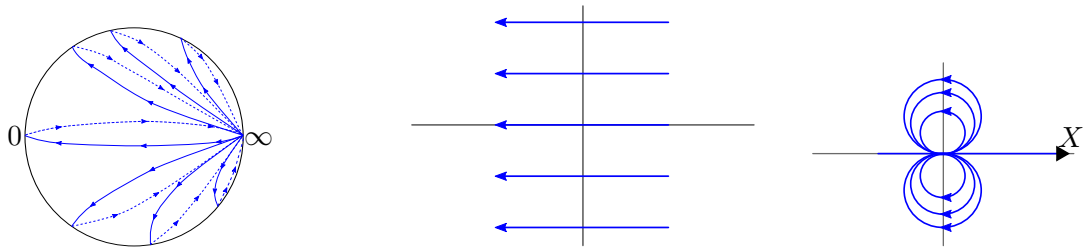

Figure 2.1.: The gradient flow of $\Re(z)$ on the sphere $\mathbb{S}^2$ and in charts around zero and infinity.

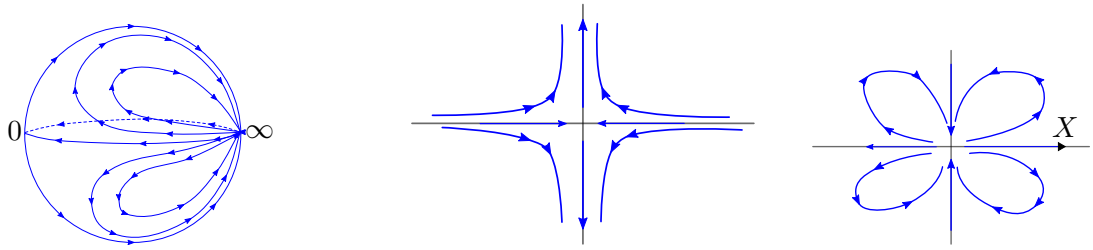

Figure 2.2.: The gradient flow of $\Re(z^2)$ on the sphere $\mathbb{S}^2$ and in charts around zero and infinity.

the critical points of u. The vertices of $\mathcal{K}_0$ are $V\mathcal{K}_0 = \mathcal{S} \cup \mathcal{P} \cup \mathcal{Q}$ and the edges $\gamma \in E\mathcal{K}_0$ are specific segments of the gradient flow of u: For two vertices $S_0 \in \mathcal{S}$ and $S_1 \in V\mathcal{K}_0$ with $t_0 = u(S_0) < u(S_1) = t_1$ (as points in $\overline{\mathbb{R}}$), a smooth curve $\gamma\colon [t_0, t_1] \longrightarrow F$ starting in S_0 and ending in S_1 is called **critical edge** if it satisfies the conditions

(i) $u(\gamma(t)) = t$ and

(ii) $\dot{\gamma}(t) = -\operatorname{grad}_u(\gamma(t)) \neq 0$ for $t_0 < t < t_1$.

In particular, curves must not traverse through critical points.

Both potential functions in Figures 2.1 and 2.2 have exactly one singularity namely at infinity. The harmonic function $\Re(z)$ has no stagnation points and $\Re(z^2)$ has exactly one. In Figure 2.4, we picture the flow of a potential function u having one dipole Q of simple order, one puncture P and one stagnation point S.

Dissecting F along the critical graph $\mathcal{K}_0$ yields r open, contractible[1] components F_1, $\ldots$, F_r called **basins**. These basins are ordered. The poles $\mathcal{Q}$ are enumerated and at every pole Q_j, the tangent vector X_j points into the first since distinguished component, whereas the others are numbered following counter-clockwise around Q_j. In Figure 2.5 we illustrate the stream lines of $\Re(z^3)$ on $\mathbb{S}^2$ around infinity. The critical flow is stressed and the basins are denoted by F_1,F_2 or F_3.

From the topological point of view, we obtain a cell decomposition. This means that the homotopy type of F, which is just its genus, can be reconstructed from glueing the disc-shaped components F_j. In order to keep track of the given complex structure, we follow

[1]Using the flow lines, each F_j is contracted to an equipotential line l_i. Observe that every potential line l_i is contractible since $\mathcal{Q}$ and $\mathcal{P}$ are removed.

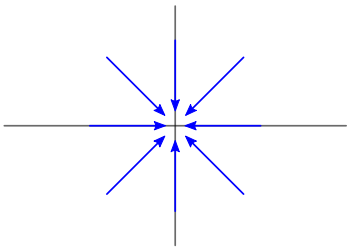

Figure 2.3.: The gradient flow of $\Re(\log(z)) = \log|z|$ near zero.

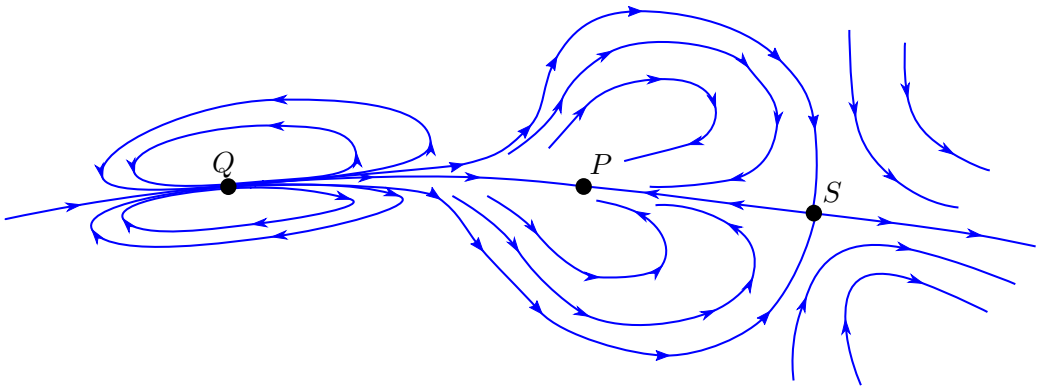

Figure 2.4.: The gradient flow of a potential function which has exactly one dipole Q of simple order, one puncture P and one stagnation point S. We have $g = 0$, $m = 1$ and $n = 1$.

[Böd90a]. On every sub-surface F_j, the harmonic function u admits a harmonic conjugate v_j, unique up to an integration constant, by letting

$$v_j(\zeta) = \int_{\zeta_o}^{\zeta} \frac{\partial u}{\partial x} dy - \frac{\partial u}{\partial y} dx \qquad \text{for some} \qquad \zeta_0 \in F_j \,.$$

The holomorphic function $w_j = u + \sqrt{-1} \cdot v_j$ maps the basin F_j injectively onto an open domain in $\mathbb{C}$ and its image is obviously the entire plane with finitely many slits removed, each slit running from some point horizontally to the left all the way to infinity. Changing the integration constant D_j corresponds to a translation parallel to the imaginary axis.

Let us go back to the examples pictured in Figures 2.2 and 2.4. Dissecting the sphere along the critical flow lines of $u = \Re(z^2)$ yields exactly two components $F_1 = \{z \in \mathbb{S}^2 - \infty \mid \Re(z) > 0\}$ and $F_2 = \{z \in \mathbb{S}^2 - \infty \mid \Re(z) < 0\}$. The tangent vector X points into the first component F_1. For the other example, consider Figure 2.6 where we added three dashed lines on which u is constant — so-called equipotential lines — and sketch the relevant clipping under the biholomorphic function. The critical graph is stressed. In Figure 2.8 on Page 27, we picture an enlarged version of Figure 2.6 with enumerated equipotential lines in order to provide more guidance.

Let $\mathfrak{H}^m_{g,n}[(r_1, \ldots, r_n)]$ be the space of all $(F, \mathcal{P}, \mathcal{Q}, \mathcal{X}, w)$ with $w = (u, v_1, \ldots, v_r)$, where u is a globally defined potential function as declared above and each v_j is a harmonic

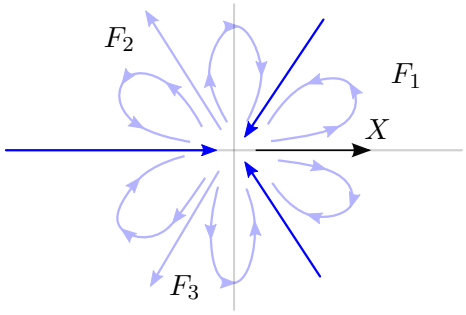

Figure 2.5.: Dissecting $\mathbb{S}^2$ along the critical graph of $\Re(z^3)$ yields three basins.

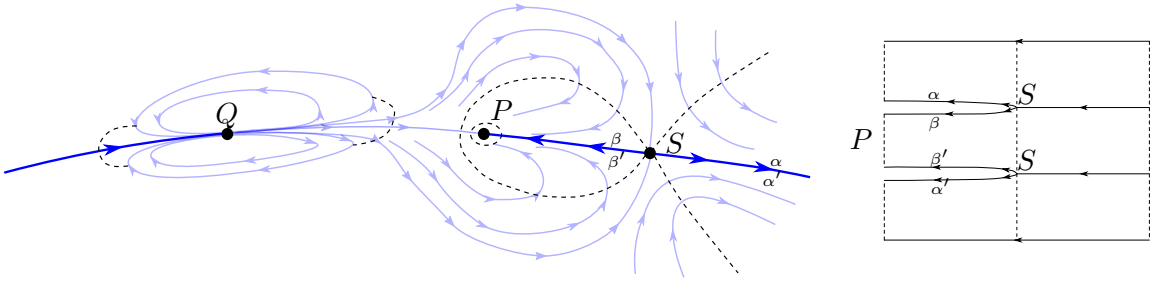

Figure 2.6.: The gradient flow of a potential function and the slit picture. We have $g = 0$, $m = 1$ and $n = 1$.

conjugates of u, defined only on F_j. There is a projection

$$\mathfrak{H}^m_{g,n}[(r_1, \ldots, r_n)] \xrightarrow{\simeq} \mathfrak{M}^m_{g,n}$$

with contractible fibres, namely the space of all $(a_{jk}, B_i^-, B_j^+, D_0, \ldots, D_r)$ subject only to the residue equation. More precisely, it is the open affine half-space $\mathbb{C}^{r-n} \times \mathbb{R}^{m+n-1}_{>0} \times \mathbb{R}^{r+1}$. This bundle would be trivial if we required both $(r_1, \ldots, r_n) = (1, \ldots, 1)$ and non-permutable punctures $\mathcal{P}$.

Its real dimension is readily computed, as $2(r-n) + m + n - 1 + 1$ real parameters correspond to a choice of u and every harmonic conjugate v_j is unique up to an additive constant, adding r real dimensions:

$$\dim \mathfrak{H}^m_{g,n}[(r_1, \ldots, r_n)] = \dim \mathfrak{M}^m_{g,n} + (2(r-n)+m+n-1+1) + r = 6g-6+3m+3n+3r = 3h\,.$$

We end this section with the following remark. There are situation in which we want to think of surfaces with boundary or, in terms of slit picutes, of the relevant clipping as seen in Figure 2.6. This is achieved by removing the critical graph as well as specific discs around the poles and punctures. Each disc around a puncture $P_j \in \mathcal{P}$ is bound by an equipotential circle beeing a closed curve on which u is constant, whereas each disc around a pole $Q_i \in \mathcal{Q}$ is bounded by a circle consisting of flow lines or equipotential lines, see Figure 2.7. Observe that this process can be reversed without loss of information as the basins are ordered.

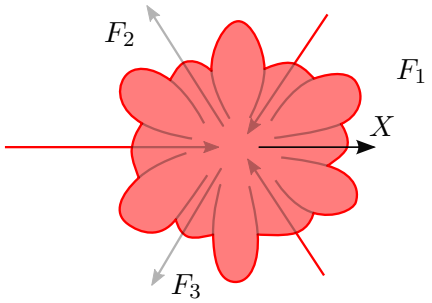

Figure 2.7.: The red matter is removed and the thick red lines are seen as the boundary curves of the resulting surface.

2.3. The Parallel Slit Complex

In this section, we review the parallel slit complex (P, P') associated with the moduli space $\mathfrak{M}^m_{g,n}$ and a given ordered partition $(r_1, \ldots, r_n)$. It is a semi-multisimplicial complex and the complement of the (realization of) the subcomplex of degenerate configurations P' is the space of parallel slit domains $\mathfrak{Par}^m_{g,n}[(r_1, \ldots, r_n)]$. This will serve as a good model for the moduli space $\mathfrak{M}^m_{g,n}$ in the sense of Theorem 2.3.15.

If not stated otherwise, the genus g, the number of punctures m, the number of boundary curves n and the ordered partition $(r_1, \ldots, r_n)$ of $r = r_1 + \ldots + r_n$ are meant to be fixed. As before, we denote $h = 2g - 2 + m + n + r$.

The following definitions express the rigidity of the geometric insights we presented in Section 2.2. Using a potential function u and harmonic conjugates $v_1, \ldots, v_r$, we obtain r copies of the complex plane $\mathbb{C}_k$ with finitely many slits removed, each slit running from some point horizontally to the left all the way to infinity. Introducing equipotential lines that are defined near the poles or run through the critical points of u, the relevant clipping of every $\mathbb{C}_k$ looks like Figure 2.6 with possibly more slits.

Let us for a moment concentrate only on one slit picture $\mathbb{C}_k$. Here the heights of the slits are denoted by the symbols $\underline{1}_k, \ldots, \underline{p}_k$. Equivalently, we number the banks using the symbols $\underline{0}_k, \ldots, \underline{p}_k$. The equipotential lines subdivide each bank into $q+1$ pieces and we encode the glueing information as indicated by Figure 2.9.

For $\underline{i}_k \neq \underline{p}_k$ and $q \geq j \geq 0$, the upper edge of the j^{th} piece of the $\underline{i}^{\text{th}}_k$ bank is glued to the lower edge of the j^{th} piece of the bank with the prediscribed symbol $\sigma_j(\underline{i}_k)$.

The $\underline{0}^{\text{th}}_k$ bank does not have a lower edge and the $\underline{p}^{\text{th}}_k$ bank does not have an upper edge but if we define $\sigma_j(\underline{p}_k) = \underline{0}_k$ we end up with $q+1$ permutations $\sigma_q, \ldots, \sigma_0$ of the symbols $\underline{0}_k$, $\ldots, \underline{p}_k$. These permutations are clearly not arbitrary, e.g. σ_0 is fixed to be cycle $\sigma_0 = (\underline{0}_k\ \underline{1}_k$ $\ldots\ \underline{p}_k)$. The $(q+1)$-tuple $(\sigma_h : \ldots : \sigma_0)$ defines the homogenous notation of a combinatorial cell (see Definition 2.3.2) whereas the inhomogeneous notation (see Definition 2.3.5) encodes the (counter-clockwise) tours around the stagnation points.

The positioning of the slits define an inner point in the multisimplex $(\Delta^{p_1} \times \ldots \times \Delta^{p_r}) \times \Delta^q$. Collapsing vertical respectively horizontal stripes defines the vertical respectively horizontal face operator (see Definition 2.3.8 respectively Definition 2.3.9). Allowing degenerate slit configurations, we end up with a semi-multisimplicial complex called the parallel slit complex (see Definition 2.3.11).

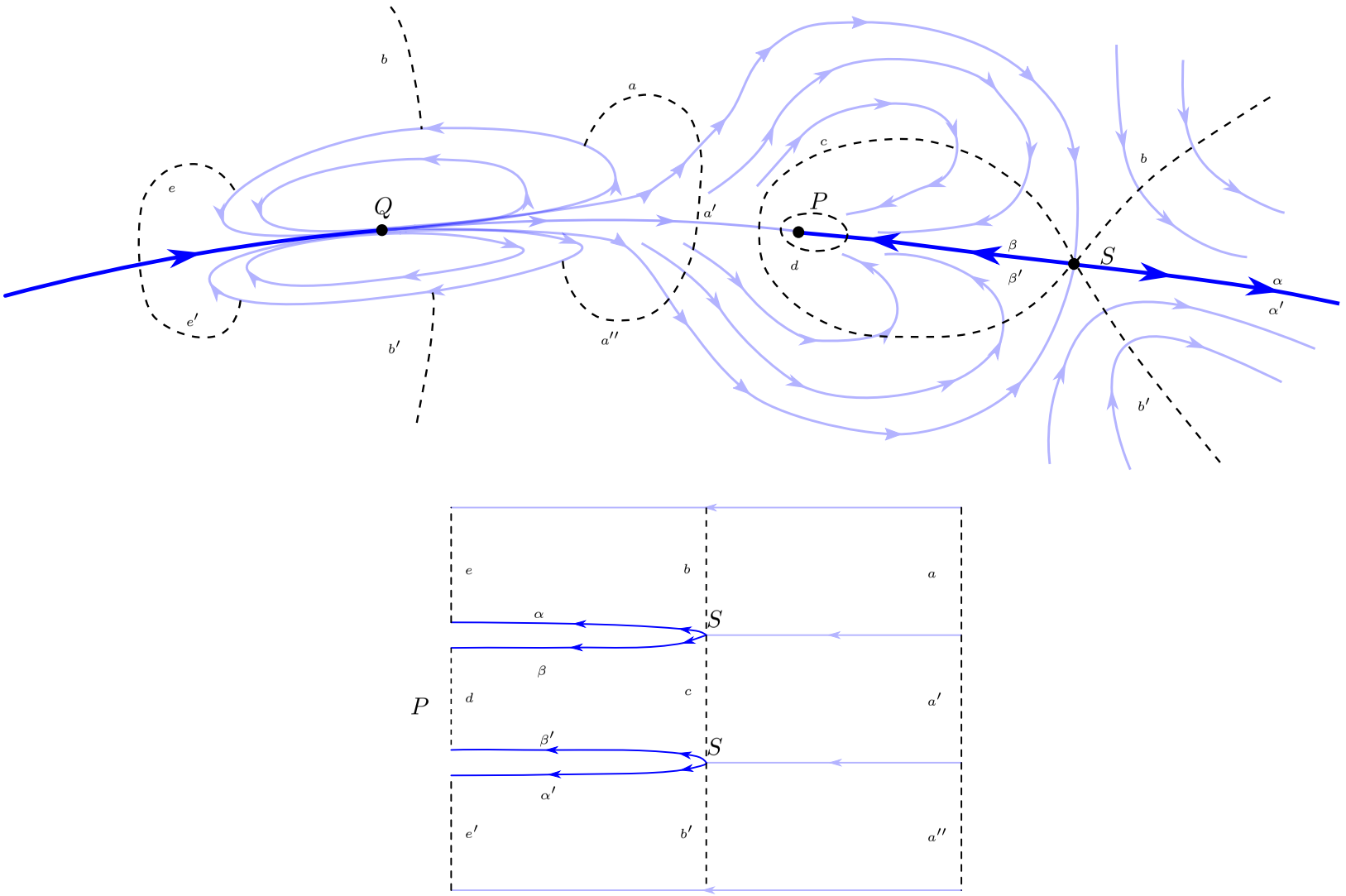

Figure 2.8.: The gradient flow of a potential function and the slit picture. The dashed curves are equipotential lines and we have $g = 0$, $m = 1$ and $n = 1$.

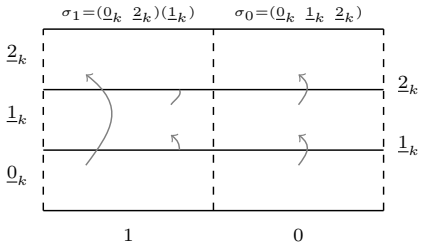

Figure 2.9.: The combinatorial description of the slit picture in Figure 2.6. We have $g = 0$, $m = 1$ and $n = 1$.

2.3.1. Cells in Homogeneous Notation

In this subsection, the partition $r = r_1 + \ldots + r_n$ is meant to be fixed. We define arbitrary cells Σ of bidegree (p, q) in the homogenous notation. Before going into details, recall our notation for the symmetric groups (see Appendix A).

Definition 2.3.1. Consider an ordered partition of the natural number $p = p_1 + \ldots + p_r$ with all p_i positive. The set

$$[p] = \{\underline{0}_1, \underline{1}_1, \ldots, \underline{p_1}_1, \ldots, \underline{0}_r, \underline{1}_r, \ldots, \underline{p_r}_r\}$$

consisting of $p + r$ elements is a **partition of** p **into** r **levels**. In what follows, we will abuse notation by abbriviating

$$\underline{p}_k = \underline{p}_{kk}\,.$$

This should not cause any confusion. The set $[p]$ is ordered canonically via

$$\underline{0}_1 < \underline{1}_1 < \ldots < \underline{p}_1 < \ldots < \underline{0}_r < \underline{1}_r < \ldots < \underline{p}_r\,.$$

Definition 2.3.2. Using the **homogeneous notation**, a combinatorial cell of bidegree (p, q) with respect to a given partition $[p]$ is a $(q + 1)$-tuple of permutations $\sigma_j \in \mathfrak{S}_{[p]}$

$$\Sigma = (\sigma_q : \ldots : \sigma_0)\,.$$

Most of the time we refere to Σ as a cell on r levels, leaving the partition $[p]$ unmentioned.

Definition 2.3.3. A cell $\Sigma = (\sigma_q : \ldots : \sigma_0)$ of bidegree (p, q) is called (parallel) **inner cell** if it is subject to the following conditions.

(i) Every σ_i maps $\underline{p}_k$ to $\underline{0}_k$ for every k.

(ii) The zero$^{\text{th}}$ permutation σ_0 is fixed to be $\sigma_0 = (\underline{0}_1\ \underline{1}_1\ \ldots\ \underline{p}_1)\ldots(\underline{0}_r\ \underline{1}_r\ \ldots\ \underline{p}_r)$.

(iii) For every $0 \leq i < q$, the permutations σ_i and σ_{i+1} are distinct.

(iv) There is no symbol $\underline{0}_k \leq \underline{j}_k < \underline{p}_k$ that is mapped to its successor $\underline{j+1}_k$ by all permutations σ_i.

(v) The levels of Σ are **ordered ascendingly** with respect to the boundary curves, i.e. σ_q induces on $\{\underline{0}_1, \ldots, \underline{0}_r\} \subseteq [p]$ the permutation $(\underline{0}_1\ \ldots\ \underline{0}_{p_1})(\underline{0}_{p_1+1}\ \ldots\ \underline{0}_{p_1+p_2})\ldots(\underline{0}_{p_{r-1}+1}\ \ldots\ \underline{0}_{p_r})$.

Reversing the process discussed in Section 2.2, an inner cell on one level is pictured as follows. We start off with the unit square which is cut up into horizontal stripes of the same size. The stripes are denoted by the symbols $\underline{0}$ to $\underline{p}$. Each stripe is divided into rectangles, denoted by the numbers 0 to q, hence we subdivided the initial square into $(p+1)(q+1)$ pieces of the same size. Now we glue the stripes according to the permutations $(\sigma_q : \ldots : \sigma_0)$ as indicated by Figure 2.10. The top side of the rectangle with coordinate $(j, \underline{i})$ is glued

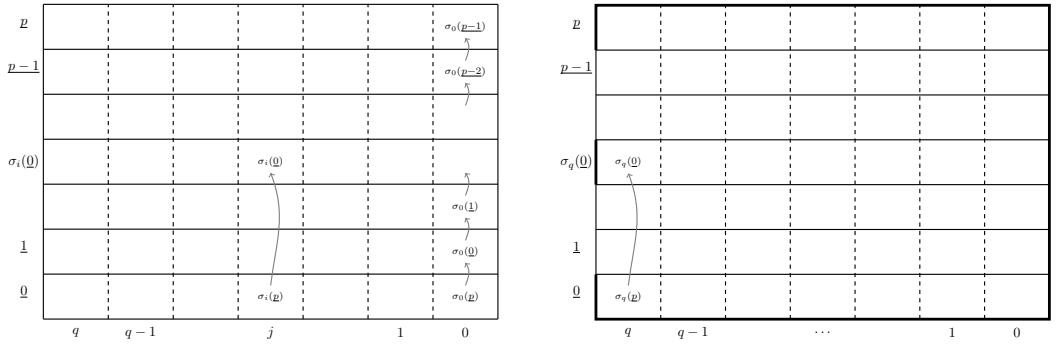

Figure 2.10.: Glueing a surface from a cell in homogeneous notation. The thick line indicates the boundary curve (which is seen as a parametrized disc around a pole).

to the bottom side of the rectangle with coordinate $(j, \sigma_j(\underline{i}))$, but we omit to glue the $\underline{p}^{\text{th}}$ rectangle to $\underline{0}^{\text{th}}$. After glueing all pieces, we receive a surface with punctures and a boundary curve (which we understand as the boundary of a contractible neighbourhood of the dipole) as follows. The cycle of σ_q containing $\underline{0}$ corresponds to the boundary curve (and therefore to the dipole), which we indicate by a thick line in Figure 2.10. All the other cycles of σ_q resemble the punctures of the surface.

The picture for an inner cell on r levels is similar. Here we start off with r unit squares $A_1, \ldots, A_r$, cut each A_k in $(p_k+1)(q+1)$ pieces and glue the collection of all pieces according to the permutations σ_i. Observe that the resulting surface has exactly n boundary curves by it may be disconnected. We will treat this case in the next definition. The cell in Figure 2.11 resembles a closed disc and corresponds to the example in the previous section, where we cut $\mathbb{S}^2$ into two pieces along the critical flow of the dipole function $\Re(z^2)$.

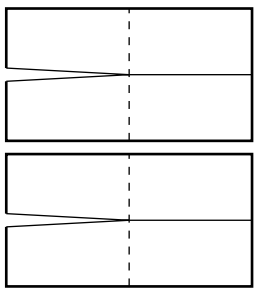

Figure 2.11.: The cells $((\underline{0}_1\ \underline{1}_2\ \underline{0}_2\ \underline{1}_1) : (\underline{0}_1\ \underline{1}_1)(\underline{0}_2\ \underline{1}_2))$ resembles a closed disc and is understood as the complement of an open disc around infinity in $\mathbb{S}^2$.

Definition 2.3.4. A combinatorial cell is **connected** if the resulting surface is connected. Wandering on the surface by traversing through the stripes horizontally or (using the glueing information) vertically, we conclude that a cell is connected if and only if the equivalence relation on $[p]$ generated by

$$i \sim j \iff \exists k : j = \sigma_k(i)$$

consists of exactly one element.

2.3.2. Cells in Inhomogeneous Notation

As before, the ordered partition $r = r_1 + \ldots + r_n$ is meant to be fixed. It is fertile to give an equivalent description for inner cells of bidegree (p, q). Let $\Sigma = (\sigma_q : \ldots : \sigma_0)$ be a inner cell and consider the permutations $\tau_j = \sigma_j \sigma_{j-1}^{-1}$ for $1 \leq j \leq h$. Every symbol $\underline{0}_k$ is fixed by every τ_i. We sometimes view these as permutations on the symbols $[p] - \{\underline{0}_k \mid 1 \leq k \leq r\}$. In the next definition we rephrase the conditions of Definition 2.3.3.

Definition 2.3.5. Using the **inhomogeneous notation**, a combinatorial cell of bidegree (p, q) with respect to a given partition $[p]$ is a q-tuple of permutations $\tau_j \in \mathfrak{S}_{[p]}$ written as

$$\Sigma = (\tau_q \mid \ldots \mid \tau_1)\,.$$

It is a (parallel) **inner cell** if it is subject to the following conditions

(i) every permutation $\tau_q, \ldots, \tau_1$ is non-trivial,

(ii) the set of common fixed points of the permutations $\tau_q, \ldots, \tau_1$ is exactly $\{\underline{0}_1, \ldots, \underline{0}_r\}$ and

(iii) the permutation $\tau_q \cdots \tau_1 \sigma_0 \in \mathfrak{S}_{[p]}$ induces on $\{\underline{0}_1, \ldots, \underline{0}_r\} \subseteq [p]$ the permutation $(\underline{0}_1 \ \cdots \ \underline{0}_{p_1})(\underline{0}_{p_1+1} \ \cdots \ \underline{0}_{p_1+p_2}) \cdots (\underline{0}_{p_{r-1}+1} \ \cdots \ \underline{0}_{p_r})$.

The following is clearly a one-to-one correspondence of inner cells with respect to a given partition $[p]$

$$(\sigma_q : \ldots : \sigma_0) \longmapsto (\tau_q \mid \ldots \mid \tau_1) \qquad \text{with} \qquad \tau_i = \sigma_i \sigma_{i-1}^{-1}\,.$$

In contrast to the homogeneous notation, where the combinatorial information describes how to traverse through the geometric cell vertically, the inhomogeneous notation portrays the tours around each (inner) corner point, which is a stagnation point in the light of Section 2.2. In Figure 2.12 we picture this for the cell $\Sigma = ((\underline{0}\ \underline{2}) : (\underline{0}\ \underline{1}\ \underline{2}))$ (written in homogeneous notation), which should remind the reader of the example portrayed in Figure 2.6.

Both the number of punctures and the number of boundary components of the corresponding surface are encoded by the permutation σ_q.

Definition 2.3.6. Consider an arbitrary cell $\Sigma = (\sigma_q : \ldots : \sigma_0)$ of bidegree (p, q).

(i) The **number of cycles** of Σ is defined to be the number of cycles of the permutation σ_q

$$\mathrm{ncyc}(\Sigma) = \mathrm{ncyc}(\sigma_q)\,,$$

where we view fixed points as cycle of length zero.

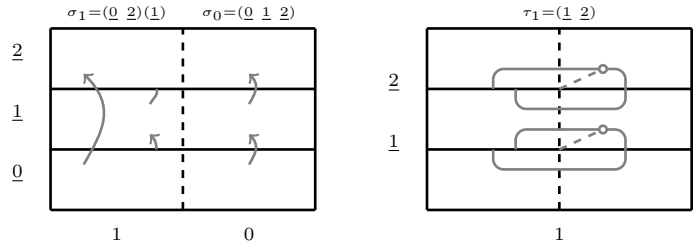

Figure 2.12.: Comparison of the homogeneous and inhomogeneous notation.

(ii) Every cycle of σ_q that contains at least one symbol $\underline{0}_k$ is called **boundary cycle** of Σ. The **number of boundaries** of Σ is denoted by

$$n(\Sigma) = \#\{\text{boundary cycle of } \Sigma\}$$

and the **number of punctures** of Σ is

$$m(\Sigma) = \mathrm{ncyc}(\Sigma) - n(\Sigma)\,.$$

(iii) The **norm** of Σ is

$$N(\Sigma) = N(\sigma_q\sigma_{q-1}^{-1}) + \ldots + N(\sigma_1\sigma_0^{-1})\,,$$

where N measures the word length in the symmetric group $\mathfrak{S}_{[p]}$ with respect to the set of all transpositions.

Remark 2.3.7. Reversing the dissection process in Section 2.2, the number of punctures and boundary curves of a combinatorial cell Σ equals the number of punctures and boundary curves of the surface F that is obtained by glueing. Moreover, an inner cell $\Sigma = (\tau_q \mid \ldots \mid \tau_1)$ defines an imbedded connected graph $\mathcal{K}_0$ whose complement are r basins. The poles, punctures and stagnation points correspond to the vertices and $N(\tau_j) + s$ is the number of edges that end in the s stagnations at the j^{th} equipotential line. The Euler characteristic of F is

$$2 - 2g = \chi(F) = \#vertices - \#edges + \#faces = m + n - h + r\,,$$

so the genus of F is uniquely determined by h, m and the partition.

$$g(\Sigma) = \frac{h - m - n - r + 2}{2}$$

2.3.3. Vertical and Horizontal Faces

Definition 2.3.8. Let $\Sigma = (\sigma_q : \ldots : \sigma_0)$ be an arbitrary cell of bidegree (p, q). The j^{th} **vertical face** of Σ is obtained by removing the j^{th} permutation, where $0 \le j \le q$:

$$d'_j(\sigma_q : \ldots : \sigma_0) = (\sigma_q : \ldots : \widehat{\sigma_j} : \ldots : \sigma_0)$$

and this translates into the inhomogeneous notation as follows.

$$d'_j(\tau_q \mid \ldots \mid \tau_1) = \begin{cases} (\tau_q \mid \ldots \mid \tau_2) & j = 1 \\ (\tau_q \mid \ldots \mid \tau_i\tau_{j-1} \mid \ldots \mid \tau_1) & 1 < j < q \\ (\tau_{q-1} \mid \ldots \mid \tau_1) & j = q \end{cases}$$

Imagining an inner cell as in Figure 2.10, we collapse the j^{th} vertical stripe of the corresponding parallel slit domain. Collapsing the i^{th} horizontal stripe corresponds to a face map in the multisimplex $\Delta^{p_1} \times \ldots \times \Delta^{p_r}$. For our techniques, it is convenient to group these face maps using the corresponding partition $[p]$. Consequently, we will speak of the i^{th} horizontal face where $i \in [p]$. Before going into the details, one might take a look at Figure 2.13.

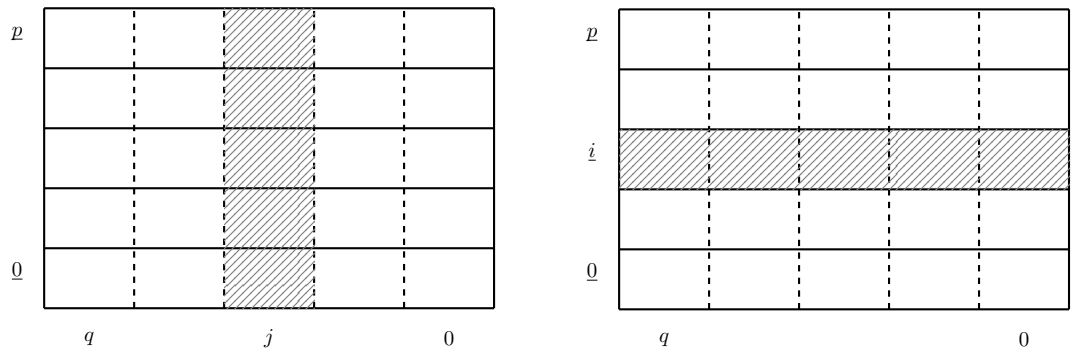

Figure 2.13.: The vertical and horizontal face operators.

Definition 2.3.9. Let $i \in [p]$. The i^{th} **horizontal face** of Σ is

$$d_i''(\Sigma) = (D_i(\sigma_q), \ldots, D_i(\sigma_0))\,,$$

where $D_i \colon \mathfrak{S}_{[p]} \longrightarrow \mathfrak{S}_{[p-1]}$ removes the symbol i from its cycle in σ (recall Definition A.3).

We usually omit the simplicial degeneracy and face maps since they only rename the symbols used. Hence we write

$$D_i(\sigma) = (i\ \sigma(i)) \cdot \sigma \qquad \text{or} \qquad D_i(\sigma) = \sigma \cdot (\sigma^{-1}(i)\ i)\,.$$

From this observation, we can easily derive a formula for the inverse of $D_i(\sigma)$, since

$$D_i(\sigma)^{-1} = ((i\ \sigma(i)) \cdot \sigma)^{-1} = \sigma^{-1} \cdot (i\ \sigma(i)) = D_i(\sigma^{-1}).$$

The next proposition reformulates the definition of the horizontal faces for the inhomogeneous notation. Using Figure 2.12 it is not hard to come up with the right idea.

Proposition 2.3.10. *Let $\Sigma = (\tau_q \mid \ldots \mid \tau_1)$ be an inner cell with homogeneous representation $(\sigma_q : \ldots : \sigma_0)$ and let $0_k < i < p_k$ for some k. Then the i^{th} horizontal face is*

$$d_i''(\Sigma) = (\tau_q'' \mid \ldots \mid \tau_1'')\,,$$

where

$$\tau_k'' = D_i(\ \tau_k \cdot (i\ \sigma_{k-1}(i))\ ) \qquad \textit{for} \qquad 1 \leq k \leq q\,.$$

In particular

$$\tau_k'' = D_i(\tau_k) \qquad \textit{if} \qquad i \notin \operatorname{supp}(\tau_k)\,.$$

Proof. For readibility, write $\rho_k = \tau_k \cdot (i\ \sigma_{k-1}(i))$. First note that

$$d_i''(\Sigma) = (D_i(\sigma_q) : \ldots : D_i(\sigma_0)) = (D_i(\sigma_q) \cdot D_i(\sigma_{q-1})^{-1} \mid \ldots \mid D_i(\sigma_1) \cdot D_i(\sigma_0)^{-1})\,.$$

Hence it suffices to show that

$$D_i(\sigma_k) \cdot D_i(\sigma_{k-1})^{-1} = D_i(\rho_k)$$

holds for each $k = 1, \ldots, q$. We have

$$D_i(\rho_k) = (i\ \rho_k(i)) \cdot \rho_k$$

and using $\tau_k = \sigma_k \cdot \sigma_{k-1}^{-1}$ its clear that $\rho_k(i) = \sigma_k(i)$, so we are left with

$$\begin{aligned} &= (i\ \sigma_k(i)) \cdot \sigma_k \cdot \sigma_{k-1}^{-1} \cdot (i\ \sigma_{k-1}(i)) \\ &= D_i(\sigma_k) \cdot D_i(\sigma_{k-1})^{-1}\,. \end{aligned}$$

□

2.3.4. The Parallel Slit Complex

Fixing the genus g, the number of punctures m, the number of boundary curves n and the ordered partition $r = r_1 + \ldots + r_n$, we are ready to define the parallel slit complex $P = P(h, m; r_1, \ldots, r_n)$.

Definition 2.3.11. Let $P_{p,q}$ be freely generated by all cells Σ on r levels of bidegree (p, q) such that the conditions

(i) $N(\Sigma) \leq h$,

(ii) $m(\Sigma) \leq m$,

(iii) $n(\Sigma) \leq n$,

(iv) Σ is connected and

(v) the levels of Σ are ordered ascendingly with respect to $(r_1, \ldots, r_n)$.

are fulfilled. A cell $\Sigma \in P$ is said to be **non-degenerate** with respect to the moduli space $\mathfrak{M}_{g,n}^m$ and the partition $(r_1, \ldots, r_n)$ if it is a connected inner cell and has exactly n boundary cycles, m punctures and norm h. All other cells in P are called **degenerate**. Observe that cells $\Sigma \notin P$ are neither degenerate nor non-degenerate with respect to $\mathfrak{M}_{g,n}^m$ and $(r_1, \ldots, r_n)$.

The **vertical boundary operator** is the alternating sum of the vertical faces

$$\partial' = \sum_{i=0}^{q} (-1)^i d_i'$$

and the **horizontal boundary operator** is the alternating sum of the horizontal faces

$$\partial'' = \sum_{j=0}^{p} (-1)^j d_j''\,.$$

The double complex $(P(h, m; r_1, \ldots, r_n), \partial', \partial'')$ is the **parallel slit complex** with respect to the moduli space $\mathfrak{M}_{g,n}^m$ and the partition $r = r_1 + \ldots + r_n$.

Remark 2.3.12. Recall that the horizontal boundary operator is the alternating sum over all face maps in $\Delta^{p_1} \times \ldots \times \Delta^{p_r}$. Hence P is indeed a semi-multisimplicial complex although we are mostly concerned with the associated bicomplex, which we denote by P as well.

Remark 2.3.13. Observe that every face $d'_0(\Sigma)$, $d'_q(\Sigma)$, $d''_{\underline{0}_k}(\Sigma)$ and $d''_{\underline{p}_k}(\Sigma)$ of a non-degenerate cell $\Sigma \in P_{p,q}$ is degenerate. Observe further that all faces of a degenerate cell remain degenerate.

Summing up the construction, we obtain the following theorem.

Theorem 2.3.14. *The parallel slit complex P is a semi-multisimplicial complex and the degenerate cells consitute a subcomplex P'. The space of parallel slit domains $\mathfrak{Par}^m_{g,n}[(r_1, \ldots, r_n)]$ is the complement of $|P'|$ inside $|P|$.*

Recall the construction of the Hilber uniformization in Section 2.1

$$\mathcal{H} \colon \mathfrak{H}^m_{g,n}[(r_1, \ldots, r_n)] \longhookrightarrow |P| \,.$$

Its corestriction to $\mathfrak{Par}^m_{g,n}[(r_1, \ldots, r_n)] = |P| - |P'|$ is a homeomorphism due to [Böd90a]. Therfore, $\mathfrak{Par}^m_{g,n}[(r_1, \ldots, r_n)] \simeq \mathfrak{M}^m_{g,n}$ serves as a good model for the corresponding mapping class group $\Gamma^m_{g,n}$:

Theorem 2.3.15. *The space of parallel slit domains $\mathfrak{Par}^m_{g,n}[(r_1, \ldots, r_n)] = |P| - |P'|$ is a manifold of dimension $3h$ in the finite, semi-bisimplical complex (P, P'). By Poincaré duality*

$$H_*(\mathfrak{M}^m_{g,n}; \mathbb{Z}) = H_*(\mathfrak{Par}^m_{g,n}[(r_1, \ldots, r_n)]; \mathbb{Z}) \cong H^{3h-*}(P, P'; \mathcal{O})$$

where $\mathcal{O}$ are the orientation coefficients.

2.4. The Bundle $\mathfrak{H}^\bullet_g(m, n)$

In this section, we want to outline the construction of the bundle $\mathfrak{H}^\bullet_g(m, n)$ over the moduli space $\mathfrak{M}^\bullet_g(m, n)$. For further details, see [Böd06].

Let $[F, \mathcal{C}^+, \mathcal{C}^-, \mathcal{P}] \in \mathfrak{M}^\bullet_g(m, n)$ be a point of the moduli space, using the same notation as in the introduction (Section 2.1). In order to describe the fiber over this point, we proceed as follows. By classical potential theory, e.g. [Tsu59, Theorem I.25], there exists a **harmonic potential** $u \colon F \longrightarrow \mathbb{R}$ without any singularities and with all critical points in the interior of F. The potential u is uniquely determined by the complex structure and by the conditions that

(i) on each boundary curve C^+_k and C^-_k, u is constant and non-negative, and

(ii) for each outer boundary curve C^+_k, the constant value is 0.

Thereby, we can only choose the constant value of u on one kind of boundary curves. Here, it will be on the outgoing ones. On the incoming boundaries, the potential u yields constants $c_k > 0$ such that $u(C^-_k) = c_k$.

Similar as in the parallel case, we construct the unstable critical graph $\mathcal{K}_0$ of the negative gradient flow $-grad_u$. Again calling the zeroes $\mathcal{S}$ of the gradient flow **stagnation points**,

note that each flow line leaving a stagnation point S either goes to another stagnation point or to a point $Q^+ \in \mathcal{C}^+$ in the outer boundary. These points shall be called **cut points**, and the set of all cut points is denoted by $\mathcal{Q}^+$. In Figure 2.14, we see an example for a surface with $n = 2$ incoming boundaries, $m = 1$ outgoing boundaries and $g = 0$. Some lines of the gradient flow are indicated in blue, whereas the unstable flow lines, which are used to build up the critical graph, are drawn bold. For reasons of clarity, only the critical flow line is drawn on the backside of the surface.

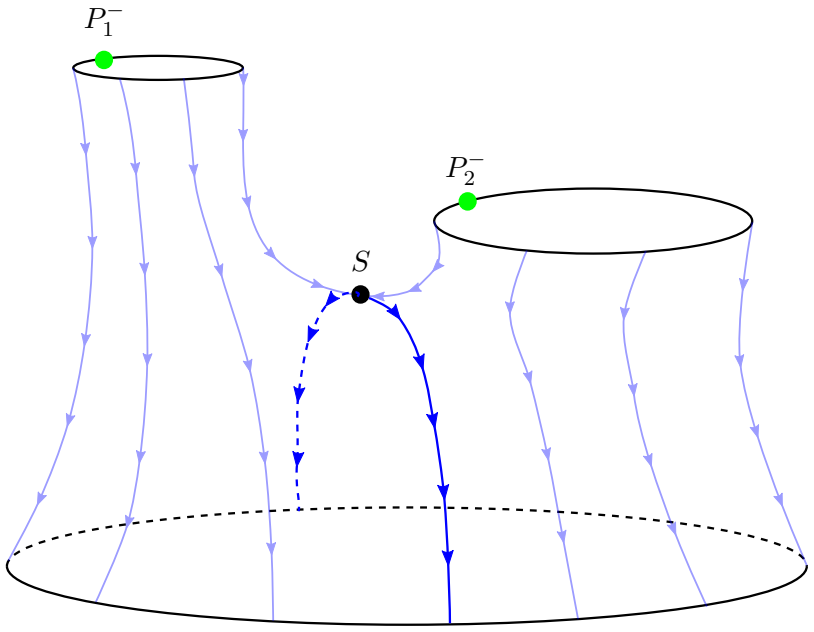

Figure 2.14.: The gradient flow of a potential function on a surface with $n = 2$, $m = 1$ and $g = 0$.

Since u is locally the real part of a holomorphic function, the stagnation points $S \in \mathcal{S}$ are saddle points of some index $-2h \leq \mathrm{ind}(S) \leq -1$. The sum of these indices has to equal the Euler characteristic $\chi(F) = -h$, thus we can conclude that there are at most h stagnation points.

The vertices of the unstable critical graph are the points in $VK_0 = S \cup \mathcal{Q}^+$. The (directed) edges of the unstable critical graph correspond to the (directed) unstable flow lines only. It is possible that $\mathcal{K}_0$ is empty, namely when F is an annulus. Note that every component of the complement of the critical graph in F contains exactly one boundary curve. Hence, we can write $F_1, \ldots, F_n$ for the components of $F \backslash \mathcal{K}_0$, which we also call **basins**. Since the gradient vector field does not have any singularities, we obtain a deformation retraction of F_k onto C_k^- by running the flow lines backwards.

In Figure 2.15, our surface from Figure 2.14 is looked at from above and dissected along the unstable critical graph, yielding one basin for each of the two incoming boundary curves.

On each basin F_k, the harmonic function $u_k = u\,|_{F_k} \colon F_k \longrightarrow \mathbb{R}$ is the real part of a holomorphic function

$$w_k = u_k + iv_k \colon F_k \longrightarrow \mathbb{C}\,,$$

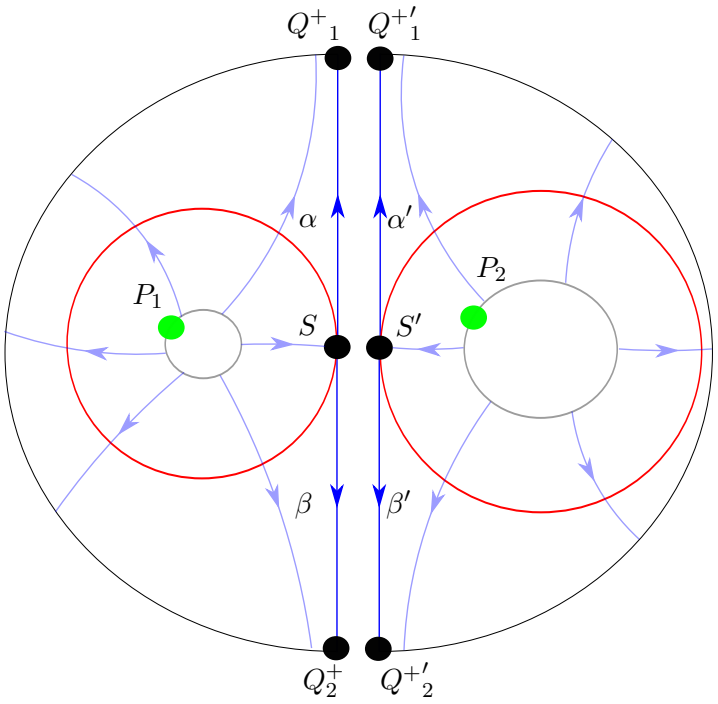

Figure 2.15.: The surface with $n = 2$, $m = 1$ and $g = 0$ of Figure 2.14 looked at from above, dissected along the unstable critical graph.

where v_k is a harmonic conjugate of u_k. The function v_k is only defined up to integer multiples of $2\pi i$, but after this it is unique up to an additive constant d_k. This we fix soon. Thus, the function

$$W_k(z) = \exp(-w_k(z)) = \exp(-u_k(z)) \exp(-iv_k(z)) \colon F_k \longrightarrow\subset \mathbb{C}$$

is well defined and maps F_k injectively into an annulus $\mathbb{A}_k$. By this, the modulus is determined by u_k and the angle by v_k. Since $\exp(-u(z))$ equals 1 when restricted to any outer boundary curve C_l^+ incident to F_k and $\rho_k := \exp(-c_k) < 1$ when restricted to C_k^-, the image of F_k under W_k is contained in an annulus $\mathbb{A}_k$ with outer radius 1 and inner radius $\rho_k < 1$. The additive constant d_k in the definition of the harmonic conjugate v_k of u_k can be chosen such that the marked point P_k on the incoming boundary curve Q_k^- is mapped to the real point $(\rho_k, 0)$ of the annulus. The image of $F_k \subset \mathbb{A}_k$ consists of the entire annulus, where finitely many slits from the outer boundary towards the center of the annulus are missing. Remembering that the surface originally was glued together along these missing slits, we can reconstruct the surface F from the image of the basins F_k on the annuli $\mathbb{A}_k$. A more detailed description of these so-called radial slit domains follows in Section 2.5.

We are now ready to finish the description of the bundle $\mathfrak{H}_g^\bullet(m,n)$. Let $\mathfrak{H}_g^\bullet(m,n)$ be the space of all

$$[F, \mathcal{C}^+, \mathcal{C}^-, \mathcal{P}, w]\,.$$

As above, $[F, \mathcal{C}^+, \mathcal{C}^-, \mathcal{P}] \in \mathfrak{M}_g^\bullet(m,n)$ is a point in the moduli space and $w = (u, (v_k)_{k=1,\dots,n})$ with $u \colon F \longrightarrow \mathbb{R}$ being the harmonic potential defined on the whole surface F, and the

functions $v_k \colon F_k \longrightarrow \mathbb{R}$ being locally defined harmonic conjugates of u on the basins F_k, for $k = 1, \ldots, n$. There is a projection

$$\mathfrak{H}_g^\bullet(m,n) \xrightarrow{\cong} \mathfrak{M}_g^\bullet(m,n)\,, [F, \mathcal{C}^+, \mathcal{C}^-, \mathcal{P}, w] \longmapsto [F, \mathcal{C}^+, \mathcal{C}^-, \mathcal{P}]\,,$$

with trivial fibres since there are no free parameters in the choice of u and v_k. Thus, the dimension of $\mathfrak{H}_g^\bullet(m,n)$ equals

$$\dim(\mathfrak{H}_g^\bullet(m,n)) = \dim(\mathfrak{M}_g^\bullet(m,n)) = 3h + n = 6g - 6 + 3m + 4n\,.$$

2.5. The Radial Slit Complex

We will now construct the radial slit complex (R, R') associated with the moduli space $\mathfrak{M}_g^\bullet(m,n)$. Recall that we have defined a homeomorphism $\mathfrak{H}_g^\bullet(m,n) \xrightarrow{\cong} \mathfrak{M}_g^\bullet(m,n)$ (compare Section 2.4). There is a space $\mathfrak{Rad}_g(m,n)$ of radial slit configurations, which is homeomorphic to $\mathfrak{H}_g^\bullet(m,n)$ and can be defined as the geometric realization of the difference $R - R'$ of the multicomplex R and its subcomplex R'. The latter are described in this section. Like the parallel slit complex (P, P'), (R, R') is only a semi-multisimplicial complex. In contrast to $\mathfrak{H}_g^\bullet(m,n)$, it has a purely combinatorical description. Hence, it is very suitable for determining the homology of

$$\begin{aligned} H_*(\mathfrak{M}_g^\bullet(m,n);\mathbb{Z}) &= H_*(\mathfrak{H}_g^\bullet(m,n);\mathbb{Z}) \\ &\cong H^{3h+n-*}(\mathfrak{H}_g^\bullet(m,n);\mathcal{O}) = H^{3h+n-*}(\mathfrak{Rad}_g(m,n);\mathcal{O}) = H^{3h+n-*}(R,R';\mathcal{O}) \end{aligned}$$

via a computer program. Here, the isomorphism is given by Poincaré duality and $\mathcal{O}$ is the orientation system, for which a simplicial definition is provided in Section 2.6.

If not stated otherwise, the genus g, the number of outgoing boundaries m and the number of incoming boundary curves n are fixed throughout this section. Be aware that these letters mean different things in the radial case than in the parallel case. Moreover, the partition $R = (r_1, \ldots, r_n)$ is always of the form $R = (1, \ldots, 1)$ here. Consequently, we have $r = n$ and can omit r as well as the paritition R. Hence, $[p]$ always denotes the set

$$[p] = \{\underline{0}_1, \underline{1}_1, \ldots, \underline{p}_1, \ldots, \underline{0}_n, \underline{1}_n, \ldots, \underline{p}_n\}\,,$$

in the radial case, where $p = p_1 + \ldots + p_n$ is a partition of p into n levels with all p_i positive (compare Definition 2.3.1 for the meaning of $[p]$ in the parallel case). As before, we write $h = 2g + m + n - 2$ in contrast to the formula for h in the parallel case.

Recall the definition of the fibre over a point $[F, \mathcal{C}^+, \mathcal{C}^-, \mathcal{P}] \in \mathfrak{M}_g^\bullet(m,n)$ in the homotopy equivalent bundle $\mathfrak{H}_g^\bullet(m,n)$ over $\mathfrak{M}_g^\bullet(m,n)$ in Section 2.4. We ended up with a function

$$W_k = \exp(-u_k)\exp(-iv_k) \colon F_k \longrightarrow \mathbb{A}_k \subset \mathbb{C}$$

for each $k = 1, \ldots, n$. This maps the basin F_k into an annulus $\mathbb{A}_k$ with inner radius $\rho_k < 1$ and outer radius 1, filling the annulus up to some missing slits. We shall now give a more detailled discription of the image of the maps W_k for $k = 1, \ldots, n$, which we call a **radial slit picture** (see Figure 2.16).

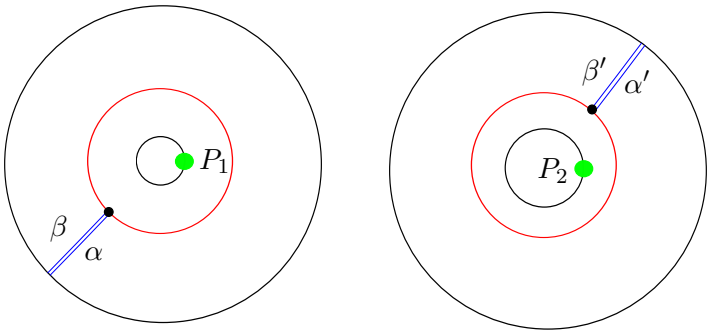

Figure 2.16.: The surface of Figures 2.14 and 2.15 with $n = 2$, $m = 1$ and $g = 0$ mapped into two annuli via W_1 and W_2.

The n annuli $\mathbb{A}_1, \dots, \mathbb{A}_n$ are called the annuli or level upon which the radial slit picture resides. The k^{th} incoming boundary curve of the surface F is mapped to the inner boundary cycle of the k^{th} annulus, and the marked point P_k on the incoming boundary curve C_k^- is mapped to the point $(\rho_k, 0)$ on this cycle. Thus we use to refer to the inner boundary cycle of the k^{th} annulus as its k^{th} inner boundary.

When we delete an edge of the unstable critical graph from F, we obtain, on either side, a bank still belonging to F. Each of these banks may belong to a different basin. After all maps W_k are applied to the basins F_k, the deleted edges of the critical graph yield missing slits on the annuli. Thereby, the banks belonging to the same edge may be seperated from each other. Since there are at most h stagnation points (compare 2.4) and each of them results in at most two missing slits, there are at most $2h$ missing slits on the annuli in total. Note that the endpoints of the slits lie anywhere on the annuli apart from their inner and outer boundary cycles.

An outer boundary curve C_l^+ of F is mapped to the outer boundary cycles of the annuli $\mathbb{A}_1, \dots, \mathbb{A}_n$, however not necessarily consecutive or even on one annulus only. While traversing C_l^+ in the surface F, one occasionally meets a cut point Q^+. In particular, this cut point is one endpoint of an edge of the unstable critical graph, so the two banks of this edge may be seperated as described above. But if we start at an arbitrary point of the image of C_l^+ under some map W_k, we can run through the entire image of C_l^+ under any map W_k in the annuli $\mathbb{A}_1, \dots, \mathbb{A}_n$. Thereby, we have to jump across paired slits whenever they are met. We thus refer to these parts of the outer boundary of all annuli $\mathbb{A}_1, \dots, \mathbb{A}_n$ as the outer boundary curve of our radial slit picture. In Figure 2.16, we can run through the single outer boundary curve along the outer boundary of the annuli clockwise if we jump from α to α' and from β' to β on our way.

By adding equipotential lines through the stagnation points, we obtain $0 \leq q \leq h$ concentrical lines on each annulus $\mathbb{A}_k$. Extending the lines of the slits towards the inner and outer boundary of $\mathbb{A}_k$, we obtain a subdivision of each annulus into regions.

This completes our description of a radial slit picture. Vice versa, the surface F can be obtained from the radial slit picture. We can re-glue previously connected basins along the missing slits in order to re-construct the surface F. Note that the resulting surface is the same if slits move in the annuli, or even if smaller slits jump across larger slits. Thus, such radial slit pictures are considered as equal.

In order to obtain a multisimplicial description of these radial slit pictures, we will normalize them in the following subsection, resulting in a new structure called cell. Note that two regions are only glued together if they lie in the same concentrical stripe of any annulus (maybe on two different annuli). Hence, we can express the glueing via one permutation $\sigma_j \in \mathfrak{S}_{[p]}$ per concentrical stripe $0 \leq j \leq q$, where $[p]$ is the set

$$[p] = \{\underline{0}_1, \underline{1}_1, \ldots, \underline{p}_1, \ldots, \underline{0}_n, \underline{1}_n, \ldots, \underline{p}_n\},$$

which denotes the radial segments of the k^{th} annulus by $\underline{0}_k, \ldots, \underline{p}_k$. In the Subsections 2.5.1 and 2.5.2, we will see how exactly this defines the cells $\Sigma = homogq$ of the relative multicomplex (R, R'), using two different perspectives.

The positions of the slits define an inner point of the multisimplex $\Delta^p \times \Delta^q$. Collapsing concentrical stripes and radial segments defines vertical and horizontal faces of the cells, see Subsection 2.5.3. After this preparation, we can introduce the radial slit complex (R, R') in Subsection 2.5.4.

2.5.1. Radial Cells in Homogeneous Notation

Recall Definition 2.3.2.

Definition 2.5.1. (Definition 2.3.2) Using the **homogeneous notation**, a combinatorial cell of bidegree (p, q) with respect to the partition $[p]$ is a $(q+1)$-tuple of permutations $\sigma_j \in \mathfrak{S}_{[p]}$

$$\Sigma = (\sigma_q : \ldots : \sigma_0).$$

Most of the time we refer to Σ as a cell on n levels, leaving the partition $[p]$ unmentioned.

Note that this definition of a cell still makes sense in the radial case. An inner cell, however, is defined differently now.

Definition 2.5.2. A cell $\Sigma = (\sigma_q : \ldots : \sigma_0)$ of bidegree (p, q) is called **radial inner cell** if it satisfies the following conditions:

(i) The zero$^{\text{th}}$ permutation σ_0 is fixed to be the levelwise cyclic permutation

$$\sigma_0 = (\underline{0}_1\ \underline{1}_1\ \ldots\ \underline{p}_1) \ldots (\underline{0}_n\ \underline{1}_n\ \ldots\ \underline{p}_n).$$

(ii) For every $0 \leq i < q$, the permutations σ_i and σ_{i+1} are distinct.

(iii) There is no symbol $\underline{0}_k \leq \underline{j}_k < \underline{p}_k$ that is mapped to its successor $\underline{j+1}_k$ by all permutations σ_i.

Note that the difference of a radial inner cell to a parallel inner cell is that the symbols $\underline{p}_k$ do not necessarily have to be mapped to $\underline{0}_k$ by each permutation σ_j. Therefore, every parallel inner cell can be viewed as a radial inner cell, and every radial inner cell, which is not a parallel cell, is the $\underline{0}_k^{\text{th}}$ face of a parallel inner cell of bidegree $(p+1, q)$.

A radial cell of bidegree (p, q) on n levels with respect to the partition $[p]$ is represented geometrically by a **radial slit annulus** in the following way.

Let $\mathbb{A}_1, \ldots, \mathbb{A}_n \subset \mathbb{C}$ be annuli in distinct complex planes. Each annulus $\mathbb{A}_k$ shall be centered at 0, having outer radius 1 and inner radius r_k for fixed $0 < r_k < 1$. Introduce

p_k+1 equally sized radial segments on the annulus $\mathbb{A}_k$, numbered clockwise by the symbols $\underline{0}_k, \ldots, \underline{p}_k$. To normalize the numeration, we require that the line preceding the 0^{th} segment $\underline{0}_k$ in clockwise ordering lies on the positive real line. Furthermore, we introduce $q+1$ concentrical, equidistant stripes on each annulus. The 0^{th} stripe is incident to the inner boundary of the annulus, and all other stripes are numbered with the symbols $1, \ldots, q$ towards the outer boundary.

This way we obtain a subdivision of each annulus $\mathbb{A}_k$ into $(q+1)(p_k+1)$ regions with coordinates $(j, \underline{i})$, where $\underline{i} \in \{\underline{0}_k, \ldots, \underline{p}_k\}$ and $j \in \{0, \ldots, q\}$. As in the parallel case, we obtain a surface by performing identifications within the set of the j^{th} stripes on each annuli, for each $j = 0, \ldots, q$. By this, the line segment preceding a region $(j, \underline{i})$ is glued with the line segment succeeding the region $(j, \sigma_j(\underline{i}))$, see Figure 2.17. It is possible that the two regions lie on two different annuli.

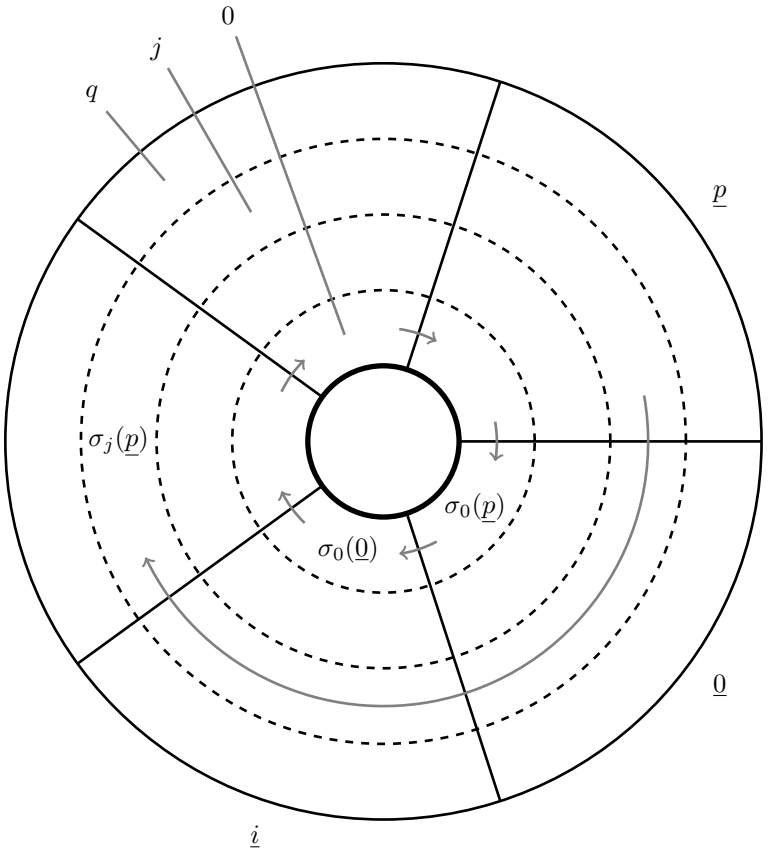

Figure 2.17.: The homogeneous representation of a radial cell.

Note that we have reversed the process described in 2.4 and at the beginning of this Subsection. The surface resulting from glueing has n incoming boundary curves arising from the n inner circles of the annuli. On each inner boundary, there is a marked point corresponding to the point $(R_k, 0)$ on the k^{th} annulus. The cycles of σ_q yield the outgoing boundary curves of the surface, which do not have a specific order. If we require the cell Σ to be connected as in Definition 2.3.4, the resulting surfaces will also be connected.

2.5.2. Radial Cells in Inhomogeneous Notation

Like a parallel inner cell, a radial inner cell can be expressed in **inhomogeneous notation** by writing

$$\Sigma = (\tau_q \mid \ldots \mid \tau_1)\,,$$

where $\tau_j = \sigma_j \cdot \sigma_{j-1}^{-1}$ for $j = 1, \ldots, q$. One should be cautious about the permutations τ_j. Whereas, in the parallel case, we could assume the τ_j to act on the symbols $[p] - \{0_k \colon 1 \leq k \leq n\}$ only, we cannot do this here since we do not require that $\underline{p}_k$ is mapped to $\underline{0}_k$ by each permutation σ_j. Therefore, the symbols $\underline{0}_k$ might be permuted non-trivially by some $\sigma_j \cdot \sigma_{j-1}^{-1}$, but they might be fixpoints of each transposition τ_j as well. We receive permutations $\tau_q, \ldots, \tau_1$ on the whole set of symbols $[p]$. Using this notation, we obtain an equivalent way to state Definition 2.5.2.

Definition 2.5.3. A combinatorial cell of bidegree (p, q) with respect to the partition $[p]$ written in **inhomogeneous notation** is a q-tuple of permutations

$$\Sigma = (\tau_q \mid \ldots \mid \tau_1)\,,$$

where each τ_j acts on the set of symbols $[p]$. It is a **radial inner cell** if satisfies the following conditions:

(i) Every permutation $\tau_q, \ldots, \tau_1$ is non-trivial.

(ii) The set of common fixed points of the permutations $\tau_q, \ldots, \tau_1$ is a subset of $\{\underline{0}_1, \ldots, \underline{0}_r\}$.

(iii) The permutations $\tau_q, \ldots, \tau_1$ do not have any fixed point in common.

Similar as in the parallel case, we draw inhomogeneous radial cells like in Picture 2.18. There could also be a slit on the positive real line, and there could be more than one slit per symbol. Again, the inhomogeneous picture of a radial cell reveals how tours around the stagnation points look like.

In order to finish a full combinatorial description for a point in the bundle $\mathfrak{H}_g^\bullet(m, n)$, we need to encode the numbers of incoming and outgoing boundaries, rewriting Definition 2.3.6 for the radial case.

Definition 2.5.4. Consider an arbitrary radial cell $\Sigma = (\sigma_q : \ldots : \sigma_0)$ of bidegree (p, q).

(i) The **number of incoming cycles** of Σ is defined to be the number $n(\Sigma)$ of annuli, on which Σ is defined, and thus equals the number of cycles of σ_0.

(ii) The **number of outgoing cycles** of Σ is defined to be the number

$$m(\Sigma) = \mathrm{ncyc}(\sigma_q)$$

of cycles of the permutation σ_q, including fixpoints.

(iii) The **norm** of Σ is

$$N(\Sigma) = N(\sigma_q \sigma_{q-1}^{-1}) + \ldots + N(\sigma_1 \sigma_0^{-1})\,,$$

where N measures the word length in the symmetric group $\mathfrak{S}_{[p]}$ with respect to the set of all transpositions.

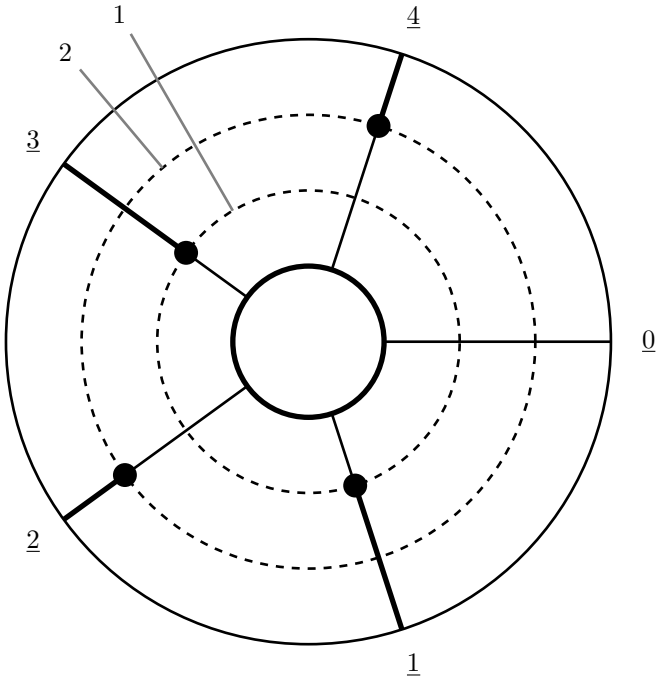

Figure 2.18.: The inhomogeneous representation of the radial cell $\Sigma = ((\underline{4}, \underline{2}) \mid (\underline{3}, \underline{1}))$ with $N(\Sigma) = 2$, $n(\Sigma) = 1$, $m(\Sigma) = 1$.

With this definition, the number of inner and outer boundary curves of a radial cell Σ coincides with the number of the surface resulting from the glueing process described in Subsection 2.5.1.

Remark 2.5.5. Recall that, for a parallel inner cell $\Sigma = (\sigma_q : \ldots : \sigma_0)$, the permutation σ_q is supposed to have $m + n$ cycles instead of m, see Definition 2.3.3. This occures because, in the parallel case, only m of these $m + n$ cycles of σ_q correspond to the m punctures of the resulting surface and the remaining cycles, which contain at least one symbol $\underline{0}_k$, correspond to the n boundary curves of the surfaces. But in the radial case, all the cycles of σ_q correspond to the m outgoing boundary curves of the surface resulting from glueing Σ.

Note that we can read off the Euler characteristic and the genus of the surface from the cell.

Proposition 2.5.6. *Let $\Sigma = (\sigma_q : \ldots : \sigma_0)$ be a radial inner cell with $m(\Sigma) = m$, $n(\Sigma) = n$ and $N(\Sigma) = h$. Then the Euler characteristic of the surface F resulting from glueing Σ according to the permutations σ_j equals*

$$\chi(F) = -h = -2g + 2 - m - n\,.$$

Proof. Note that the slits and the concentrical lines of Σ yield an embedded graph $\mathcal{K}_0 \subset F$, the unstable critical graph. The vertices correspond to the cut points $\mathcal{Q}^+$ on the outgoing boundaries and to the stagnation points $\mathcal{S}$. On the j^{th} equipotential line, all stagnation

points are connected by a cycle and there are $N(\tau_j)$ edges connecting stagnation points to the outgoing boundaries. The number of faces of $\mathcal{K}_0$ equals n.

Since we want to use this embedded graph for determining the Euler characteristic, we would like it to be connected with contractible faces. In order to obtain a connected graph, we add edges around the outgoing boundary curves. After having done so, there is one additional edge for each cut point Q^+. If we additionally introduce one vertex per incoming boundary C_k^-, together with one loop around C_k^- and one edge connecting it to some vertex of the critical graph (without introducing any crossings), each face of the resulting graph is contractible and the number of faces remains n. Hence, the Euler characteristic of F is given by

$$\begin{aligned}\chi(F) &= \#vertices - \#edges + \#faces \\ &= |\mathcal{Q}^+| + |\mathcal{S}| + n - (|\mathcal{S}| + h + |\mathcal{Q}^+| + 2n) + n \\ &= -h\,.\end{aligned}$$

□

Corollary 2.5.7. *Let $\Sigma = (\sigma_q : \ldots : \sigma_0)$ be a radial inner cell with $m(\Sigma) = m$, $n(\Sigma) = n$, $N(\Sigma) = h$. Then, the genus of the surface F resulting from glueing Σ according to the permutations σ_j equals*

$$g(\Sigma) = \frac{h - m - n + 2}{2}\,.$$

2.5.3. Faces

Using the same formulas as in parallel case (see Definitions 2.3.8 and 2.3.9), we define **vertical** and **horizontal faces** for radial cells Σ of bidegree (p, q). In particular, note that Proposition 2.3.10 also holds for radial inner cells. Geometrically, the j^{th} vertical face of Σ arises from Σ by deleting its j^{th} concentrical stripe, for $j \in \{0, \ldots, q\}$. The $\underline{i}^{\text{th}}$ horizontal face arises by deleting the $\underline{i}^{\text{th}}$ radial segment for $\underline{i} \in [p]$ (see Figure 2.19).

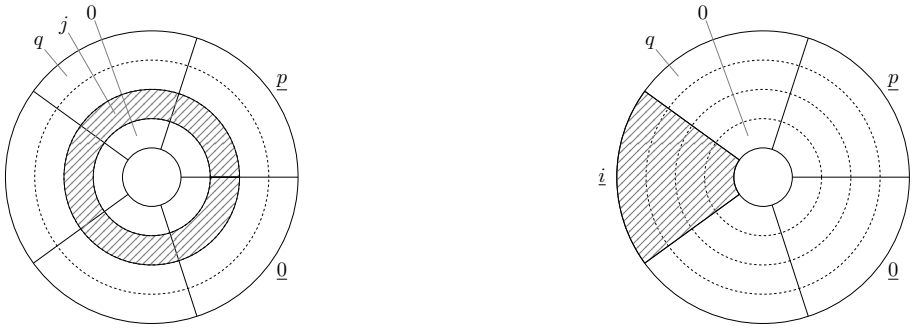

Figure 2.19.: The vertical and horizontal face operators.

2.5.4. The Radial Slit Complex

Write $h = 2g - 2 + m + n$. We are finally able to introduce the **radial slit complex**, a relative finite multisimplicial complex (R, R'), whose homology is just the homology of the

moduli space $\mathfrak{M}_g^\bullet(m,n)$. As a first step, define a complex $R = R(g,m,n)$ with possibly non-zero modules $\overline{R}_{p,q}$ in bidegree (p,q) for each $1 \leq p \leq 2h$ and $1 \leq q \leq h$. Similar to the parallel case, the module $R_{p,q}$ is freely generated over $\mathbb{Z}$ by all those radial cells $\Sigma = (\sigma_q, \ldots, \sigma_0)$ of bidegree (p,q) with

(i) $N(\Sigma) \leq h$,

(ii) $m(\Sigma) \leq m$,

(iii) $n(\Sigma) \leq n$.

A cell $\Sigma \in R_{p,q}$ is called **non-degenerate** with respect to $\mathfrak{M}_g^\bullet(m,n)$ if it is a connected inner radial cell that fulfills each of the above conditions with equality. All other cells in $R_{p,q}$ are called **degenerate**.

As in the parallel case, the vertical respectively horizontal boundary operator of a radial cell in R is given by the alternating sum of its horizontal respectively vertical faces. Again, faces of degenerate radial cells and the 0^{th} vertical face of a non-degenerate radial cell are always degenerate. But now the $\underline{0}_k^{\text{th}}$ and $\underline{p}_k^{\text{th}}$ horizontal face of a radial cell Σ is not necessarily degenerate since the condition that all $\underline{p}_k$ have to be mapped to $\underline{0}_k$ by each σ_q is dropped for radial cells.

By construction, we have

Theorem 2.5.8. *The radial slit complex R is a semi-multisimplicial complex and the degenerate cells consitute a subcomplex R'. The space of radial slit domains $\mathfrak{Rad}_g(m,n)$ is the complement of $|R'|$ inside $|R|$.*

As in the parallel case, we have reviewed the Hilbert uniformization

$$\mathcal{H}\colon \mathfrak{H}_g^\bullet(m,n) \hookrightarrow |R|\,,$$

for which the restriction to $\mathfrak{Rad}_g(m,n) = |R| - |R'|$ is a homoeomorphism due to [Böd06]. Summarizing, we obtain

Theorem 2.5.9. *The space of radial slit domains $\mathfrak{Rad}_g(m,n) = |R| - |R'|$ is a manifold of dimension $3h+n$ in the finite, semi-multisimplical complex (P,P'). So by Poincaré duality*

$$H_*(\mathfrak{M}_g^\bullet(m,n);\mathbb{Z}) = H_*(\mathfrak{Rad}_g(m,n);\mathbb{Z}) \cong H^{3h+n-*}(R,R';\mathcal{O})\,,$$

where $\mathcal{O}$ are the orientation coefficients.

2.6. The Orientation System

Let $\mathfrak{M}$ denote the moduli space $\mathfrak{M}_{g,r}^m$ or $\mathfrak{M}_g^\bullet(m,n)$ with fixed g, m, n, and possibly r, Let $\mathfrak{H}$ denote the corresponding bundle over $\mathfrak{M}$. For simplicity, we always use the letter P for the associated relative multisimplicial complex (P,P') instead of writing (R,R') in the radial case.

Since $\mathfrak{H}$ is non-orientable when $m > 1$, we need to use a local orientation system $\mathcal{O}$ to compute its homology via generalized Poincaré duality

$$H_*(\mathfrak{M};\mathbb{Z}) = H_*(\mathfrak{H};\mathbb{Z}) \cong H^{d-*}(\mathfrak{H};\mathcal{O}) = H^{d-*}(P,P';\mathcal{O})\,,$$

where $\mathcal{O}$ are the orientation coefficients and d denotes the dimension of $\mathfrak{H}$. We follow Mehner's approach to define the orientation system (see [Meh11, Chapter 3.7]) because it can be applied to the parallel case as well as to the radial case and because its implementation is a simple calculation (compare Subsubsection 6.3.2.5). In the following, we describe the idea of our orientation system, starting with the notion of orientation in the manifold $\mathfrak{H}$ and continuing with the bisemisimplicial orientation system for (P, P').

By $\tilde{\mathfrak{H}}$, we denote the orientable covering space of $\mathfrak{H}$ that arises from $\mathfrak{H}$ by numbering the m punctures in the parallel case, respectively the m outgoing boundary curves in the radial case. The symmetric group $\mathfrak{S}_m$ acts on $\tilde{\mathfrak{H}}$ by permuting the punctures respectively outgoing boundaries, with $\mathfrak{H} = \tilde{\mathfrak{H}}/\mathfrak{S}$. The elements of the alternating group $\mathfrak{A}_m \subset \mathfrak{S}_m$ are exactly those elements that act orientation-preserving, compare [Meh11, Chapter 3.4]. Hence, it is a simple exercise to see that the quotient $\overline{\mathfrak{H}} = \tilde{\mathfrak{H}}/\mathfrak{A}_m$ arising from $\tilde{\mathfrak{H}}$ is orientable. As an orientable twofold covering of $\mathfrak{H}$ with orientation reversing deck transformations, $\overline{\mathfrak{H}}$ is isomorphic to the orientation covering of $\mathfrak{H}$ and thus can be used to define an orientation system for $\mathfrak{H}$.

In order to perform explicit calculations, we need to see how this notion of orientation transfers to the bicomplex P. By $(\tilde{P}, \tilde{P}')$, we denote the relative bicomplex corresponding to $\tilde{\mathfrak{H}}$. Recall that, in the radial case, the m outgoing boundary curves of a surface correspond to the m cycles of the permutation σ_q belonging to a cell $\Sigma \in R$; while in the parallel case, the m punctures correspond to those m cycles of σ_q belonging to $\Sigma \in P$ that do not contain any symbol $\underline{0}_k$. Thus, a permutation of the punctures corresponds to a permutation of the cycles of σ_q, apart from the cycles containing some $\underline{0}_k$ in the parallel case. Hence, a cell $\tilde{\Sigma} \in \tilde{P}$ can be written as a pair $\tilde{\Sigma} = (\Sigma, \nu)$, where the function $\nu \colon [p] \longrightarrow \{0, \dots, m\}$ defines a numeration of the cycles, i.e.

(i) ν is invariant under σ_q,

(ii) ν induces a bijection
- $[p]/\sigma_q \longrightarrow \{0, \dots, m\}$ in the parallel case,
- $[p]/\sigma_q \longrightarrow \{1, \dots, m\}$ in the radial case, and

(iii) in the parallel case, we have $\nu(\underline{0}_k) = 0$ for all $k = 1, \dots, r$.

Note that the application of the vertical face operator d'_j to Σ leaves σ_q and hence ν invariant, for $j = 1, \dots, q-1$. Thus, the vertical boundary of $\tilde{P}$ is simply given by

$$\tilde{\partial}'_j = (\partial'_j(\Sigma), \nu)\,.$$

When the horizontal face operator d''_i is applied to Σ, $i \in [p]$, the symbol i is erased from its cycle in σ_q. We obtain a numeration of the cycles of $d''_i(\Sigma)$ by keeping the cycle numbers for all remaining symbols. This yields the formula

$$\tilde{\partial}''_i(\Sigma) = (\partial''_i(\Sigma), \nu \circ d_i^{\Delta})$$

after to renormalization. A cell $(\Sigma, \nu) \in \tilde{P}$ is degenerate if and only if $\Sigma \in P$ is degenerate, and $\tilde{P}' \subset \tilde{P}$ is the subset of degenerate cells.

Defining an orientation system for the bicomplex (P, P') means that we may need to alter the definition of the vertical and horizontal differentials by additional signs in order

to correct the change of orientation induced by permutations of the punctures or outgoing boundaries. To be precise, we choose a distinguished lift to $\tilde{P}$ for all cells of P. Considering some $\Sigma \in P$, we obtain a cell $\tilde{\Sigma} = (\Sigma, \nu)$ with a distinguished numeration ν of the cycles of σ_q. Then we apply any face operator d to Σ and, correspondingly, $\tilde{d}$ to $\tilde{\Sigma}$. As $\widetilde{d\Sigma}$ and $\tilde{d}(\tilde{\Sigma})$ lie in the same orbit under $\mathfrak{S}_m$, there is a permutation $\pi \in \mathfrak{S}_m$ that transforms the two different numerations of the cycles of σ_q into each other. Projecting everything down to the orientation covering $\overline{P}$, the projections of the two lifts $\widetilde{d\Sigma}$ and $\tilde{d}(\tilde{\Sigma})$ give two orientations of the cell $d(\Sigma)$. Therefore, the differential d is orientation preserving if and only if π is a permutation in the alternating group $\mathfrak{A}_m$. If d is orientation reversing, we correct this by using an additional sign in the differential for (P, P') depending on Σ. Thus we aim at defining differentials

$$\hat{\partial}' = \sum_{j=0}^{q} (-1)^j \varepsilon'_j(\Sigma) d'_j(\Sigma)$$

and

$$\hat{\partial}'' = \sum_{i \in [p]} (-1)^i \varepsilon''_i(\Sigma) d''_i(\Sigma)$$

on the cells of P, P' with signs $\varepsilon'_j, \varepsilon''_i \in \{\pm 1\}$ such that each face operator $\varepsilon'_j(\Sigma)d'_j(\Sigma)$ and $\varepsilon''_i(\Sigma)d''_i(\Sigma)$ preserves orientations.

Let us now see how the minimum symbols of the cycles of σ_q determine the distinguished lift.

Definition 2.6.1. Let $\Sigma = (\sigma_q : \ldots : \sigma_0) \in P$ be a cell in homogeneous notation. The **distinguished lifting** for Σ to $\tilde{P}$ is given by the cell $\tilde{\Sigma} = (\Sigma, \nu)$, where ν is defined by the following procedure:

(i) Decompose σ_q into disjoint cycles, yielding a decomposition
- $\sigma_q = \alpha_0 \ldots \alpha_m$ in the parallel case,
- $\sigma_q = \alpha_1 \ldots \alpha_m$ in the radial case.

(ii) Denote the minimum symbol of each cycle α_k by a_k.

(iii)
- In the parallel case, choose the indices $0, \ldots, m$ such that $a_0 < \ldots < a_m$,
- In the radial case, choose the indices $1, \ldots, m$ such that $a_1 < \ldots < a_m$.

(iv) For a symbol $i \in [p]$ belonging to cycle α_k, set $\nu(i) = k$.

Note that for $m = 1$, $\mathfrak{H}$ and $\tilde{\mathfrak{H}}$ coincide, and we can keep the differentials unchanged.

For the j^{th} vertical face operator, recall that $\tilde{d}'_j(\tilde{\Sigma})$ preserves the numeration ν, hence we can always set $\varepsilon'_j(\Sigma) = 1$. But already for $m = 2$, there are situations when the horizontal differential changes the orientation of a cell.

Example 2.6.2. Let $\Sigma \in P$ be a parallel cell on one level with $\sigma_q = (\underline{0}\ \underline{4})(\underline{1}\ \underline{3})(\underline{2})$. Then $\tilde{\Sigma}$ is given by Σ together with the distinguished numeration ν of the cycles

$$\begin{array}{cccccc} i & \underline{0} & \underline{1} & \underline{2} & \underline{3} & \underline{4} \\ \nu(i) & 0 & 1 & 2 & 1 & 0 \end{array}.$$

The application of the horizontal face operator $\tilde{d}''_{\underline{1}}$ erases the symbol $\underline{1}$ from σ_q and renormalizes the permutation. The new numeration of the cycles of $d''_1(\Sigma)$ is given by

$$\begin{array}{cccccc} i & \underline{0} & \underline{1} & \underline{2} & \underline{3} \\ \nu(i) & 0 & 2 & 1 & 0 \end{array}.$$

On the other hand, first applying $d''_{\underline{1}}$ to Σ and then lifting it to $\tilde{P}$ yields the distinguished numeration

$$\begin{array}{cccccc} i & \underline{0} & \underline{1} & \underline{2} & \underline{3} \\ \nu(i) & 0 & 1 & 2 & 0 \end{array}.$$

Hence the difference of the two permutations is the transposition (1 2), yielding $\varepsilon''_{\underline{1}}(\Sigma) = -1$ because this means that $d''_{\underline{1}}$ reverses orientations.

More generally, let $\Sigma \in P_{p,q}$ be an oriented parallel or radial cell together with the distinguished numeration ν of the cycles of σ_q. Consider $i \in [p]$. In the parallel case, we can assume that $i \neq \underline{0}_k, \underline{p}_k$ since then the i^{th} faces are always degenerate. Examine the sign difference $\varepsilon''_i(\Sigma)$ of the numeration of the cycles of σ_q given by $\tilde{d}''_i(\tilde{\Sigma})$ and the distinguished numeration of $d''_i\Sigma$. Assume that the decomposition $\sigma_q = (\alpha_0)\alpha_1 \ldots, \alpha_m$ and the minimum symbols $(a_0 <)a_1 < \ldots < a_m$ are chosen as above, and that the symbol i is contained in the cycle α_k.

(i) The symbol i is a fixed point of σ_q. Then the number of cycles of $\partial_i(\Sigma)$ is m instead of $m+1$, thus $\partial''_i(\Sigma)$ is degenerate and this case is not of interest.

(ii) The symbol i is not the minimum symbol of the cycle α_k. Then ν is not affected by the application of d''_i, meaning that $\varepsilon''_i(\Sigma) = 1$.

(iii) We have $a_k = i$. When d''_i is applied, the symbol i is removed from its cycle, leaving another element $i' > i$ as the smallest element of the cycle α_k. Now the numeration $\nu_i = \nu \circ {d_i}^{\Delta}$ is not necessarily the distinguished numeration of $d''_i(\Sigma)$ since we do not know whether $i' < a_{k+1}$. But we can transform ν_i into the distinguished numeration by swapping i' with all a_l such that $i < a_l < i'$. This means that the sign difference $\varepsilon''_i(\Sigma)$ is exactly $(-1)^{l-k}$, where l is the maximum symbol with $i < a_l < i'$.

Hence, setting $\hat{d}''_i(\Sigma) = \varepsilon''_i(\Sigma)d''_i(\Sigma)$ corrects all the changes in orientations. We obtain

Proposition 2.6.3. *The homology of the moduli spaces $\mathfrak{M} = \mathfrak{M}^m_{g,n}$ respectively $\mathfrak{M}^\bullet_g(m,n)$ can be determined via*

$$H_*(\mathfrak{M};\mathbb{Z}) = H^{d-*}(P,P';\mathcal{O}) = H^{d-*}(\hat{P},\hat{P}')\,.$$

Here, (P,P') is the relative parallel respectively radial bicomplex. The relative bicomplex $(\hat{P},\hat{P}')$ consists of the same cells as (P,P') together with the vertical differential $\hat{\partial}' = \partial'$ and, for $\Sigma \in \hat{P}$, the horizontal differential

$$\hat{\partial}'' = \sum_{i\in[p]} (-1)^i \varepsilon''_i(\Sigma) d''_i(\Sigma)$$

with $\varepsilon''_i(\Sigma)$ as above.

2.7. Comparison of the Parallel and Radial Models

We now want to relate the moduli spaces $\mathfrak{M}_{g,n}^m$ and $\mathfrak{M}_g^\bullet(m,n)$. The most important, well-known fact about their correlation is

Proposition 2.7.1. *The moduli spaces $\mathfrak{M}_{g,n}^m$ and $\mathfrak{M}_g^\bullet(m,n)$ are homotopy equivalent.*

In particular, the homology of the two spaces coincides. In the remaining part of this section, we will construct maps from one kind of these moduli spaces into the other or, equivalently, maps between the corresponding bundles $\mathfrak{H}_{g,n}^m[(r_1,\dots,r_n)]$ and $\mathfrak{H}_g^\bullet(m,n)$ or between the spaces $\mathfrak{Par}_{g,n}^m[(r_1,\dots,r_n)]$ and $\mathfrak{Rad}_g(m,n)$ of parallel and radial slit domains.

2.7.1. Parallelization

Consider a surface F with m permutable outgoing boundary curves and n marked incoming boundary curves with a potential function u. For each outgoing boundary component C_j^+, we glue in a disc D_j^+ and declare its origin as a logarithmic sink of u. For each incoming boundary component C_i^-, we glue in a disc D_i^- and declare at its origin

(i) a tangent vector X_i pointing towards the marked point on C_i^- and

(ii) a pole of order r_i respecting the tangent vector X_i.

We sketch this in Figure 2.20. Note that the number of stagnation points in D_i^- is exactly r_i. We obtain a surface F' with m permutable punctures and n poles with tangent vectors attached. Thus, we have constructed a map

$$\mathrm{par}\colon \mathfrak{H}_g^\bullet(m,n) \longrightarrow \mathfrak{H}_{g,n}^m[(r_1,\dots,r_n)]\,.$$

On moduli spaces, this construction can be viewed as in Figure 2.21. We simply declare the incoming boundary curves of a surface $F \in \mathfrak{M}_g^\bullet(m,n)$ as boundary curves of a resulting surface F'. Outgoing boundary curves are transformed into punctures by glueing half-open cylinders onto them. Thus we also have described the parallelization map

$$\mathrm{par}\colon \mathfrak{M}_g^\bullet(m,n) \longrightarrow \mathfrak{M}_{g,n}^m$$

on moduli spaces.

From Figure 2.20, we can also read off how to realize the parallelization map on the spaces of slit domains. Consider a radial slit domain A corresponding to a surface $F \in \mathfrak{H}_g^\bullet(m,n)$, where the slits reside on n annuli $\mathbb{A}_1,\dots,\mathbb{A}_n$. Let an ordered partition $r = r_1 + \dots + r_n$ be given, with $r_i \geq 1$ for all i. We want to transform A into a parallel slit domain on r levels.

Concentrate on a single annulus $\mathbb{A}_i$. Since the inner boundary of $\mathbb{A}_i$ corresponds to an inner boundary curve C_i^-, we have to imitate the process of glueing a pole of order r_i to C_i^-. Similar to what is happening to the critical graph on the surface, we split up the annulus $\mathbb{A}_i$ into r_i segments, ordered cyclically, starting at the marked point of A on the real horizontal line. Each of the segments is mapped onto one level of the arising parallel slit domain as in Figure 2.22. Here, we choose to map all endpoints of slits into the unit square, and scale all distances between slits the same way they were scaled in the segment of the annulus before. The levels are ordered at first by the number of the boundary curve,

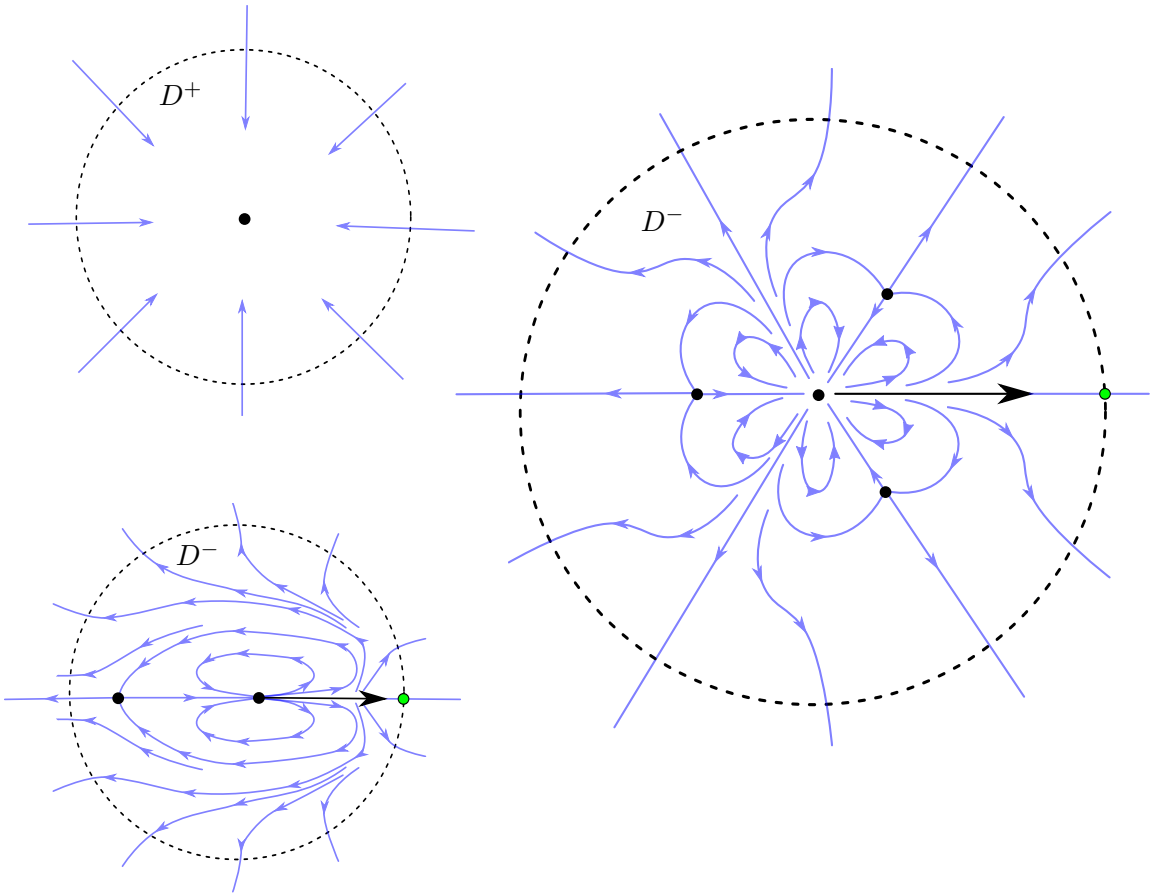

Figure 2.20.: Three examples of extending the potential u. The tangent vector is colored black, the marked point is green and the flow lines of u are light blue.

and among those levels corresponding to the same boundary curve by the cyclic ordering of the segments on the annulus $\mathbb{A}_i$.

Now it remains to preserve the information that the segments on the i^{th} annulus have to be glued together cyclically. Thus, we insert a new pair of slits between the levels corresponding to each two neighboring segments, and these slits have to be longer than any of the other slits. Compare again Figure 2.22, and note that the insertion of the new slits corresponds to the insertion of stagnation points in Figure 2.20.

Remark 2.7.2. It does not matter where exactly the segments of one annulus are seperated from each other since on the resulting parallel slit domain, the slits of neighboring segments can jump over the newly inserted pairs of slits.

This completes the description of the parallelization map

$$\mathrm{par}\colon \mathfrak{Rad}_g(m,n) \longrightarrow \mathfrak{Par}^m_{g,n}[(r_1,\ldots,r_n)]$$

in terms of radial slit pictures. Altogether, we obtain

Definition 2.7.3. There is a map

$$\mathrm{par}\colon \mathfrak{M}^\bullet_g(m,n) \longrightarrow \mathfrak{M}^m_{g,n}$$

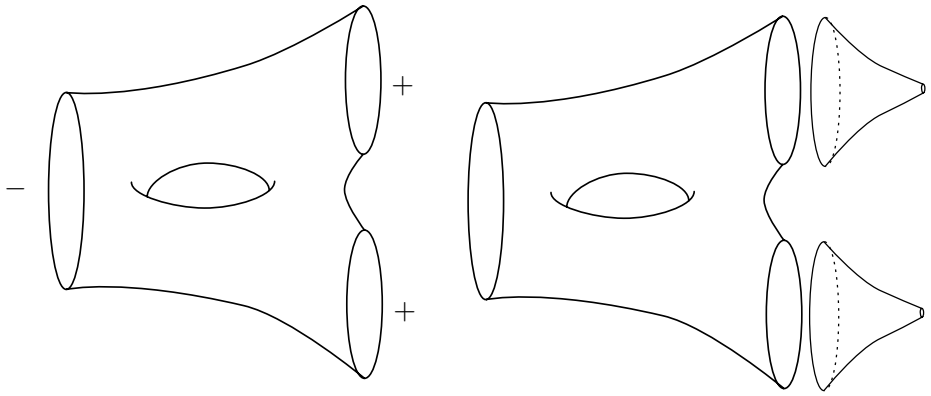

Figure 2.21.: The parallelization map applied to a surface.

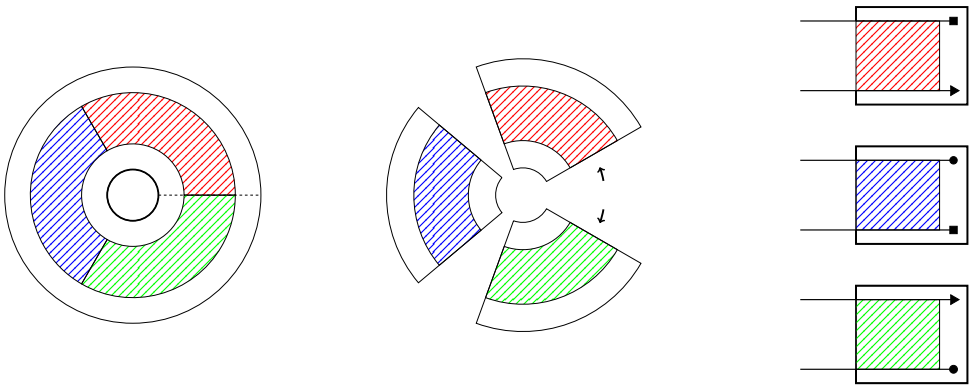

Figure 2.22.: The parallelization map applied to a radial slit domain on one level, with $r = 3$.

called the **parallelization map**, which is described by the above process. The parallelization map can also be expressed on the corresponding bundles and slit domains.

In the special cases when $n = 1$ or $m = 1$, the parallelization map factors through the space $\mathfrak{Par}_{g,n}^{m,1}[1, \ldots, 1]$ of parallel slit domains with one distinguished puncture. On parallel slit pictures, these punctures that are touched by the new slits are distinguished. When $n = 1$, this defines a single puncture; when $m = 1$, there is only one puncture anyway. Note that, when $n > 1$ and $m > 1$, it is possible that this description defines an arbitrary number t of $1 \leq t \leq \min(n, m)$ puncture. In general, we can therefore not determine a number of distinguished punctures for parallelized radial slit domain which is independent of the slits.

Proposition 2.7.4. *Let $n = 1$ or $m = 1$. Then the parallelization map factors through the*

space $\mathfrak{Par}^{m,1}_{g,n}[(1,\dots,1)]$ *as in the following diagram:*

$$\begin{array}{ccc} \mathfrak{Rad}_g(m,n) & \xrightarrow{\quad\text{par}\quad} & \mathfrak{Par}^{m}_{g,n}[(1,\dots,1)] \\ & \searrow^{\text{par}^1} \quad \nearrow & \\ & \mathfrak{Par}^{m,1}_{g,n}[(1,\dots,1)] & \end{array}$$

Here, the map $\text{par}^1\colon \mathfrak{Rad}_g(m,n) \longrightarrow \mathfrak{Par}^{m,1}_{g,n}[(1,\dots,1)]$ *is defined as the factorization of the parallelization map through* $\mathfrak{Par}^{m,1}_{g,n}[(1,\dots,1)]$*, and the unnamed map forgets that one of the punctures is distinguished.*

2.7.2. Radialization

The resembling descriptions of the parallel and radial multicomplex suggest a simple map from $\mathfrak{M}^m_{g,n}$ to $\mathfrak{M}^\bullet_g(m+n,n)$. To see this, remember that a non-degenerate parallel cell $\Sigma = (\sigma_q : \ldots : \sigma_0)$ of bidegree (p,q) can also be viewed as a non-degenerate radial cell Σ of bidegree (p,q) (see Definition 2.5.1). Recall that, in the parallel case, the parameter $m(\Sigma)$ equals the number of cycles of σ_q subtracted by the number n of boundaries of Σ, and in the radial case, it equals the number of cycles of σ_q. Hence, the parameter $m(\Sigma)$ increases by n during the transformation of Σ from a parallel to a radial cell. Note that if r is the number of levels of Σ, the number of levels of the radial version of Σ also is r.

Unfortunately, this map $P(g,m,n;r) \longrightarrow R(g,m+n,r)\,,\ \Sigma \longmapsto \Sigma$, is not cellular. Considering for example the cell

$$\Sigma = (((\underline{2}\ \underline{0})(\underline{1})) : (\underline{0}\ \underline{1}\ \underline{2})) \in P(1,1;1)\,,$$

we see that the 2^{nd} horizontal boundary of Σ is

$$\Sigma' = ((\underline{1})(\underline{0}) : (\underline{0}\ \underline{1}))\,.$$

This cell is not an inner cell of the parallel slit complex since $\sigma'_1 = (\underline{1})(\underline{0})$ does not map the symbol $\underline{1}$ to $\underline{0}$. But in the radial slit complex, Σ' is even non-degenerate.

We still can realize the desired map in terms of slit pictures as in Figure 2.23. Let

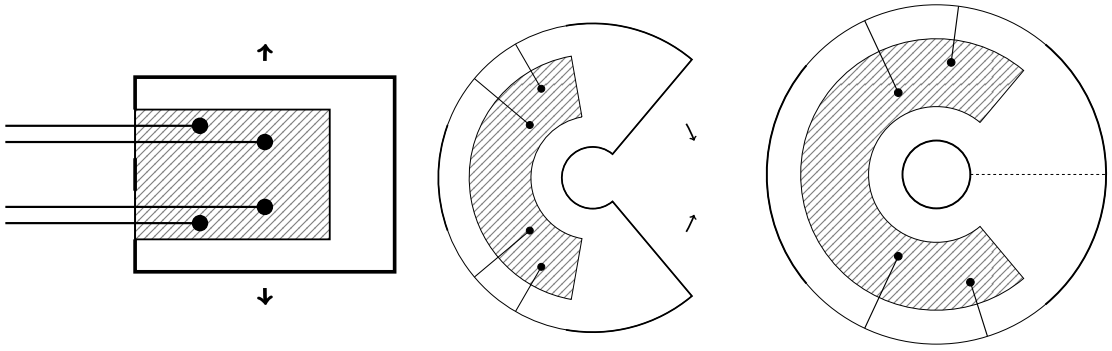

Figure 2.23.: The radialization map applied to a parallel slit domain on one level

$L \in \mathfrak{Par}^m_{g,n}[(r_1, \ldots, r_n)]$ be a parallel slit domain on r levels. For the i^{th} such level, we embed the i^{th} copy of the complex plane belonging to the parallel slit picture into an annulus $\mathbb{A}_i \subset \mathbb{C}$ with inner radius c_i and outer radius 1. Thereby, the ends of the slits are put into the interior of the annulus. In the picture, the slits all lie in the shaded region. In the parallel slit picture, the slits run infinitely to the left, and in the resulting radial slit picture, they run towards the outer boundary of the annulus. Note that no slit is put onto the real horizontal line of the annulus.

Tracing the relevant clipping of the levels of the parallel slit picture (e.g. in Figure 2.23) indicates how to describe the radialization map in terms of moduli spaces. So let $F \in \mathfrak{M}^m_{g,n}$ be a surface with permutable punctures and numbered boundary curves. The punctures of F can be read off from the left border of the relevant clipping. Thus, the punctures of F are adopted as outgoing boundary curves during radialization. In the pictures, there is a bold line indicating what happens to the part of a boundary curve belonging to the relevant clipping of A on one level. When A is transformed into a radial slit domain, the boundary curve is spit up into to pieces; the inner boundary of the annulus and portions of the outer boundary. Note that, when the boundary curve belongs to more than one level, we obtain inner boundary curves for each of the levels, but only one outcoming boundary curve for the whole boundary curve.

Thus, we obtain

Definition 2.7.5. There is a map

$$\text{rad}\colon \mathfrak{M}^m_{g,n} \longrightarrow \mathfrak{M}^\bullet_g(m+n, n)\,,$$

which shall be called **radialization map**. There are realizations of the radialization on slit pictures and on bundles.

On moduli spaces, the radialization map can be described like in Figure 2.24. The

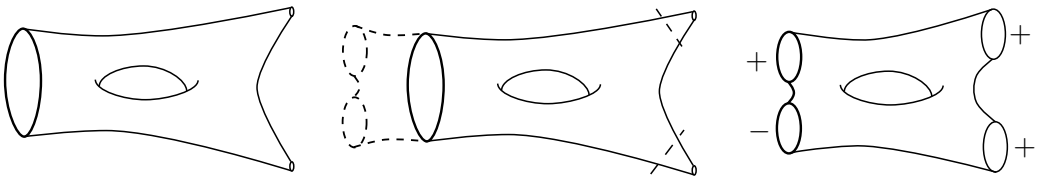

Figure 2.24.: The radialization map applied to a surface.

punctures are transformed into outgoing boundary curves by cutting out small disks around them. Onto each boundary curve, we glue a pair of pants with one outgoing and one incoming boundary.

We have already seen how to construct the radialization map

$$\text{rad}\colon \mathfrak{Par}^m_{g,n}[(r_1, \ldots, r_n)] \longrightarrow \mathfrak{Rad}_g(m+n, r)$$

on the niveau of slit domains. Thus, it remains to express it via bundles. So let $F \in \mathfrak{H}^m_{g,n}$ be a surface with punctures, poles, tangent vectors and a gradient flow. We describe the radialization as a map

$$\text{rad}\colon \mathfrak{H}^m_{g,n} \longrightarrow \mathfrak{H}^\bullet_g(m+n, r)\,.$$

Here, we also cut out small disks around the punctures and immediately obtain outgoing boundary curves instead. This reverses the process displayed in Figure 2.20, but only for the punctures, not for the poles. We have already understood how we have to alter the gradient flow around each pole. We want to glue in an outgoing boundary curve around the pole and, for each basin of the pole, an incoming boundary curve such that the gradient flow remains the same outside an excerpt around the pole. Figure 2.25 shows how this is achieved for the pole of order 3 visible in Figure 2.20.

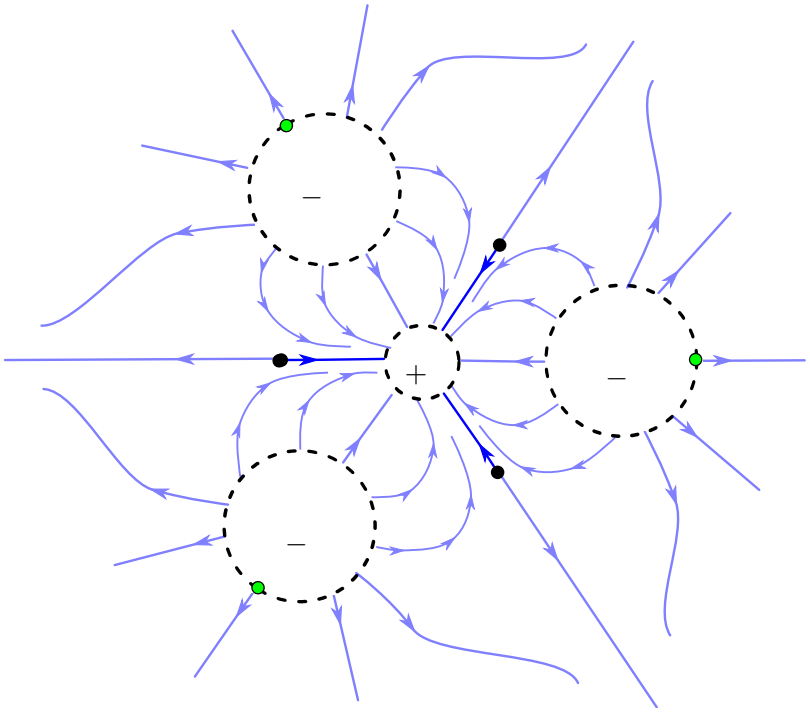

Figure 2.25.: Transforming a pole of order 3 into one outgoing and three incoming boundary curves.

In the special cases when $n = 1$ or $m = 1$, Proposition 2.7.4 yields the following

Proposition 2.7.6. *If $n = 1$ or $m = 1$, the radialization map is split injective and hence induces a split injective map*

$$\mathrm{rad}_*\colon H_*(\mathfrak{M}^m_{g,n}) \longrightarrow H_*(\mathfrak{M}^\bullet_g(m+n, n))$$

on homology.

Proof. Choose $r = n = 1 + \cdots + 1$ the trivial partition. Consider the composition

$$\mathfrak{Par}^m_{g,n}[(1,\dots,1)] \xrightarrow{\text{rad}} \mathfrak{Rad}(g, m+n, n) \xrightarrow{\text{par}^1} \mathfrak{Par}^{m+n}_{g,n}1[(1,\dots,1)] \xrightarrow{\text{forget}} \mathfrak{Par}^m_{g,n}[(1,\dots,1)]$$

of the radialization map with the parallelization map from Proposition 2.7.4 and the forgetful map that forgets the distinguished puncture. In Figure 2.26, we see that this composition is the identity. This proves the claim.

□

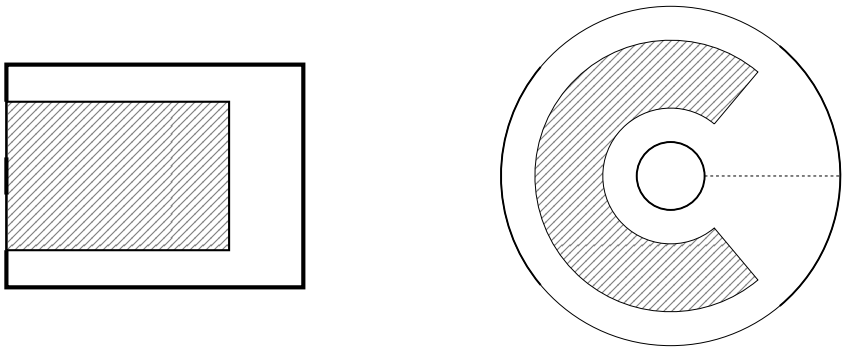

Figure 2.26.: The parallel slit picture A and its radialization $\mathrm{rad}(A)$.

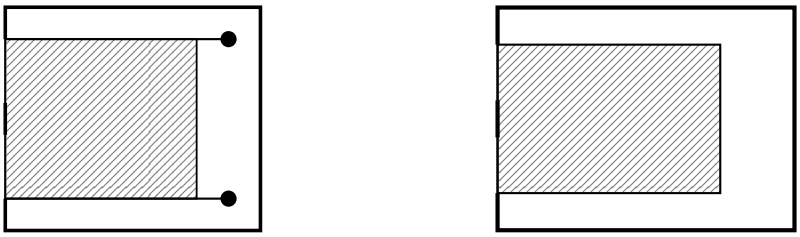

Figure 2.27.: The parallel slit pictures $\mathrm{par}(\mathrm{rad}(A))$ and $\mathrm{forget}(\mathrm{par}(\mathrm{rad}(A))) = A$.

Note that we have to set $r = n$ in the preceding proof since the radialization map always yields a radial slit picture with r annuli. In Corollary 4.4.3, we will be able to show the statement for arbitrary m and n.

2.8. The Ehrenfried Complex

In this section, we treat the radial slit complex and parallel slit complex at once. In order to reduce notation, we only mention the parallel model most of the time.

The homology of the moduli spaces as well as homology operations are derived via the relative cohomology of the dual of P/P'. Due to Ehrenfried, there is a considerably smaller, quasi-isomorphic subcomplex $\mathbb{E}$ of the total complex $Tot(P/P')$ for $n = 1$. The subcomplex $\mathbb{E}$ has a distinguished basis and is called the **Ehrenfried complex associated with** $\mathfrak{M}^m_{g,1}$. Using Visy's techniques, we construct the Ehrenfried complex for arbitrary $P(h, g; r_1, \ldots, r_n)$ and $R(g, n, m)$ as follows.

2.8.1. Construction of the Ehrenfried Complex

We proceed as indicated in Section 2.1. A brief review on factorable groups can be found in Appendix B. Here, we use some basic tools from group homology which are introduced in [Bro82]. Further, we assume that the reader is used to work with spectral sequences. There are several introductions to the theory of spectral sequences and we recommend working through [Wei95, Chapter 5] or [Spa94, Chapter 9].

Denote by E the spectral sequence associated with the vertical homology of the double complex P/P'. Observe that P/P' vanishes if the vertical degree is larger then h.

Definition/Theorem 2.8.1. The first page of the spectral sequence E is concentrated in the h^{th} row

$$\mathbb{K}_\bullet = E^1_{\bullet,h} = \ker(\partial'_{\bullet,h})\,.$$

Proof. Consider the bar resolution $B_\bullet(\mathfrak{S}_p^\times)$ of the symmertric group $\mathfrak{S}_p^\times = Aut(\{1,\dots,p\})$ and let N denote the word length norm with respect to the generating set of all transpositions. This norm induces a filtration

$$F_tB_q = \langle (g_q \mid \dots \mid g_1) \mid N(g_q) + \dots + N(g_1) \leq t \rangle$$

on the bar resolution. The spectral sequence associated with this filtration is by definition the norm complex $\mathcal{N}[\mathfrak{S}_p^\times]$ with zero$^{\text{th}}$ term $\mathcal{N}^0[\mathfrak{S}_p^\times]_{t,q} = F_tB_q/F_{t-1}B_q$. We refere to the following theorem.

Theorem 2.8.2 ([Vis10] Theorem 4.1.1 and Theorem 5.2.1)**.** *The symmetric group with the above norm is factorable. The homology of $\mathcal{N}^0[\mathfrak{S}_p^\times]_{\bullet,h}$ is therefore concentrated in the top degree $\bullet = h$.*

It remains to show that for fixed p, $E_\bullet = E^0_{p,\bullet}$ is a direct summand of $\mathcal{N}[\mathfrak{S}_p^\times]^0_{\bullet,h}$. As a module, $\mathcal{N}[\mathfrak{S}_p^\times]_{q,h}$ is freely generated by all $(g_q \mid \dots \mid g_1)$ with

(i) $1 \neq g_j \in \mathfrak{S}_p^\times$ for all j and

(ii) $N(g_q) + \dots + N(g_1) = h$.

The module E_q is freely generated by all non-degenerate cells. Using the inhomogenous notation, E_q is hence freely generated by all $\Sigma = (g_q \mid \dots \mid g_1)$ with

(i) $1 \neq g_j \in \mathfrak{S}_p^\times$ for all j,

(ii) $N(g_q) + \dots + N(g_1) = h$,

(iii) the $g_q, \dots, g_1$ do not have a common fixed point,

(iv) $m = m(\Sigma)$ and $n = n(\Sigma)$,

(v) the levels of Σ are ordered ascendingly with respect to the partition $(r_1, \dots, r_n)$ and

(vi) Σ is connected.

A direct computation shows that the canonical inclusion $E_\bullet \hookrightarrow \mathcal{N}[\mathfrak{S}_p^\times]_{\bullet,h}$ of modules induces a chain monomorphism that splits as the latter four conditions are invariant under $\partial^{\mathcal{N}[\mathfrak{S}_p^\times]}$. □

Corollary 2.8.3. *The canonical inclusion of the chain complex $\mathbb{K}_\bullet$ into the top row of P/P' defines a quasi-isomorphism*

$$\mathbb{K}_\bullet \xhookrightarrow{\simeq} Tot(P/P')_{\bullet+h}\,.$$

Proof. The canonical inclusion $\mathbb{K}_p \longrightarrow Tot(P/P')_{p,h}$ defines a chain map since $\mathbb{K} = \ker(\partial'_{\bullet,h})$. From the preceding Theorem 2.8.1, we obtain $H_*(\mathbb{K}) = E^2_{*,h} = H_{*+h}(P, P')$. □

Let us construct an distinguished basis for $\mathbb{K}_\bullet$. In order to do so, recall the definition of the factorization map η (discussed in Appendix B.2). It splits a permutation α into $\alpha = \overline{\alpha}\alpha'$ with $\overline{\alpha} = (c\ \alpha^{-1}(c))$ where $c = \mathrm{ht}(\alpha)$.

Definition 2.8.4. For an arbitrary cell $\Sigma = (\tau_q \mid \ldots \mid \tau_1)$ of bidegree (p, q) and $q > j \geq 1$, let

$$\Upsilon_j(\Sigma) = (\tau_q \mid \ldots \mid \overline{\tau_{j+1}\tau_j} \mid (\tau_{j+1}\tau_j)' \mid \ldots \mid \tau_1)\,.$$

In other words, the map Υ_j considers the j^{th} vertical face of Σ by multiplying τ_j with τ_{j+1}, and then factors this product via the factorization map from above. Consequently, the symbol $\Upsilon = \eta\mu$ should remind us of this process and is therefore called **mueta**.

Definition 2.8.5. We define the homomorphism κ by extending

$$\kappa = \kappa_h = K_h \circ \ldots \circ K_1$$

linearly, where

$$K_q = \sum_{j=1}^{q} (-1)^{q-j} \Phi^q_j$$

and

$$\Phi^q_j = \Upsilon_j \circ \ldots \Upsilon_{q-1}\,.$$

Definition 2.8.6. As a module, let $\mathbb{E}_p$ be freely generated by all top dimensional, non-degenerate cells $\Sigma = (\tau_h \mid \ldots \mid \tau_1)$ that are monotonous, i.e.

$$\mathrm{ht}(\tau_h) \geq \ldots \geq \mathrm{ht}(\tau_1)\,.$$

Lemma 2.8.7. *The map $\kappa\colon \mathbb{E}_p \longrightarrow \mathbb{K}_p$ is an isomorphism of modules.*

Proof. In order to prove this, we use the notation introduced in the proof of Theorem 2.8.1. Due to Visy's work on factorable groups [Vis10, Theorem 5.4.1] – which was generalized to factorable monoids due to [Hes12, Proposition 3.3.6] –, there is a homomorphism of modules

$$\mathbb{V}_p \xrightarrow{\kappa} \mathcal{N}^1[\mathfrak{S}^\times_p]_{h,h} \qquad \text{is inverse to} \qquad \mathcal{N}^1[\mathfrak{S}^\times_p]_{h,h} \xrightarrow{\pi} \mathbb{V}_p\,,$$

where $\mathbb{V}_p$ is freely generated by all top dimensional, monotonous cells and π is the projection onto the monotonous ones. By construction, $E^0_{p,\bullet} \subseteq \mathcal{N}^0[\mathfrak{S}^\times_p]_{\bullet,h}$ has a direct complement $C_\bullet$ that is freely generated by all cells that satisfy conditions (i) and (ii) but violate at least one of the other conditions (c.f. 2.8.1). In particular, we have

$$\mathbb{K}_p \oplus H_h(C_\bullet) = H_h(E^1_{p,\bullet}) \oplus H_h(C_\bullet) \cong \mathcal{N}^1[\mathfrak{S}^\times_p]_{h,h}$$

since $\mathbb{K}_p = H_h(E^1_{p,\bullet})$ by Definition 2.8.1. The module $\mathbb{E}_p \subset \mathbb{V}_p$ has a direct complement D_p which is freely generated by all top dimensional that satisfy the first three conditions in Definition 2.3.11 but are not non-degenerate — which is not equivalent to being degenerate. Now the claim follows from

$$\pi(\mathbb{K}_p) \subseteq \mathbb{E}_p \qquad \text{and} \qquad \pi(H_h(C)) \subseteq D_p$$

as all modules are finite dimensional. □

Definition 2.8.8. The chain modules $\mathbb{E}_p$ of the Ehrenfried complex $(\mathbb{E}, \partial_{\mathbb{E}})$ are freely generated by all top-dimensional non-degenerate cells. The boundary maps $\partial_{\mathbb{E}} = \pi \circ \partial'' \circ \kappa$ make the diagram

$$\begin{array}{ccc} \mathbb{E}_p & \xrightarrow{\partial_{\mathbb{E}}} & \mathbb{E}_{p-1} \\ \cong\downarrow\kappa & & \cong\uparrow\pi \\ \mathbb{K}_p & \xrightarrow{\partial''} & \mathbb{K}_{p-1} \end{array}$$

commutative. If we want to distinguish the parallel case from the radial case, we write $\mathbb{E}(h, m; r_1, \ldots, r_n)$ respectively $\mathbb{E}(h, m, n)$.

Theorem 2.8.9. *The dual Ehrenfried complex is a quasi-isomorphic direct summand of (the total complex of) $(P/P')^*$, respectively $(R, R')^*$. In particular the homology of the moduli space is by Poincaré duality*

$$H_*(\mathfrak{M}^m_{g,n}; \mathbb{Z}) \cong H^{2h-*}(\mathbb{E}(h, m; r_1, \ldots, r_n); \mathcal{O}) \qquad \textit{with} \qquad h = 2g - 2 + m + n + r\,,$$

respectively

$$H_*(\mathfrak{M}^\bullet_g(m, n); \mathbb{Z}) \cong H^{2h+n-*}(\mathbb{E}(h, m); \mathcal{O}) \qquad \textit{with} \qquad h = 2g - 2 + m + n\,.$$

Proof. The Ehrenfried complex is a quasi-isomorphic direct subcomplex of $Tot(P/P')$ as it is isomorphic to $\mathbb{K}$ (compare Corollary 2.8.3). The projection onto the monotonous cells $\pi\colon Tot(P/P') \longrightarrow \mathbb{E}$ is a retraction to κ, so $\mathbb{E} \hookrightarrow Tot(P/P')$ is a quasi-isomorphism. After dualizing, $\pi^*\colon \mathbb{E}^* \hookrightarrow Tot(P/P')^*$ is the canonical inclusion with retraction κ^*. By naturality of the universal coefficient theorem, $\mathbb{E}^* \hookrightarrow Tot(P/P')^*$ is also a quasi-isomorphism. □

2.8.2. Some Useful Properties

In this subsection, we present some properties and formulas that will become handy in later parts of this thesis or in our computer program.

The following definition is inspired by [Hes12, Lemma 2.3.33] but uses a different indexing convention.

Definition 2.8.10. Let a and b be positive integers. Denote $I_a^b = (a, a+1, \ldots, b-1, b)$ for $a \leq b$ and let $I_a^b = ()$ be the empty sequence for $a > b$. The set of **κ-sequences** is

$$\Lambda_1\{()\} \qquad \text{and by concatenation} \qquad \Lambda_{n+1} = \{I_1^n, \ldots, I_n^n, I_{n+1}^n\}.\Lambda_n\,.$$

For a κ-sequence $I = (i_1, \ldots, i_k)$ we set

$$\kappa_I = \mathfrak{X}_{i_1} \circ \ldots \circ \mathfrak{X}_{i_k}\,.$$

Lemma 2.8.11. *The map κ is the alternating sum of all κ-sequences:*

$$\kappa_h = \sum_{(i_1,\ldots,i_k)\in\Lambda_h} (-1)^k \kappa_{(i_1,\ldots,i_k)}\,.$$

Proof. By Definition 2.8.5

$$\kappa_h = \prod_{q=1}^{h} \left(\sum_{j=1}^{q} (-1)^{q-j} (\mathfrak{X}_j \circ \ldots \circ \mathfrak{X}_{q-1}) \right) .$$

We proof the equality by induction on h. For $h = 1$, it is readily verified.

To proof the induction step $h \longmapsto h+1$ let $\mathcal{I} = \{I_1^h, \ldots, I_h^h, I_{h+1}^h\}$. Then

$$\kappa_{h+1} = \left(\sum_{j=1}^{h+1} (-1)^{h+1-j} (\mathfrak{X}_j \circ \ldots \circ \mathfrak{X}_h) \right) \circ \prod_{q=1}^{h} \left(\sum_{j=1}^{q} (-1)^{q-j} (\mathfrak{X}_j \circ \ldots \circ \mathfrak{X}_{q-1}) \right) \tag{2.1}$$

$$= \left(\sum_{(i_1,\ldots,i_j)\in\mathcal{I}} (-1)^j \kappa_{(i_1,\ldots,i_j)} \right) \circ \left(\sum_{(i_1,\ldots,i_k)\in\Lambda_h} (-1)^k \kappa_{(i_1,\ldots,i_k)} \right) \tag{2.2}$$

and composing maps yields

$$= \sum_{(i_1,\ldots,i_k)\in\mathcal{I}.\Lambda_h} (-1)^k \kappa_{(i_1,\ldots,i_k)} \tag{2.3}$$

which is the desired result. □

To avoid unneccessary computations in later discussions, we need simple way to detect the cases when $d_i''(\Sigma)$ is degenerate for cells $\Sigma \in \mathbb{E}$ of the Ehrenfried complex. The next proposition will aid us many times.

Proposition 2.8.12. *Let $\Sigma \in P(h, m; r_1, \ldots, r_n)_{p,h}$ be a non-degenerate top dimensional cell and $\underline{1}_k \leq i < \underline{p}_k$. The i^{th} horizontal face of Σ is degenerate if and only if there exists $1 \leq j \leq h$ with*

$$\tau_j = (i \ \sigma_{j-1}(i)) \qquad or \qquad \sigma_j(i) = i \, .$$

Proof. Denote the i^{th} face of $\Sigma = (\tau_h \mid \ldots \mid \tau_1)$ by $\tilde{\Sigma} = (\tilde{\tau}_h \mid \ldots \mid \tilde{\tau}_1)$. By Proposition 2.3.10, we have $\tilde{\tau}_j = D_i(\tau_j \cdot (i \ \sigma_{j-1}(i))$ for all j.

If there exists $1 \leq j \leq h$ with (1) $\tau_j = (i \ \sigma_{j-1}(i))$, then $\tilde{\tau}_j = 1$ and $\tilde{\Sigma}$ is degenerate. If (2) $\sigma_j(i) = i$, then let us assume that j is maximal with this property, i.e. either $j = h$ or $j < h$. Therefore, we either collapse a puncture of Σ which makes $\tilde{\Sigma}$ degenerate or we have $\tau_{j+1}(i) \neq i$ thus $\tilde{\tau}_{j+1} = D_i(\tau) = 1$ which shows that $\tilde{\Sigma}$ is again degenerate.

Conversely, if there is no such j we conclude that all $\tilde{\tau}_j$ are non-trivial and $\tilde{\Sigma}$ has the same number of punctures as Σ. The result follows from the non-degeneracy of Σ. □

2.9. The Dual Ehrenfried Complex

In this section, we introduce the notion of coboundary traces to provide explicit formulas for both the horizontal coface operator $(\partial'')^*$ and the coboundary operator $\partial_{\mathbb{E}}^*$. Moreover, we study some usefull properties of κ^* and classify the cells of a given Ehrenfried complex.

Let us sketch the process of constructing horizontal cofaces of a given top dimensional cell $\Sigma = (\tau_h \mid \ldots \mid \tau_1)$. Every transposition defines a slit of pairs where shorter slits sit atop of longer slits if they are of the same height. In some pictures (e.g. Lemma 2.9.15),

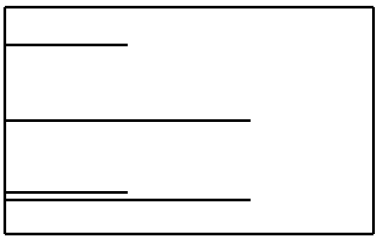

Figure 2.28.: The cell $((\underline{3}\ \underline{1})|(\underline{2}\ \underline{1}))$. Here $g = 1$, $n = 1$ and $m = 0$.

we indicate this pairing by an arc joining the two slits. In Figure 2.28 we picture the cell $\Sigma = ((\underline{3}\ \underline{1})|(\underline{2}\ \underline{1}))$.

We obtain a coboundary by glueing a stripe inbetween the two slits of height $\underline{1}$. More sophisticated, we let the shorter slit jump through the longer slit, in order to end up below the long slit of height $\underline{2}$, and glue in the stripe afterwards. The two coboundaries are sketched in Figure 2.29 where we shade the stripe which was glued in.

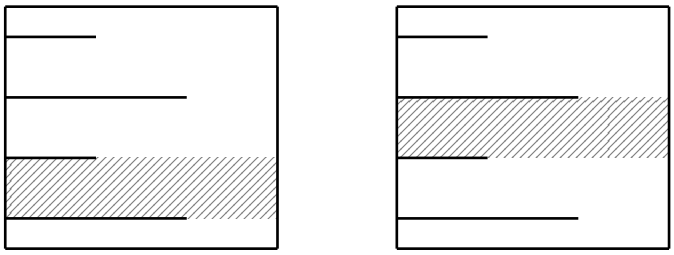

Figure 2.29.: Two coboundaries of $((\underline{3}\ \underline{1})|(\underline{2}\ \underline{1}))$. Still $g = 1$, $n = 1$ and $m = 0$.

For a cell with more slits we might have more choices for jumps as seen in the next example. The cell $\Sigma = \big((\underline{4}\ \underline{1})|(\underline{3}\ \underline{1})|(\underline{3}\ \underline{1})|(\underline{2}\ \underline{1})\big)$ is skeched in Figure 2.30 and we construct

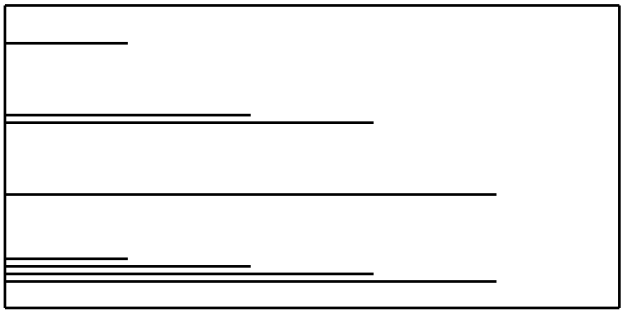

Figure 2.30.: The cell $\big((\underline{4}\ \underline{1})|(\underline{3}\ \underline{1})|(\underline{3}\ \underline{1})|(\underline{2}\ \underline{1})\big)$. Here $g = 2$, $n = 1$ and $m = 0$.

the three coboundaries seen in Figure 2.31. To obtain coboundary (1), we let slits 2, 3 and 4 of height $\underline{1}$ jump through slit 1. For coboundary (2), we let slits 3 and 4 of height $\underline{1}$ jump through slit 2, and for coboundary (3), we slits 2 and 3 of height $\underline{1}$ jump through slit 1.

The key insight is that an i^{th} coboundary $\tilde{\Sigma}$ is determined by its sequence $\tilde{\sigma}_j(i)$. By this, we see that constructing a coboundary should be the same as constructing such a sequence by choosing which slits are going to jump. We encode our geometric intuition in the notion

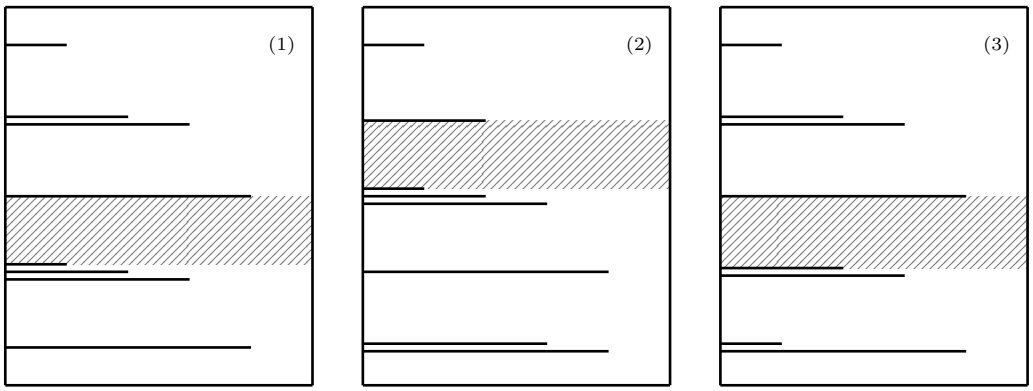

Figure 2.31.: Three coboundaries of $((\underline{4}\ \underline{1})|(\underline{3}\ \underline{1})|(\underline{3}\ \underline{1})|(\underline{2}\ \underline{1}))$ that arise from different jumps.

of i^{th} coboundary trace (see Definition 2.9.2) and show that the canonical map from the set of i^{th} coboundary traces $T_i(\Sigma)$ to the set of i^{th} cofaces $\text{cf}_i(\Sigma)$ is bijective (see Proposition 2.9.7). The coface corresponding to a given coboundary trace a is denoted by $a.\Sigma$. Using our notation, the coboundary operator of the Ehrenfried complex is

$$\partial^*_{\mathbb{E}}(\Sigma) = \sum_{i=1}^{p} (-1)^i \sum_{a \in T_i(\Sigma)} \kappa^*(a.\Sigma)\,.$$

Most importantly the explicit formula and a better understanding of κ^* (developed in Subsection 2.9.2) allows us to define homology operations on the moduli space via coboundary maps defined on the dual Ehrenfried complex, see Chapter 4.

Moreover, we classify the cells of a fixed Ehrenfried complex. Cofaces $\tilde{\Sigma}$ are said to arise as basic expansions of Σ if the construction involves no jumps, in the sense of the above paragraphs. Cells that do not arise this way are called thin. Applying basic expansions is commutative (this is made precise by Proposition 2.9.23) and every cell in $\mathbb{E}$ arises uniquely from a thin cell by applying a set of basic expansions:

Proposition (2.9.26)**.** *Denote the set of thin cells by $Thin^m_{g,n}[(r_1,\dots,r_n)]$, the set of basic expansions of a cell Σ by $Bsupp(\Sigma)$ and the power set operator by $\mathcal{P}ow$. There is a bijection*

$$ex\colon \coprod_{\Sigma \in Thin^m_{g,n}[(r_1,\dots,r_n)]} \mathcal{P}ow(Bsupp(\Sigma)) \longrightarrow Cells(\mathbb{E}) \qquad \text{with} \qquad Bsupp(\Sigma) \supseteq J \longmapsto J.\Sigma\,.$$

In particular, the number of cells of a given degree is the sum of certain binomial coefficients and the dimension of $\mathbb{E}$ is

$$\dim \mathbb{E} = \sum_{p=2}^{2h} 2^{(2h-p)} \cdot |\{\Sigma \in \mathbb{E}_p \text{ thin}\}|\,.$$

2.9.1. The Coface Operator via Coboundary Traces

In this subsection, we proceed as described above. We encode our geometric intuition in the notion of i^{th} coboundary trace and show that the canonical map from the set of i^{th}

coboundary traces $T_i(\Sigma)$ to the set of i^{th} cofaces $\mathrm{cf}_i(\Sigma)$ is bijective. Hereby, we focus on the parallel Ehrenfried complex as our proofs become more compact and the radial case is treated analogously.

Recall that the horizontal boundary operator is defined as the alternating sum of the faces of $\Delta^{p_1} \times \ldots \times \Delta^{p_r}$. It is therefore computed "levelwise" and it might be helpful to think of parallel slit domains with exactly one level.

Definition 2.9.1. Let $\Sigma = (\tau_h \mid \ldots \mid \tau_1)$ be a non-degenerate cell in the double complex P/P' of bidegree (p, h). The set of its i^{th} cofaces is denoted by

$$\mathrm{cf}_i(\Sigma) = \{\tilde{\Sigma} \in P_{p+1,h} \mid d_i''(\tilde{\Sigma}) = \Sigma\}.$$

Definition 2.9.2. Let $\Sigma = (\tau_h \mid \ldots \mid \tau_1)$ be a parallel non-degenerate top dimensional cell with respect to $[p]$ and let $\underline{0}_k < i \leq \underline{p}_k$. A sequence $(a_h : \ldots : a_0)$ in $[p]$ is called i^{th} **coboundary trace of** Σ if it satisfies the following conditions:

(i) $a_0 = i + 1$.

(ii) If $a_j \neq a_{j-1}$, then $a_j = (S_i\tau_j)(a_{j-1})$ (or equivalently: if $a_j \neq (S_i\tau_j)(a_{j-1})$, then $a_j = a_{j-1}$).

(iii) $a_j \neq (S_i\tau_j)(a_{j-1})$ at least once.

(iv) $a_j \neq a_{j-1}$ at least once.

The set of all i^{th} coboundary traces of Σ is denoted by

$$T_i(\Sigma) = \{(a_h : \ldots : a_0) \text{ is an } i^{\text{th}} \text{ coboundary trace of } \Sigma\}.$$

Let us elaborate on the above definition. Condition (i) is the normalization corresponding to $\sigma_0(i) = i+1$. The second condition encodes jumping slits and glueing in stripes. In this sense, condition (iii) forbids glueing in a stripe below all stripes of height i and condition (iv) forbids glueing in a stripe above all stripes of height i. Recalling that the $\underline{0}_k^{\text{th}}$ slit of a radial cells might be empty the next definition is the obvious analogue to Definition 2.9.2.

Definition 2.9.3. Let $\Sigma = (\tau_h \mid \ldots \mid \tau_1)$ be a radial non-degenerate top dimensional cell with respect to $[p]$ and let $\underline{0} < i \leq \underline{p+1}_k$. A sequence $(a_h : \ldots : a_0)$ in $[p]$ is called i^{th} **coboundary trace of** Σ if it satisfies the following conditions:

(i) $a_0 = \begin{cases} i+1 & i \neq \underline{p+1}_k \\ \underline{0}_k & i = \underline{p+1}_k \end{cases}$.

(ii) If $a_j \neq a_{j-1}$, then $a_j = (S_i\tau_j)(a_{j-1})$ (or equivalently: if $a_j \neq (S_i\tau_j)(a_{j-1})$, then $a_j = a_{j-1}$).

(iii) If $i \neq \underline{0}_k$ we have $a_j \neq (S_i\tau_j)(a_{j-1})$ at least once.

(iv) If $i \neq \underline{p+1}_k$ we have $a_j \neq a_{j-1}$ at least once.

The set of all i^{th} coboundary traces of Σ is denoted by

$$T_i(\Sigma) = \{(a_h : \ldots : a_0) \text{ is an } i^{\text{th}} \text{ coboundary trace of } \Sigma\}.$$

Remark 2.9.4. Observe that the symbol i does not occur in an i^{th} coboundary trace.

Definition 2.9.5. Let $\Sigma = (\tau_h \mid \ldots \mid \tau_1)$ be a non-degenerate top dimensional cell with respect to $[p]$ and let $i = \underline{i}_k \in [p]$ and $a \in T_i(\Sigma)$. Then we define

$$a.\Sigma = (\tilde{\tau}_h \mid \ldots \mid \tilde{\tau}_1)$$

with

$$\tilde{\tau}_j = \begin{cases} S_i\tau_j & a_j = (S_i\tau_j)(a_{j-1}) \\ (i\ a_{j-1})S_i\tau_j(i\ a_{j-1}) & a_j \neq (S_i\tau_j)(a_{j-1}) \end{cases}$$

and with respect to the partition of $p+1 = p_1 + \ldots + p_{k-1} + (p_k+1) + p_{k+1} + \ldots + p_r$.

Remark 2.9.6. For $a \in T_i(\Sigma)$ and $a.\Sigma = (\tilde{\tau}_h \mid \ldots \mid \tilde{\tau}_1)$, we have

$$a_j \neq (S_i\tau_j)(a_{j-1}) \quad \text{iff} \quad \tilde{\tau}_j(i) \neq i \quad \text{iff} \quad \tilde{\tau}_j = (i\ (S_i\tau_j)(a_{j-1}))\,.$$

Proposition 2.9.7. *Consider $P = P(h, m; r_1, \ldots, r_n)$, the bisimplicial complex associated with $\mathfrak{M}^m_{g,n}$. For every non-degenerate cell $\Sigma \in P_{p,h}$ and $\underline{1}_k \leq i \leq \underline{p}_k$, the map*

$$\Phi\colon T_i(\Sigma) \longrightarrow \mathrm{cf}_i(\Sigma) \qquad \textit{with} \qquad a \longmapsto a.\Sigma$$

is bijective. The p^{th} coboundary operator of the associated Ehrenfried complex is therefore

$$\partial^*_{\mathbb{E}}(\Sigma) = \sum_{i=1}^{p}(-1)^i \sum_{a\in T_i(\Sigma)} \kappa^*(a.\Sigma)\,.$$

We prove this proposition using the following basic properties.

Lemma 2.9.8. *Consider $\Sigma = (\tau_h \mid \ldots \mid \tau_1)$ and $\Sigma' = (\tau'_h \mid \ldots \mid \tau'_1)$ of bidegree (p, h) that have their i^{th} horizontal face in common. Assume that $\sigma_j(i) = \sigma'_j(i)$ for all j. Then already $\Sigma = \Sigma'$.*

Proof. Using the definition of the horizontal differential (see 2.3.3), we have

$$(i\ \sigma_j(i))\sigma_j = D_i(\sigma_j) = D_i(\sigma'_j) = (i\ \sigma'_j(i))\sigma'_j = (i\ \sigma_j(i))\sigma'_j$$

for arbitrary j, up to renormalization. Hence $\sigma_j = \sigma'_j$ for all j and the claim follows. □

Lemma 2.9.9. *Let $a = (a_h : \ldots : a_0)$ be an i^{th} coboundary trace of Σ and denote $a.\Sigma = (\tilde{\sigma}_h : \ldots : \tilde{\sigma}_0)$. Then we have*

$$a_j = \tilde{\sigma}_j(i)\,.$$

Proof. By construction $a_0 = i+1 = \tilde{\sigma}_0(i)$. We assume there is a minimal index j with $a_j \neq \tilde{\sigma}_j(i)$. Hence

$$a_j \neq \tilde{\sigma}_j(i) = \tilde{\tau}_j(\tilde{\sigma}_{j-1}(i)) = \tilde{\tau}_j(a_{j-1}) = \begin{cases} (S_i\tau_j)(a_{j-1}) & a_j = (S_i\tau_j)(a_{j-1}) \\ ((i\ a_{j-1})S_i\tau_j(i\ a_{j-1}))(a_{j-1}) = a_{j-1} & a_j \neq (S_i\tau_j)(a_{j-1}) \end{cases}$$

by definition of $\tilde{\tau}_j$. The first case is clearly impossible, and the second case implies $\sigma_j(i) = a_{j-1} = a_j$ by (ii) in Definition 2.9.2. □

Lemma 2.9.10. *Let $a \in T_i(\Sigma)$. Then*

$$d_i''(a.\Sigma) = \Sigma\,.$$

Proof. Denote $a.\Sigma = (\tilde{\tau}_h \mid \ldots \mid \tilde{\tau}_1) = (\tilde{\sigma}_h : \ldots : \tilde{\sigma}_0)$ and $d_i''(a.\Sigma) = (\tilde{\tau}_h'' \mid \ldots \mid \tilde{\tau}_1'')$. For $q \geq j \geq 1$, by Proposition 2.3.10 and Lemma 2.9.9, we have

$$\tilde{\tau}_j'' = D_i(\tilde{\tau}_j \cdot (i\ a_{j-1})) = \begin{cases} D_i(S_i\tau_j \cdot (i\ a_{j-1})) & a_j = (S_i\tau_j)(a_{j-1}) \\ D_i((i\ a_{j-1}) \cdot S_i\tau_j) & a_j \neq (S_i\tau_j)(a_{j-1}) \end{cases}.$$

Now $(i\ a_{j-1})$ is disregarded in both cases by Proposition 2.3.10 and we are done as $D_iS_i\tau_j = \tau_j$. □

Lemma 2.9.11. *Consider a non-degenerate cell $\Sigma \in P_{p,h}$ and let $a \in T_i(\Sigma)$. Then the cell $a.\Sigma \in P_{p+1,h}$ is also non-degenerate.*

Proof. Denote

$$\Sigma = (\tau_h \mid \ldots \mid \tau_1) = (\sigma_h : \ldots : \sigma_0) \qquad \text{and} \qquad a.\Sigma = \tilde{\Sigma} = (\tilde{\tau}_h \mid \ldots \mid \tilde{\tau}_1) = (\tilde{\sigma}_h : \ldots : \tilde{\sigma}_0)\,.$$

We show that $\tilde{\Sigma}$ is a connected inner cell with the correct number of punctures and boundaries.

Clearly, $\tilde{\tau}_j \neq 1$ for all $q \geq j \geq 1$. Recall that the $\tilde{\tau}_q, \ldots, \tilde{\tau}_1$ have a fixed point k in common if and only if $\tilde{\sigma}_j(k-1) = k$ for all j. By assumtion, $D_i(\tilde{\sigma}_j) = \sigma_j$ and Σ is an inner cell. Hence, it suffices to check $k = i, i+1$. By condition (iii) in Definition 2.9.2, there is at least one $a_j \neq (S_i\tau_j)(a_{j-1})$. This implies $\tilde{\tau}_j(i) \neq i$ (see Remark 2.9.6). By condition (iv) in Definition 2.9.2, there is at least one j with $a_j \neq a_{j-1}$. This implies $\tilde{\sigma}_j(i) \neq i+1$ for at least one j. Thus $\tilde{\Sigma}$ is an inner cell.

By Lemma 2.9.10, $\tilde{\Sigma}$ is an i^{th} coboundary of Σ. In particular, it is connected. Moreover, $\tilde{\sigma}_j(i) = a_j \neq i$ (by Lemma 2.9.9 and Remark 2.9.4) and $D_i(\tilde{\sigma}_j) = \sigma_j$. Therefore

$$\operatorname{ncyc}(\tilde{\Sigma}) = \operatorname{ncyc}(\Sigma)$$

and, by construction, $N(\tilde{\Sigma}) = h$. The levels of $\tilde{\Sigma}$ are ordered ascendingly as this is true for Σ. □

Proof of Proposition 2.9.7. The map Φ is well defined by Lemma 2.9.11 and Lemma 2.9.10.

By Lemma 2.9.9, every i^{th} coboundary trace $a \in T_i(\Sigma)$ defines a coboundary $a.\Sigma = (\tilde{\sigma}_h : \ldots : \tilde{\sigma}_0)$ with $a_j = \tilde{\sigma}_j(i)$. We conclude that Φ is injective (as a consequence of Lemma 2.9.8).

Using Lemma 2.9.9 and Lemma 2.9.8, it remains to show that every i^{th} coboundary $\tilde{\Sigma} = (\tilde{\sigma}_h : \ldots : \tilde{\sigma}_0)$ defines an i^{th} coboundary trace a of Σ with $a_j = \tilde{\sigma}_j(i)$. Both the conditions

$$\tilde{\sigma}_0(i) = i+1 \qquad \text{and} \qquad \tilde{\sigma}_j(i) \neq \tilde{\sigma}_{j-1}(i) \text{ at least once}$$

are clearly satisfied; it remains to prove (ii) and (iii).

In order to show condition (ii) of Definition 2.9.2, let $\tilde{\sigma}_{j-1}(i) \neq \tilde{\sigma}_j(i) = \tilde{\tau}_j(\tilde{\sigma}_{j-1}(i))$. But $\tilde{\sigma}_{j-1}(i) \neq i \neq \tilde{\sigma}_j$ by Proposition 2.8.12, hence $\tau_j(i) = i$. Now, by Proposition 2.3.10,

$$\tau_j = D_i(\tilde{\tau}_j(i\ \tilde{\sigma}_{j-1}(i))) = D_i(\tilde{\tau}_j)\,, \qquad \text{hence} \qquad \tilde{\tau}_j = S_i\tau_j\,.$$

We have shown that

$$\tilde{\sigma}_j(i) \neq \tilde{\sigma}_{j-1}(i) \qquad \text{implies} \qquad \tilde{\sigma}_j(i) = \tilde{\tau}_j(\tilde{\sigma}_{j-1}(i)) = (S_i\tau_j)(\tilde{\sigma}_{j-1}(i))\,.$$

It remains to proof condition (iii) of Definition 2.9.2. By assumption, $\tilde{\Sigma}$ is an inner cell, so $\tilde{\tau}_j = (i\ c)$ for at least one j with $c \neq \tilde{\sigma}_{j-1}(i)$ by Proposition 2.8.12. We have

$$\tau_j = D_i(\tilde{\tau}_j(i\ \tilde{\sigma}_{j-1}(i))) \qquad \text{hence} \qquad S_i\tau_j = (c\ \tilde{\sigma}_{j-1}(i))$$

and therefore

$$(S_i\tau_j)(\tilde{\sigma}_{j-1}(i)) = c \neq \tilde{\sigma}_{j-1}(i)\,.$$

□

The next proposition states in what sense two cofaces might differ.

Proposition 2.9.12. *Let $\Sigma = (\tau_h \mid \ldots \mid \tau_1)$ and $\Sigma' = (\tau'_h \mid \ldots \mid \tau'_1)$ be cells of bidegree (p,h) that have their i^{th} face in common. If we assume $\sigma_j(i) = \sigma'_j(i)$ for all j then $\Sigma = \Sigma'$. In any case, the transpositions τ_j and τ'_j satisfy*

(1) If $\tau_j(i) = i = \tau'_j(i)$, then

$$\tau'_j = \tau_j\,.$$

(2) Otherwise we can assume without loss of generality $\tau_j = (i\ c)$.

(2.1) If in addition $\sigma_{j-1}(i) = \sigma'_{j-1}(i)$, then

$$\tau'_j = (\sigma_{j-1}(i)\ c) \qquad \text{or} \qquad \tau'_j = (i\ c)\,.$$

(2.2) If in addition $\sigma_{j-1}(i) \neq \sigma'_{j-1}(i)$, then

$$\tau'_j = (\sigma_{j-1}(i)\ c) \qquad \text{or} \qquad \tau'_j = (i\ \sigma_{j-1}(i))\,.$$

Proof. The first statement is Lemma 2.9.8, so we concentrate on the second one. We denote the i^{th} face of the above cells by $d''_i(\Sigma) = (\bar{\tau}_q \mid \ldots \mid \bar{\tau}_1)$ and omit the subscripts since j is fixed. Identifying the permutations in $\mathfrak{S}_{p-1}$ with their image under the i^{th} pseudo degeneracy $S_i\colon \mathfrak{S}_{p-1} \hookrightarrow \mathfrak{S}_p$, Proposition 2.3.10 yields

$$\bar{\tau} = \tau \qquad \text{for } \tau(i) = i\,, \tag{2.4}$$

$$\bar{\tau} = (\sigma(i)\ c) \neq \mathrm{id} \qquad \text{for } \tau = (i\ c)\,, \tag{2.5}$$

This implies (1). The cases (2.1) and (2.2) follow immediately from

$$(\sigma(i)\ c) \overset{(2.5)}{=} \bar{\tau} = \bar{\tau}' = \begin{cases} \tau' & \text{for } \tau'(i) = i \text{ by (2.4)} \\ (\sigma'(i)\ c') & \text{for } \tau'(i) \neq i \text{ by (2.5)} \end{cases},$$

since for $(\sigma(i)\ c) = (\sigma(i)'\ c')$, equation (2.5) yields

$$\tau' = \begin{cases} (i\ c) & \text{for } \sigma(i) = \sigma'(i) \\ (i\ \sigma(i)) & \text{for } \sigma(i) \neq \sigma'(i) \end{cases}.$$

□

2.9.2. The Dual of κ

The map π^* is the canonical inclusion and we understood the horizontal coboundary operator $(\partial'')^*$ in terms of coboundary traces via Proposition 2.9.7. It remains to gain some insights on the dual of κ.

Definition 2.9.13. Let a and b be positive integers. Denote $J_a^b = (b, b-1, \ldots, a+1, a)$ for $a \leq b$ and let $J_a^b = ()$ be the empty sequence for $a > b$. The set of κ^***-sequences** is

$$\Lambda_1^*\{()\} \qquad \text{and by concatenation} \qquad \Lambda_{n+1}^* = \Lambda_n^*.\{J_1^n, \ldots, J_n^n, J_{n+1}^n\}\,.$$

For a κ^*-sequence $J = (i_1, \ldots, i_k)$ we set

$$\kappa_J^* = \Upsilon_{i_1}^* \circ \ldots \circ \Upsilon_{i_k}^*\,.$$

Lemma 2.9.14. *The map κ^* is the alternating sum of all κ^*-sequences:*

$$\kappa_h^* = \sum_{(i_1,\ldots,i_k)\in\Lambda_h^*} (-1)^k \kappa_{(i_1,\ldots,i_k)}^*\,.$$

Proof. This is just the dual statement of Lemma 2.8.11. □

To get our hands on κ^*, we have to understand Υ_j^*. From the definition of the factorization map and κ^*, it suffices to examine the image of a cell $(\tau_2 \mid \tau_1)$ of bidegree $(p, 2)$ with $p = 2, 3, 4$ under $\Upsilon = \Upsilon_1$.

Lemma 2.9.15. *We have*

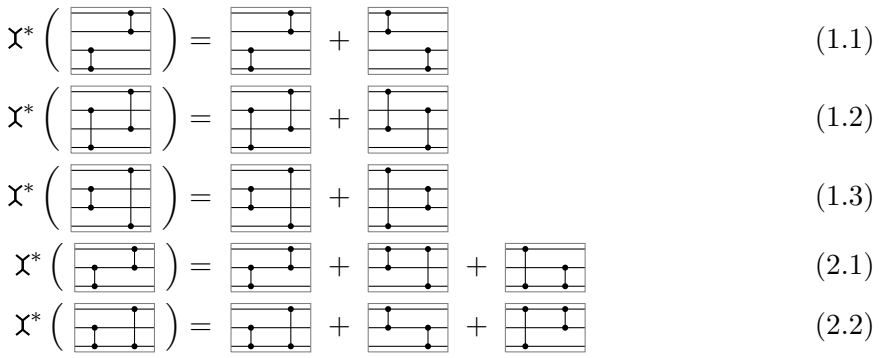

(1.1)

(1.2)

(1.3)

(2.1)

(2.2)

and for every Σ not listed above we have

$$\Upsilon^*(\Sigma) = 0 \tag{3}$$

Proof. This is follows directly from a case-by-case analysis of $\Upsilon(\tau_2 \mid \tau_1)$ for all inner cells of bidegree $(p, 2)$ with $p = 2, 3, 4$. □

Lemma 2.9.16. *Let $\Sigma = (\tau_q \mid \ldots \mid \tau_1)$ be an inner cell with $\mathrm{ht}(\tau_{j+1}) > \mathrm{ht}(\tau_j)$ for some $q > j \geq 1$. Then*

$$\Upsilon_j^*(\Sigma) = 0\,.$$

Proof. This follows immediately from the definition of the factorization map or from the lemma above. □

Definition 2.9.17. Let Σ be a top dimensional cell. A κ^*-sequence $I \in \Lambda^*$ is **relevant** if $\kappa_I^*(\Sigma) \neq 0$ and **irrelevant** else. The set of relevant κ^*-sequences with respect to Σ is denoted by R^Σ.

The next lemma will become handy in the study of homology operations see Chapter 4. It states that every relevant κ^*-sequences of a cell pictured in Figure 2.32 is (up to a canonical shift) the concaternation of κ^*-sequences of Σ' and Σ''

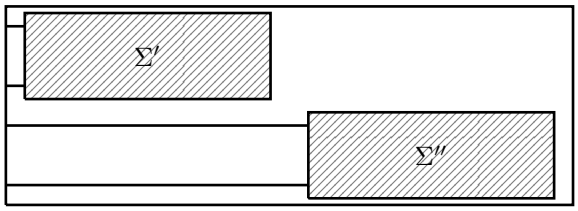

Figure 2.32.: This cell might be seen as the product of Σ' and Σ'' (see Definition 4.1.2).

Lemma 2.9.18. *Consider a top dimensional cell* $\Sigma = (\tau_{t+q} \mid \ldots \mid \tau_{t+1} \mid \tau_t \mid \ldots \mid \tau_1)$ *with*

$$\operatorname{supp}(\tau_t, \ldots, \tau_1) \subseteq \{\underline{1}, \ldots, \underline{s}\} \qquad \textit{and} \qquad \operatorname{supp}(\tau_{t+q}, \ldots, \tau_{t+1}) \subseteq \{\underline{s+1}, \ldots, \underline{s+p}\}\,.$$

Then, the set of relevant κ^**-sequences with respect to* Σ *is the concatenation*

$$R^\Sigma = R^{(\tau_t|\ldots|\tau_1)}.S_t R^{(\tau_{t+q}|\ldots|\tau_{t+1})}\,,$$

where S_t *is defined on* κ^**-sequences to be* $S_t(i_1, \ldots, i_k) = (t + i_1, \ldots, t + i_k)$.

Proof. The supports of $\tau_{t+q}, \ldots, \tau_{t+1}$ and $\tau_t, \ldots, \tau_1$ satisfy the inequality

$$\min \operatorname{supp}(\tau_{t+q}, \ldots, \tau_{t+1}) > \max \operatorname{supp}(\tau_t, \ldots, \tau_1)$$

and so does every term of $\kappa_I^*(\Sigma)$ for I a relevant κ^*-sequence (compare Lemma 2.9.15). Then, by Lemma 2.9.16, there is not a single κ^*-sequence $(i_1, \ldots, i_k)$ with $i_j = t$ for some j. Therefore every relevant κ^*-sequence $I \in R^\Sigma$ is the concatenation of two relevant κ^*-sequences $I \in R^{(\tau_t|\ldots|\tau_1)}.S_t R^{(\tau_{t+q}|\ldots|\tau_{t+1})}$ and vice versa. □

2.9.3. The dual Ehrenfried complex of $\mathfrak{M}_{1,1}^0$.

The following example is indented to give the reader a better understanding for explicit computations. We consider the dual Ehrenfried complex associated with the moduli space $\mathfrak{M}_{1,1}^0$ of genus one surfaces with one boundary component and no punctures. Here, we use the trivial partition $r = (1)$. Recall that the orientation coefficients $\mathcal{O}$ are constant since $m \leq 1$, so we drop them in the notation. Clearly,

$$h = 2g - 2 + m + n + r_1 + \ldots + r_n = 2$$

and therefore we have cells in range $2 = h \leq p \leq 2h = 4$. We show that the homology of the moduli space $\mathfrak{M}_{1,1}^0$ is

$$H_*(\mathfrak{M}_{1,1}^0; \mathbb{Z}) \cong H^{4-*}(\mathbb{E}^*; \mathcal{O}) \cong \begin{cases} \mathbb{Z} & * = 0 \\ \mathbb{Z} & * = 1 \\ 0 & else \end{cases}.$$

Recall that a p-cell Σ in the (dual) Ehrenfried complex is $\Sigma = (\tau_2 \mid \tau_1)$ with $\tau_1, \tau_2 \in \mathfrak{S}_p^\times$ such that the following two conditions are satisfied. Let us write $\tau_i = (a_i\ b_i)$ with $a_i > b_i$. We require

$$a_2 \geq a_1 \tag{2.6}$$

and

$$\tau_2\tau_1(0\ 1\ \ldots\ p) \quad \text{has exactly one cycle}\,. \tag{2.7}$$

Therefore, we have exactly one 2-cell

$$e_1 = \quad ,$$

we have exactly two 3-cells

$$f_1 = \qquad \text{and} \qquad f_2 =$$

and we have exactly one 4-cell

$$g_1 = \quad .$$

Let us compute the transformation matrices of the dual Ehrenfried complex.

$$\mathbb{Z}\langle e_1\rangle \xrightarrow{(\partial_{\mathbb{E}}^*)_2} \mathbb{Z}\langle f_1, f_2\rangle \xrightarrow{(\partial_{\mathbb{E}}^*)_3} \mathbb{Z}\langle g_1\rangle \tag{2.8}$$

The coboundary map $\partial_{\mathbb{E}}^*$ is computed as the composition $\partial_{\mathbb{E}}^* = \kappa^*\partial_{\mathbb{K}}^*\pi^*$. The map π^* is the canonical inclusion. Using either the geometric idea of the cofaces or listing all coboundary traces we compute

$$d_1^*(\ \ ) = \quad +$$

and

$$d_2^*(\ \ ) = \quad + \quad .$$

By construction $\partial_{\mathbb{K}}^* = \sum_{i=1}^{p-1}(-1)^i d_i^*$ therefore

$$\partial_{\mathbb{K}}^*(\ \ ) = - \quad + \quad .$$

The map κ^* is the sum all κ^*-sequences (compare Lemmata 2.9.14 and 2.8.11). Therefore we use Lemma 2.9.15 to conclude that the transformation matrix of the second coboundary $\partial_{\mathbb{E}}^*$ is

$$(\partial_{\mathbb{E}}^*)_2 = \begin{pmatrix} 2 \\ 1 \end{pmatrix} .$$

By the same arguments, the transformation matrix of the third coboundary $\partial_{\mathbb{E}}^*$ vanishes.

Now, diagram (2.8) is seen to be

$$\mathbb{Z}\langle e_1\rangle \xrightarrow{\begin{pmatrix} 2 \\ 1 \end{pmatrix}} \mathbb{Z}\langle f_1, f_2\rangle \xrightarrow{\begin{pmatrix} 0 & 0 \end{pmatrix}} \mathbb{Z}\langle g_1\rangle$$

thus the homology of the moduli space $\mathfrak{M}^0_{1,1}$ is

$$H_*(\mathfrak{M}^0_{1,1};\mathbb{Z}) \cong H^{4-*}(\mathbb{E}^*;\mathcal{O}) \cong \begin{cases} \mathbb{Z} & *=0 \\ \mathbb{Z} & *=1 \\ 0 & else \end{cases}.$$

2.9.4. Classification of the Cells of the Ehrenfried Complex

In this subsection, we encode the geometric ideas presented in the first paragraphs of Section 2.9 in order to study cofaces that are obtained by glueing a stripe inbetween two slits of the same height. As we concentrate on the Ehrenfried complex $\mathbb{E}$ (and its dual), we are only interested in top dimensional cells of the bicomplex. Hence the position of a stripe, which is about to be glued in, is just a coordinate (j,i) with $h \geq j \geq 1$ and $p \geq i \geq 1$. Proposition 2.9.23 states that glueing in different stripes is commutative (up to relabeling the heights). A cell that does not arise from such a process will be called thin and Proposition 2.9.26 states that every cell of $\mathbb{E}$ is uniquely obtained from a thin cell by such an expansion.

Definition 2.9.19. Consider a cell $\Sigma \in \mathbb{E}$. An i^{th} coboundary trace $(a_h \mid \ldots \mid a_1)$ is **basic** it there exists an index j with

(i) $a_{j-1} = \ldots = a_0 = i+1$,

(ii) $a_j = (S_i\tau_j)(a_{j-1}) \neq a_{j-1}$ (i.e. $\tau_i = (i\ d_i^\Delta(a_j))$) and

(iii) $a_{k+1} = (S_i\tau_{k+1})(a_k)$ for $h \geq k \geq j$.

In this case, the coface $a.\Sigma$ is called **basic expansion** of Σ.

Lemma 2.9.20. *Let $a = (a_h : \ldots : a_0)$ be a basic coboundary trace of Σ. Then, the j mentioned in Definition 2.9.19 is unique and $(a_h : \ldots : a_0)$ is an i^{th} coboundary trace with $i = \tau_j(d_i^\Delta(a_j))$. Moreover,*

$$a.\Sigma = (S_i\tau_h \mid \ldots \mid S_i\tau_j \mid S_{i+1}\tau_{j-1} \mid \ldots \mid S_{i+1}\tau_1)\,. \tag{2.9}$$

Proof. The index j is clearly unique and a_j fulfills $a_j = (S_i\tau_j)(i+1) \neq i+1$, so $a_j = s_i^\Delta(\tau_j(i))$ or equivalently $d_i^\Delta(a_j) = \tau_j(i)$.

Equation (2.9) is readily verified using Definitions 2.9.5 and 2.9.19. □

Lemma 2.9.21. *For $\Sigma \in \mathbb{E}_p$, the set $Btrace(\Sigma)$ of basic coboundary traces is in one-to-one correspondence to the disjoint union*

$$Bsupp(\Sigma) = \coprod_{h \geq j \geq 1} \operatorname{supp}(\tau_j) \cap \operatorname{supp}(\tau_{j-1}, \ldots, \tau_1)\,,$$

where $(a_h : \ldots : a_0) \in Btrace(\Sigma)$ is mapped to the unique index i in the j^{th} component, with j and $i = \tau_j(d_i^\Delta(a_j))$ as in Lemma 2.9.20. In particular, the number of basic coboundary traces is

$$|Btrace(\Sigma)| = |Bsupp(\Sigma)| = 2h - p\,.$$

Proof. By Definitions 2.9.2 and 2.9.19, the sequence $(a_h : \ldots : a_0)$ is a basic coboundary trace with respect to j if and only if

(i) $a_{j-1} = \ldots = a_0 = i + 1$,

(ii) $a_k \neq (S_i\tau_k)(a_{k-1})$ at least once,

(iii) $a_j = (S_i\tau_j)(a_{j-1})$ and

(iv) $a_k = (S_i\tau_k)(a_{k-1})$ for $h \geq k > j$.

Thus, the indicated map is a bijection $Btrace(\Sigma) \cong Bsupp(\Sigma)$.

A symbol i occures in $Bsupp(\Sigma)$ exactly k times if and only if it is in the support of exactly $k + 1$ transpositions. Thus

$$\begin{aligned}\left|\coprod_{h\geq j\geq 1} \operatorname{supp}(\tau_j) \cap \operatorname{supp}(\tau_{j-1}, \ldots, \tau_1)\right| &= \sum_i \left(\left(\sum_j |\{i\} \cap \operatorname{supp}(\tau_j)|\right) - 1\right) \\ &= \left(\sum_{i,j} |\{i\} \cap \operatorname{supp}(\tau_j)|\right) - p \\ &= \left(\sum_j |\operatorname{supp}(\tau_j)|\right) - p \\ &= 2h - p\,.\end{aligned}$$

□

Notation 2.9.22. In order to forumlate Proposition 2.9.23 we introduce yet another notation. We want to ignore the index shifts that occures if we compare $Bsupp(\Sigma)$ with $Bsupp(a.\Sigma)$ for a basic coboundary trace $a = (a_h : \ldots : a_0)$: It suffices to compare the relative index in the support of every transposition. For $s_j = \operatorname{supp}(\tau_j) \cap \operatorname{supp}(\tau_{j-1}, \ldots, \tau_1)$, we have $|s_j| \leq 2$. Thus we write

$$s_j \ni c = j^\varepsilon \qquad \text{with} \qquad \varepsilon = \begin{cases} 0 & c = \min(s_j) \\ 1 & c = \max(s_j) \end{cases} \qquad \text{and identify} \qquad j^0 = j^1 \quad \text{if} \quad |s_j| = 1\,.$$

Using the bijection in Lemma 2.9.21, we write $a(j^\varepsilon)$ for the basic coboundary trace corresponding to $j^\varepsilon \in Bsupp(\Sigma)$ and denote by $j^\varepsilon.\Sigma$ the coboundary $a(j^\varepsilon).\Sigma$.

Proposition 2.9.23. *Using the above notation, let $j^\varepsilon \in Bsupp(\Sigma)$. Then*

$$Bsupp(j^\varepsilon.\Sigma) = Bsupp(\Sigma) - \{j^\varepsilon\}\,. \tag{2.10}$$

Moreover, basic expansions commute, i.e. for two distinct basic coboundary traces $j_1^{\varepsilon_1}$ and $j_2^{\varepsilon_2} \in Bsupp(\Sigma)$, we have

$$j_2^{\varepsilon_2}.(j_1^{\varepsilon_1}.\Sigma) = j_1^{\varepsilon_1}.(j_2^{\varepsilon_2}.\Sigma)\,. \tag{2.11}$$

Proof. Using Lemma 2.9.20, we have

$$a(j^\varepsilon).\Sigma = (S_i\tau_h \mid \ldots \mid S_i\tau_j \mid S_{i+1}\tau_{j-1} \mid \ldots \mid S_{i+1}\tau_1) = (\tilde{\tau}_h \mid \ldots \mid \tilde{\tau}_1)$$

for $i = \tau_j(d_i^\Delta(a_j))$. Up to an order preserving renaming of the symbols, we have

$$\mathrm{supp}(\tilde{\tau}_k) \cap \mathrm{supp}(\tilde{\tau}_{k-1}, \ldots, \tilde{\tau}_1) = s_i^\Delta(\ \mathrm{supp}(\tau_k) \cap \mathrm{supp}(\tau_{k-1}, \ldots, \tau_1)\ )$$

if i is not in the support of τ_k. Otherwise a case by case analysis yields

$$\mathrm{supp}(\tilde{\tau}_k) \cap \mathrm{supp}(\tilde{\tau}_{k-1}, \ldots, \tilde{\tau}_1) = \begin{cases} s_{i+1}^\Delta(\ \mathrm{supp}(\tau_k) \cap \mathrm{supp}(\tau_{k-1}, \ldots, \tau_1)\ ) & \text{for } k < j \\ s_i^\Delta(\ (\mathrm{supp}(\tau_k) \cap \mathrm{supp}(\tau_{k-1}, \ldots, \tau_1)\ ) - \{i+1\} & \text{for } k = j \\ s_i^\Delta(\ \mathrm{supp}(\tau_k) \cap \mathrm{supp}(\tau_{k-1}, \ldots, \tau_1)\ ) & \text{for } k > j \end{cases},$$

and (2.10) is an immediate consequence.

The commutativity (2.11) follows from (2.10) and the behaviour of the bijection $Bsupp(\Sigma) = Btrace(\Sigma)$ in Lemma 2.9.21. □

Definition 2.9.24. Consider a cell $\Sigma \in \mathbb{E}$ and a non-empty subset $J = \{j_1^{\varepsilon_1}, \ldots, j_t^{\varepsilon_t}\} \subseteq Bsupp(\Sigma)$. The cell

$$J.\Sigma = j_1^{\varepsilon_1}. \cdots .j_t^{\varepsilon_t}.\Sigma$$

is called an **expansion** of Σ.

Definition 2.9.25. A cell $\Sigma \in \mathbb{E}$ that is not an expansion of some other cell is called **thin**. The set of thin cells is $Thin_{g,n}^m[(r_1, \ldots, r_n)]$.

Proposition 2.9.26. *Every cell $\Sigma \in \mathbb{E}$ is a unique expansion of a thin cell, i.e. denoting the power set operator by $\mathcal{P}ow$, there is a bijection*

$$ex\colon \coprod_{\Sigma \in Thin_{g,n}^m[(r_1,\ldots,r_n)]} \mathcal{P}ow(Bsupp(\Sigma)) \longrightarrow Cells(\mathbb{E}) \qquad \text{with} \qquad Bsupp(\Sigma) \supseteq J \longmapsto J.\Sigma\,.$$

Proof. The expansion map ex is surjective by the definition of thin cells.

In order to proof injectivity, consider thin cells $\tilde{\Sigma}$ and $\tilde{\Sigma}'$ together with $J \subseteq Bsupp(\tilde{\Sigma})$ of minimal size and some $K \subseteq Bsupp(\tilde{\Sigma}')$ such that $J.\tilde{\Sigma} = K.\tilde{\Sigma}'$. We show that J has to be empty to deduce $\tilde{\Sigma} = K.\tilde{\Sigma}'$, so K is also empty (because $\tilde{\Sigma}$ is thin).

Assume J is non-empty and consider $j^\varepsilon \in J$ and $k^\delta \in K$. We denote

$$\Sigma = (J - \{j^\varepsilon\}).\tilde{\Sigma} = (\tau_h \mid \ldots \mid \tau_1) \qquad \text{and} \qquad \Sigma' = (K - \{k^\delta\}).\tilde{\Sigma}' = (\tau_h' \mid \ldots \mid \tau_1')\,.$$

By assumption,

$$j^\varepsilon.\Sigma = (S_a\tau_h \mid \ldots \mid S_a\tau_j \mid S_{a+1}\tau_{j-1} \mid \ldots \mid S_{a+1}\tau_1) \tag{2.12}$$

$$= (S_b\tau_h' \mid \ldots \mid S_b\tau_k' \mid S_{b+1}\tau_{k-1}' \mid \ldots \mid S_{b+1}\tau_1') = k^\delta\Sigma' \tag{2.13}$$

for some unique a and b.

Here, $a = b$ is impossible: If $j = k$, the index set J was clearly not minimal, but for $j > k$, we have $S_{a+1}\tau_k = S_a\tau_k'$ with $a \in \mathrm{supp}(\tau_k)$ by (ii) in Definition 2.9.19, so $\mathrm{supp}(S_{a+1}\tau_k) \not\ni a+1 \in \mathrm{supp}(S_a\tau_k')$.

Without loss of generality, let $a < b$. Similar to the previous consideration, $a + 1 = b$ and $j > k$ must not hold at once as otherwise $S_a\tau_j = S_b\tau'_j = S_{a+1}\tau'_j$ with $\mathrm{supp}(S_{a+1}\tau_j) \ni a + 1 \notin \mathrm{supp}(S_{a+1}\tau'_j)$.

Now that we excluded all troublesome cases, the transpositions of $j^\varepsilon.\Sigma$ and $k^\delta.\Sigma'$ at the l^{th} spot are

$$S_c\tau_l = S_d\tau'_l$$

for appropriate $c < d$. We deduce

$$S_d\tau'_l = S_cS_{d-1}\tau'' \qquad \text{with} \qquad \tau''_l = D_c\tau'_l \neq 1_{\mathfrak{S}}$$

as (by the identities in Proposition A.8)

$$S_c\tau_l = S_cD_cS_c\tau_l \qquad \text{and} \qquad D_cS_d\tau''_l = S_{d-1}D_c\tau'_l\,.$$

Substituting the transpositions of $k^\delta.\Sigma'$ in equation (2.13), it is readily seen that J was not minimal. □

3. Cluster Spectral Sequence

We assume that the reader is familiar with spectral sequences. There are several introductions to the theory of spectral sequences and we recommend working through [Wei95, Chapter 5] or [Spa94, Chapter 9].

As before, we discuss the parallel and radial slit complex $P(h, m; r_1, \ldots, r_n)$ and $R(h, m, n)$ at once. In order to have a compact notation, we concentrate on the parallel case and we keep g, n, m and $(r_1, \ldots, r_n)$ fixed. The double complex is denoted by $P_{\bullet,\bullet} = P_{\bullet,\bullet}(h, m, ; r_1, \ldots, r_n)$, the relative bicomplex associated with a fixed $P_{\bullet,\bullet}(h, m, ; r_1, \ldots, r_n)$ is $\mathbb{P}_{\bullet,\bullet} = (P/P')_{\bullet,\bullet}$ and the corresponding Ehrenfried complex is $\mathbb{E} = \mathbb{E}_\bullet(h, m; r_1, \ldots, r_n)$.

In this chapter, we follow [Böd14]. We define a filtration on the bicomplex $\mathbb{P}_{\bullet,\bullet}$ inducing a filtration on the Ehrenfried complex $\mathbb{E}_\bullet$. In both cases, we obtain a first quadrant spectral sequence which collapses at the second page.

3.1. The Cluster-Filtration on $\mathbb{P}_{\bullet,\bullet}$ and $\mathbb{E}_\bullet$

The upcoming filtration is inspired by the following observation. For a surface F and a potential function u, we obtain the critical graph $\mathcal{K}_0$ on F. Observe that $\mathcal{K}_0$ is connected. Removing all poles and punctures from $\mathcal{K}_0$ yields a possibly disconnected graph $\mathcal{K}_-$ with c connected components. We imagine the horizontal and vertical face operators, which were defined on slit domains, as follows. The critical flow lines and the equipotential lines which run through the stagnation points indicate vertical and horizontal stripes. Each vertical or horizontal face operator collapses its corresponding stripe. Let us assume that the surface, which results from a single collapse, is non-degenerate in order to study how $\mathcal{K}_-$ is altered. It is readily seen that vertical faces leave the number of connected components of $\mathcal{K}_-$ fixed since vertical faces only collapse edges inside $\mathcal{K}_-$. The horizontal face operator collapses a horizontal stripe l along an equipotential line. Therefore, it identifies the edges of $\mathcal{K}_-$ which form the upper margin of l with the edges of $\mathcal{K}_-$ that form the lower margin of l. The number of connected components of the new graph is therefore at most c and at least $c - 1$. Keeping this in mind, following definitions and lemmata are straightforward.

Definition 3.1.1. Consider a cell $\Sigma = (\sigma_q : \ldots : \sigma_0) = (\tau_q \mid \ldots \mid \tau_1) \in \mathbb{P}_{p,q}$ with respect to $[p] = \{\underline{0}_1, \ldots, \underline{p}_1, \ldots, \underline{0}_r, \ldots, \underline{p}_r\}$. On $[p]$, we declare a relation $\sim_{\mathrm{CL}}$ as follows.

$$i \sim_{\mathrm{CL}} i' \quad \text{if} \quad i \text{ and } i' \text{ are in the same cycle of some } \tau_j.$$

The transitive closure of $\sim_{\mathrm{CL}}$ is an equivalence relation. Equivalence classes are called **(index) cluster** of Σ. The number $c(\Sigma) = c$ of equivalence classes is called the **cluster number** of Σ and we set $c(0) = 0$.

Remark 3.1.2. Obviously, we have $1 \leq c(\Sigma) \leq h$ for every generator Σ.

Definition 3.1.3. The modules of the bicomplex $\mathbb{P}$ are filtred as follows. For $c = 1, \ldots, h$, let

$$F_c\mathbb{P}_{p,q} = \langle \Sigma \quad \text{with} \quad c(\Sigma) \leq c \rangle .$$

This filtration of the chain modules is a filtration of the chain complex by the next lemma.

Lemma 3.1.4. *For a generator $\Sigma \in \mathbb{P}_{p,q}$ we have*

(i) $c(d'_j(\Sigma)) = c(\Sigma)$ *for all* j *and*

(ii) $c(\Sigma) - 1 \leq c(d''_i(\Sigma)) \leq c(\Sigma)$ *for all* $i \in [p]$,

if the faces are non-degenerate and therefore generators.

Proof. The index set $[p]$ of a non-degenerate vertical face $d'_j(\Sigma)$ agrees with the index set of Σ. In fact, the equivalence relation $\sim_{\mathrm{CL}}$ coincides on these index sets.

The index set of a horizontal face $d''_{\underline{i}_k}(\Sigma)$ is reduced by one, namely — in the inhomogeneous notation — by identifying $\underline{i}_k$ with $\underline{i+1}_k$. This changes the number of clusters if and only if $\underline{i}_k \not\sim_{\mathrm{CL}} \underline{i+1}_k$, and obviously we have at most one cluster less.

Thus $c(\partial(\Sigma)) \leq c(\Sigma)$ and the filtration is a filtration of a chain complex. □

The definition of the equivalence relation $\sim_{\mathrm{CL}}$ on the index set $[p]$ of a cell Σ is valid for all non-degenerate cells Σ. In particular, we have a cluster number $c(\Sigma)$ defined for the generators of the Ehrenfried complex. We need to see how it behaves under the boundary operator $\partial_{\mathbb{E}}$. Recall that $\mathbb{E}$ is a quasi-isomorphic direct summand[1] of the total complex of $\mathbb{P}$. The projection π onto the top dimensional monotone cells is just the projection onto this summand. The inverse of π is κ, compare Section 2.8.

Definition 3.1.5. The modules of $\mathbb{E}$ are filtred as follows. For $c = 1, \ldots, h$, let

$$F_c\mathbb{E}_p = \langle \Sigma \quad \text{with} \quad c(\Sigma) \leq c \rangle .$$

This filtration of the chain modules is a filtration of the chain complex by the next lemma since $\partial_{\mathbb{E}} = \pi \circ \partial'' \circ \kappa$.

Lemma 3.1.6. *For a generator $\Sigma \in \mathbb{E}_p$ we have*

(i) $c(\pi(\Sigma)) = c(\Sigma)$ *and*

(ii) $c(\kappa(\Sigma)) = c(\Sigma)$.

This lemma is an immediate consequence of Section 2.8 as $\mathbb{E}$ is a direct summand of $Tot(\mathbb{P})$. However, we give another proof.

Proof. The projection π preserves the cluster number if Σ is monotone.

Recall that κ is the alternating sum of all κ-sequences

$$\kappa_{(j_1,\ldots,j_k)} = \curlywedge_{j_1} \circ \ldots \circ \curlywedge_{j_k}$$

[1] To be precise, the Ehrenfried complex is, up to a shift in the homological degree, identified with a direct summand. The inclusion induces an isomorphism in homology.

and $\curlywedge_l$ is the composition $\eta\mu$ of the multiplication μ with the factorability structure η, applied to $\tau_{j+1}|\tau_j$ in the h-tuple $\Sigma = (\tau_h \mid \ldots \mid \tau_1)$. Since $d'_j(\curlywedge_l(\Sigma)) = d'_j(\Sigma)$ for all $j = 1, \ldots, h-1$ it follows from (i) in Lemma 3.1.4, that $c(\curlywedge_l(\Sigma))$ is either zero or equal to the cluster number of Σ. Thus the same is true for iterations of these $\curlywedge_l$ for various l. In the linear combination $\kappa(\Sigma)$ all non-zero terms therefore have the same cluster number as Σ. Since Σ itself is such a term, claim (ii) follows. □

Proposition 3.1.7. *Let Σ be a generator in $\mathbb{P}$ or $\mathbb{E}$ and denote the respective boundary operator by $\partial = \partial_{\mathbb{P}}$ or $\partial_{\mathbb{E}}$. The cluster number of every non-vanishing term $\tilde{\Sigma}$ in $\partial(\Sigma)$ satisfies*

$$c(\Sigma) - 1 \leq c(\tilde{\Sigma}) \leq c(\Sigma)\,.$$

Proof. The claim is an immediate consequence of Lemmata 3.1.4 and 3.1.6 since $\partial_{\mathbb{E}} = \pi \circ \partial'' \circ \kappa$. □

3.2. The Cluster Spectral Sequence for $\mathbb{P}_{\bullet,\bullet}$ and $\mathbb{E}_\bullet$

Throughout this section, we fix a ring A. Consequently, we treat $\mathbb{P}$ and $\mathbb{E}$ as complexes over A.

Proposition 3.2.1. *Let g, n, m and $(r_1, \ldots, r_n)$ be given and set $h = 2g-2+m+n+r_1+\ldots+r_n$. There are two first quadrant spectral sequences*

$$E^0_{k,c}(\mathbb{P}) = \bigoplus_{p+q=k} [F_c\mathbb{P}_{p,q}(h, m; r_1, \ldots, r_n)/F_{c-1}\mathbb{P}_{p,q}(h, m; r_1, \ldots, r_n)]$$

converging towards

$$E^0_{k,c}(\mathbb{P}) \Rightarrow H_{k+c}(\mathbb{P}_{\bullet,\bullet}(h, m; r_1, \ldots, r_n); A)$$

and

$$E^0_{p,c}(\mathbb{E}) = F_c\mathbb{E}_p(h, m; r_1, \ldots, r_n)/F_{c-1}\mathbb{E}_p(h, m; r_1, \ldots, r_n)$$

converging towards

$$E^0_{p,c}(\mathbb{E}) \Rightarrow H_{p+c}(\mathbb{E}_\bullet(h, m; r_1, \ldots, r_n); A)\,.$$

Both spectral sequences collapse at the second page.

Proof. The existence of both spectral sequences is evident. Both complexes $\mathbb{P}$ and $\mathbb{E}$ are bounded, so the associated spectral sequence is first quadrant and convergent. The only non-trivial differentials are page zero and one by Proposition 3.1.7, see Lemma 3.2.3. □

Remark 3.2.2. If A is a field, then we have

$$H_*(\mathbb{E}_\bullet(h, m; r_1, \ldots, r_n); A) = \bigoplus_{p+c=*} E^2_{p,c}(\mathbb{E})\,.$$

This is one foundation of our computer-aided computations.

Lemma 3.2.3. *Consider a chain complex (C, ∂) with filtration F_cC and assume ∂ decreases the filtration degree by at most s. Then, the associated spectral sequence collapses at E^{s+1}.*

Proof. In order to prove the convergence theorem for reasonable filtred chain complexes (c.f. [Spa94, Chapter 9, Theorem 2]) one finds

$$Z^r_{p,c} = \{x \in F_pC_{p+c} \mid \partial x \in F_{p-r}C_{p+c-1}\}$$

and

$$E^r_{p,c} = Z^r_{p,c}/(Z^{r-1}_{p-1,c+1} + \partial(Z^{r-1}_{p+r-1,c-r+2}))\,.$$

The r^{th} differential $d^r_{p,c}\colon E^r_{p,c} \longrightarrow E^r_{p-r,c+r-1}$ is induced by ∂ since

$$\partial(Z^r_{p,c}) \subseteq Z^r_{p-r,c+r-1} \qquad \text{and} \qquad \partial(Z^{r-1}_{p-1,c+1} + \partial(Z^{r-1}_{p+r-1,c-r+2})) \subseteq \partial(Z^{r-1}_{p-1,c+1})\,.$$

For $r \geq s+1$, we assumed $\partial(Z^r_{p,c}) = 0$. We conclude $d^r = 0$ and $E^\infty = E^{s+1}$. □

3.3. The Cluster Spectral Sequence in Terms of Matrices

Let us study the differentials of the spectral sequence associated with the Ehrenfried complex. The presented arguments can be applied to $\mathbb{P}$ as well.

The Ehrenfried complex is a based chain complex and the cluster-filtration has a remarkable effect on the transformation matrices. We exploit this fact in our computer program, compare Section 6. The filtration of $\mathbb{E}$ is induced by a filtration of the bases elements. For each degree p, we regroup the basis elements with identical cluster number and order the groups ascendingly. The boundary operator reduces the filtration degree by at most one by Proposition 3.1.7. The p^{th} transformation matrix is therefore a block matrix.

$$\begin{pmatrix} d^0 & d^1 & & & \\ & d^0 & d^1 & & \\ & & d^0 & d^1 & \\ & & & & \ddots \end{pmatrix}$$

The submatrices d^0 or d^1 correspond to the differentials of the zeroth respectively first page. Observe that the second term E^2 is given by

$$\ker(d^1|_{\ker(d^0)})/\left[\operatorname{im}(d^0) + \operatorname{im}(d^1|_{\ker(d^0)})\right]\,.$$

For actual computation, it is worthwile to detect the homology via determining and diagonalizing the transformation matrix block by block.

4. Homology Operations

In this chapter, we discuss well-known homology operations defined on the space of parallel slit domains or the space of radial slit domains. We relate them via the parallelization and radialization map and realize them by cochainmaps using our formula for the coboundary operator.

4.1. Operations on $\mathfrak{Par}_1$ by Patching Slit Pictures

In this section, we review some of the homology operations provided by [Böd90b]. They are defined on the space of all parallel slit domains on exactly one level. In order to make the notation more compact, we write $\mathfrak{Par}_{g,1}^m = \mathfrak{Par}_{g,1}^m[(1)]$ and $\mathfrak{Par}_1 = \coprod_{g,m} \mathfrak{Par}_{g,1}^m$. The mentioned homology operations on $\mathfrak{Par}_1$ are induced by the action of a little cubes operad, namely of the ordered configuration spaces of the complex plane. The precise background on little cubes operads can be found in [May72].

The k^{th} ordered configuration space of the complex plane is

$$\tilde{C}^k = \tilde{C}^k(\mathbb{C}) = \{(z_1, \ldots, z_k) \in \mathbb{C}^k \mid z_i \neq z_j \text{ for } i \neq j\}$$

where the trivial configuration $() \in \tilde{C}^0$ is seen as the origin of the complex plane. Recall that the family of all configuration spaces $\left(\tilde{C}^k(\mathbb{C})\right)_{k\geq 0}$ constitutes an operad as follows: For a configuration $z = (z_1, \ldots, z_l) \in \tilde{C}^l$ and configurations $x^{(1)} \in \tilde{C}^{k_1}, \ldots, x^{(l)} \in \tilde{C}^{k_l}$, we continuously choose l paraxial disjoint squares of the same size centred at the points $z_1, \ldots, z_l$, in which we insert the configurations $x^{(1)}, \ldots, x^{(l)}$. This yields a configuration $\theta(z, x^{(1)}, \ldots, x^{(l)})$ in $\tilde{C}^{k_1+\ldots+k_l}$ (see Figure 4.1). The trivial configuration is seen as the origin of the complex plane and therefore serves as identity $\mathbb{1}$. Moreover, we have a canonical associativity law.

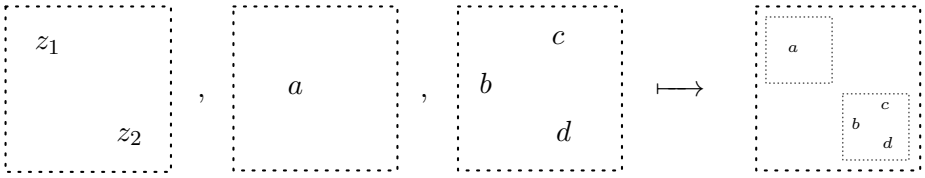

Figure 4.1.: The configuration spaces $\tilde{C}^k(\mathbb{C})$ define a little cubes operad.

Let us review the action of this little cube operad on the disjoint union $\mathfrak{Par}_1 = \coprod_{g,m} \mathfrak{Par}_{g,1}^m$ of all parallel slit domains with one boundary curve by defining

$$\tilde{\vartheta} \colon \tilde{C}^k \times \mathfrak{Par}_{g_1,1}^{m_1} \times \ldots \times \mathfrak{Par}_{g_k,1}^{m_k} \longrightarrow \mathfrak{Par}_{g,1}^m$$

with $g = g_1 + \ldots + g_k$ and $m = m_1 + \ldots + m_k$. Consider $(z_1, \ldots, z_k) \in \tilde{C}^k$ at which we want to place given slit pictures $L_1, \ldots, L_k$. In the naive approach, we continuously choose

k disjoint, paraxial squares of equal size B_i with center z_i in which we want to patch L_1, $\ldots, L_k$, but the insertion of a single slit picture implies the removal of certain slits and the introduction of glueing information. Ignoring this fact, we may produce degenerate slit configurations, compare Figure 4.2. In order to obtain non-degenerate slit pictures, we

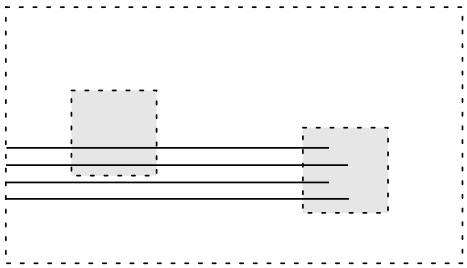

Figure 4.2.: The naive / wrong definition of the action of the little cubes operad does not respect the introduced slits.

have to alter our approach. The geometric idea is to insert the squares from the rightmost point z_{j_1} to to the leftmost point z_{j_k} one after another, by letting the box B_i float vertically from a point near infinity down to $x_i + \sqrt{-1} \cdot y_i$ while jumping through all slits it passes. We picture this process for $k = 2$ in Figure 4.3.

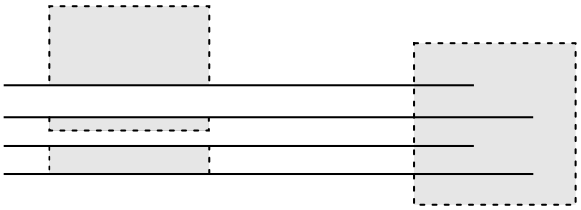

Figure 4.3.: The appropriate definition of the action of the little cubes operad.

From the geometric viewpoint, this is clearly an action of the little cubes operad; the details are discussed in [Böd90b, Section 3].

Theorem 4.1.1 ([Böd90b, Theorem 3.6.2])**.** *There are operations*

$$\tilde{\vartheta} \colon \tilde{C}^k \times \mathfrak{Par}_{g_1,1}^{m_1} \times \ldots \times \mathfrak{Par}_{g_k,1}^{m_k} \longrightarrow \mathfrak{Par}_{g,1}^{m}$$

with the following properties.

(i) (associativity) The diagram

$$\begin{array}{ccc} \tilde{C}^l \times (\tilde{C}^k \times \mathfrak{Par}_{g_1,1}^{m_1} \times \ldots \times \mathfrak{Par}_{g_k,1}^{m_k})^l & \xrightarrow{\mathrm{id} \times \tilde{\vartheta}^k} & \tilde{C}^l \times (\mathfrak{Par}_{g,1}^{m})^l \\ \downarrow{\scriptstyle \theta \times \mathrm{id}} & & \downarrow{\scriptstyle \tilde{\vartheta}} \\ \tilde{C}^{lk} \times (\mathfrak{Par}_{g_1,1}^{m_1} \times \ldots \times \mathfrak{Par}_{g_k,1}^{m_k})^l & \xrightarrow{\tilde{\vartheta}} & \mathfrak{Par}_{lg,1}^{lm} \end{array}$$

commutes for $g = g_1 + \ldots + g_k$ and $m = m_1 + \ldots + m_k$.

(ii) (equivariant associativity) If in addition $g_1 = \ldots = g_k$ and $m_1 = \ldots = m_k$ holds, then the above diagram commutes equivariantly with respect to permutations of the points in a given configuration in $\tilde{C}^k$ and permutations of the factors of $(\mathfrak{Par}^m_{g,1})^k$. In particular, dividing out the action of $\mathfrak{S}_k^\times = Aut(\{1,\ldots,k\})$ defines operations

$$\vartheta\colon \tilde{C}^k \times_{\mathfrak{S}_k^\times} (\mathfrak{Par}^m_{g,1})^k \longrightarrow \mathfrak{Par}^{km}_{kg,1}$$

such that the following diagram commutes

$$\begin{array}{ccc} \tilde{C}^l \times_{\mathfrak{S}_l^\times} (\tilde{C}^k \times_{\mathfrak{S}_k^\times} (\mathfrak{Par}^m_{g,1})^k)^l & \xrightarrow{\mathrm{id}\times\vartheta^k} & \tilde{C}^l \times_{\mathfrak{S}_l^\times} (\mathfrak{Par}^m_{g,1})^l \\ \downarrow{\scriptstyle \theta\times\mathrm{id}} & & \downarrow{\scriptstyle \vartheta} \\ \tilde{C}^{lk} \times_{\mathfrak{S}_l^\times k} ((\mathfrak{Par}^m_{g,1})^k)^l & \xrightarrow{\qquad\vartheta\qquad} & \mathfrak{Par}^{lm}_{lg,1} \end{array}$$

(iii) (unity) The composition

$$\mathfrak{Par}_1 \xrightarrow{\mathbb{1}\times\mathrm{id}} \tilde{C}^1 \times \mathfrak{Par}_1 \xrightarrow{\tilde{\vartheta}} \mathfrak{Par}_1$$

is homotopic to the identity.

Definition/Corollary 4.1.2. The restriction

$$\mu = \tilde{\vartheta}|_{(-1+i,1-i)}\colon \mathfrak{Par}_1 \times \mathfrak{Par}_1 \longrightarrow \mathfrak{Par}_1\,,$$

which places the first slit picture into the upper left and the second slit picture into the lower right (see Figure 4.4), equips $\mathfrak{Par}_1$ with the structure of an h-commutative, h-associativ, H-space which admits a two-sided h-unit, the trivial slit picture $\emptyset$.

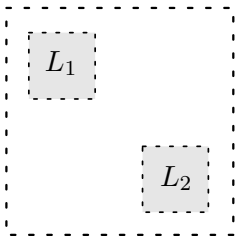

Figure 4.4.: Patching two slit pictures into the complex plane via μ.

Proof. By the above theorem, it remains to specify a homotopy which makes μ h-commutative. In $\tilde{C}^2$ we use some path joining the configurations $(-1+i, 1-i)$ and $(1-i, -1+i)$, so

$$\mu = \tilde{\vartheta}|_{(-1+i,1-i)} \simeq \tilde{\vartheta}|_{(-1+i,1-i)} = \mu \circ t$$

with t being the swapping map. □

Definition 4.1.3. Using the homology cross product we obtain a family of homology operations

$$\tilde{\vartheta}_*\colon H_s(\tilde{C}^k) \otimes H_{t_1}(\mathfrak{Par}^{m_1}_{g_1,1}) \otimes \ldots \otimes H_{t_k}(\mathfrak{Par}^{m_k}_{g_k,1}) \longrightarrow H_{s+t}(\mathfrak{Par}^{m}_{g,1})$$

defined by

$$\tilde{v} \otimes x_1 \otimes \ldots \otimes x_k \longmapsto \tilde{\vartheta}_\star(\tilde{v} \otimes x_1 \otimes \ldots \otimes x_k)$$

with $g = g_1 + \ldots + g_k$, $m = m_1 + \ldots + m_k$, $t = t_1 + \ldots + t_k$ and $\tilde{\vartheta}_\star$ the induced map in homology.

4.1.1. The Action of $\tilde{C}^2(\mathbb{C})$ on $\mathfrak{Par}_1$ in Detail

Throughout this thesis, we are mainly interested in the case $k = 2$ and we remark that this is not an actual restriction: The configuration spaces $\tilde{C}^k(\mathbb{C})$ serve as classifying spaces for the braid groups B^k on k strings whose homology is understood due to [CLM76]. The inclusion into the braid group B^∞ on infinitely many strings induces a monomorphism in homology and identifies the p-torsion $H_*(B^k; \mathbb{Z}/p\mathbb{Z})$ with a sub-polynomial-algebra generated by infinitely many generators $a_1, \ldots, b_1, \ldots$, where each generator is identified with $a_j = Q_1^{j-1}(a_1)$ or $b_j = \beta a_{j+1}$ with a_1 the distinguished generator in the first homology, Q_1^k an iterated Dyer–Lashof operation and β the Bockstein. The action of the Dyer-Lashof algebra is therefore determined by the action of $\tilde{C}^2(\mathbb{C})$. A more elaborate description of this fact can be found in the survey article [Ver98].

Note that the ordered configuration space $\tilde{C}^2$ defines a canonical two-fold covering over the unordered configuration space C^2 and this covering map is homotopic (as a covering) to the well-known covering $\mathbb{S}^1 \longrightarrow \mathbb{R}P^1$, by regarding the first point of an ordered configuration as (wandering) basepoint.

Definition 4.1.4. Under the above identification, we fix the generator $\tilde{v}_0 = [(-1+i, 1-i)] \in H_0(\tilde{C}^2)$ and the generator $\tilde{v}_1 \in H_1(\tilde{C}^2) = H_1(\mathbb{S}^1)$ which is represented by the identity map $\mathbb{S}^1 \longrightarrow \mathbb{S}^1$, compare Figure 4.5.

Figure 4.5.: The generators $\tilde{v}_0 \in H_0(\tilde{C}^2)$ and $\tilde{v}_1 \in H_1(\tilde{C}^2)$.

Definition/Corollary 4.1.5. The map μ defines the Pontryagin product

$$H_s(\mathfrak{Par}_1) \otimes H_t(\mathfrak{Par}_1) \longrightarrow H_{s+t}(\mathfrak{Par}_1)$$

denoted by

$$x \otimes y \longmapsto x\#y = \tilde{\vartheta}_*(\tilde{v}_0 \otimes x \otimes y)$$

which equips $\bigoplus_* H_*(\mathfrak{Par}_1)$ with the structure of a commutative, unital ring.

Definition 4.1.6. Using the distinguished homology class $\tilde{v}_1$, the Browder operation

$$R_1 \colon H_s(\mathfrak{Par}_1) \otimes H_t(\mathfrak{Par}_1) \longrightarrow H_{s+t+1}(\mathfrak{Par}_1)$$

is sketched in Figure 4.6 and defined by

$$R_1(x \otimes y) = \tilde{\vartheta}_*(\tilde{v}_1 \otimes x \otimes y)\,.$$

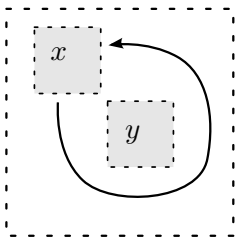

Figure 4.6.: We picture the Browder operation $R(x, y)$.

In order to define the Dyer–Lashof operations Q_0 and Q_1, we restrict ourselves either to homology classes x in $\mathfrak{Par}_1$ of even degree or to coefficients in the field $\mathbb{F}_2$. A direct computation shows that every chain $\tilde{w}$ in $\tilde{C}^2 \simeq \mathbb{S}^1$ which projects to a cycle w in the unordered configuration space $C^2 \simeq \mathbb{R}P^1$ defines a cycle $\tilde{w} \otimes x \otimes x$ in $\tilde{C}^2 \times_{\mathfrak{S}_2^\times} (\mathfrak{Par}^m_{g,1} \times \mathfrak{Par}^m_{g,1})$.

Definition 4.1.7. Using the homology cross product we obtain a family of homology operations

$$\vartheta_* \colon H_s(\tilde{C}^2) \otimes H_t(\mathfrak{Par}^m_{g,1}) \longrightarrow H_{s+2t}(\mathfrak{Par}^{2m}_{2g,1})$$

by

$$w \otimes x \longmapsto \vartheta_\star(\tilde{w} \otimes x \otimes x)$$

with $\tilde{w}$ a chain in $\tilde{C}^2$ which projects onto w and $\vartheta_\star$ the induced map in homology.

Definition 4.1.8. We fix the chains $\tilde{w}_0$ respectively $\tilde{w}_1$ in $\tilde{C}^2$ mapping to the distinguished non-vanishing classes in $H_0(C^2)$ respectively $H_1(C^2)$, compare Figure 4.7.

Figure 4.7.: The generators $w_0 \in H_0(C^2)$ and $w_1 \in H_1(C^2)$.

Definition 4.1.9. The Dyer–Lashof operations Q_0 and Q_1 are

$$Q_0 \colon H_t(\mathfrak{Par}^m_{g,1}) \longrightarrow H_{2t}(\mathfrak{Par}^{2m}_{2g,1}) \qquad \text{with} \qquad Q_0(x) = \vartheta_*(\tilde{w}_0 \otimes x \otimes x)$$

and

$$Q_1 \colon H_t(\mathfrak{Par}^m_{g,1}) \longrightarrow H_{2t+1}(\mathfrak{Par}^{2m}_{2g,1}) \qquad \text{with} \qquad Q_1(x) = \vartheta_*(\tilde{w}_1 \otimes x \otimes x)\,.$$

They are sketched in Figure 4.8.

Figure 4.8.: The Operations Q_0 and Q_1.

4.1.2. Formulas for Q_0, Q_1 and R_1

In this subsection, we remind ourselves of well-known formulas for the Dyer–Lashof operations Q_0, Q_1 and R_1 which hold for coefficients in the field $\mathbb{F}_2$, see [CLM76, Pages 214–218] or [Böd90b, Sections 4.3–4.5].

Proposition 4.1.10. *The operations Q_0 satisfy*

(i) (squaring)

$$Q_0(x) = x\#x = x^2\,,$$

(ii) (linearity)

$$Q_0(x+y) = Q_0(x) + Q_0(y)\,,$$

(iii) (multiplicativity)

$$Q_0(x\#y) = Q_0(x)\#Q_0(y)\,,$$

(iv) (stability)

$$Q_0(\rho x) = \rho^2(Q_0(x))$$

for $\rho = (\psi\phi)_*$ the stabilization map on Page 8,

(v) (units)

$$Q_0(1) = 1$$

for the respectively units in $H_0(\mathfrak{Par}^m_{g,1})$ or $H_0(\mathfrak{Par}^{2m}_{2g,1})$,

(vi) (Nishida relation)

$$Sq_{2t}(Q_0(x)) = Q_0(Sq_t(x))$$

and

$$Sq_{2t+1}(Q_0(x)) = 0$$

for Sq_t the dual Steenrod squares.

Proposition 4.1.11. *The operations Q_1 are not in general additive and the Browder operations measure this defect. They satisfy*

(i) (linearity)

$$Q_1(x+y) = Q_1(x) + R_1(x,y) + Q_1(y)\,,$$

(ii) (Cartan formula)

$$Q_1(xy) = x^2 Q_1(y) + xR_1(x,y)y + Q_1(y)y^2\,,$$

(iii) (nullification)

$$Q_1(1) = 0$$

for the unit in $H_0(\mathfrak{Par}^m_{0,1})$,

(iv) (Nishida relations)

$$Sq_{2t}(Q_1(x)) = Q_1(Sq_t(x)) + \sum_{\substack{i+j=2t\\ i<j}} R_1(Sq_i(x), Sq_j(x))$$

and

$$Sq_{2t+1}(Q_1(x)) = Q_0(Sq_t(x)) + \sum_{\substack{i+j=2t+1\\ i<j}} R_1(Sq_i(x), Sq_j(x))\,.$$

Proposition 4.1.12. *The Browder operations* R_1 *satisfy*

(i) (commutativity)

$$R_1(x,y) = R_1(y,x)\,,$$

(ii) (unit)

$$R_1(1,x) = 0 = R_1(x,1)$$

for the unit in $H_0(\mathfrak{Par}^m_{0,1})$,

(iii) (nullification)

$$R_1(x,x) = 0\,,$$

(iv) (Cartan formula)

$$R_1(xy, x'y') = xR_1(y,x')y' + R_1(x,x')yy' + xx'R_1(y,y') + x'R_1(x,y')y'\,,$$

(v) (Jacobi identity)

$$R_1(x, R_1(y,z)) + R_1(y, R_1(z,x)) + R_1(z, R_1(x,y)) = 0\,,$$

(vi) (Nishida relation)

$$Sq_t(R_1(x,y)) = \sum_{i+j=t} R_1(Sq_i(x), Sq_j(x))\,,$$

(vii) (Bockstein relation)

$$\beta R_1(x,y) = R_1(\beta x, y) + R_1(x, \beta y)\,,$$

(viii) (Ádem relations)

$$R_1(x, Q_0(y)) = 0 = R_1(Q_0(x), y)$$

and

$$R_1(x, Q_1(y)) = 0 = R_1(Q_1(x), y)\,.$$

4.2. Operations for Parallel Slit Domains on Several Levels

In this section, we propose a generalization of the above operations to parallel slit domains on several levels. Hereby, we imagine the parallel slit domains in question as slit pictures and surfaces with boundaries simultaneously. Consequently, we picture the product of two parallel slit domains $L_1 \in \mathfrak{Par}_{g_1,1}^{m_1}[(1)]$ and $L_2 \in \mathfrak{Par}_{g_2,1}^{m_2}[(1)]$ as follows. We view L_1 and L_2 as disjoint paraxial rectangles that miss several slits and identify them with the associated surfaces F_1 and F_2 which have exactly one boundary curve, see Figure 4.9.

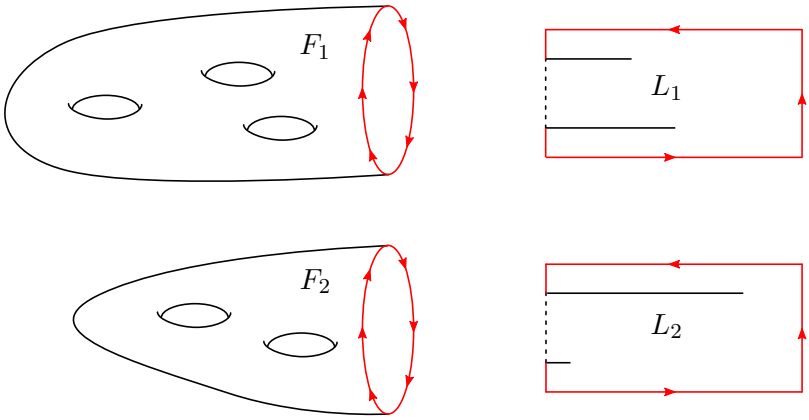

Figure 4.9.: Two surfaces with boundary and their associated parallel slit domains.

The slit picture $\mu(L_1, L_2)$ is obtained by glueing in a stripe which joins the top of L_2 with the bottom of L_1. The boundary of the surfaces F_1 respectively F_2 admits a distinguished arc c_2^+ respectively c_1^-, which corresponds to the top respectively bottom of the associated slit picture. Joining c_1^- with c_2^+ by glueing a stripe inbetween gives rise to the surface associated with $\mu(L_1, L_2)$, compare Figure 4.10. In order to define the glueing construction,

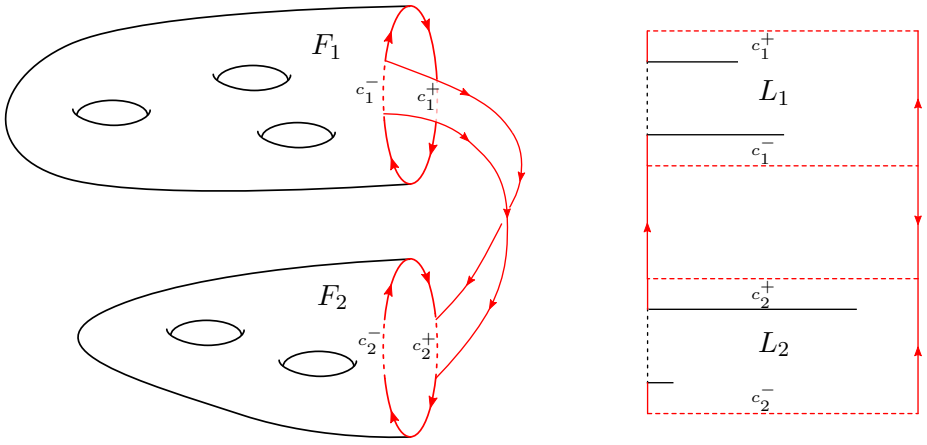

Figure 4.10.: The surface associated with the parallel slit domain $\mu(L_1, L_2)$.

we will think of two surfaces to stand opposite to each other, compare Figure 4.11.

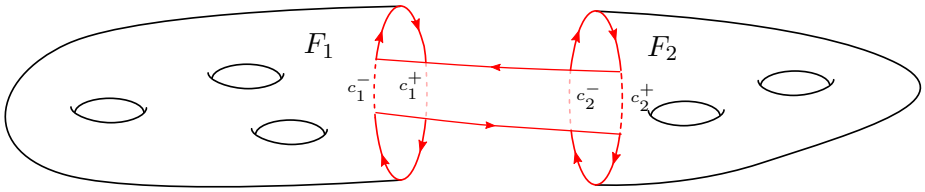

Figure 4.11.: The surface associated with the parallel slit domain $\mu(L_1, L_2)$.

4.2.1. The Glueing Construction

In order to treat the general case, consider a parallel slit domain $L \in \mathfrak{Par}^m_{g,n}[(r_1, \ldots, r_n)]$. The associated surface F has exactly n boundary curves $C_1, \ldots, C_n$, each C_i is subdivided into r_i increasingly enumerated regions and each region admits two arcs c^+_{ij} and c^-_{ij} which correspond to the top and bottom of the incidential level of the parallel slit domain L.

Fix parallel slit domains $L_1 \in \mathfrak{Par}^{m_1}_{g_1,n_1}[(r^{(1)}_1, \ldots, r^{(1)}_{n_1})]$ and $L_2 \in \mathfrak{Par}^{m_2}_{g_2,n_2}[(r^{(2)}_1, \ldots, r^{(2)}_{n_2})]$. We discuss the glueing construction for the associated surfaces F_1 and F_2 at first. Imagine F_1 to stand left of F_2. Moreover, the boundary curves of F_1 form the boundaries of tubes that tend to F_2 and analogously the boundary curves of F_2 form the boundaries of tubes that tend to F_1 as is sketched in Figure 4.12.

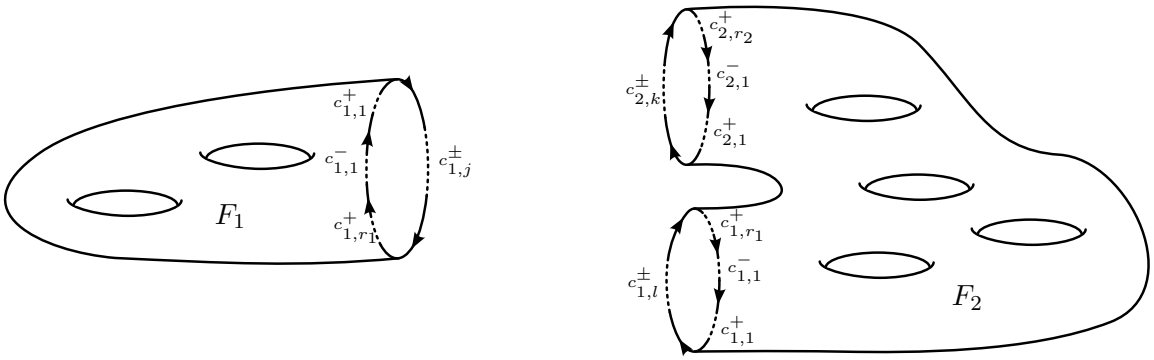

Figure 4.12.: Two surfaces looking at each other.

In the first step, we match some of the arcs c^- of F_1 with some of the arcs c^+ of F_2. The matching is not allowed to be empty (this would produce a disconnected surface). In the second step, we join the matched arcs by glueing (untwisted) stripes inbetween. The resulting surface F has $m = m_1 + m_2$ punctures, but both the genus g and the number of boundary curves n is subject to the chosen matching. In the third step, we choose an enumeration of the boundaries of F and for each boundary C_i of F there are r_i arcs c^- which were not used in the glueing process (e.g. all arcs c^- in F_2). The resulting (ordered) partition is therefore $r = r_1 + \ldots + r_n$. Moreover, we choose an arc c^-_i for each boundary curve C_i of F and the levels of the associated parallel slit domain are ordered with respect to the occurence of the incidential arcs c^- by wandering through the corresponding boundary curve starting at the arc c^-_i chosen above.

In terms of parallel slit domains, we start with the choice of a partial, non-empty matching of the respective levels of L_1 and L_2. Using the action of the little cubes operad for each pair of levels, we emplace each pair into its own complex plane. The number of punctures

is $m = m_1 + m_2$, the norm is $h = h_1 + h_2$, but both the number n of boundary curves and the number r_i of levels per boundary curve have to be computed — note that the number of levels is not determined by $r^{(1)}$, $r^{(2)}$ and the size of the matching — and the genus is given by $g = \frac{h+2-m-n-r}{2}$. Having this done, we choose an enumeration of the n boundary curves by declaring a first level for each boundary. The remaining levels are ordered by their occurence of the permutation induced by σ_h. This ends the construction of a non-degenerate parallel slit domain in $\mathfrak{Par}_{g,n}^{m}[(r_1, \ldots, r_n)]$.

We reflect the construction discussed above in the next

Definition 4.2.1. The **combinatorial type** G which specifies the glueing construction **depends on** the parameters

$$\mathfrak{P}(G) = (g_1, g_2, n_1, n_2, m_1, m_2, (r_1^{(1)}, \ldots, r_{n_1}^{(1)}), (r_1^{(2)}, \ldots, r_{n_2}^{(2)}))$$

and **consists of** the following two data.

(i) A partial, non-empty matching of the levels.

The size of the matching is denoted by $s(G)$. The corresponding surface of genus $g(G)$ has $m(G) = m_1 + m_2$ punctures and $n(G)$ (yet unordered) boundary curves each consisting of several levels.

(ii) A partial enumeration of the levels such that each boundary curve belongs to exactly one selected level.

The corresponding ordered configuration is $(r_1^{(G)}, \ldots, r_{n(G)}^{(G)})$. The **set of combinatorial types** that specify a glueing construction is denoted by $\mathcal{G}$.

Using the introduced notation we have proven the following

Proposition 4.2.2. *For every combinatorial type $G \in \mathcal{G}$ with parameters*

$$\mathfrak{P}(G) = (g_1, g_2, n_1, n_2, m_1, m_2, (r_1^{(1)}, \ldots, r_{n_1}^{(1)}), (r_1^{(2)}, \ldots, r_{n_2}^{(2)}))$$

there are operations

$$\tilde{\vartheta}_G \colon \left(\coprod_{s(G)} \tilde{C}^2(\mathbb{C}) \right) \times \mathfrak{Par}_{g_1,n_1}^{m_1}(r_1^{(1)}, \ldots, r_{n_1}^{(1)}) \times \mathfrak{Par}_{g_2,n_2}^{m_2}(r_1^{(2)}, \ldots, r_{n_2}^{(2)}) \longrightarrow \mathfrak{Par}_{g(G),n(G)}^{m(G)}(r_1^{(G)}, \ldots, r_{n(G)}^{(G)}) \,,$$

where each $\tilde{C}^2(\mathbb{C})$ acts on exactly one predescribed pair of matched levels. Using the homology cross product, we obtain homology operations

$$(\tilde{\vartheta}_G)_* \colon H_i(\tilde{C}^2(\mathbb{C}))^{\oplus s(G)} \otimes H_j(\mathfrak{Par}_{g_1,n_1}^{m_1}(r_1^{(1)}, \ldots, r_{n_1}^{(1)})) \otimes H_k(\mathfrak{Par}_{g_2,n_2}^{m_2}(r_1^{(2)}, \ldots, r_{n_2}^{(2)})) \longrightarrow H_{i+j+k}(\mathfrak{Par}_{g(G),n(G)}^{m(G)}(r_1^{(G)}, \ldots, r_{n(G)}^{(G)})) \,.$$

Now that we have established the general framework, let us discuss three special cases of the glueing construction. The first operation $\mu^{\uparrow\uparrow}$ is discussed in terms of parallel slit domains, the second operation $\mu^{\uparrow\downarrow}$ is discussed in terms of surfaces with boundaries and the third operation μ^{cs} is discussed in terms of the dual Ehrenfried complex.

4.2.2. The Operation $\mu_*^{\uparrow\uparrow}$

The first homology operation is induced by a product called $\mu^{\uparrow\uparrow}$ and is defined for all parallel slit domains in $\mathfrak{Par}_n[(r_1,\dots,r_n)] = \coprod_{g,m} \mathfrak{Par}_{g,n}^m[(r_1,\dots,r_n)]$ with n and $r = r_1 + \dots + r_n$ fixed. For two parallel slit domains $L_1 \in \mathfrak{Par}_{g_1,n}^{m_1}[(r_1,\dots,r_n)]$ and $L_2 \in \mathfrak{Par}_{g_2,n}^{m_2}[(r_1,\dots,r_n)]$, we match the levels with the same index and insert each pair into a complex plane via μ. The resulting parallel slit domains are sketched in Figure 4.13 where L_1 is colored green and L_2 is colored blue. Note that for each pair of boundary curves C_i of L_1 and L_2

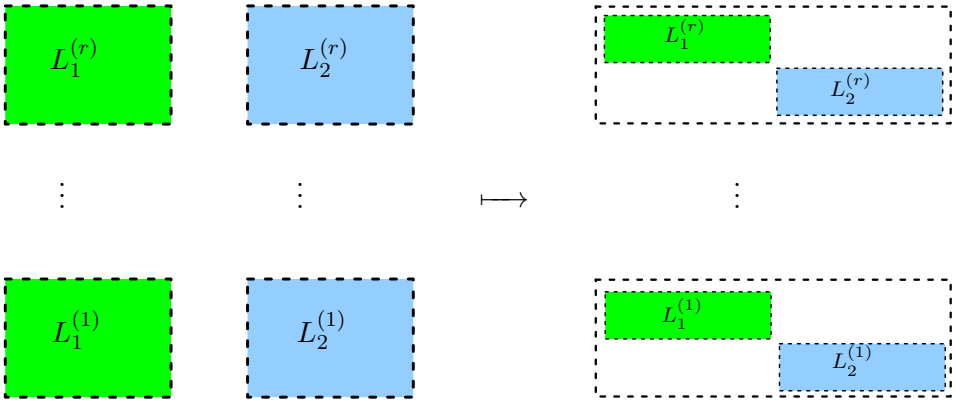

Figure 4.13.: The parallel slit domain $\mu^{\uparrow\uparrow}(L_1, L_2)$.

with $r_i \equiv_2 1$ the resulting parallel slit domain L receives exactly one boundary curve, but for $r_i \equiv_2 0$ we receive two boundaries. This is due to the fact that the induced ordering of the levels of L is

$$\left((\underline{0}_1,\dots,\underline{0}_{r_1})(\underline{0}_{r_1+1},\dots,\underline{0}_{r_2})\dots\right)^2 = (\underline{0}_1,\underline{0}_3,\dots)\dots .$$

We order the boundaries and levels ascendingly, i.e. the lowest level corresponds to the first level of the first boundary. The subsequent levels are ordered with respect to their occurence in $(\underline{0}_1,\dots,\underline{0}_{r_1})^2$. On the remaining levels we repeat this process until all levels are ordered. The resulting parallel slit domain L has $\tilde{m} = m_1 + m_2$ punctures, $\tilde{n} = n + \#\{r_i \equiv_2 0\}$ boundary components, the ordered partition $(\tilde{r}_1,\dots\tilde{r}_{\tilde{n}})$ arises from $(r_1,\dots,r_n)$ by replacing every even $(\dots,r_i,\dots)$ by $(\dots,\frac{r_i}{2},\frac{r_i}{2},\dots)$ and the genus is $\tilde{g} = g_1 + g_2 + \frac{n+r-\#\{r_i\equiv_2 0\}}{2} - 1$. We write $\mu^{\uparrow\uparrow}(L_1, L_2)$ to remind us that the levels of both parallel slit domains occured ascendingly. This ends the discussion of the first selected homology operation. Summing up, we have

Definition/Proposition 4.2.3. Using the homology cross product we obtain a family of homology operations

$$\mu_*^{\uparrow\uparrow} : H_s(\mathfrak{Par}_{g_1,n}^{m_1}[(r_1,\dots,r_n)]) \otimes H_t(\mathfrak{Par}_{g_2,n}^{m_2}[(r_1,\dots,r_n)]) \longrightarrow H_{s+t}(\mathfrak{Par}_{\tilde{g},\tilde{n}}^{\tilde{m}}[(\tilde{r}_1,\dots,\tilde{r}_{\tilde{n}})])$$

by

$$x \otimes y \longmapsto \mu_\star^{\uparrow\uparrow}(x \otimes y)\,,$$

with $\tilde{g}$, $\tilde{m}$, $\tilde{n}$ and $\tilde{r}$ as above and $\mu_\star^{\uparrow\uparrow}$ the induced map in homology.

4.2.3. The Operation $\mu_*^{\uparrow\downarrow}$

The second homology operation is induced by a product called $\mu^{\uparrow\downarrow}$ and is defined for all parallel slit domains in $\mathfrak{Par}_n[(r_1,\ldots,r_n)] = \coprod_{g,m} \mathfrak{Par}_{g,n}^m[(r_1,\ldots,r_n)]$ with n and $r = r_1 + \ldots + r_n$ fixed. Consider two parallel slit domains $L_1 \in \mathfrak{Par}_{g_1,n}^{m_1}[(r_1,\ldots,r_n)]$ and $L_2 \in \mathfrak{Par}_{g_2,n}^{m_2}[(r_1,\ldots,r_n)]$ and imagine their associated surfaces F_1 and F_2 such that the boundary components with the same numbering are in the face of each other. For each boundary curve we join the arcs c^- in F_1 with the arcs c^+ on the opposite side in F_2. In Figure 4.14, we sketch this for parallel slit domains $L_1 = L_2$ with combinatorial type $\Sigma_1 = \Sigma_2 = ((\underline{1}_3\ \underline{1}_2)|(\underline{2}_3\ \underline{1}_1))$ and we obtain the same surface by connecting the boundary

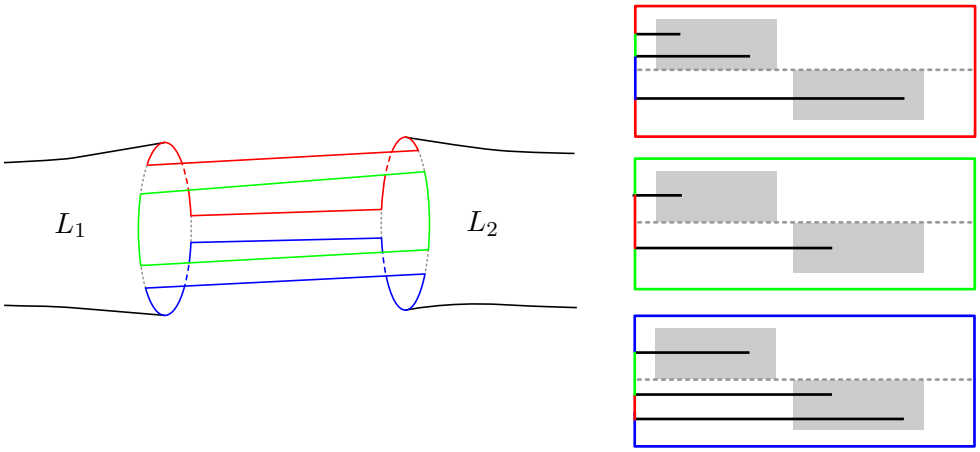

Figure 4.14.: The multiplication of two closed discs on three levels, where $g = m = 0$, $n = 1$ and $r = 3$.

component of L_1 with the boundary component of L_2 by a tube which has three additional, enumerated boundary curves, see Figure 4.15. In general, every two boundary components

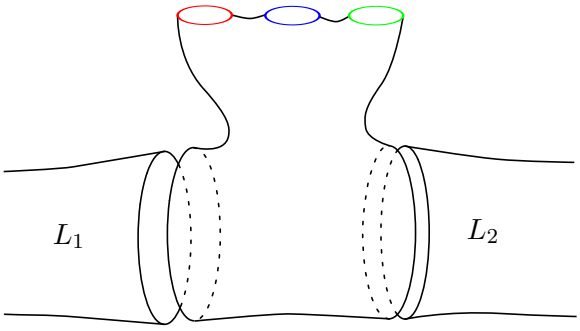

Figure 4.15.: A better picture for the multiplication of two closed discs on three levels, where $g = m = 0$, $n = 1$ and $r = 3$.

with the same numbering say i are connected by a tube with r_i additional boundary curves enumerated by the arcs c^- in F_1. The resulting surface has $\tilde{n} = r$ enumerated boundary components and it is clear that the associated partition is $(1 + \ldots + 1)$. Moreover, the number of punctures of the resulting parallel slit domain is $\tilde{m} = m_1 + m_2$ and by taking a

glance at Figure 4.16 it is clear that its genus is $g_1 + g_2 + n - 1$.

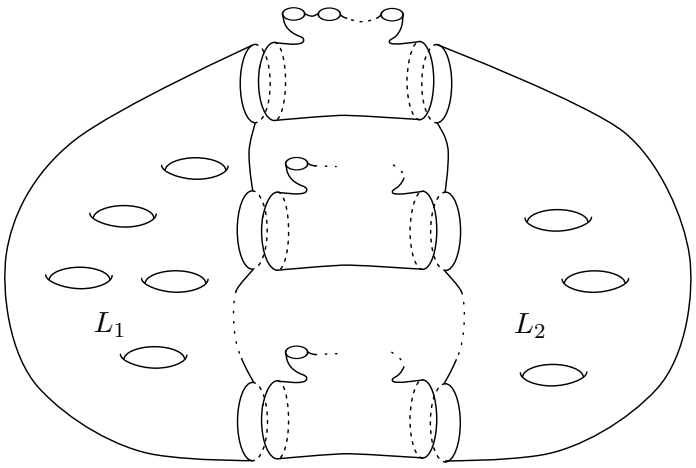

Figure 4.16.: The genus of the resulting surface is g_1+g_2+n-1, it has m_1+m_2 punctures and r enumerated boundary components. The associated partition is $(1, \ldots, 1)$.

As operation on parallel slit domains, we match the ascending levels of L_1 with the descending levels of L_2. This is denoted by the symbol $\mu^{\uparrow\downarrow}$. This ends the discussion of the second selected homology operation. Summing up, we provided

Definition/Proposition 4.2.4. Using the homology cross product we obtain a family of homology operations

$$\mu_*^{\uparrow\downarrow} : H_s(\mathfrak{Par}_{g_1,n}^{m_1}[(r_1,\ldots,r_n)]) \otimes H_t(\mathfrak{Par}_{g_2,n}^{m_2}[(r_1,\ldots,r_n)]) \longrightarrow H_{s+t}(\mathfrak{Par}_{\tilde{g},\tilde{n}}^{\tilde{m}}[(\tilde{r}_1,\ldots,\tilde{r}_n)])$$

by

$$x \otimes y \longmapsto \mu_\star^{\uparrow\downarrow}(x \otimes y),$$

with $\tilde{g} = g_1 + g_2 + n - 1$, $\tilde{m} = m_1 + m_2$, $\tilde{n} = r$ and partition $(1, \ldots, 1)$, and $\mu_\star^{\uparrow\downarrow}$ the induced map in homology.

4.2.4. The Operation μ_*^{cs}

The third homology operation is induced by a product called μ^{cs} and is defined for all parallel slit domains in $\mathfrak{Par} = \coprod_{g,m,(r_1,\ldots,r_n)} \mathfrak{Par}_{g,n}^{m}[(r_1,\ldots,r_n)]$. If we think of parallel slit domains as surfaces with poles, the well-known product μ, which was defined above for $n = r = 1$, is understood as the connected sum at the distinguished dipole. The product μ^{cs} (which we are about to define) does the same and its superscript should remind us of the connected sum operation. For two parallel slit domains $L_1 \in \mathfrak{Par}_{g_1,n_1}^{m_1}[(r_1^{(1)},\ldots,r_{n_2}^{(1)})]$ and $L_2 \in \mathfrak{Par}_{g_2,n_2}^{m_2}[(r_1^{(2)},\ldots,r_{n_2}^{(2)})]$, we consider the connected sum of the two associated surfaces with respect to the first level of L_1 and the last level of L_2, see Figure 4.17.

Let us describe this operation in terms of the dual Ehrenfried complex.

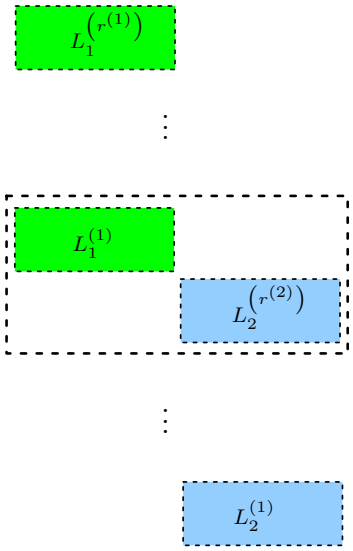

Figure 4.17.: The parallel slit domain $\mu^{cs}(L_1, L_2)$.

Definition 4.2.5. Consider cells $\Sigma = (\tau_q \mid \ldots \mid \tau_1) \in P^*(h, m; r_1, \ldots, r_n)$ of bidegree (p, q) and $\Sigma' = (\tau'_q \mid \ldots \mid \tau'_1) \in P^*(h', m'; r'_1, \ldots, r'_n)$ of bidegree (s, t) and denote the s^{th} iterated pseudo degeneracy $S = S_0 \circ \cdots \circ S_0 \colon \mathfrak{S}_p \longrightarrow \mathfrak{S}_{s+p}$. The **connected sum of** Σ and Σ' is

$$\mu^{cs}(\Sigma, \Sigma') = (-1)^{pq}(S\tau_q \mid \ldots \mid S\tau_1 \mid \tau'_t \mid \ldots \mid \tau'_1)$$

as cell in $P(h + h', m + m'; r'_1, \ldots, r'_{n'-1}, r'_{n'} + r_1, r_2, \ldots, r_n)$.

Proposition 4.2.6. *The connected sum defines a cochain map*

$$\mu^{cs} \colon \mathbb{E}^*(h, m; r_1, \ldots, r_n) \otimes \mathbb{E}^*(h', m'; r'_1, \ldots, r'_n) \longrightarrow \\ \mathbb{E}^*(h + h', m + m'; r'_1, \ldots, r'_{n'-1}, r'_{n'} + r_1, r_2, \ldots, r_n)$$

and therefore a homology operation on the associated moduli spaces.

Notation 4.2.7. In order to simplify notation, we write $\Sigma \cdot \Sigma'$ instead of $\mu^{cs}_*(\Sigma, \Sigma')$. Moreover, we assume $r = [(1)] = r'$, since the general case is proven in the same way.

Lemma 4.2.8. *If Σ and Σ' are non-degenerate cells, then the same holds true for $\Sigma \cdot \Sigma'$.*

Proof. Consider non-degenerate cells $x = (x_q \mid \ldots \mid x_1) \in \mathbb{E}^*(q, m; 1)_p$ and $y = (y_t \mid \ldots \mid y_1) \in \mathbb{E}^*(t, m'; 1)_s$ and denote their product by

$$z = (z_{t+q} \mid \ldots \mid z_1) = (Sx_q \mid \ldots \mid Sx_q \mid y_t \mid \ldots \mid y_1)\,.$$

By assumption, there is neither $1 = x_i$ respectively $1 = y_i$ nor a common fixed point of x_q, $\ldots, x_1$ respectively $y_t, \ldots y_1$, so the same holds true for z. Moreover, $N(z) = N(x) + N(y)$. Thus, z is non-degenerate in $\mathbb{E}^*(t + q, m + m'; 1)_{s+p}$ if the number of boundary curves is

$$n(z) = n(x) + n(y) - 1 \tag{4.1}$$

and the number of punctures is

$$m(z) = m(x) + m(y)\,. \tag{4.2}$$

We compare the cycles of

$$\alpha = z_{t+q} \cdots z_1 \cdot (\underline{0} \ \ldots \ \underline{s+p})$$

with the cycles of

$$\sigma = x_q \cdots x_1 \cdot (\underline{0} \ \ldots \ \underline{p}) \qquad \text{and} \qquad \rho = y_t \cdots y_1 \cdot (\underline{0} \ \ldots \ \underline{s})\,.$$

By construction $z_{t+q} \cdots z_{t+1}$ respectively$z_t \cdots z_1$ is an automorphism of the set $\{\underline{s+1}, \ldots, \underline{s+p}\}$ respectively$\{\underline{1}, \ldots, \underline{s}\}$, so

$$\alpha|_{\{\underline{0},\ldots,\underline{s-1}\}} = \rho|_{\{\underline{0},\ldots,\underline{s-1}\}}$$

and

$$\alpha|_{\{\underline{s},\ldots,\underline{s+p-1}\}} = S(\sigma)|_{\{\underline{s},\ldots,\underline{s+p-1}\}}\,.$$

Therefore, $\underline{0}$ and $\underline{s}$ are in the same orbit of α whereas every other cycle corresponds to exactly one cycle of either σ or ρ. Both (4.1) and (4.2) are immediate consequences.

In order to prove the general case, observe that $\mu_*^{cs}(\Sigma, \Sigma')$ is connected. Observe that its levels are ordered appropriately. □

Lemma 4.2.9. *The connected sum is subject to the Leibniz rule*

$$(\partial_{\mathbb{K}}^* \pi^* x) \cdot y + (-1)^{|x|} x \cdot (\partial_{\mathbb{K}}^* \pi^* y) = \partial_{\mathbb{K}}^* \pi^* (x \cdot y)$$

Proof. The signs are readily checked. It suffices to show that the following relation,

$$\mathrm{cf}_{i-p'}(x) \sqcup \mathrm{cf}_i(y) \sim \mathrm{cf}_i(x \cdot y)$$

with

$$\mathrm{cf}_{i-p'}(x) \ni \tilde{x} \sim \tilde{x} \cdot y \qquad \text{and} \qquad \mathrm{cf}_i(y) \ni \tilde{y} \sim x \cdot \tilde{y}$$

is a bijection. By Proposition 2.9.7 it suffices to compare the corresponding coboundary traces. But a coboundary trace of $x \cdot y$ is a sequence in either $\{\underline{0}, \ldots, \underline{s}\}$ or $\{\underline{s+1}, \ldots, \underline{s+p}\}$ and therefore corresponds to a coboundary trace of either x or y. The converse is true by the same argument. □

Lemma 4.2.10. *The map κ^* commutes with connected sums, i.e.*

$$\kappa^*(\Sigma \cdot \Sigma') = (\kappa^* \Sigma) \cdot (\kappa^* \Sigma')\,.$$

Proof. This is an immediate consequence of Lemma 2.9.18. □

Proof of Proposition 4.2.6. The product of two monotoneous cells is clearly monotoneous.

We have

$$(\partial_{\mathbb{K}}^* \pi^* x) \cdot y + (-1)^{|x|} x \cdot (\partial_{\mathbb{K}}^* \pi^* y) = \partial_{\mathbb{K}}^* \pi^* (x \cdot y)$$

by Lemma 4.2.9 and κ^* commutes with products by Lemma 4.2.10.

$$(\kappa^* \partial_{\mathbb{K}}^* \pi^* x) \cdot \kappa^* y + (-1)^{|x|} \kappa^* x \cdot (\kappa^* \partial_{\mathbb{K}}^* \pi^* y) = \kappa^* \partial_{\mathbb{K}}^* \pi^* (x \cdot y)$$

The cells x and y are monotoneous, thus by Lemma 2.9.16

$$\kappa^*(x) = x \qquad \text{and} \qquad \kappa^*(y) = y\,.$$

□

This ends the discussion of the third selected homology operation. Summing up, we provided

Definition/Proposition 4.2.11. By Poincaré duality the operation on the dual Ehrenfried complex defines an operation

$$\mu_*^{cs}\colon H_s(\mathfrak{M}_{g_1,n_1}^{m_1}) \otimes H_t(\mathfrak{M}_{g_2,n_2}^{m_2}) \longrightarrow H_{s+t}(\mathfrak{M}_{g_1+g_2,n_1+n_2}^{m_1+m_2})\,.$$

4.3. Operations on $\mathfrak{Par}$ via Bundles

We assume that the reader is familiar with spectral sequences. There are several introductions to the theory of spectral sequences and we recommend working through [Wei95, Chapter 5] or [Spa94, Chapter 9].

In this section, we sketch three homology operations that are induced by certain bundle maps. For a more detailed discussion we refere the reader to [Meh11, Chapter 4]. Moreover, we realize the homology operation T via the dual Ehrenfried complex using our description of the coboundary operator.

For trivial bundles $F \longrightarrow X \longrightarrow B$ with F a q-dimensional, connected, oriented, closed manifold, taking the cross product with the fundamental class defines a homomorphism in integral homology

$$H_p(B) \longrightarrow H_{p+q}(X)\,.$$

For oriented bundles a similar construction is possible and there are many ways to state naturality of this construction. The next proposition is an algebraic solution. For a given bundle with fibre F, denote by $\dim(F)$ the largest homological degree with $H_{\dim(F)}(F) \neq 0$. In this case, we call X a $\dim(F)$-dimensional bundle over B.

Proposition 4.3.1. *Fix a coefficient ring R and a homological degree q. For the category of R-oriented[1], q-dimensional bundles $F \longrightarrow X \longrightarrow B$ there is a natural map*

$$\otimes\colon H_p(B;R) \otimes H_q(F;R) \longrightarrow H_{p+q}(X;R)$$

which agrees with the homological cross product in case X is a trivial bundle and $H_*(F)$ is of finite rank and torsion free.

Proof. Recall the construction of the homological Leray–Serre spectral sequence ([Spa94, Chapter 9]). The base B is (up to CW-replacement) a CW-complex and the preimage of the cellular filtration F_pB of B defines a filtration of X. The associated spectral sequence is the Leray–Serre spectral squence with second page

$$E^2_{p,q} = H_p(B; H_q(F;R)) \Rightarrow H_{p+q}(X;R)\,.$$

[1] We assume that the induced action of the fundamental groupoid on $H_*(F;R)$ is trivial. Geometrically speaking, the tour along a closed path in X is always orientation preserving (with respect to the fibres and the coefficient ring).

The local coefficient system is trivial by assumption. In particular, we have natural, exact sequences

$$H_p(B;R) \otimes H_q(F;R) = E^2_{p,q} \xrightarrow{\alpha} E^\infty_{p,q} \longrightarrow 0$$

and

$$0 \longrightarrow E^\infty_{p,q} \xrightarrow{\beta} H_{p+q}(X;R)$$

since $E^\infty_{p,q} = F_pH_{p+q}(X;R)/F_{p-1}H_{p+q}(X;R)$ and $E^\infty_{p-k,q+k} = 0$ for $k > 0$. Thus

$$\otimes = \beta\alpha\colon H_p(B;R) \otimes H_q(F;R) \longrightarrow H_{p+q}(X;R)$$

is a natural homomorphism.

For X the trivial bundle $B \times F \longrightarrow B$ the filtration of X is just $F_pX = F_pB \times F$. By the Eilenberg-Zilber theorem, we have a natural chain homotopy equivalence

$$C(X) \simeq C(B) \otimes C(F)\,,$$

so the induced filtration on the right hand side is $(F_pC(B)) \otimes C(F)$. But this filtration induces the Tor spectral sequence which collapses at the second page (as $H_*(F)$ is torsion free and of finite rank). In particular, the Leray–Serre spectral squence of $B \times F \longrightarrow F$ is natural isomorphic to this Tor spectral sequence, so the map $\otimes$ agrees (up to natural isomorphism) with the homology cross product. □

Consider the space of parallel slit domains with a distinguished punctures $\mathfrak{Par}^{m-1,1}_{g,n}[(r_1, \ldots, r_n)]$. This is a non-trivial m-fold covering $\mathfrak{Par}^{m-1,1}_{g,n} \xrightarrow{\pi} \mathfrak{Par}^m_{g,n}[(r_1, \ldots, r_n)]$ and we have the transfer map[2]

$$tr\colon H_*(\mathfrak{Par}^m_{g,n}[(r_1, \ldots, r_n)]) \longrightarrow H_*(\mathfrak{Par}^{m-1,1}_{g,n}[(r_1, \ldots, r_n)])\,.$$

For varying slit domains, we continuously insert a small circle around the distinguished puncture. This defines a non-trivial orientable circle bundle $\mathbb{S}^1 \longrightarrow \mathfrak{I}_T \longrightarrow \mathfrak{Par}^{m-1,1}_{g,n}[(r_1, \ldots, r_n)]$. Adding a pair of slits, one slit ending in a given point z of the small circle and its partner above all other slits (take a glance at Figure 4.18) defines a continuous map

$$\tilde{\vartheta}_T\colon \mathfrak{I}_T \longrightarrow \mathfrak{Par}^{m-1}_{g+1,n}[(r_1, \ldots, r_n)]\,.$$

Topologically, we forget the distinguished puncture, remove small discs around the two points and glue in a handle, increasing the genus of the surface by one.

Definition 4.3.2. The map $\tilde{\vartheta}_T$ induces the homology operation

$$T\colon H_s(\mathfrak{Par}^m_{g,n}[(r_1, \ldots, r_n)]) \longrightarrow H_{s+1}(\mathfrak{Par}^{m-1}_{g+1,n}[(r_1, \ldots, r_n)])$$

by

$$x \longmapsto (\tilde{\vartheta}_T)_\star(tr(x) \otimes [\mathbb{S}^1])\,,$$

where $[\mathbb{S}^1]$ is the fundamental class of the circle and $\otimes$ as in Proposition 4.3.1 and $(\tilde{\vartheta}_T)_\star$ the induced homomorphism in homology. We imagine $(\tilde{\vartheta}_T)_*$ as seen in Figure 4.18.

[2]The transfer map is already defined on the singular complexes by summing over the m choices of lifting singular chains. Note that $\pi_* \circ tr$ is just the multiplication by m.

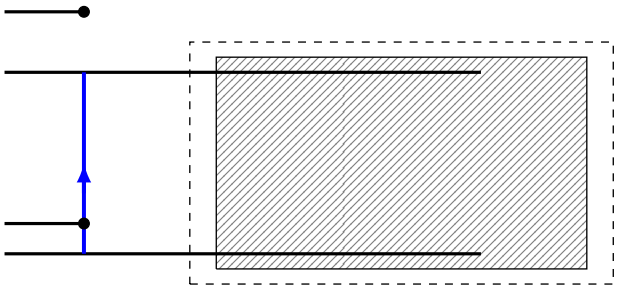

Figure 4.18.: The operation $(\tilde{\vartheta}_T)_*$ inserts a new pair of slits while rotating the slit sitting in the distinguished puncture.

Similar to the construction above, we continuously embed a circle C near a distinguished puncture and consider two distinct points on C This is, up to homotopy, a non-trivial orientable circle bundle $\mathbb{S}^1 \longrightarrow \mathfrak{I}_F \longrightarrow \mathfrak{Par}_{g,n}^{m-1,1}[(r_1,\ldots,r_n)]$. Inserting a pair of slits which end in the two marked points on the circle (take a glance at Figure 4.19) defines a continuous map

$$\tilde{\vartheta}_F \colon \mathfrak{I}_F \longrightarrow \mathfrak{Par}_{g,n}^{m+1}[(r_1,\ldots,r_n)]\,.$$

Topologically, we introduce a new puncture near the distinguished one.

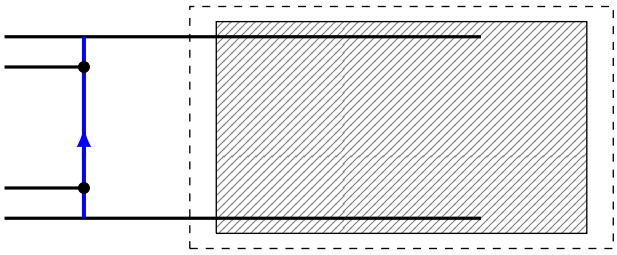

Figure 4.19.: The operation $(\tilde{\vartheta}_F)_*$ inserts a new pair of rotating slits sitting in the distinguished puncture.

Definition 4.3.3. For $m \geq 1$, the map $\tilde{\vartheta}_F$ induces the homology operation

$$F \colon H_s(\mathfrak{Par}_{g,n}^{m}[(r_1,\ldots,r_n)]) \longrightarrow H_{s+1}(\mathfrak{Par}_{g,n}^{m+1}[(r_1,\ldots,r_n)])$$

by

$$x \longmapsto (\tilde{\vartheta}_F)_\star(tr(x) \otimes [\mathbb{S}^1])$$

where $[\mathbb{S}^1]$ is the fundamental class of the circle and $\otimes$ as in Proposition 4.3.1 and $(\tilde{\vartheta}_F)_\star$ the induced homomorphism in homology, see Figure 4.19.

Similarly, for the space of parallel slit domains with two distinguished, enumerated punctures $\mathfrak{Par}_{g,n}^{m-2,1,1}[(r_1,\ldots,r_n)]$, there is a non-trivial orientable torus bundle $\tilde{\mathfrak{I}}_E \longrightarrow \mathfrak{Par}_{g,n}^{m-2,1,1}[(r_1,\ldots,r_n)]$ by considering two enumerated circles on the surface, each near one of the two enumerated punctures. Dividing out the obvious action of $\mathfrak{S}_2^\times = Aut(\{1,2\})$ (defined by interchanging the coordinates in the torus respectively the enumerated punctures)

defines a $\mathbb{F}_2$-orientable torus bundle

$$\mathbb{S}^1 \times \mathbb{S}^1 \longrightarrow \mathfrak{I}_E \longrightarrow \mathfrak{Par}_{g,n}^{m-2,2}[(r_1, \ldots, r_n)]$$

with $\mathfrak{Par}_{g,n}^{m-2,2}[(r_1, \ldots, r_n)]$ the space of parallel slit domains with two distinguished, unordered punctures. Inserting a pair of slits which end in the two marked points on the two unordered circles (take a glance at Figure 4.20) defines a continuous map

$$\tilde{\vartheta}_E \colon \mathfrak{I}_E \longrightarrow \mathfrak{Par}_{g+1,n}^{m-2}[(r_1, \ldots, r_n)]\,.$$

Topologically, we forget the two distinguished punctures, remove small discs around the two points and glue in a handle, increasing the genus of the surface by one. In order to define the homology operation, observe that the forgetful map

$$\mathfrak{Par}_{g,n}^{m-2,2}[(r_1, \ldots, r_n)] \longrightarrow \mathfrak{Par}_{g,n}^{m}[(r_1, \ldots, r_n)]$$

is a $\binom{m}{2}$-fold non-trivial covering, so we have again a transfer map tr.

Definition 4.3.4. For $m \geq 2$, the map $\tilde{\vartheta}_E$ induces the homology operation

$$E \colon H_s(\mathfrak{Par}_{g,n}^{m}[(r_1, \ldots, r_n)]) \longrightarrow H_{s+2}(\mathfrak{Par}_{g+1,n}^{m-2}[(r_1, \ldots, r_n)])$$

by

$$x \longmapsto (\tilde{\vartheta}_E)_\star(tr(x) \otimes [\mathbb{S}^1 \times \mathbb{S}^1])$$

where $[\mathbb{S}^1 \times \mathbb{S}^1]$ is the fundamental class of the torus and $\otimes$ as in Proposition 4.3.1 and $(\tilde{\vartheta}_E)_\star$ the induced homomorphism in homology. We sketch our geometric interpretation of $(\tilde{\vartheta}_E)_*$ in Figure 4.20.

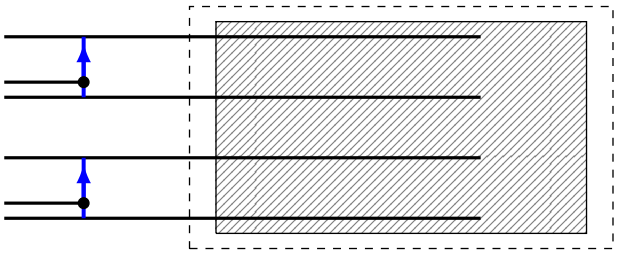

Figure 4.20.: The operation $(\tilde{\vartheta}_E)_*$ inserts a new pair of independently rotating slits sitting in the distinguished punctures.

4.3.1. The Operation T via the Dual Ehrenfried Complex

In this subsection, we construct the operation T in terms of the dual Ehrenfried complex. Geometrically speaking, we start with a combinatorial cell Σ and have to introduce two new slits, one rotating in a puncture and the other on top of all other slits. In the algebraic model, there is no notion of rotating slits but it is easy to come up with the right definition. In order to reduce the cohomological degree of the resulting cell by one, we append every cell by a transposition $(\underline{p_r + 1}_r \; c)$ with c a symbol in a puncture. Using the geometric intuition of jumping slits and relevant κ^*-sequences, it is easy to see that we defined a coboundary map.

Definition 4.3.5. Let $\Sigma = (\tau_h \mid \ldots \mid \tau_1) = (\sigma_h : \ldots : \sigma_0)$ be a top dimensional, non-degenerate cell in $P(h, m; r_1, \ldots, r_n)$. Denote the cycles of σ_h that correspond to the m punctures by $\alpha_1, \ldots, \alpha_m$. The **symbols corresponding to the punctures of** Σ are

$$\mathrm{punc}(\Sigma) = \mathrm{supp}(\alpha_1, \ldots, \alpha_m)\,.$$

Notation 4.3.6. Since T adds a new slit above all other slits, we obtain the ordered partition $p{+}1 = p_1{+}\ldots{+}p_{r-1}{+}(p_r{+}1)$. In particular, the largest symbol is $\underline{p_r + 1}_r = p_r{+}1$.

Definition 4.3.7. Then the operation T is defined on generators $\Sigma \in \mathbb{E}^*$ by

$$T(\Sigma) = \sum_{c \in \mathrm{punc}(\Sigma)} \Sigma_c$$

where

$$\Sigma_c = (\ (\underline{p_r + 1}_r\ c) \mid \tau_q \mid \ldots \mid \tau_1)\,.$$

Proposition 4.3.8. *The operation T defines a cochain map*

$$T\colon \mathbb{E}^{*+1}(h, m; r_1, \ldots, r_n) = \mathbb{E}^*(h, m; r_1, \ldots, r_n) \otimes \mathbb{Z}[1] \longrightarrow \mathbb{E}^*(h+1, m-1; r_1, \ldots, r_n)\,.$$

Lemma 4.3.9. *If Σ is top dimensional, non-degenerate cell of bidegree (p, h) in $P^m_{g,n}[(r_1, \ldots, r_n)]$, then every term Σ_c of $T(\Sigma)$ is a top dimensional, non-degenerate cell of bidegree $(p+1, h+1)$ in $P(h+1, m-1; r_1, \ldots, r_n)$.*

Proof. Consider $\Sigma = (\tau_h \mid \ldots \mid \tau_1) = (\sigma_h : \ldots : \sigma_0)$ and let $\Sigma_c = (x_{h+1} \mid \ldots \mid x_1) = (\sigma_c : \sigma_h : \ldots : \sigma_0)$ be a term of $T(\Sigma)$, i.e. $\Sigma_c = ((\underline{p_r + 1}_r\ c) \mid \tau_q \mid \ldots \mid \tau_1)$ and $\sigma_c = (\underline{p_r + 1}_r\ c)\sigma_h$, with $c \in \mathrm{punc}(\Sigma)$.

The following is evident: $N(\Sigma_c) = N(\Sigma) + 1 = h + 1$, Σ_c is connected, the levels are ordered and there is neither $1 = x_i$ nor a common fixed point of $x_{q+1}, \ldots, x_1$. From $\sigma_c = (\underline{p_r + 1}_r\ c)\sigma_h$ and $\underline{p_r + 1}_r \notin \mathrm{punc}(\Sigma) \ni c$ we deduce

$$n(\Sigma_c) = n(\Sigma) \qquad \text{and} \qquad m(\Sigma_c) = m(\Sigma) - 1\,.$$

□

Lemma 4.3.10. *We have*

$$T\partial^*_{\mathbb{K}}\pi^* = \partial^*_{\mathbb{K}}\pi^* T\,.$$

In order to prove the lemma, we use Proposition 2.9.7 to show that every term in $T\partial^*_{\mathbb{K}}\pi^*(\Sigma)$ occures in $\partial^*_{\mathbb{K}}\pi^* T(\Sigma)$. Then, using Proposition 2.9.7 again, the difference of both sums is zero.

Proof. By Proposition 2.9.7, the terms of $\partial^*_{\mathbb{K}}\pi^*(\Sigma)$ correspond bijectively to all coboundary traces of Σ. Applying T, every term x of $T\partial^*_{\mathbb{K}}\pi^*(\Sigma)$ is identified with an i^{th} coboundary trace $a = a(x)$ and a symbol $c = c(x)$ corresponding to one of the punctures of $a.\Sigma$.

If $c \neq i$, we identify x with the term $\tilde{a}.\Sigma_{\tilde{c}}$, where $\tilde{c} = d_i^{\Delta}(c)$ and $\tilde{a}$ is the i^{th} coboundary trace of $\Sigma_{\tilde{c}}$ with

$$\tilde{a}_j = \begin{cases} a_j & j \leq h \\ (\underline{p_r + 1_r}\ c)(a_h) & j = h+1 \end{cases} \tag{4.3}$$

as both $\tilde{a} \in T_i(\Sigma_{\tilde{c}})$ and $x = \tilde{a}.\Sigma_{\tilde{c}}$ are readily verified.

Otherwise, i.e if $c = i$, we identify x with the term $a'.\Sigma_{c'}$ where $c' = d_i^{\Delta}(a_h)$ and a' is the i^{th} coboundary trace of $\Sigma_{c'}$ with

$$a'_j = \begin{cases} a_j & j \leq h \\ a_h & j = h+1 \end{cases} \tag{4.4}$$

as both $a' \in T_i(\Sigma_{c'})$ and $x = a'.\Sigma_{c'}$ are again readily verified.

Observe that in case (4.3) we have

$$\tilde{a}_{h+1} = S_i(\underline{p_r + 1_r}\ \tilde{c})(a_j)$$

and in case (4.4) we have

$$\tilde{a}_{h+1} \neq S_i(\underline{p_r + 1_r}\ c')(a_j)\,.$$

We identify the terms of $T\partial_{\mathbb{K}}^*\pi^*(\Sigma)$ with all coboundary traces $a = (a_{h+1} : \ldots : a_0)$ of all terms of $T(\Sigma)$ that satisfy both

$$a_j \neq a_{j-1} \quad \text{for some} \quad j \leq h \qquad \text{and} \qquad a_j \neq (S_i\tau_j)(a_{j-1}) \quad \text{for some} \quad j \leq h\,.$$

The remaining terms of $\partial_{\mathbb{K}}^*\pi^*T(\Sigma) - T\partial_{\mathbb{K}}^*\pi^*(\Sigma)$ are identified with the coboundary traces of all terms $\Sigma_c = (x_{h+1} \mid \ldots \mid x_1)$ of $T(\Sigma)$ that satisfy

$$a_j = a_{j-1} = i+1 \quad \text{for all} \quad j \leq h \qquad \text{and} \qquad a_{h+1} \neq a_h \tag{4.5}$$

or

$$a_j = (S_i x_j)(a_{j-1}) \quad \text{for all} \quad j \leq h \qquad \text{and} \qquad a_{h+1} \neq (S_i x_{h+1})(a_h)\,. \tag{4.6}$$

Let us reformulate (4.5) and (4.6). Clearly

$$\begin{aligned} a \in T_i(\Sigma_c) \text{ satisfies (4.5)} &\iff S_i(\underline{p_r + 1_r}\ c)(i+1) \neq i+1 && (4.7)\\ &\iff c = i && (4.8)\\ &\iff a = (\underline{p_r + 1_r} : i+1 : \ldots : i+1) \quad \text{and} \quad i \in \text{punc}(\Sigma) && (4.9)\\ &\iff a = (\underline{p_r + 1_r} : i+1 : \ldots : i+1) \quad \text{and} \quad \sigma_h(i) \in \text{punc}(\Sigma) && (4.10) \end{aligned}$$

and

$$a \in T_{i+1}(\Sigma_c) \text{ satisfies (4.6)} \iff S_{i+1}(\underline{p_r + 1_r}\ c)(a_h) \neq a_h \tag{4.11}$$

using $a_j = S_{i+1}(\tau_j \cdots \tau_1)(i+2) = s^{\Delta}_{i+1}(\sigma_j(i))$ yields

$$\iff c = a_h = \sigma_h(i) \tag{4.12}$$

$$\iff a = (s^{\Delta}_{i+1}(\sigma_h(i)) : s^{\Delta}_{i+1}(\sigma_h(i)) : \ldots : s^{\Delta}_{i+1}(\sigma_0(i))) \quad \text{and} \quad \sigma_h(i) \in \mathrm{punc}(\Sigma)\,. \tag{4.13}$$

By (4.10) and (4.13) the remaining terms of $\partial^*_{\mathbb{K}}\pi^* T(\Sigma) - T\partial^*_{\mathbb{K}}\pi^*(\Sigma)$ come in pairs, where

$$a \in T_i(\Sigma_i) \qquad \text{is paired with} \qquad a' \in T_{i+1}(\Sigma_{\sigma_h(i)})$$

and a direct computation shows

$$a.\Sigma_i = (\ (\underline{p_r + 1}_r\ i+1) \mid S_{i+1}\tau_q \mid \ldots \mid S_{i+1}\tau_1) = a'.\Sigma_{\sigma_h(i)}$$

which finishes the proof:

$$\partial^*_{\mathbb{K}}\pi^* T(\Sigma) - T\partial^*_{\mathbb{K}}\pi^*(\Sigma) = \sum_{a \in T_i(\Sigma_i)} (-1)^i a.\Sigma_i + (-1)^{i+1} a'.\Sigma_{\sigma_h(i)} = 0\,.$$

□

Proof of Proposition 4.3.8. The map T is well defined by Lemma 4.3.9, it commutes up to κ^* with $\partial^*_{\mathbb{E}} = \kappa^* \partial^*_{\mathbb{K}} \pi^*$ by Lemma 4.3.10, so the comparision of relevant κ^*-sequences using Lemma 2.9.16 ends the proof. □

4.4. The Operation α

During this section, let $n = r = 1 + \cdots + 1$ the trivial partition.

Consider a surface F with genus g, m punctures and n boundary curves, and choose the k^{th} of these boundary curves. We can then add another puncture to F by glueing a cylinder with a puncture to this boundary curve, see Figure 4.21.

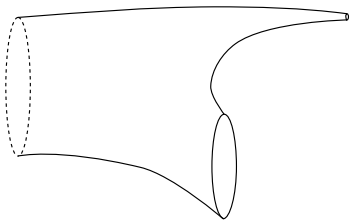

Figure 4.21.: Adding a puncture to a surface.

In order to realize this map on parallel slit pictures, consider the k^{th} level of a parallel slit picture L. Recall that the border of the relevant clipping of L can be identified with the boundary curves and punctures of L. The k^{th} boundary curve needs to be seperated into one new boundary curve and one new puncture. Therefore, we insert a new pair of slits per level as in Figure 4.22. The new slits are longer than any other slit of the slit picture, and they are placed below respectively above all other slits.

In [BT01, Theorem 1.3], Bödigheimer and Tillmann prove the following

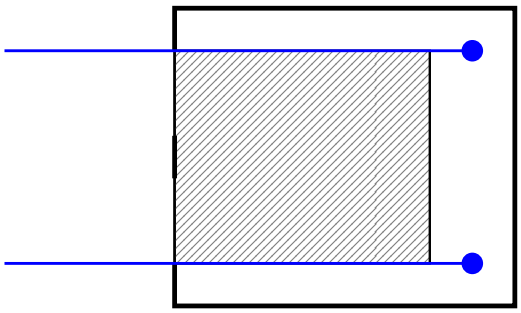

Figure 4.22.: Adding a puncture to a parallel slit picture.

Theorem 4.4.1. *The map* $\alpha_k \colon \mathfrak{M}_{g,n}^m \longrightarrow \mathfrak{M}_{g,n}^{m+1}$ *admits a stable retraction. In particular,* α_k *induces an injective splitting in homology.*

By applying the map α_k successively for all $k = 1, \ldots, n$, we obtain

Definition/Proposition 4.4.2. The map

$$\alpha = \alpha_n \circ \ldots \circ \alpha_1 \colon \mathfrak{M}_{g,n}^m \longrightarrow \mathfrak{M}_{g,n}^{m+n}$$

induces a split injective map

$$\alpha_* \colon H_*(\mathfrak{M}_{g,n}^m) \longrightarrow H_*(\mathfrak{M}_{g,n}^{m+n})$$

in homology.

As promised in Subsection 2.7.2, we can now proof

Corollary 4.4.3. *The radialization map*

$$\mathrm{rad} \colon \mathfrak{M}_{g,n}^m \longrightarrow \mathfrak{M}_g^\bullet(m,n)$$

induces a split injective map on homolgoy.

Proof. Note that

$$\alpha = \mathrm{par} \circ \mathrm{rad}\,,$$

which can be seen in Figure 4.23. The claim follows with Proposition 4.4.2. □

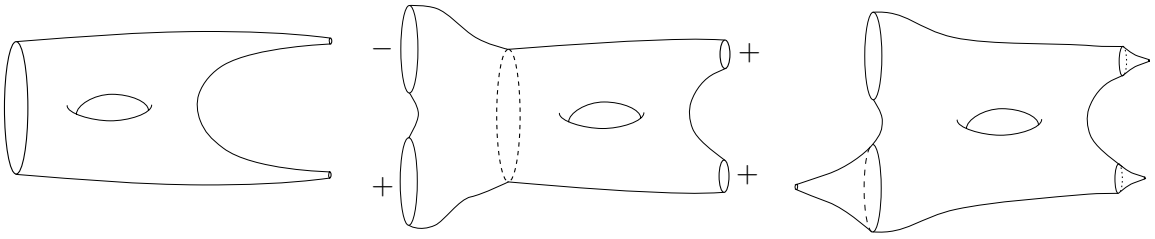

Figure 4.23.: Applying radialization and then parallelization to a surface with punctures and boundaries.

4.5. Radial Multiplication

We will now define a multiplication for radial slit pictures, which looks very analogous to the multiplication for parallel slit pictures. Nevertheless, it will turn out that the radialization map defined in Subsection 2.7.2 is not multiplicative with respect to these multiplications, compare Remark 4.5.7.

So let A respectively A' be two radial slit domains, each on n annuli. We merge each corresponding pair of annuli of the radial slit pictures of A and A' into one as in Picture 4.24. We subdivide the new annulus equally into an outer and an inner ring, putting A

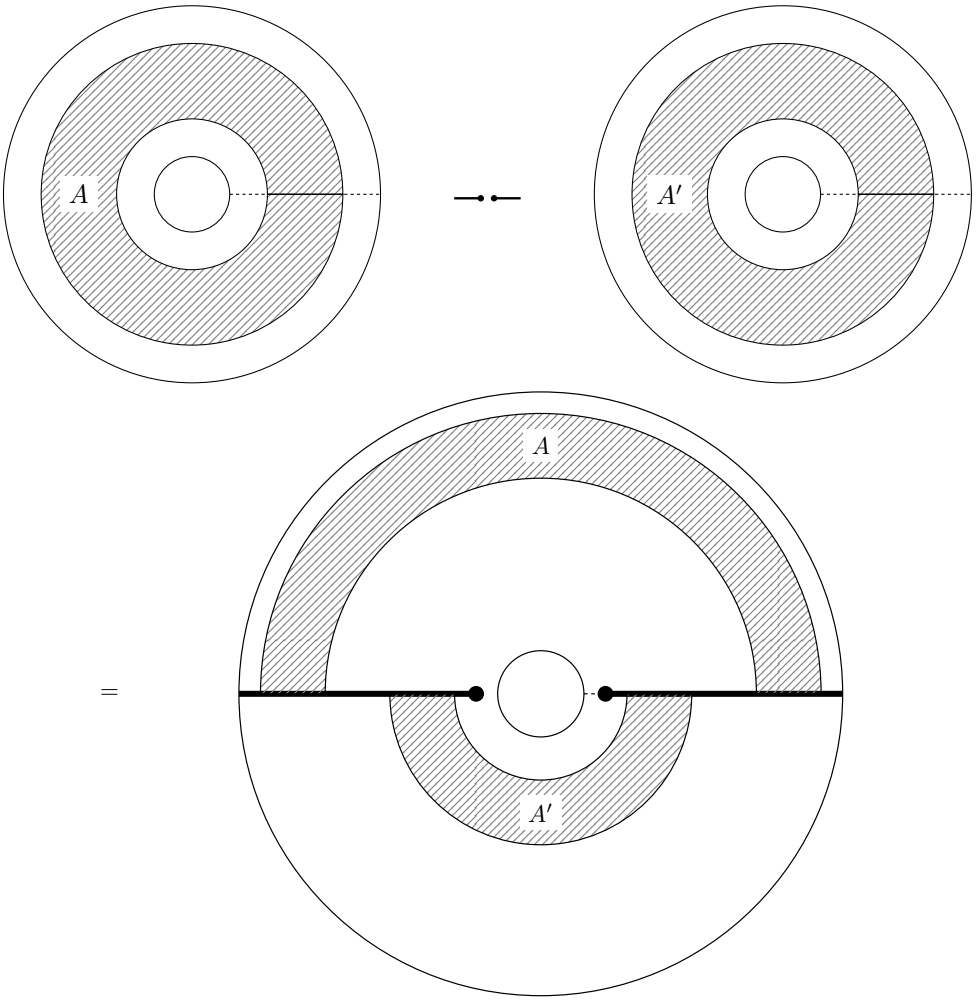

Figure 4.24.: Two radial slit pictures A and A' and their product $A \multimap\!\bullet\!\multimap A'$.

into the outer ring and A' into the inner ring, whereby A' uses the lower half of the slits and A' the upper half. Be aware that the slits of A also start at the outer boundary of the annulus. Thus we introduce a new slit pair on each annulus in order to ensure that the outer boundary curves of A and A' do not interfere. We obtain

Definition 4.5.1. Let $A \in \mathfrak{Rad}_g(m,n)$ and $A' \in \mathfrak{Rad}_{g'}(m',n)$ be two radial slit domains

with the same number of incoming boundary curves. The **product**

$$A \multimap\!\bullet\!\multimap A'$$

of A and A' is given by the radial slit domain obtained by the process described above. We shall refer to this multiplication as **radial multiplication**.

Proposition 4.5.2. *The radial multiplication is a map*

$$\multimap\!\bullet\!\multimap : \mathfrak{Rad}_g(m,n) \times \mathfrak{Rad}_{g'}(m',n) \longrightarrow \mathfrak{Rad}_{\tilde{g}}(\tilde{m},n)\,,$$

where $\tilde{g} = g + g' + n - 1$ *and* $\tilde{m} = m + m'$.

Proof. By construction, we obtain $n(A \multimap\!\bullet\!\multimap A') = n$. Due to the insertion of the new slits, we assert

$$m(A \multimap\!\bullet\!\multimap A') = m(A) + m(A')\,.$$

Using the formula $N(A) = 2g(A) - 2 + m(A) + n(A)$ for A, A' and $A \multimap\!\bullet\!\multimap A'$, we obtain

$$g(A \multimap\!\bullet\!\multimap \mathbb{A}') = g + g' + n - 1\,.$$

□

In order to develop a deeper understanding why these formulas are correct, let us see how radial multiplication looks on surfaces, compare Figure 4.25.

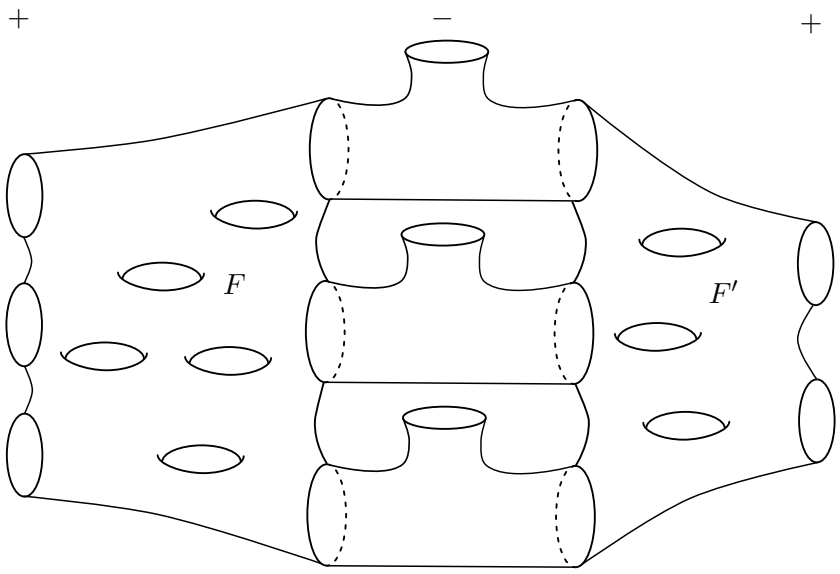

Figure 4.25.: Radial multiplication applied to surfaces F and F'.

The k^{th} inner boundary curves of F and F' are connected by a tube, upon which a new k^{th} inner boundary curve arises. Thereby, each two neighboring tubes contribute to the genus of the new surface. The newly inserted slits make sure that the outer boundary curves of the new surface are simply the outer boundary curves of F and F'.

Now we come to several properties we expect to be fulfilled by a multiplication, and see which of them are indeed satisfied by this radial multiplication.

Proposition 4.5.3. *Radial multiplication is associative up to homotopy.*

Proof. Let A, B, C be three radial slit pictures. In Figure 4.26, we see how $A \rightarrowtail\!\bullet\!\leftarrowtail (B \rightarrowtail\!\bullet\!\leftarrowtail C)$ can be homotoped into $(A \rightarrowtail\!\bullet\!\leftarrowtail B) \rightarrowtail\!\bullet\!\leftarrowtail C$ by successively applying slit jumps and changing the lengths of slits. □

If we consider the definition of the radial multiplication on surfaces, we immediately see

Proposition 4.5.4. *Radial multiplication is commutative up to homotopy.*

Note that the insertion of a new pair of slits on each annulus nicely maintains all glueing information, but also cause several disadvantages.

Remark 4.5.5. Radial multiplication does not have a unit (even up to homotopy): Consider a radial slit domain A and try to imagine another radial slit domain B, for which $A \rightarrowtail\!\bullet\!\leftarrowtail B$ is homotopic to A. But since we always insert a new pair of slits isolating A from the rest of the annulus, we will always obtain an additional outgoing boundary curve, no matter how B looks like (even if it is empty).

Remark 4.5.6. Since the radial multiplication of two slit pictures involves inserting new slits, we cannot directly describe it in terms of operads. See Section 4.6 for an associative operation that does fulfill this property, but that is only defined under limited conditions.

Remark 4.5.7. The radialization map

$$\mathrm{rad}\colon \mathfrak{M}_{g,n}^{m} \longrightarrow \mathfrak{M}_g(m+n, n)$$

defined in Subsection 2.7.2 is not multiplicative with respect to the radial multiplication and any of the multiplications $\mu^{\uparrow\uparrow}$, $\mu^{\uparrow\downarrow}$ or μ^{cs} from Subsections 4.2.2, 4.2.3 and 4.2.4. To see this, let F respectively F' be two surfaces with m respectively m' punctures, and with n boundary curves each. Compare $\mathrm{rad}(F) \rightarrowtail\!\bullet\!\leftarrowtail \mathrm{rad}(F')$ and $\mathrm{rad}(F \cdot F')$ with $\_ \cdot \_$ denoting any of these parallel multiplications. Recall that the radialization map applied to F transforms the punctures of F in outgoing boundaries and creates one additional outgoing boundary for each boundary curve of F. Hence, the number of outgoing boundaries of $\mathrm{rad}(F) \rightarrowtail\!\bullet\!\leftarrowtail \mathrm{rad}(F')$ equals $m+n+m'+n$. On the other hand, the product $F \cdot F'$, however the parallel multiplication is chosen among $\mu^{\uparrow\uparrow}$, $\mu^{\uparrow\downarrow}$ or μ^{cs}, only keeps the punctures from F and F' and does not create any new ones. Thus, we have

$$m(\mathrm{rad}(F \cdot F')) = m + m' + n \neq m + m' + 2n = m(\mathrm{rad}(F) \rightarrowtail\!\bullet\!\leftarrowtail \mathrm{rad}(F'))$$

for $n > 0$, which is always presumed.

Summarizing the positive results, we obtain

Corollary 4.5.8. *Radial multiplication yields an associative and commutative homology operation*

$$\rightarrowtail\!\bullet\!\leftarrowtail_*\colon H_*(\mathfrak{M}_g(m,n)) \otimes H_*(\mathfrak{M}_{g'}(m',n)) \longrightarrow H_*(\mathfrak{M}_{g+g'+n-1}(m+m',n))\,.$$

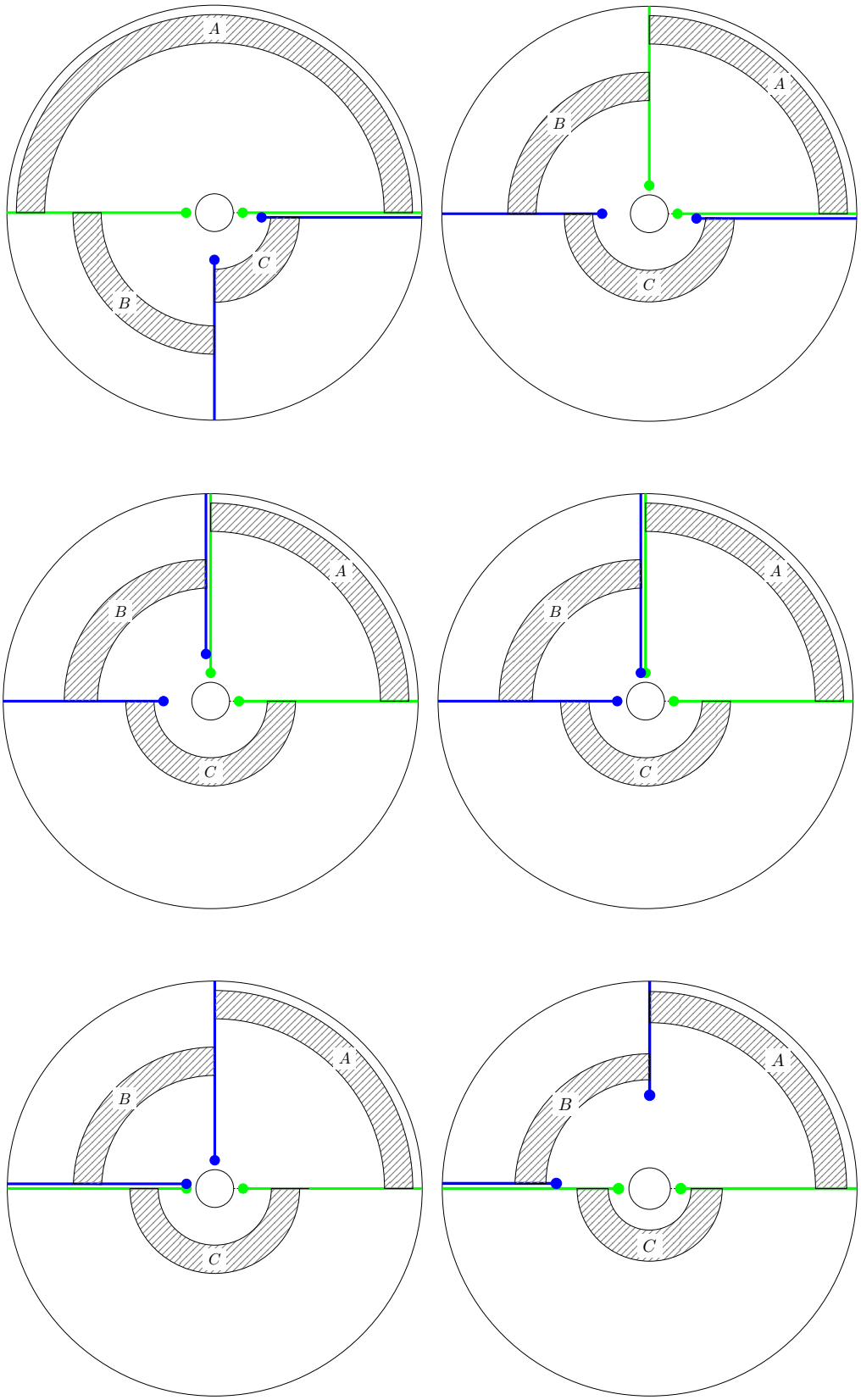

Figure 4.26.: Transforming $A \multimap\!\bullet\!\!-(B \multimap\!\bullet\!\!- C)$ into $(A \multimap\!\bullet\!\!- B) \multimap\!\bullet\!\!- C$, to be read from the left to the right and then from up to down.

4.6. Composition of Radial Slit Pictures

In this section, we will describe a homology operation on the space of radial slit domains that can be expressed via operads (compare also Section 4.1).

This time, we will first give a description of a new operation in terms of surfaces. Let F and F' be two surfaces, where F has m outcoming boundary curves and n marked incoming boundary curves, and F' has l outgoing boundary curves and m marked incoming boundary curves. We want to define a canonical composition of these surfaces, compare Figure 4.27, where the m outgoing boundary curves of F are glued together with the m incoming boundary curves of F'. Since there is a marked point P'^-_k on each incoming boundary C'^-_k of F', we additionally have to require that each outgoing boundary C^+_k of F also has a marked point P^+_k.

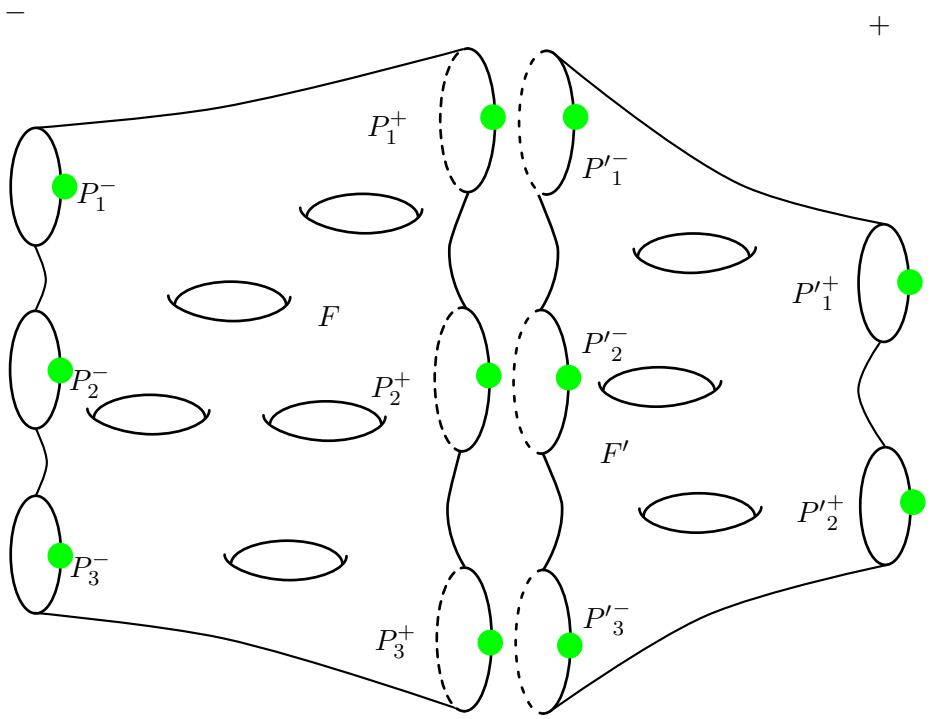

Figure 4.27.: The composition $F \odot F'$ of two surfaces F and F'.

In order to formalize the composition, we therefore give

Definition 4.6.1. Let $\mathfrak{M}_g^{\bullet\bullet}(m,n)$ denote the moduli space parametrizing Riemann surfaces with genus g, n incoming and m outgoing boundary curves with one marked point P_i^- on each incoming boundary curve C_i^-, but also one marked point P_j^+ on each outgoing boundary curve C_j^+. Analogously, the associated space of radial slit pictures is denoted by $\mathfrak{Rad}_g^{\bullet\bullet}(m,n)$.

Now, we can state

Definition 4.6.2. The **composition** of surfaces is the map

$$\odot\colon \mathfrak{M}_g^{\bullet\bullet}(m,n) \times \mathfrak{M}_{g'}^{\bullet\bullet}(l,m) \longrightarrow \mathfrak{M}_{\tilde{g}}^{\bullet\bullet}(l,n)\,, (F,F') \longmapsto F \odot F'\,,$$

which glues the surfaces F and F' along their incoming respectively outgoing boundary curves. Thereby, we have

$$\tilde{g} = g + g' + m - 1\,.$$

Note that we actually only need marked points on the outgoing boundary curve of the surface in the second factor, and that the formula for $\tilde{g}$ is due to the observation that each two neighboring glued boundary curves contribute to the genus.

It remains to realize the composition via radial slit pictures, see also Figures 4.28 up to 4.31. Therefore, consider two radial slit domains $A = (\sigma_q : \ldots : \sigma_0)$ and $A' = (\sigma'_q : \ldots : \sigma'_0)$ with $m(A) = n(A') = m$, $n(A) = n$ and $m(A') = l$, e.g. those two in Figures 4.28 and 4.29. In the pictures, we color the outgoing boundary curves of A and the incoming boundary curves of A' and each of their marked points since they have to be glued together. We call the annuli upon that the slits of A respectively A' lie $\mathbb{A}_1, \ldots, \mathbb{A}_n$ respectively $\mathbb{A}'_1, \ldots, \mathbb{A}'_m$. If F and F' are the surfaces resulting from glueing A and A', we want to construct a radial slit domain $B = A \odot A'$, which results in the surface $F \odot F'$ after glueing. Hence, the new slit picture B resides on n annuli $\mathbb{A}_1^{\odot}, \ldots, \mathbb{A}_n^{\odot}$ and fulfills $m(B) = l$.

For the construction of B, at first concentrate on one annulus $\mathbb{A}_i^{\odot}$. We subdivide $\mathbb{A}_i^{\odot}$ equally into an inner and an outer ring, where the ends of the slits of A and A' will be placed, and imagine these rings to be seperated by a line. The outer boundary of $\mathbb{A}_i$ has to correspond to the inner boundary of $\mathbb{A}'_i$. Thus, it makes sense to scale down the annulus $\mathbb{A}_i$ and to place it into the inner ring of $\mathbb{A}_i^{\odot}$, see Figure 4.30. The slits of A have to be extended towards the outer boundary of the annulus $\mathbb{A}_i^{\odot}$.

Now, the seperating lines of the annuli $\mathbb{A}_1^{\odot}, \ldots, \mathbb{A}_n^{\odot}$ are divided into arcs by the slits of A. Each of these arcs belongs to one of the m outgoing boundary curves of A. Due to the definition of the composition, we have to glue the j^{th} outgoing boundary curve of A to the inner boundary of the annulus $\mathbb{A}'_j$. We obtain a closed path corresponding to the j^{th} outgoing boundary curve of A by starting at the marked point ${P_j}^+$ and wandering along the seperating lines counter-clockwise, jumping across slits of A when they are met. Reparametrizing the inner boundary of the annulus $\mathbb{A}'_j$ such that it can be mapped onto this closed path, especially ${P'_j}^-$ onto ${P_j}^+$, we insert all slits of A'_j into the outer rings of the annuli ${\mathbb{A}_1}^{\odot}, \ldots, {\mathbb{A}_n}^{\odot}$. Thereby, all angles have to be preserved. In Figure 4.31, we see how the annuli $\mathbb{A}'_1, \mathbb{A}'_2, \mathbb{A}'_3$ are put into the annulus $\mathbb{A}^{\odot}$ this way.

This process to describe a radial slit version of the composition yields

Definition 4.6.3. Let the map

$$\odot\colon \mathfrak{Rad}_g^{\bullet\bullet}(m,n) \times \mathfrak{Rad}_{g'}^{\bullet\bullet}(l,m) \longrightarrow \mathfrak{Rad}_{g+g'+m-1}^{\bullet\bullet}(l,n)\,, (A,A') \longmapsto A \odot A'\,,$$

be given by the process defined above. We call $A \odot A'$ the **composition** of the two radial slit pictures A and A'.

The composition map fulfills the following properties.

Proposition 4.6.4. *The composition yields an H-space structure on the disjoint union* $\mathfrak{Rad}^{\bullet\bullet} = \coprod_{g,m,n} \mathfrak{Rad}_g^{\bullet\bullet}(m,n)$ *respectively* $\mathfrak{M}^{\bullet\bullet} = \coprod_{g,m,n} \mathfrak{M}_g^{\bullet\bullet}(m,n)$.

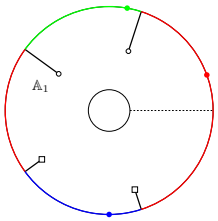

Figure 4.28.: A radial slit domain A with $m(A) = 3$, $n(A) = 1$, $g(A) = 0$.

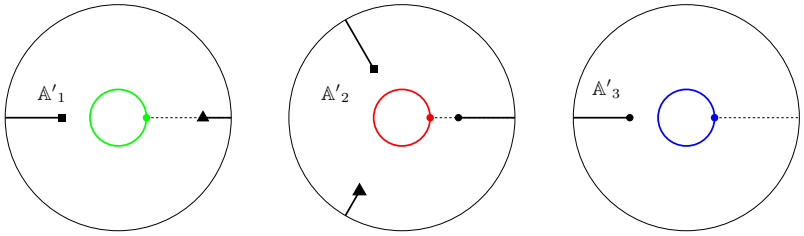

Figure 4.29.: A radial slit domain A' with $m(A') = 2$, $n(A') = 3$, $g(A') = 0$.

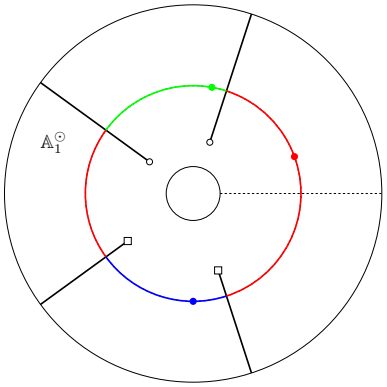

Figure 4.30.: The slits of A put into the annulus $\mathbb{A}_1^{\odot}$.

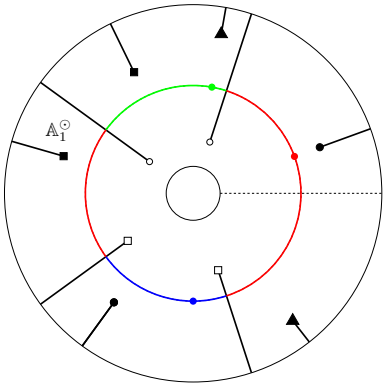

Figure 4.31.: The slit picture $A \odot A'$ with $m(A \odot A') = 2$, $n(A \odot A') = 1$, $g(A \odot A') = 2$.

Proof. We have to show that composition is assotiative up to homotopy, but this is evident if we consider the composition map on surfaces. □

Note that if we allow disconnected surfaces, the disjoint union of the appropriate number of cylinders serves as a right / left unit up to homotopy. Using a generalization of this composition map, we can equip $\mathfrak{Rad}_g^{\bullet\bullet}(m,n)$ with the structure of an operad.

Definition 4.6.5. Define the composition map

$$\odot_M \colon \mathfrak{M}_g^{\bullet\bullet}(m,n) \times \left(\mathfrak{M}_{g_1}^{\bullet\bullet}(l_1,m_1)\dots\mathfrak{M}_{g_s}^{\bullet\bullet}(l_s,m_s)\right) \longrightarrow \mathfrak{M}_{g+g'+m-s}^{\bullet\bullet}(l,n)\,,(A,A') \longmapsto A\odot A'\,,$$
$$(F,(F_1,\dots,F_s)) \longrightarrow F\odot(F_1,\dots,F_s)\,,$$

by glueing the incoming boundary curves of s surfaces $F_1,\dots,F_s$ to the outgoing boundary curves of a single surface F. Here, $m=m_1+\dots+m_s$ is an ordered partition with all $m_i>0$, mentioned in the map $\odot_M$ as $M=(m_1,\dots,m_s)$. We have $g'=g_1+\dots+g_s$ and $l=l_1+\dots+l_s$.

That $m=m_1+\dots+m_s$ is an ordered partition means that the m_1 incoming boundary curves of F_1 are glued with the first m_1 outgoing boundaries of F and so forth. This generalized composition maps equip the family of spaces $\mathfrak{M}_g^{\bullet\bullet}(m,n)$ with the structure of an operad. Due to Proposition 4.6.4, we immediately see that the associativity conditions (i) and (iii) of Theorem 4.1.1 are also fulfilled for the maps $\odot_M$. For equivariant associativity, i.e., condition (ii), we need to restrict to $n=1$ and $m_1=\dots=m_2=1$. Then, the symmetric group $\mathfrak{S}_m$ acts on $\mathfrak{M}_g^{\bullet\bullet}(m,n)$ by permuting the outgoing boundary curves and it is clear that equivariant associativity is fulfilled. This results in

Proposition 4.6.6. *The operations $\odot_M$ equip the family of spaces $\mathfrak{M}_g^{\bullet\bullet}(m,n)$ with an operad structure. We have to restrict to the subfamily of spaces $\mathfrak{M}_g^{\bullet\bullet}(m,n)$ with $m=1$ and $n=1$ in order to guarantee equivariant associativity.*

Another closely related generalization of the composition map arises as follows. Consider again the two surfaces in Figure 4.27. We pair the outer boundary curves of F with the inner boundary curves of F' according to their numeration and glue them together in order to obtain the new surfaces $F\odot F'$. Alternatively, we can choose any pairing of the outer boundary curves of F and the inner boundary curves of F', or even any partial pairing. We obtain

Definition 4.6.7. Consider two moduli spaces $\mathfrak{M}_g^{\bullet\bullet}(m,n)$ and $\mathfrak{M}_{g'}^{\bullet\bullet}(m',n')$. Define a partial pairing π_k of the outgoing boundary curves of F and the incoming boundary curves of F' of cardinality k. The **composition** of surfaces **with respect to the partial pairing** π_k is the map

$$\odot_{\pi_k} \colon \mathfrak{M}_g^{\bullet\bullet}(m,n)\times\mathfrak{M}_{g'}^{\bullet\bullet}(m',m') \longrightarrow \mathfrak{M}_{\tilde{g}}^{\bullet\bullet}(\tilde{m},\tilde{n})\,,(F,F') \longmapsto F\odot_{\pi_k}F'\,,$$

which glues the surfaces F and F' along the paired incoming respectively outgoing boundary curves. Thereby, we have

- $\tilde{g}=g+g'+k-1$,
- $\tilde{m}=m-k+m'$,
- $\tilde{n}=n+n'-k$.

Obviously, this generalized composition is still assotiative.

4.7. Rotation of Radial Slit Pictures

In this section, we want to construct an operation on the space $\mathfrak{Rad}_g(m,n)$ of radial slit domains that looks like a rotation of the annuli on which radial slit pictures reside.

Consider the bundle $\mathfrak{H}_g^\bullet(m,n) \cong \mathfrak{Rad}_g(m,n)$ first. Recall that its elements are tuples $[F, \mathcal{C}^+, \mathcal{C}^-, \mathcal{P}, w]$. For an explanation of the notation and more details about the following explanation, see Section 2.4. Here, we only mention that $\mathcal{P} = (P_1, \dots, P_n)$ is the set of marked points on the enumerated incoming boundary curves $C_1^-, \dots, C_n^-$ of the surface F, On each incoming boundary curve C_k^-, we can let the sphere act by rotating the marked point P_k by an angle θ_k. We obtain

Definition 4.7.1. There is a group operation

$$\psi \colon (\mathbb{S}^1)^n \times \mathfrak{H}_g^\bullet(m,n) \longrightarrow \mathfrak{H}_g^\bullet(m,n)$$

given by

$$(\theta_1, \dots, \theta_n).[F, \mathcal{C}^+, \mathcal{C}^-, (P_1, \dots, P_n), w] = [F, \mathcal{C}^+, \mathcal{C}^-, (\theta_1 P_1, \dots, \theta_n P_n), w] \,.$$

Here, $\theta_k P_k$ is a shorthand for

$$\theta_k P_k = \varphi_k(\theta_k \varphi_k^{-1}(P_k)) \in C_k^- \,,$$

where $\varphi_k \colon \mathbb{S}^1 \longrightarrow C_k^-$ parametrizes the k^{th} incoming boundary curve.

Recall that we obtain a radial slit picture from $[F, \mathcal{C}^+, \mathcal{C}^-, \mathcal{P}, w]$ by mapping it into n annuli $\mathbb{A}_1, \dots, \mathbb{A}_n$, whereby the marked point P_k is mapped to the real point of the inner boundary of the annulus $\mathbb{A}_k$. Hence, a rotation of P_k by an angle θ_k implies a rotation of the marked point on $\mathbb{A}_k$ by θ_k. Equivalently, we can leave the marked point on the annulus in the same place as before and rotate all slits on the annulus by an angle $-\theta_k$ instead. We chose the latter variant in order to avoid confusions about the location of the marked point. By composing the induced map of this group operation in homology with the homology cross product, we obtain

Definition 4.7.2. There is a map

$$H_i((\mathbb{S}^1)^n) \otimes H_j(\mathfrak{H}_g^\bullet(m,n)) \longrightarrow H_{i+j}(\mathfrak{H}_g^\bullet(m,n)) \,, \gamma \otimes x \longmapsto \psi_*(\gamma \times x) \,.$$

The restriction

$$\mathrm{rot}_\gamma \colon H_j(\mathfrak{H}_g^\bullet(m,n)) \longrightarrow H_{j+1}(\mathfrak{H}_g^\bullet(m,n)) \,, \mathrm{rot}_\gamma = \psi_*(\gamma \times x)$$

of this map is called the **rotation map** with respect to $\gamma \in H_1((\mathbb{S}_1)^n)$.

Proposition 4.7.3. *The rotation map satisfies the following properties:*

(i) Rotation is associative, i.e. for $\gamma_1, \gamma_2 \in H_1((\mathbb{S}_1)^n)$, we have

$$\mathrm{rot}_{\gamma_1} \mathrm{rot}_{\gamma_2} = \mathrm{rot}_{\gamma_1 \cdot \gamma_2} \,.$$

Here, $\_ \cdot \_$ denotes the Pontryagin product.

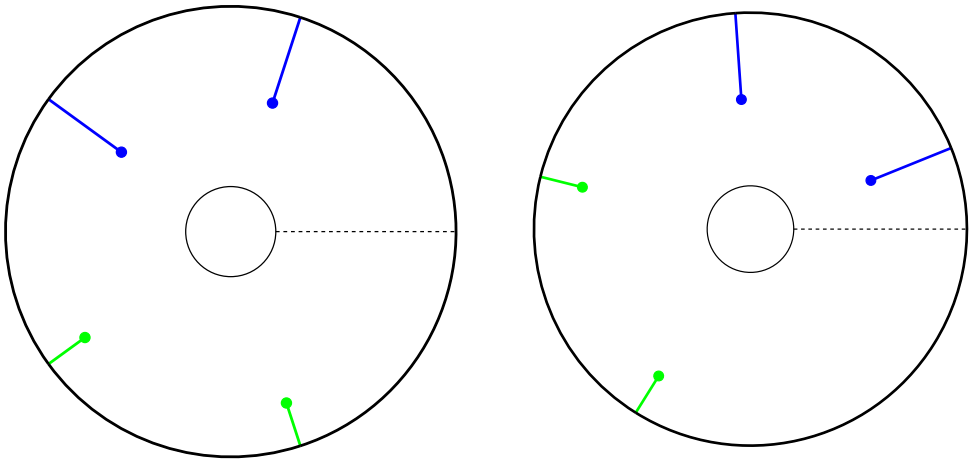

Figure 4.32.: Rotating a radial slit picture by an angle of 50 degree.

(ii) Rotation defines a differential of degree $+1$ *on* $H_*(\mathfrak{H}_g^\bullet(m,n))$*, i.e.* $\mathrm{rot}_\gamma^2 = 0$ *for* $\gamma \in H_1(\mathbb{S}_1)$*.*

Proof. The first statement is obvious since ψ is a group operation and the cross product is an isomorphism in our case. The second claim follows from the first one since the ring $H_*((\mathbb{S}^1)^k)$ is strictly anticommutative, i.e., $\gamma^2 = 0$ if the degree of γ is odd, which is the case here. Hence,

$$\mathrm{rot}_\gamma^2 = \mathrm{rot}_{\gamma^2} = \mathrm{rot}_0 = 0\,.$$

□

4.8. Correlation of Parallel and Radial Homology Operations

In this section, we will use the radialization and parallelization maps to compare parallel and radial homology operations, or obtain operations of the space of parallel slit domains on the space of radial slit domains. Thereby, let always $r = n = 1 + \cdots + 1$ be the trivial partition, and denote $\mathfrak{Par}_{g,1}^{m_1} = \mathfrak{Par}_{g,1}^{m_1}[(1,\ldots,1)]$. Thus, the two multiplications $\mu^{\uparrow\uparrow}$ and $\mu^{\uparrow\downarrow}$ on parallel slit domains coincide and will be denoted by a simple dot during this chapter. In our case, the parallel multiplication is hence a map

$$\_\cdot\_\colon \mathfrak{Par}_{g_1,n}^{m_1} \times \mathfrak{Par}_{g_2,n}^{m_2} \longrightarrow \mathfrak{Par}_{\tilde{g},n}^{m_1}$$

with $\tilde{g} = g_1 + g_2 + n - 1$.

4.8.1. Placing Parallel Slit Pictures into Annuli via Operads

First, we would like to let $\mathfrak{Par}_1 = \coprod g, m\mathfrak{Par}_{g,1}^m$ act on $\mathfrak{Rad}(n) = \coprod_{g,m} \mathfrak{Rad}_g(m,n)$ via little cubes operads, for fixed $n > 0$.

Therefore, let $\mathbb{A} \subset \mathbb{C}$ be an annulus in the complex plane, and let

$$\tilde{C}^k(\mathbb{A}) = \{(z_1,\ldots,z_n) \in \mathbb{A} \mid z_i \neq z_j \text{ for } i \neq j\}$$

denote the k^{th} ordered configuration space of $\mathbb{A}$. We want to use this configuration space to emplace k parallel slit pictures into $\mathbb{A}$, resulting in a radial slit picture.

Assume we are given a configuration $(z_1, \dots, z_k) \in \tilde{C}^k(\mathbb{A})$ and k parallel slit pictures $L_1, \dots, L_k$, where slit picture L_i fulfills $m(L_i) = m_i$, $h(L_i) = h_i$ and $n(L_i) = 1$. Since the points $z_1, \dots, z_k$ are pairwise distinct, we can choose pairwise disjoint regions around them. Here, a region is the intersection of a radial segment and a concentrical stripe of the annulus, see also Figure 4.33. Into the i^{th} such region, we insert the radialization of the parallel slit picture L_i.

Similar as in Figures 4.2 and 4.3, we thereby have to be careful that we insert the slits in the right order and way: We have to put the slit pictures L_i into the annulus $\mathbb{A}$ by increasing distance of the point z_i from the center of the annulus. Whenever, during the insertion of some slit picture L_i, there are already some slits in the region we chose for L_i to reside in, we have to thread in the new slit picture through the old slits. For a better understanding of this process, compare Figure 4.33 and the exact definition of threading in Section 4.6.

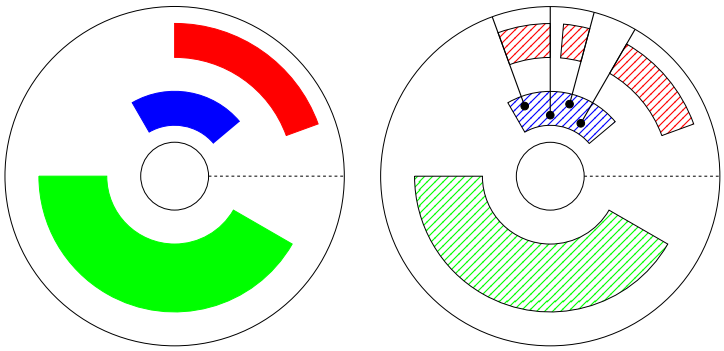

Figure 4.33.: The operation ρ on slit pictures At first, a blue parallel slit domain is inserted into the inner ring of the annulus via radialization. Afterwards, the green radial slit picture is threaded in into the outer ring.

Note that, when the first slit picture, say this is L_1, is inserted into $\mathbb{A}$, the number of punctures of the resulting radial slit picture is $m_1 + 1$ since this process is simply the radialization map, compare Subsection 2.7.1. Each further inserted slit picture L_i causes the number of punctures to increase by m_i since it is threaded in into one of the cycles of the slit picture, which has been built up so far. Since the number h of slit pairs of the final slit picture is the sum of the slit pairs of $L_1, \dots, L_k$, we can compute that the genus of the resulting slit picture will be the sum of all the genuses. Thus, this process results in

Proposition 4.8.1. *There is a map*

$$\tilde{\vartheta} \colon \tilde{C}^k(\mathbb{A}) \times \mathfrak{Par}_{g_1,1}^{m_1} \times \cdots \times \mathfrak{Par}_{g_k,1}^{m_k} \longrightarrow \mathfrak{Rad}_{\tilde{g}}(\tilde{m}+1, 1)$$

defined by an action of the little cubes operade. The map is given by choosing k distinct points on the annulus $\mathbb{A}$ and emplacing each of the k parallel slit pictures into disjoint regions as described above. Hereby, we have $\tilde{g} = \sum_{i=1}^{k} g_i$ and $\tilde{m} = \sum_{i=1}^{k} m_i$.

Note that the map $\tilde{\vartheta}$ defined here restricts to the map $\tilde{\vartheta}$ defined in Theorem 4.1.1. To give the precise statement, let $\tilde{C}^k(\mathbb{C}) \overset{\iota}{\longrightarrow} \tilde{C}^k(\mathbb{A})$ denote the inclusion, where the complex plane

is wrapped around the annulus $\mathbb{A}$. Now, the definitions of the maps $\tilde{\vartheta}$ and rad immediately yield

Proposition 4.8.2. *The map $\tilde{\vartheta}$ restricts to the action of the little cubes operad on parallel slit domains (compare Theorem 4.1.1). To be precise, the diagram*

$$\begin{array}{ccc} \tilde{C}^k(\mathbb{A}) \times \mathfrak{Par}_{g_1,1}^{m_1} \times \cdots \times \mathfrak{Par}_{g_k,1}^{m_k} & \xrightarrow{\tilde{\vartheta}} & \mathfrak{Rad}_{\tilde{g}}(\tilde{m}+1,1) \\ \uparrow{\scriptstyle \iota \times id} & & \uparrow{\scriptstyle \mathrm{rad}} \\ \tilde{C}^k(\mathbb{C}) \times \mathfrak{Par}_{g_1,1}^{m_1} \times \cdots \times \mathfrak{Par}_{g_k,1}^{m_k} & \xrightarrow{\tilde{\vartheta}} & \mathfrak{Par}_{\tilde{g},1}^{\tilde{m}} \end{array}$$

commutes, where, as above, $\tilde{g} = \sum_{i=1}^k g_i$ and $\tilde{m} = \sum_{i=1}^k m_i$.

With the homology cross product, we obtain

Proposition 4.8.3. *The map $\tilde{\vartheta}$ yields a family of homology operations*

$$\tilde{\vartheta}_* \colon H_s(\tilde{C}^k(\mathbb{A})) \otimes H_{t_1}(\mathfrak{Par}_{g_1,1}^{m_1}) \otimes \cdots \otimes H_{t_k}(\mathfrak{Par}_{g_k,1}^{m_k}) \longrightarrow H_{s+\tilde{t}}(\mathfrak{Rad}_{\tilde{g}}(\tilde{m}+1,1))\,,$$

where $\tilde{g} = \sum_{i=1}^k g_i$, $\tilde{m} = \sum_{i=1}^k m_i$ and $\tilde{t} = \sum_{i=1}^k t_i$.

For later uses, it is a good idea to imagine what the map $\tilde{\vartheta}$ looks like on surfaces, compare Figure 4.34. At the bottom of the picture, we see the boundary curves of three surfaces with

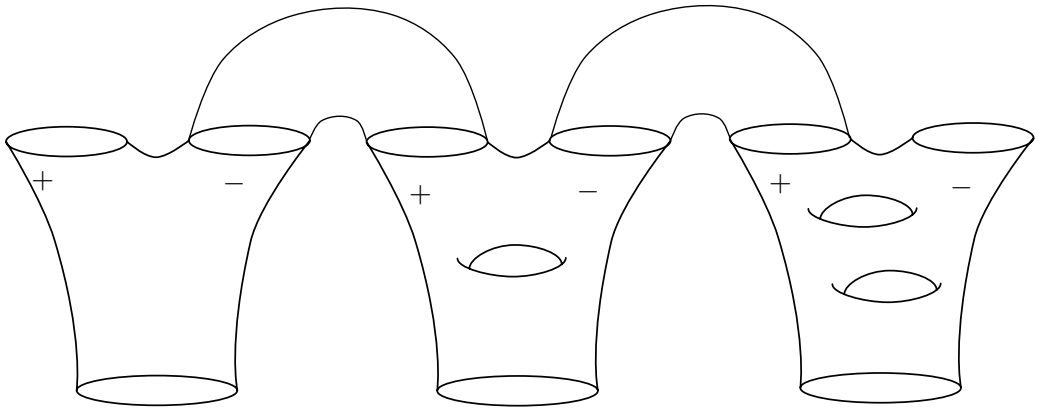

Figure 4.34.: An excerpt of the map $\tilde{\vartheta}$ applied to three surfaces.

punctures and each one boundary curve. Since the map $\tilde{\vartheta}$ at first applies the radialization map to each of these surfaces, there are pairs of pants glued to each boundary curve, with one leg an outgoing and one leg an incoming boundary curve. Secondly, we need to carry over the meaning of the configuration space for the surfaces. Recalling the definition of $\tilde{\vartheta}$ on slit pictures, we see that a configuration in $\tilde{C}^k(\mathbb{A})$ determines an order in which to insert the k parallel slit pictures into the annulus. During the insertion of a new parallel slit picture L , it also determines an already placed slit domain L' and inserts the new picture into one of its outgoing boundary curves. On the corresponding surfaces F and F',

this outgoing boundary curve of F' is hence glued to the incoming boundary curve of F. So Figure 4.34 shows an excerpt of one possibility how $\tilde{\vartheta}$ acts with the surfaces. It is not neccessarily the new outgoing boundary curve arising by radialization that is glued with some incoming boundary curve.

We can easily generalize the map $\tilde{\vartheta}$ by inserting parallel slit pictures into n annuli instead of one.

Definition 4.8.4. Write $n\mathbb{A} = \mathbb{A}_1 \sqcup \ldots \sqcup \mathbb{A}_n$ for the disjoint union of n annuli in the complex plane. There is a map

$$\tilde{\vartheta} \colon \tilde{C}^k(n\mathbb{A}) \times \mathfrak{Par}_{g_1,1}^{m_1} \times \cdots \times \mathfrak{Par}_{g_k,1}^{m_k} \longrightarrow \mathfrak{Rad}_{\tilde{g}}(\tilde{m}+n, n)$$

given by placing k parallel slit pictures into n annuli using the same method as above. By this, we have $\tilde{g} = \sum_{k=1}^{k} g_i$ and $\tilde{m} = \sum_{i=1}^{k} m_i$.

Here, the regions where parallel slit pictures are inserted can lie on different annuli, but each slit picture is placed completely into a single annulus. Thus, the resulting radial slit picture is not connected for $n > 1$, and it is even possible that one annulus stays empty. The parameters of the target space of this generalized map $\tilde{\vartheta}$ are obvious. In Proposition 4.8.11, we will use this map to describe how parallel slit pictures can also be placed into radial slit pictures and not only into empty annuli. Thus, we also need to generalize the above proposition to

Proposition 4.8.5. *Let $\mathbb{A} = \mathbb{A}_1 \sqcup \ldots \sqcup \mathbb{A}_n$ be the disjoint of n complex annuli. Then, the generalized map $\tilde{\vartheta}$ restricts to a similarly generalized action of the little cubes operad on parallel slit domains. To be precise, the diagram*

$$\begin{array}{ccc} \tilde{C}^k(n\mathbb{A}) \times \mathfrak{Par}_{g_1,1}^{m_1} \times \cdots \times \mathfrak{Par}_{g_k,1}^{m_k} & \xrightarrow{\tilde{\vartheta}} & \mathfrak{Rad}_{\tilde{g}}(\tilde{m}+n, 1) \\ \uparrow{\scriptstyle \iota \times id} & & \uparrow{\scriptstyle \mathrm{rad}} \\ \tilde{C}^k(n\mathbb{C}) \times \mathfrak{Par}_{g_1,1}^{m_1} \times \cdots \times \mathfrak{Par}_{g_k,1}^{m_k} & \xrightarrow{\tilde{\vartheta}} & \mathfrak{Par}_{\tilde{g},n}^{\tilde{m}} \end{array}$$

commutes, where $\tilde{g} = \sum_{i=1}^{k} g_i$ and $\tilde{m} = \sum_{i=1}^{k} m_i$.

4.8.2. $\mathfrak{Par}$ as a Module over $\mathfrak{Rad}$

We will now develop an operation that makes the homology of $\mathfrak{Par}(n) = \coprod_{g,m} \mathfrak{Par}$ a module over the homology of $\mathfrak{Rad}(n) = \coprod_{g,m} \mathfrak{Rad}_g(m,n)$.

Therefore, let $L \in \mathfrak{Par}$ and $A \in \mathfrak{Rad}$ be two slit pictures with $n(L) = n(A)$. We want to merge L and A into a radial slit picture on n new annuli $\tilde{\mathbb{A}}_1, \ldots, \tilde{\mathbb{A}}_n$. For a visualization of the following description, see Figure 4.35. Consider a fixed annulus $\tilde{\mathbb{A}}_k$ and seperate it equally into an inner and an outer ring. Put the k^{th} level of the parallel slit picture x into the inner ring of $\tilde{\mathbb{A}}_k$ like via the radialization map, extending the slits to the outer boundary of the annulus. We obtain a new distinguished outgoing boundary curve that arises during radialization, marked red in the picture. Starting at the real horizontal line, we insert the k^{th} level of the radial slit picture y into the outer ring of the annulus, threading in the slits into the distinguished cycle similarly as in Subsection 4.8.1.

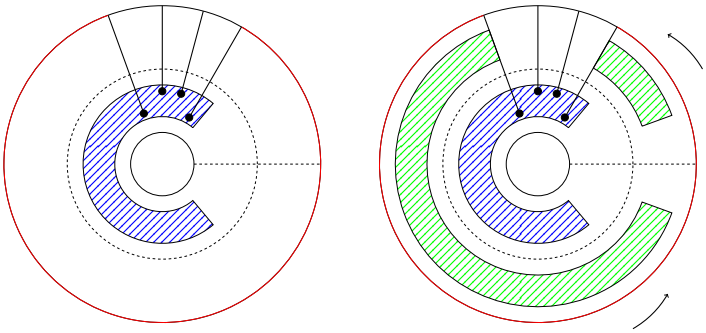

Figure 4.35.: Three regions of an annulus, into which three parallel slit pictures are placed, and how slits have to be threaded in.

Definition 4.8.6. The above procedure defines a a map

$$\rho\colon \mathfrak{Rad}(n) \times \mathfrak{Par}(n) \longrightarrow \mathfrak{Rad}(n)\,, (A, L) \longmapsto \rho(A, L) = A.L\,.$$

We also denote the map ρ with a low dot since it will turn out that it is a module operation in the sense of operads. Before we show that, we take a closer look at the map ρ itself.

Proposition 4.8.7. *For $A \in \mathfrak{Rad}_{g_1}(m_1, n)$ and $L \in \mathfrak{Par}^{m_2}_{g_2,n}$, we have $A.L \in \mathfrak{Rad}_{\tilde{g}}(\tilde{m}, n)$ with $\tilde{g} = g_1 + g_2 + n - 1$ and $\tilde{m} = m_1 + m_2$.*

Proof. By construction, the radial slit picture $A.L$ has n incoming boundary curves. Since the n incoming boundary curves of A are glued to the n outgoing boundary curves that arise due to radialization, we have

$$\tilde{m} = (m_2 + n) - n + m_1 = m_1 + m_2\,.$$

Using the formulas for h for each of the three spaces involved, we obtain

$$\tilde{g} = g_1 + g_2 + n - 1\,.$$

□

In Figure 4.36, one can see that the genus increases by one for each two neighboring incoming boundary curves of A. Note that here, it is always the new outgoing boundary curves of L arising from radialization that are glued together with the incoming boundary curves of A.

Proposition 4.8.8. *Let $n > 0$. There is a right module structure*

$$H_*(\mathfrak{Rad}(n)) \otimes H_*(\mathfrak{Par}(n)) \longrightarrow H_*(\mathfrak{Rad}(n))$$

induced by an action of the litte cubes operade.

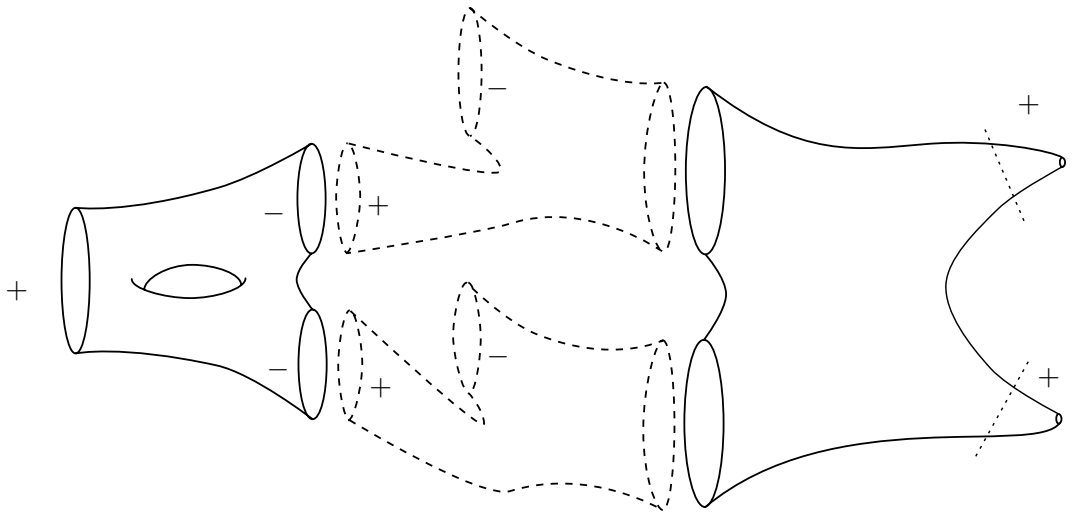

Figure 4.36.: The operation ρ on surfaces.

Proof. We define the right module structure by the composition

$$H_*(\mathfrak{Rad}(n)) \otimes H_*(\mathfrak{Par}(n)) \xrightarrow{\otimes} H_*(\mathfrak{Rad}(n) \times \mathfrak{Par}(n)) \xrightarrow{\rho_*} H_*(\mathfrak{Rad}(n))\,.$$

The map ρ is induced by a little cubes operade in the following way. We can restrict the map $\tilde{\theta}$ of Proposition 4.8.1 for $k = 1$ to the point $z = -1$ in the configuration space $\tilde{C}^1(\mathbb{A})$ in order to choose the position for inserting one level of a parallel slit picture into one annulus $\mathbb{A}$. We can apply this to a parallel slit picture on n levels by treating the levels seperately. It is also possible to do this if there is already a radial slit picture residing on the annuli since we can thread in the slits of the parallel slit picture.

It remains to verify that, for $L_1, L_2 \in \mathfrak{Par}(n)$ and $A \in \mathfrak{Rad}(n)$, we have $A.(L_1 \cdot L_2) \simeq (A.L_1).L_2$. Using the definition of ρ on the surfaces resulting from glueing the slit pictures, it is not difficult to see that this formula if fulfilled. Now we can compose the induced map ρ_* with the homology cross product in order to obtain the desired operation. □

4.8.3. Formulas

In this subsection, we will see several formulas relating all the maps and operations we have seen so far.

First, we obtain another property of the radialization map from Section 2.7.2. The radialization map may not be multiplicative with respect to the radial multiplication (see 4.5.7). However, it is compatible with the operation ρ defined in Subsection 4.8.2.

Proposition 4.8.9. *The radialization map is compatible with the operation ρ and the parallel multiplication, i.e., for L_1, $L_2 \in \mathfrak{Par}(n)$, we have*

$$\mathrm{rad}(L_1 \cdot L_2) \simeq \mathrm{rad}(L_1).L_2\,.$$

Proof. See Figure 4.37 for a proof. Here, L_1 is colored green and L_2 blue. The first picture shows the radial slit picture $\mathrm{rad}(L_1).L_2$. Note that the slits of L_1 are threaded in into a

single outgoing boundary curve of $\mathrm{rad}(L_2)$. We can reverse this threading process in order to move all slits of L_1 into a connected part of the annulus. This happens in the second picture. From the radial slit picture shown there, the slits only have to be rotated around the annulus, and their lengths have to be changed, and then we arrive at the third radial slit picture, $\mathrm{rad}(L_1 \cdot L_2)$.

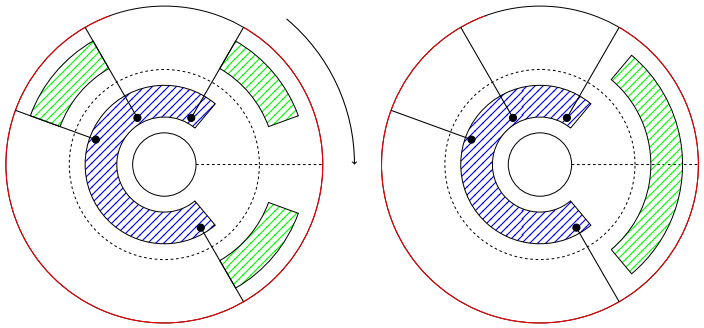

Figure 4.37.: Proof of Proposition 4.8.9.

□

Next, we obtain another little formula that relates radialization and the operation ρ with the composition of radial slit pictures defined in Section 4.6.

Proposition 4.8.10. *Denote the map swapping the two factors of a product by t. The diagram*

$$\begin{array}{ccc} \mathfrak{Rad}^{\bullet\bullet}_{g_1}(n,n) \times \mathfrak{Par}^{m}_{g_2,n} & \xrightarrow{\rho} & \mathfrak{Rad}_{g}(m,n)^{\bullet\bullet}_{g_1+g_2+n-1}(m+n,n) \\ \downarrow{\scriptstyle \mathrm{id}\times\mathrm{rad}} & & \uparrow{\scriptstyle \odot_{\pi_n}} \\ \mathfrak{Rad}^{\bullet\bullet}_{g_1}(n,n) \times \mathfrak{Rad}^{\bullet\bullet}_{g_2}(m+n,n) & \xrightarrow{t} & \mathfrak{Rad}^{\bullet\bullet}_{g_2}(m+n,n) \times \mathfrak{Rad}^{\bullet\bullet}_{g_1}(n,n) \end{array}$$

commutes, where the partial pairing π_n pairs the k^{th} incoming boundary curve of the second factor with the outgoing boundary curves of the first factor arising from the k^{th} boundary curve by radialization.

Proof. Recall how the operation ρ is defined on surfaces $F \in \mathfrak{M}^{\bullet\bullet}_{g_1}(n,n)$ and $F' \in \mathfrak{M}^{m}_{g_2,n}$, see Figure 4.36. The surface F' is at first radialized, i.e. each puncture is transformed into an outgoing boundary, and onto each boundary curve, a pair of pants with one incoming and one outgoing boundary curve is glued. Now the k^{th} new outgoing boundary curve arising from the k^{th} boundary curve of F' is glued together with the k^{th} incoming boundary curve of F. But this is exactly what the map $\odot_{\pi_n} \circ t \circ (\mathrm{id} \times \mathrm{rad})$ does. □

Note that we need to restrict to these parameters in order to state the preceeding formula. The number of incoming boundary curves of the radial and the parallel slit picture in this formula have to coincide since this is required by the operation ρ. Furthermore, the number of outgoing boundary curves of the radial slit picture needs to equal the same number due to the composition map.

We can use this proposition to show that, in some special cases, we can relate the operad structure on $\mathfrak{Par}$ with the radial composition map by the operation of $\mathfrak{Par}$ on $\mathfrak{Rad}$. The next corollary will state that the diagram

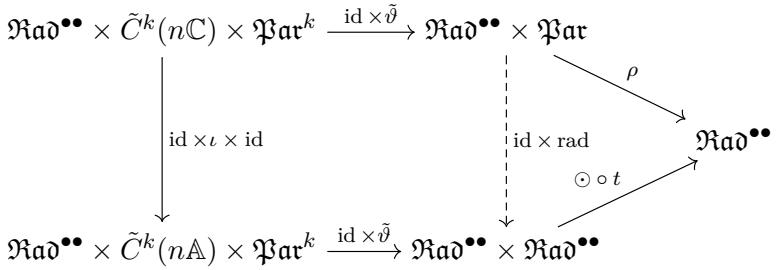

commutes up to homotopy, whenever it makes sense to write down the compositions of the participating maps. We will come to state a more formal version of this diagram. But without all the indices, it is easier to see that the left square consists of the commutative diagram in Proposition 4.8.5 and the triangle of the commutative diagram in Proposition 4.8.10.

Furthermore, we can already interpret the diagram in this simple version. There are two canonical ways to emplace parallel slit pictures into a given radial slit picture in order to obtain another radial slit picture via little cubes operads. Firstly, by composing the parallel map $\tilde{\theta}$ given by operads on the parallel slit pictures with the operation ρ of $\mathfrak{Par}$ on $\mathfrak{Rad}$; secondly, by using the radial map $\tilde{\theta}$ given by operads followed by the radial composition. According to the diagram, these processes coincide whenever they are comparable. We now formalize the diagram in

Corollary 4.8.11. *Let π_k and t as in the preceeding proposition. The diagram*

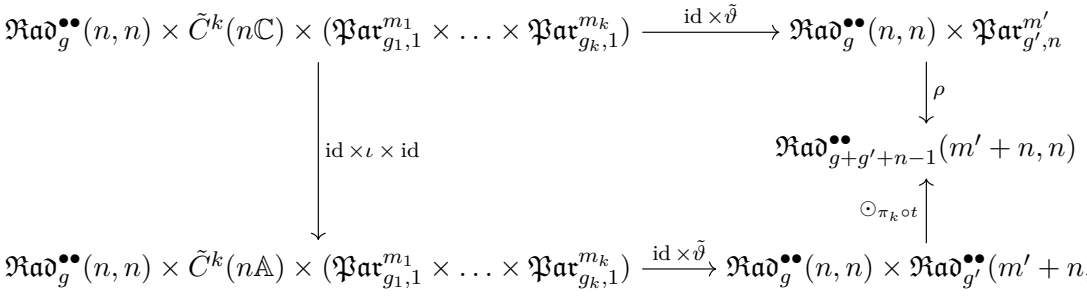

commutes up to homotopy. Here, we have $m' = \sum_{i=1}^k m_i$ and $g' = \sum_{i=1}^k g_i$.

Proposition 4.8.12. *Let A be a parallel slit picture on n levels, B a radial cell with $n(A) = n(B) = n$. Then the parallel slit pictures $\alpha(A \cdot \mathrm{par}(B))$ and $\mathrm{par}(\mathrm{rad}(A) \rightarrowtail\!\bullet\!\leftarrowtail B)$ coincide.*

Proof. Consider the product $\mathrm{rad}(A) \rightarrowtail\!\bullet\!\leftarrowtail B$ and its parallelization $\mathrm{par}(\mathrm{rad}(A) \rightarrowtail\!\bullet\!\leftarrowtail B)$, see Figure 4.38. Comparing this with Figure 4.39, we see that $\mathrm{par}(\mathrm{rad}(A) \rightarrowtail\!\bullet\!\leftarrowtail B)$ results from $\alpha(A \cdot \mathrm{par}(B))$ by moving the lowest green slit upwards a little, which means that the two slit pictures agree. □

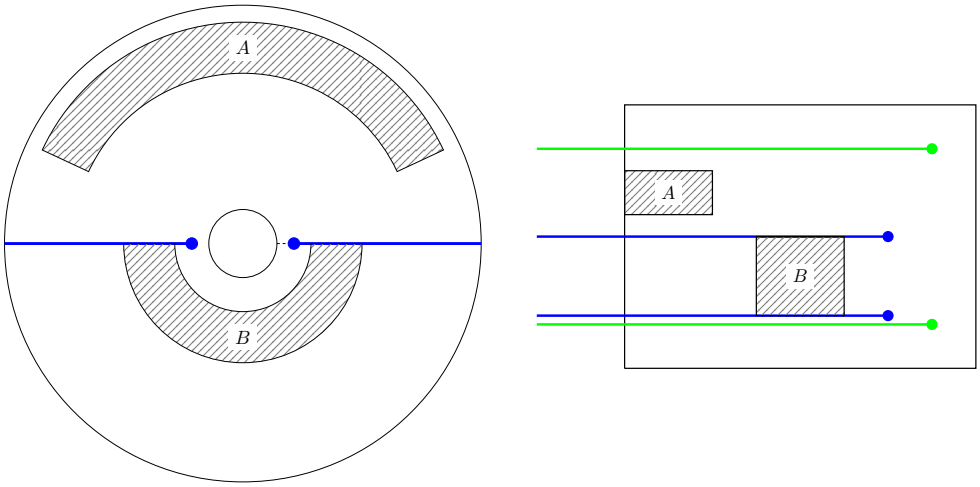

Figure 4.38.: The radial / parallel slit pictures $\mathrm{rad}(A)\multimap\bullet\!\!-B$ and $\mathrm{par}(\mathrm{rad}(A)\multimap\bullet\!\!-B)$.

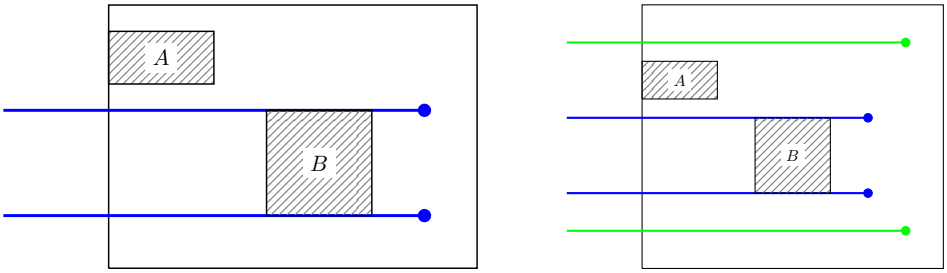

Figure 4.39.: The parallel slit pictures $A \cdot \mathrm{par}(B)$ and $\alpha(A \cdot \mathrm{par}(B))$.

Proposition 4.8.13. *Let A be a parallel slit domain on n levels, B a radial slit domain with $n(A) = n(B) = n$. Then the radial slit domains* $\mathrm{rad}(A)\multimap\bullet\!\!-B$ *and* $\mathrm{rad}(A \cdot \mathrm{par}(B))$ *coincide.*

Proof. Comparing Figures 4.40 and 4.41, we see that we can transform $\mathrm{rad}(A \cdot \mathrm{par}(B))$ into $\mathrm{rad}(A)\multimap\bullet\!\!-B$ by rotating all slits a little.

□

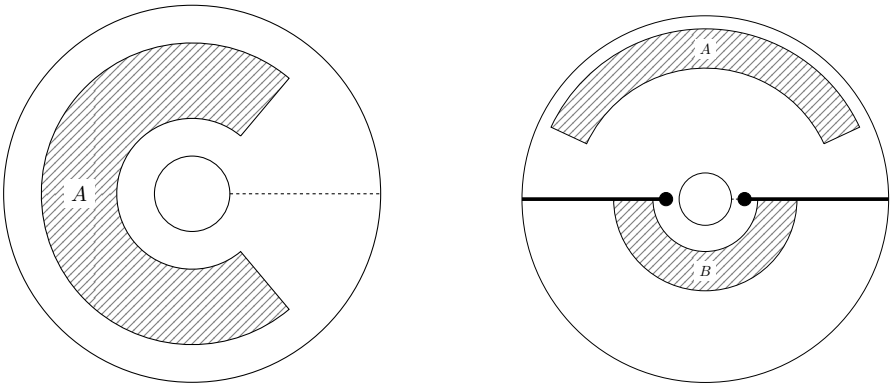

Figure 4.40.: The radial slit pictures $\mathrm{rad}(A)$ and $\mathrm{rad}(A)\text{—••—}B$.

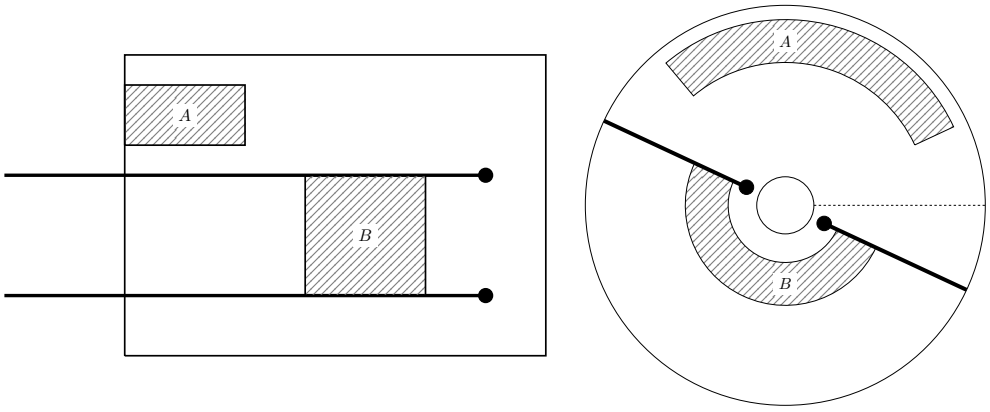

Figure 4.41.: The slit pictures $A \cdot \mathrm{par}\, B$ and $\mathrm{rad}(A \cdot \mathrm{par}\, B)$.

5. On the Computational Complexity

This chapter serves as a brief review on nearby complexity concerns. The first section explains why computation require much space even for small valued for h — which is $h = 2g - 2 + m + n + r$ in the parallel case and $h = 2g - 2 + m + n$ in the radial case — whereas the second section explains why computations require much time.

5.1. An Estimation of the Number of Cells of $\mathbb{E}(h, m; 1)$

In this section, we concentrate on combinatorial cells on exatcly one level, i.e. $n = 1$ and $r = (1)$. Recalling definitions 2.3.5 and 2.8.6, the combinatorial type of a non-degenerate cell Σ in the Ehrenfried complex is a finite word $\Sigma = (\tau_q \mid \ldots \mid \tau_1)$ of transpositions $\tau_k \in \mathfrak{S}_p$ with

$$\text{every element } 1 \leq k \leq p \text{ is permuted non-trivially by at least one transposition} \tag{Σ1}$$
$$\mathrm{ht}(\tau_q) \geq \ldots \geq \mathrm{ht}(\tau_1). \tag{Σ2}$$

Let us denote the sum of all Ehrenfried complexes by

$$\underline{\mathbb{E}} = \bigoplus_{g,m} \mathbb{E}(h, m; 1)\,.$$

Clearly, this sum is finite in each bidegree (p, q). More precisely:

Proposition 5.1.1. *The number of cells of $\underline{\mathbb{E}}_{p,q}$ is*

$$A(p, q) = \dim(\underline{\mathbb{E}}_{p,q}) = \sum_{k=1}^{p-1} a_{p,k} \cdot k^{q-1}\,, \tag{5.1}$$

where the coefficients $a_{p,k}$ are

$$a_{2,1} = 1 \tag{5.2}$$
$$a_{p,k} = 0 \qquad \textit{for} \quad p \leq k \tag{5.3}$$
$$a_{p,k} = -\frac{p-1}{p-1-k}(a_{p-2,k} + 2a_{p-1,k}) \qquad \textit{for} \quad 1 \leq k \leq p-2 \tag{5.4}$$
$$a_{p,p-1} = -\sum_{k=1}^{p-2} a_{p,k} \qquad \textit{for} \quad 3 \leq p\,. \tag{5.5}$$

Before going into the proof, we provide an essential remark and list some values of $A(p, q)$ in Figure 5.1.

Corollary 5.1.2. *The number of cells of $\underline{\mathbb{E}}_{p,q}$ depends polynomially on p and exponentially on q and the number of cells of the radial Ehrenfried complex in bidegree (p,q) is*

$$B_{p,q} = A_{p,q} + A_{p+1,q}\,.$$

Proof. The first statement is evident. Let us take a look at the number of cells $B_{p,q}$ in the radial Ehrenfried complex. Recall that its basis is given by all radial cells $\Sigma = (\tau_q \mid \ldots, \mid \tau_1)$, where all τ_i are transpositions on the symbols $\{\underline{0}, \ldots, \underline{p}\}$ subject to the conditions (Σ1) and (Σ2) from above. Thus, in radial bidegree (p,q), we have all the parallel cells of bidegree (p,q), and for all parallel cells Σ of bidegree $(p+1,q)$ the 0^{th} face $d_0(\Sigma)$. □

Remark 5.1.3. Since, for fixed g and m, the parallel Ehrenfried complex consists of cells with $q = 2g+m$ transpositions, but the radial of cells with $q = 2g+m-1$ transpositions, the preceding corollaries recommend to use the radial model for homology computations instead of the parallel one.

$A(p,q)$	$q=1$	$q=2$	$q=3$	$q=4$	$q=5$	$q=6$	$q=7$	$q=8$
$p=2$	1	1	1	1	1	1	1	1
$p=3$	0	4	12	28	60	124	252	508
$p=4$	0	3	36	183	720	2523	8316	26463
$p=5$	0	0	40	496	3560	20240	101640	474096
$p=6$	0	0	15	655	9150	84950	639765	4256805
$p=7$	0	0	0	420	13356	211296	2408616	22738716
$p=8$	0	0	0	105	11200	329434	5858832	79210803
$p=9$	0	0	0	0	5040	326368	9572256	189588288
$p=10$	0	0	0	0	945	200025	10639755	320787891
$p=11$	0	0	0	0	0	69300	7957180	388089460
$p=12$	0	0	0	0	0	10395	3839220	334326685
$p=13$	0	0	0	0	0	0	1081080	200600400
$p=14$	0	0	0	0	0	0	135135	79774695
$p=15$	0	0	0	0	0	0	0	18918900
$p=16$	0	0	0	0	0	0	0	2027025

Figure 5.1.: The number of cells of $\underline{\mathbb{E}}_{p,q}$ for small p and q.

We deduce Proposition 5.1.1 from the following oberservation.

Lemma 5.1.4. *The numbers $A(p,q)$ fulfill*

$$A(1,q) = 0 \tag{5.6}$$
$$A(2,q) = 1 \tag{5.7}$$
$$A(p,q) = (p-1)\big(A(p-2,q-1) + 2A(p-1,q-1) + A(p,q-1)\big) \quad \textit{for} \quad p > 2 \tag{5.8}$$
$$A(p,q) = 0 \quad \textit{for} \quad p > 2q\,. \tag{5.9}$$

Proof. Properties (5.6), (5.7) and (5.9) are consequences of ($\Sigma 1$). The following Figure 5.2 destincts the possible cases of appending a cell by one transposition and therefore proofs the remaining property (5.8). □

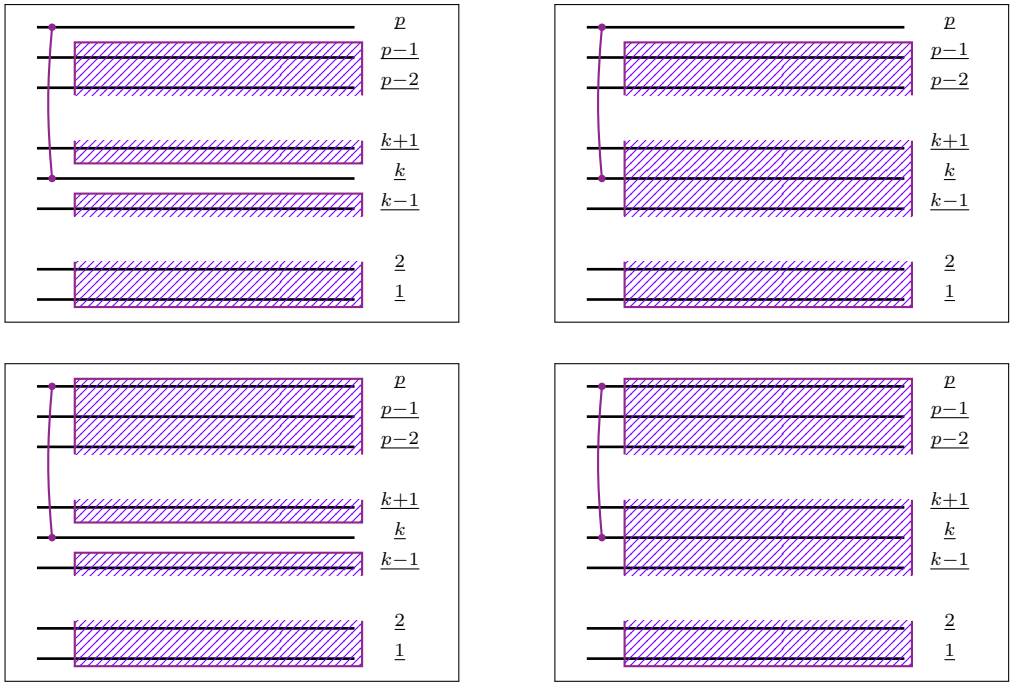

Figure 5.2.: The possible cases of appending a monotonous cell by one transposition.

Proof of Proposition 5.1.1. We are going to prove proposition 5.1.1 by induction on p. The base cases $p = 1$ and $p = 2$ are immediate by (5.6) and (5.7).

To deduce the induction step, we start with (5.8)

$$A(p,q) = (p-1)(A(p-2,q-1) + 2A(p-1,q-1) + A(p,q-1))$$

which is by the induction hypotheses (5.1) and (5.3)

$$\begin{aligned} &= (p-1)\left(\sum_{k=1}^{p-2} a_{p-2,k}\cdot k^{q-2} \quad + \quad 2\sum_{k=1}^{p-2} a_{p-1,k}\cdot k^{q-2} \quad + \quad A(p,q-1)\right) \\ &= (p-1)\left(\sum_{k=1}^{p-2} a_{p-2,k}\cdot (p-1)^0 k^{q-2} \quad + \quad 2\sum_{k=1}^{p-2} a_{p-1,k}\cdot (p-1)^0 k^{q-2} \quad + \quad A(p,q-1)\right). \end{aligned}$$

Fix $1 \le k \le p-2$ in the above equation and use lemma 5.1.4 to substitute $A(p,l)$ successively. We obtain

$$(p-1)(a_{p-2,k} + 2a_{p-1,k}) \sum_{l=0}^{q-2} (p-1)^l k^{q-2-l}\,.$$

Using $(a-b)\sum_{k=0}^{q-2} a^k \cdot b^{q-2-k} = a^{q-1} - b^{q-1}$ yields

$$\begin{aligned} &= (p-1)(a_{p-2,k} + 2a_{p-1,k})\frac{(p-1)^{q-1} - k^{q-1}}{p-1-k} \\ &= -\frac{p-1}{p-1-k}(a_{p-2,k} + 2a_{p-1,k}) \cdot k^{q-1} \quad + \quad \frac{p-1}{p-1-k}(a_{p-2,k} + 2a_{p-1,k}) \cdot (p-1)^{q-1}\,. \end{aligned}$$

The left hand side is the coefficient of k^{q-1} and the right hand side is a summand of the coefficient of $(p-1)^{q-1}$, hence

$$a_{p,k} = -\frac{p-1}{p-1-k}(a_{p-2,k} + 2a_{p-1,k}) \qquad \text{and} \qquad a_{p,p-1} = -\sum_{k=1}^{p-2} a_{p,k}\,.$$

But $a_{p,k} = 0$ for $k \geq p$ is also clear. □

5.2. Comparison of Computational Approaches

In this section, we will see arguments that emphasize further why computing the homology of the moduli spaces is such a hard problem. Besides, we argue why we chose our strategies for the computations.

Review our computational approach for determining the homology of $\mathfrak{M}_{g,n}^m$ and $\mathfrak{M}_g^\bullet(m,n)$ for $n = 1$ with rational and finite fields coefficients. We construct the parallel or radial Ehrenfried complex (see Section 2.8) with its filtration by cluster sizes (compare Chapter 3). Thereby, the bases of the Ehrenfried complex are ordered in such a way that the differentials have a certain block form, see Subsection 3.3. At this point, there are many ways to derive the homological data. We diagonalize the differentials via parallelized Gaussian elimination while exploiting the special structure of the matrices due to the cluster filtration. In the preceding section, we saw that the modules of the Ehrenfried complex are extremely large, so we have to diagonalize its differentials as efficient as possible.

The study of manifolds via Morse Theory is well-known. In [For02], Forman proposes a discrete analogon for semisimplicial complexes with respect to arbitrary coefficients. Here a large discrete Morseflow yields a small, homotopy equivalent subcomplex. Unfortunately, finding an optimum Morse flow is generally NP-hard due to Joswig and Pfetsch (compare [JP06]). In practice, a simple greedy algorithm will produce a Morse flow not far away from an optimum solution. The construction of the associated smaller complex is the most time consuming process. It is (in terms of complexity theory) slightly faster than the state of the art SNF algorithms that do not make use of concurrency. It is slower than the Gaussian elimination algorithm. For calculations with coefficients in $\mathbb{Z}$ or $\mathbb{Z}/p^k\mathbb{Z}$, we recommend Jäger's parallelized algorithm based on the Smith normal form.

For coefficients in a field, diagonalizing even reduces to determining the rank. We imagined that there are numerical ways of improving our techniques. However, due to Beuchler (see [Beu14]), numerical algorithms for rank determination do not fit our requirements. These algorithms are in general unstable, i.e. they do not compute the rank exactly. They become more stable the smaller the kernel of the matrix is. But in our case, the kernels of the huge matrices are about half of their size. Hence, we cannot rely on such algorithms at all.

Beuchler recommended using preconditioning algorithms on our matrices instead, e.g. the nested dissection methods presented in [GL81, Chapter 8]. Such algorithms are applied before the actual computation in order to bring the matrix into a form that makes diagonalizing easier. Thus, rows or columns are reordered such that there are less row or column operations neccessary, or such that the entries of the matrix do not become too big during the computation. For instance, our application of the cluster spectral sequence can be seen as a preconditioning method that exploits the special shape of the matrix. Hence, we do not use any further preconditioning.

6. The Software Project

Based on the foundations presented in this thesis, we provide a computer program for determining the homology of the moduli spaces $\mathfrak{M}_{g,1}^m$ and $\mathfrak{M}_g^\bullet(m,1)$. Our software project aims at several goals. Above all, we put a lot of effort into optimizing the performance of our program since in Section 5.1, we see that our homology computations demand an economical use of memory and running time. Secondly, our objective is to present software which can easily be adapted to future methods of homology computations. Therefore, we designed well documented program code with a modularized structure that allows to exchange, improve or extend the different aspects of the homology computation smoothly. For instance, our program can readily be extended to computing the homology of $\mathfrak{M}_{g,n}^m$ and $\mathfrak{M}_g^\bullet(m,n)$ for arbitrary n.

The project is split into two almost independent units. The library **libhomology** offers an extendible framework for generic homology computations applied to chain complexes and certain types of spectral sequences that collapse at the second page. We propose coefficient ring, matrix types and algorithms for diagonalizing matrices.

We provide an implementation for rational and finite fields coefficients together with matrices that are diagonalized using parallelized Gaussian elemination. For coefficients in the field $\mathbb{F}_2$, we create an own coefficient type based on the observation that they can be stored in a single bit. This results in vast improvements concerning memory and runtime, see also Section 6.1.

Recall that the homology of $\mathfrak{M}_{g,1}^m$ respectively $\mathfrak{M}_g^\bullet(m,1)$ equals the cohomology of the parallel respectively radial Ehrenfried complex $\mathbb{E}(h,m;1)$ respectively $\mathbb{E}(h,m,1)$ (compare Section 2.8). Since our program can deal with both cases, we shall denote by $\mathbb{E}$ the radial or parallel Ehrenfried complex during this chapter. Thus, the program **kappa** generates $\mathbb{E}$ and computes some of its properties. Most importantly, we use our library **libhomology** to derive its cohomology. Thereby, we filter the Ehrenfried complex by the number of clusters (compare Chapter 3) in order to reduce the size of the differentials that have to be diagonalized. This again causes an enormous reduction of memory usage, which especially is useful in the case of rational coefficients that consume a lot of memory. The effect upon the running time is also highly positive since diagonalizing has cubic complexity and thus several small matrices are faster to diagonalize than a single huge matrix.

In order to get a better feeling for $\mathbb{E}$, we also offer the possibility to compute characteristics of its differentials as the number of non-zero entries or the number of blocks.

We chose the programming language C++11 to realize this project since it is one of the prefered programming languages for mathematical projects, and since the new standard together with some additional libraries suits our needs perfectly. The C++11 standard allows us to parallelize all time consuming steps of our project easily such that we can exhaust the full hardware architecture of the computer. We make use of the **GNU multiple precision arithmetic library** [GMP] for operations on signed integers, rational numbers, and floating-point numbers and of the **boost C++ libraries** [boost], which is

a set of portable libraries that offer high-quality solutions to standard problems as basic linear algebra, graph theory or file compression.

We are starting this chapter in Subsection 6.1 with an overview on the performance gain of our programming techniques in order to motivate our work. Afterwards, we will explain the library **libhomology** (see Section 6.2) and the program **kappa** (see Section 6.3) in detail. Additionally, we hand out advise about how to compile our computer programs (see Section 6.4). Finally, we present our results, i.e., the homology groups and cluster spectral sequences we have computed (compare Section 6.5).

6.1. Runtime and Memory Improvements

Recall that the enormous size of the Ehrenfried complex forces us to take care of the runtime and memory consumption of our computer program (compare Section 5.1). Via some example calculations, we show how we have improved the performance of our computer program step by step.

Consider the moduli spaces $\mathfrak{M}_{3,1}^1$ and $\mathfrak{M}_3(m,n)$. The E^0 term of the corresponding cluster spectral sequence on the parallel Ehrenfried complex looks as follows:

	$g=3$, $m=1$: Parallel $E^0_{p,l}$ for $\mathbb{F}_2$						
p \ l	1	2	3	4	5	6	7
2	1						
3	252						
4	7563	18					
5	81360	2010					
6	424920	48855	195				
7	1141056	469938	13230				
8	1305876	2069844	247898	1540			
9		3593880	1810368	70476			
10			4737360	915390	8715		
11				3702820	258720		
12					1765335	31878	
13						477906	
14							56628

We were not able to calculate the entire homology of $\mathfrak{M}_{3,1}^1$ via this spectral sequence since there are a lot of modules with several million of basis elements, exeeding our possibilities concerning runtime and memory. But we can use the radial Ehrenfried complex cluster spectral sequence for our calculations instead due to Proposition 2.7.1. This reduces the dimensions of the modules of the E^0 page enourmously:

	$g = 3$, $m = 1$: Radial $E^0_{p,l}$ for $\mathbb{F}_2$						
p \ l	1	2	3	4	5	6	7
1	1						
2	82	1					
3	1212	91					
4	7200	1652	9				
5	20400	12890	500				
6	23760	49380	7706	60			
7		77924	48104	2310			
8			111588	25676	294		
9				91384	7497		
10					44850	945	
11						12375	
12							1485

The biggest module on the first page for the radial case has dimension 111588, and not dimension 4737360 as in the parallel case. Using all our strategies to improve the performance of our program, we can now determine the homology of $\mathfrak{M}^1_{3,1}$ and $\mathfrak{M}_3(m,n)$ within less than half an hour. In each row of the following table, we see running time and maximum memory consumption of one run of our computer program with different improvement techniques.

Runtime and Memory Results for $g = 3$, $m = 1$					
Radial	CSS	Bool	# Threads	Runtime [h:min:sec]	Max. Memory Used [MB]
x	x	x	$t_w = 8$, $t_r = 4$	0 : 27 : 43	7056
x	x	x	$t_w = 11$, $t_r = 1$	0 : 39 : 03	7071
x	x	x	$t = 1$	1 : 37 : 49	7031
x		x	$t_w = 8$, $t_r = 4$	1 : 25 : 39	10819
x	x		$t_w = 8$, $t_r = 4$	18 : 36 : 22	92857
	x	x	$t_w = 8$, $t_r = 4$	/	/

Thereby, a cross marks whether

- we use the radial Ehrenfried complex or the parallel one,
- we filter this by cluster sizes,
- we use our special implementation of boolean coefficients (compare Subsubsection 6.2.4),

and we specify whether we run the program single threaded ($t = 1$) or parallel, and if parallel, how many threads we use as working threads (t_w) and as remaining threads (t_r). For an explanation of the meaning of these threads, see Subsubsection 6.2.6.

We see that the most significant effect on both runtime and memory consumption arises by implementing boolean coefficients in a clever way – the runtime decreases by a factor 40 and memory by a factor 13. Using this implementation of boolean coefficients, another important step to improve performance is to filter the Ehrenfried complex by cluster sizes, which yields another factor 3 of runtime and a factor 1.5 of memory consumption improvement. Unfortunately, parallelizing the program with 12 threads does not gain another factor 12 concerning runtime since diagonalizing is not smoothly parallelizable. Still, another factor 2.5 of runtime improvement, when only the jobs of the so-called working threads are distributed, and even a factor of 3.6, when also the so-called remaining work is distributed, results in valuable reduction of running time.

6.2. The Library Libhomology

With **libhomology** we provide an expandable framework for all kinds of homology computations. In our context, it is used as the foundation of the program kappa (see Section 6.3). In the following we explain use and essential details of its classes.

The template class `ChainComplex` is the core of **libhomology**. Here we think of a chain complex as a finite sequence of compatible matrices D_n satisfying $D_{n-1}D_n = 0$ which we call differential. We do not mention bases. Given a `ChainComplex`, our goal is to determine its homology. Therefore one needs an implementation of the coefficient ring `CoefficientT` (see Subsection 6.2.2) and the matrix type `MatrixT` (see Subsection 6.2.3) of the differentials. The class `HomologyT` (see Subsection 6.2.7) specifies the scope of homological information one wants to extract. These should be derived using the class `DiagonalizerT` (see Subsection 6.2.5) which diagonalizes matrices by applying row or column operations.

The implementations of the classes `ChainComplex`, `MatrixT`, `DiagonalizerT` and `HomologyT` are interdependent, so we recommend to skim over the details on the first reading.

6.2.1. The Class ChainComplex

We start with the description of the members of the template class

```
template< class CoefficientT,
          class MatrixT,
          class DiagonalizerT,
          class HomologyT >
class ChainComplex;
```

A `ChainComplex` is a finite sequence of differentials which we represent by

```
std::map< int32_t, MatrixT > differential;
```

It is reasonable to define the following pass-through methods. You access the n^{th}differential by calling

```
MatrixT& operator[]( const int32_t n );
```

or its `const` counter part

```
const MatrixT& at( const int32_t n ) const;
```

You can test whether the n^{th}differential is defined by checking whether

```
size_t count( const int32_t n ) const;
```

evaluates to zero. The n^{th}differential is deleted by the following method.

```
void erase( const int32_t n );
```

All homology modules are computed by calling

```
HomologyT homology();
```

In order to compute the n^{th}homology, one calls

```
HomologyT homology( const int32_t n );
```

If you are interested in the kernel and torsion parts of the n^{th} differential, you should call

```
HomologyT compute_kernel_and_torsion( int32_t n );
```

These operations consume by far the most time and we recommend using a parallelized diagonalization process (compare Subsection 6.2.6).

The DiagonalizerT in use, is accessed via

```
      DiagonalizerT& get_diagonalizer();
const DiagonalizerT& get_diagonalizer() const;
```

In order to derive the homology of the moduli spaces, we have to handle very large differentials (compare Section 5.1). Thus we work with a single differential at a time, which is accessed via

```
// Access the current differential.
      MatrixT& get_current_differential();
const MatrixT& get_current_differential() const;

// Erases the current differential.
void erase();

// Access the coefficient of the current differential.
CoefficientT& operator() ( const uint32_t row, const uint32_t col );

// Return number of rows resp. columns of the current differential
size_t num_rows() const;
size_t num_cols() const;
```

6.2.2. The Type CoefficientT

The coefficient ring must be represented by a class that meets the requirements discussed in Subsubsection 6.2.2.1.

6.2.2.1. Obligatory Operations for CoefficientT

Clearly, one has to provide the basic ring operations.

```
CoefficientT& operator= ( const CoefficientT& );        // Assignment
bool          operator==( const CoefficientT& ) const;  // Comparison
bool          operator!=( const CoefficientT&, const CoefficientT& );
```

```
CoefficientT  operator- () const;                          // Negation
CoefficientT& operator+=( const CoefficientT& );          // Addition
CoefficientT  operator+ ( const CoefficientT&, const CoefficientT& );
CoefficientT& operator-=( const CoefficientT& );          // Subtraction
CoefficientT  operator- ( const CoefficientT&, const CoefficientT& );
CoefficientT& operator*=( const CoefficientT& );          // Multiplication
CoefficientT  operator* ( const CoefficientT&, const CoefficientT& );
```

If the coefficients form a field, we suggest to implement the division operators.

```
CoefficientT& operator/=( const CoefficientT& );
CoefficientT  operator/ ( const CoefficientT&, const CoefficientT& );
```

The integers are initial in the category of rings, thus it is reasonable to implement the following methods.

```
CoefficientT& operator= ( const int );                      // Assignement
bool          operator==( const int ) const;                // Comparision
CoefficientT  operator* ( const CoefficientT&, const int ); // Multiplication
```

In our project **kappa**, we intend to save differentials so you should provide a method that stores a `CoefficientT` (See Subsection 6.2.8).

6.2.2.2. Coefficients in the Rationals and the Integers Mod m

We offer the classes `Q` respectively `Zm` that represent coefficients in $\mathbb{Q}$ respectively $\mathbb{Z}/m\mathbb{Z}$: The class `Q` is defined via the following `typedef`.

```
typedef mpq_class Q;
```

The class `mpq_class` itself is the C++ variant of the **GMP** type `mpq_t`. Before using the class `Zm`, you have to call the static member function

```
static void set_modulus(const uint8_t p, const uint8_t e = 1);
```

that defines $m = p^e$. Omitting the call will throw a segmentation fault which is the result of a division by zero. The following self-explaining member functions might be useful.

```
static void const print_modulus();
static void const print_inversetable();
static bool       is_field();
```

6.2.3. The Type MatrixT

6.2.3.1. Existing Template Classes

Before writing your own `MatrixT` you may want to have a look at the **ublas library** provided by **boost**. They offer several matrix templates for sparse and dense matrices as well as BLAS implementations for numerical computations. Moreover, our **libhomology** provides the template class

```
template < class CoefficientT >
class MatrixField;
```

for exact computations with matrix coefficients in a given field. In the following, we present an overview of the requirements any implementation of MatrixT has to fulfill, whereas in Subsection 6.2.4 we treat more specialized implementations.

6.2.3.2. Requirements on MatrixT

Your implementation of MatrixT has to meet some requirements. These are inspired by the **boost ublas library** as we make heavy use of it to compactify implementation details. We denote the coefficients of the matrix by CoefficientT. A MatrixT is created as follows:

```
MatrixT ( size_t number_rows, size_t number_cols );
```

The coefficient in the i^{th} row and the j^{th} column is accessed by calling

```
CoefficientT& operator()( size_t i, size_t j );
```

The number of rows is

```
size_t size1() const;
```

and the number of columns is

```
size_t size2() const;
```

As we intend to save differentials in our project **kappa**, you should provide a method that stores a MatrixT (See Subsection 6.2.8).

6.2.3.3. Optional Requirements on MatrixT

If you provide your own MatrixT with coefficients in a field, you may want to use our class DiagonalizerField (see Subsection 6.2.6) to compute rank and torsion of your matrices. In order to do so, you have to provide the member function

```
void row_operation( size_t row_1, size_t row_2, size_t col );
```

that applies a row operation on the matrix, i.e. adds the appropriate multiple of `row_1` to `row_2` in order to erase the entry `(row_2, col)` of the matrix. Our implementation makes use of multithreading, therefore you have to be careful with race conditions. You have to ensure that row operations for fixed `row_1` and `col` with varying `row_2` can be applied concurrently.

6.2.4. Special Implementations of MatrixField

6.2.4.1. MatrixField for Coefficients in $\mathbb{F}_2$

For coefficients in the field $\mathbb{F}_2$, our implementation provides siginificant improvements concerning memory and execution duration, see Section 6.1. Using well-known techniques, we store multiple entries of a row in a single data entity. Note that, since the only invertible element in $\mathbb{F}_2$ is 1, a row operation corresponds to the bitwise `XOR`-instruction.

Using these insights, we provide an implementation called MatrixBool. It behaves almost like MatrixField but has a few technical limitations (which are unavoidable as these are direct consequences of the enormous performance gain). E.g. for a matrix of type MatrixBool, it is not possible to access its coefficients by reference.

```
bool operator() ( const size_t i, const size_t j );
bool at         ( const size_t i, const size_t j ) const;
```

Observe that for our purpose, it suffices to add 1 to a given entry which is provided by the method

```
void add_entry( const size_t i, const size_t j );
```

It should be easy to equip MatrixBool with more member functions if needed.

6.2.4.2. MatrixField for the Cluster Spectral Sequence

In order to exploit the cluster spectral squence, we provide the adapted version MatrixFieldCSS of MatrixField and also MatrixBoolCSS of MatrixBool. Here, one should think of a spectral sequence that collapses at the second page as a subdivision of the differentials: The bases are ordered in a way such that the transposed differential D consists of a diagonal of block matrices d^0 which respect the filtration degree and below a single second diagonal of block matrices which decrease the filtration degree by one.

$$D = \begin{pmatrix} d^1 & d^0 & & \\ & d^1 & d^0 & \\ & & d^1 & d^0 \\ & & & \ddots \end{pmatrix}$$

Such a matrix is diagonalized as follows. We construct the first line given by d^1 and d^0 in the top left corner. Then we apply row operations to d^0 until its image is determined and then apply row operations to the remaning rows of d^1 until the image of the first row is fully understood. Afterwards, we may forget the matrix d^1 in the top left corner, construct the matrix d^1 of the next line and apply the needed row operations that are due to the matrix d^0 from above. Now we forget the entire first line, construct the next matrix d^0 and iterate this process.

During this procedure, we store at most two submatrices of D, namely one of type d^0 and one of type d^1, so our implementation MatrixFieldCSS and MatrixBoolCSS does exactly the same. We provide two ways to access the two submatrices d^0 and d^1. To use the first approach, the method

```
void define_operations( const OperationType );
```

defines on which submatrix we are currently working, where OperationType is an enumeration type and set to be main_and_secondary to access d^0 or secondary to access d^1. Now one calls member functions of MatrixFieldCSS respectively MatrixBoolCSS which have the same name as the member functions of MatrixField respectively MatrixBool. Let us give a simple example by printing d^0 and d^1 to the screen.

```
M.define_operations( main_and_secondary );
std::cout << M; \\ prints d^0 to screen.

M.define_operations( secondary );
std::cout << M; \\ prints d^1 to screen.
```

In the second approach, one calls a member method corresponding to d^0 by adding the prefix `main_`, whereas `sec_` applies to d^1. The following listing is an example for the member functions `size1` and `size2`.

```
size_t main_size1() const; // Returns the number of rows of d^0.
size_t main_size2() const; // Returns the number of columns of d^0.
size_t sec_size1() const;  // Returns the number of rows of d^1.
size_t sec_size2() const;  // Returns the number of columns of d^1.
```

A row operation on d^0 clearly affects the submatrix d^1 in the same line. In the algorithm presented above, we apply only those operations to d^1 that leave d^0 unchanged. Therefore we provide the following member functions.

```
void row_operation_main_and_secondary
    ( const size_t row_1, const size_t row_2, const size_t col );
void row_operation_secondary
    ( const size_t row_1, const size_t row_2, const size_t col );
```

6.2.5. The Type DiagonalizerT

Given a differential $C_n \xrightarrow{\partial} C_{n-1}$ of a chain complex, one wants to derive its kernel and image in order to compute the homology of the chain complex. In our situation, we are given a differential of the type `MatrixT`, so we want to apply a range of base changes to end up with a matrix where reading off these informations is easy. These base changes depend heavily on the coefficient ring. For field coefficients, one can apply Gaussian elimination, but for integral coefficients, one has to work much harder. Some state of the art algorithms can be found in [Jäg03] and [JW09]. We emphasize that this is the most time consuming operation (see Chapter 5) and suggest to carry out an algorithm that makes use of concurrency.

The `DiagonalizerT` is a function object, so you have to provide the method

```
void operator()( MatrixT& matrix );
```

that diagonalizes the given matrix. Afterwards, kernel and torsion of the matrix should be available by the diagonalizer's member functions

```
HomologyT::KernT kern();
HomologyT::TorsT tors();
```

where `HomologyT` is the class we use to store the homology of a chain complex (compare Subsection 6.2.7).

Moreover, we are interested in the defect and the rank of the matrix, so you have to provide the following two member functions.

```
uint32_t dfct();
uint32_t rank();
```

There are situations in which one wants to generate a chain complex without computing homological data: The size of the differentials of the Ehrenfried complex (see Section 2.8) is enourmous by Proposition 5.1, so it is impossible to compute the number of non-vanishing entries per column by hand. Therefore we offer the template class

```
template < class MatrixT >
class DiagonalizerDummy;
```

that does absolutely nothing, so you can use it together with HomologyDummy (see Subsubsection 6.2.7.2) as a template parameter for the template class ChainComplexT (see Subsection 6.2.1).

In the following, we shall describe our implementations of the class DiagonalizerField.

6.2.6. The Class DiagonalizerField

The DiagonalizerField applies a slightly modified version of the Gaussian elimination to a given matrix. Note that for computing the homology of a chain complex with field coefficients, it is sufficient to determine the rank and defect of all its differentials. Thus, the class DiagonalizerField merely transforms row operations upon the matrix in order to determine its rank, but does not exchange columns in order to obtain a triangular matrix. Since computing the rank is equivalent to diagonalizing for our purpose, we refer to this process as diagonalizing nevertheless. After giving an overview on the usage of this class, we will explain implementation details and runtime results of our parallelized diagonalization algorithm.

6.2.6.1. Overview and Usage of DiagonalizerField

For field coefficients, we offer the following template class.

```
template < class CoefficientT >
class DiagonalizerField;
```

Here we assume that MatrixT is given by

```
typedef MatrixField< CoefficientT > MatrixT;
```

and it is trivial to alter the class definition in order to allow arbitrary matrices.

The member variable current_rank of the class DiagonalizerField keeps track of the progress of an ongoing computation as it stores the number of linearly independent rows the algorithm has already found. Operations on variables of the type atomic_uint are atomic, i.e. reading, writing, incrementing and so forth is free of race conditions. We suggest to make use of this feature as follows. You start two threads, one computes kernel and torsion and the other monitors the progress.

```
ChainComplex< ... > complex;
// Define the differentials of matrix_complex.
// ...

atomic_uint& rank = diagonalizer.current_rank;
measure_duration = Clock(); // Measures duration.

// Set the value of state to 1 if and only if kernel and torsion are computed.
// This is done to terminate the 'monitoring thread'.
atomic_uint state(0);

// Diagonalizing thread.
auto partial_homology_thread = std::async( std::launch::async, [&]()
{
    auto ret = complex.compute_current_kernel_and_torsion( p );
    state = 1;
```

```
    return ret;
} );

// Monitoring thread.
auto monitor_thread = std::async( std::launch::async, [&]()
{
    while( state != 1 )
    {
        std::cout << "Diagonalization␣" << current_rank << "\r";
        std::this_thread::sleep_for( std::chrono::milliseconds( 50 ) );
    }
} );
```

The current progress is printed to screen and updated every 50 milliseconds till the computation is done.

6.2.6.2. Implementation Details

Our key algorithm for computing the rank of a matrix via Gaussian elimination is given by

Algorithm 1: Rank Computation

Input: A matrix $A = (a_{ij})$ with coefficients in a field $\mathbb{F}$
Output: The rank $\mathrm{rk}(A)$

Let R be the set of rows of A
Set $R_r := \emptyset$ `// Let` R_r `denote the set of rows contributing to the rank`
foreach *column* c **do**
    Let $j \in R \backslash R_r$ be a row index with a_{jc} invertible in $\mathbb{F}$
    if *No such* j *exists* **then**
        continue
    Let $S \subset R \backslash R_r$ be the subset of rows $s \neq j$ with a_{sc} invertible in $\mathbb{F}$
    if $S \neq \emptyset$ **then**
        Set $R_r := R_r \cup \{j\}$
    foreach *row* $s \in S$ **do**
        Perform `A.row_operation(j, s, c)`
return $|R|$

Hereby, `row_operation` is the member function of the class `MatrixType` described in Subsubsection 6.2.3.3.

A sequential version of this algorithm is implemented as the member function

```
uint32_t diag_field( MatrixType& matrix );
```

of `DiagonalizerField`. For the parallelized version, the method

```
uint32_t diag_field_parallelized( MatrixType& matrix );
```

is used. Since – at least for our matrices of type `MatrixBool` – a single row operation is performed very fast, we do not use several threads to parallelize row operations, but subdivide the set of row operations such that several row operations are performed simultaneously.

We define two helper classes for parallelizing, which we will explain here roughly, using the notation from Algorithm 1. The class `JobQueue` keeps track of all significant data used in Algorithm 1. Obviously, a `JobQueue` has to know the

```
MatrixType & matrix;
```

which is supposed to be diagonalized, and the column

```
size_t col;
```

and row

```
size_t row_1;
```

that are currently considered, where, in the notation of Algorithm 1, we have `col` $= c$ and `row_1` $= r$. Furthermore, the `JobQueue` maintains the

```
std::vector rows_to_work_at;
```

which resembles the set S, and the

```
std::vector remaining_rows;
```

consisting of the rows t not yet contributing to the rank for that the entry a_{tc} is not invertible in $\mathbb{F}$, i.e. of $R \backslash (R_r \cup S)$. Since the `JobQueue` contains all the information necessary to perform the required row operations for a given column c, only two tasks remain: updating these data members when passing over from one column to the next and parallelizing the row operations as well as the update.

For each thread used, we create an instantiation of the class `Worker`, which will not be discussed in this thesis, to perform computations. Experiments showed that having two different kinds of `Workers` is more efficient: Firstly, we define a family of `Workers` that actually perform the diagonalizing work. The `JobQueue` distributes the rows `rows_to_work_at` among these `Workers` equally. Afterwards, each of these `Workers` considers all its assigned rows s, performs the row operation upon s and marks whether s will also be in the set S for the next column. This means that the already defined `Workers` update parts of the arrays `rows_to_work_at` and `remaining_rows`, and that it remains to update these arrays with respect to the set of `remaining_rows`. This is the task the other family of `Workers` execute, where the `remaining_rows` are again distributed equally among the `Workers` by the `JobQueue`.

The input parameters `num_threads` respectively `num_remaining_threads` define how many threads are occupied for the first respectively second type of `Workers`, see also Subsection 6.3.1.

6.2.7. The Type HomologyT

In order to derive the homology of a chain complex, we compute all kernels and images of the differentials, given by transposed transformation matrices. In our situation, we start with a `ChainComplex` (see Subsection 6.2.1) that is essentially a finite series of matrices of the type `MatrixT` (see Subsection 6.2.3). The function object `DiagonalizerT` (see Subsection 6.2.5) applies row and column operations until both kernel and image can be read off. This data should then be communicated to `HomologyT`.

6.2.7.1. Essential Members

The type HomologyT requires the following members. You have to provide the types HomologyT::KernT respectively HomologyT::TorsT that store the kernel respectively the image of a differential. This can be achieved by including the following two lines in the public section of the class definition.

```
class HomologyT{
public:
    typedef /* ... */ KernT;
    typedef /* ... */ TorsT;
};
```

You have to define the following two constructors

```
HomologyT ();
HomologyT ( int32_t n, KernT& k, TorsT& t ); // Sets k and t at the spot n.
```

and member functions for storing kernels and images.

```
void set_kern ( int32_t , KernT& );
void set_tors ( int32_t , TorsT& );
```

Moreover, we want to print the homology to the screen, thus the class definition has to include the following line.

```
friend std::ostream& operator<< ( std::ostream& , const HomologyT& );
```

6.2.7.2. The Class HomologyDummy

As mentioned in Subsection 6.2.5, there are situations in which one wants to generate a chain complex without computing homological data. For this purpose, we offer the class

```
class HomologyDummy
```

that does absolutely nothing, so you can use it together with DiagonalizerDummy (see Subsection 6.2.5) as a template parameter for the template class ChainComplexT (see Subsection 6.2.1).

6.2.7.3. The Class HomologyField

Using field coefficients, the homology modules are all vector spaces. For those who are only interested in the Betti numbers, we offer the class HomologyField. Here we store only the dimensions of kernel and image. The class definition is essentially as follows, where the member functions should be self-explaining.

```
class HomologyField{
public:
    typedef int64_t KernT;
    typedef int64_t TorsT;

    HomologyField ();
    HomologyField ( int32_t, KernT, TorsT );
```

```
    void  set_kern   ( int32_t, KernT );
    void  set_tors   ( int32_t, TorsT );
    KernT get_kern   ( int32_t ) const;
    TorsT get_tors   ( int32_t ) const;
    void  erase_kern ( int32_t );
    void  erase_tors ( int32_t );
    friend std::ostream& operator<< ( std::ostream&, const HomologyField& );
private:
    std::map< int32_t, int64_t > kern_rep;
    std::map< int32_t, int64_t > tors_rep;
};
```

6.2.8. Serialization

The transformation of data and objects of a running computer program into storable information (which can be saved on a hard disk) is called serialization. In our project, we want to generate basis elements and differentials to save them for later use, i.e. we want to serialize them. Therefore, we provide the general purpose template functions

```
template < class StorableType >
void save_to_file_bz2
    ( StorableType& t, std::string filename, bool print_duration=true );
```

and

```
template < class StorableType >
void load_from_file_bz2
    ( StorableType& t, std::string filename, bool print_duration=true);
```

Both functions, use the `bzip2` algorithm for fast file compresseion, so we produce much smaller files.

6.2.8.1. Storable Types

A type can be handled by the above template functions, if it is defined by the C++11 standard (such as `int` or `std::vector< char >`) or the **boost C++library**. Otherwise your class has to meet the following conditions. First of all, it has to be a friend of `boost::serialization::access`, i.e. its class description includes the following line.

```
class my_class
{
    ...
    friend class boost::serialization::access;
    ...
};
```

There are two ways of proceeding from here. Most commonly, the process of saving and loading is the same. In this situation one defines the template member function

```
template < class Archive >
void serialize( Archive &ar, const unsigned int version );
```

whereas the template parameter `Archive` is filled in by **boost** (and you do not need to know what it is). Now saving and loading is achieved via the binary operator `&` applied to

`ar` and every member variable we want to save and load. In the example below, we tell the serialization function, to save and load two out of three member variables.

```
class my_class
{
    ...
    int keep_this;
    int this_is_also_important;
    int useless;

    friend class boost::serialization::access;
    template < class Archive >
    void serialize( Archive &ar, const unsigned int )
    {
        ar & keep_this;
        ar & this_is_also_important;
    }
};
```

There are rare situations, in which a saving mechanism differs from its loading counter part. Then one has to implement the function

```
template< class Archive >
void save( Archive & ar, const unsigned int version ) const;
```

and its counter part

```
template< class Archive >
void load( Archive & ar, const unsigned int version );
```

and one has to tell **boost** to use these two functions by calling the macro

```
BOOST_SERIALIZATION_SPLIT_MEMBER()
```

afterwards. A simple example could look like this.

```
class my_class
{
    ...
    int keep_this;
    int this_is_also_important;
    int useless;

    friend class boost::serialization::access;
    template< class Archive >
    void save( Archive & ar, const unsigned int ) const
    {
        ar & keep_this & this_is_also_important;
    }
    template< class Archive >
    void load( Archive & ar, const unsigned int )
    {
        ar & keep_this & this_is_also_important;
        useless=0;
    }
    BOOST_SERIALIZATION_SPLIT_MEMBER()
};
```

For more information one should consider the online manual of [boost].

6.3. The Program Kappa

The program **kappa** mainly uses the previously introduced **libhomology** (compare Section 6.2) and the theory developed in Chapter 2 in order to determine the homology of the moduli spaces $\mathfrak{M}_{g,1}^m$ and $\mathfrak{M}_g^\bullet(m,1)$. Thus, it computes the cohomology of the parallel or radial Ehrenfried complex $\mathbb{E}$, filtered by cluster sizes.

Recall that the homology of $\mathfrak{M}_{g,1}^m$ and $\mathfrak{M}_g^\bullet(m,1)$ coincides for $m > 0$, see Proposition 2.7.1. For computing the homology of $\mathfrak{M}_{g,1}^m$ for fixed g and m, it is more efficient to use the radial Ehrenfried complex rather than the parallel one, since its modules and thus differentials are much smaller, see Section 5.1. However, for $m = 0$, we cannot use the radial model, so we also offer the computation of the homology of $\mathfrak{M}_{g,1}^m$ via the parallel model. Since we also determine the dimensions of the modules of the cluster spectral sequence, computation with the parallel model produces new homological information for $m > 0$.

A central class of our computer program is hence the class `ClusterSpectralSequence`, see Subsection 6.3.3, which stores the parallel or radial Ehrenfried complex filtered by cluster sizes.

Since the basis elements of $\mathbb{E}$ are monotonous tuples of transpositions, another important class of the program kappa is the class `Tuple` (see Subsection 6.3.2), which represents such a basis element and offers many functions that are applied to it during the generation of the `ClusterSpectralSequence`.

With these foundations, we can offer the tool `compute_css` (see Subsection 6.3.1) for computing the first three pages of the cluster spectral sequences corresponding to the moduli spaces $\mathfrak{M}_{g,1}^m$ and $\mathfrak{M}_g^\bullet(m,1)$ and especially their homology.

We also provide the tool `compute_cache`, which computes the bases and the differentials of $\mathbb{E}$ and stores them in files via serialization. For most g and m, the computation of both takes a lot of time, and it is thus functional to have the opportunity to store the data of $\mathbb{E}$ for later uses.

For example, `compute_cache` can be used to examine the structure of the Ehrenfried complex via the tools `compute_statistics` and `print_basis`. After `compute_cache` has been performed, one can call `compute_statistics` to find out various properties of the Ehrenfried complex $\mathbb{E}$ like the sizes of the differentials or their largest entry per column. Alternatively, a call of `print_basis` outputs the basis of the Ehrenfried complex.

Since all these tools mentioned are organized in a similar way, we shall only describe the tool `compute_css` in detail, see Subsection 6.3.1. Thereafter, we illustrate the above mentioned classes `Tuple` (compare Subsection 6.3.2) and `ClusterSpectralSequence` (compare Subsection 6.3.3), which describe the Ehrenfried complex.

6.3.1. The Tool `compute_css`

The tool `compute_css`, which computes the homology of the moduli spaces $\mathfrak{M}_{g,1}^m$ and $\mathfrak{M}_g^\bullet(m,1)$ by deriving the second term of the corresponding cluster spectral sequence, is the most important tool supported by the project **kappa**. In Subsubsection 6.3.1.1, we describe how one operates this tool, while in Subsubsection 6.3.1.2, we explain its implementation.

6.3.1.1. Usage

For the computation of the homology of the moduli space $\mathfrak{M}_g^\bullet(m,1)$, one can use the command

```
.\compute_css -g arg -m arg (-q | -s arg)
```

Thereby,

- the parameter `g` is the genus of the moduli space,
- the parameter `m` is the number of punctures of the moduli space,
- one can either use the parameter q or the parameter s. If q is chosen – without any argument – homology with rational coefficients will be computed. If the parameter s is set to some positive prime, we will compute homology with coefficients in $\mathbb{Z}/s\mathbb{Z}$.

As the output of this command, one obtains a description of the E^0, E^1 and E^2 term of the cluster spectral sequence associated with $\mathfrak{M}_g^\bullet(m,1)$, and can read off the homology from the E^2 page.

Recall that, for $m > 0$, the homology of the moduli space $\mathfrak{M}_{g,1}^m$ coincides with the homology of the moduli space $\mathfrak{M}_{g,1}^m$ (compare Proposition 2.7.1). For determining the homology of $\mathfrak{M}_{g,1}^m$ for $m = 0$ or the dimensions of the modules in the cluster spectral sequence of $\mathfrak{M}_{g,1}^m$, one can set the optional parameter

- `parallel`

to true.

For instance, the call

```
./compute_css -g 1 -m 3 -s 2
```

computes the homolgy of the moduli space $\mathfrak{M}_1^\bullet(3,1)$ with $\mathbb{Z}/2\mathbb{Z}$ coefficients, while the call

```
./compute_css -g 1 -m 3 -q --parallel 1
```

determines the homolgy of the moduli space $\mathfrak{M}_{3,1}^1$ with rational coefficients.

There are other optional parameters that improve the performance or handling of the program.

- The optional parameter `t` is the number of threads that are allowed to be used for parallelization, which is 1 by default.
- In addition, one can use the optional parameter `num_remaining_threads` to determine how exactly computations are parallelized. For a detailed explanation, see 6.2.6.2. The total number of threads used will then be

  `num_threads + num_remaining_threads,`

  and we recommend to use one third of the total number of threads as remaining threads.

- The optional parameters `first_diff` respectively `last_diff` are the minimal respectively maximal $p \in \mathbb{N}$ for which the homology $H_p(\mathfrak{M}_{g,1}^m)$ is supposed to be computed, which are 0 respectively $2h$ by default.

If the command `help` is used or if the input is not valid, instructions for use will be printed to the console.

During the computations, we offer intermediate results and progress bars as console output. When the computation of the homology is finished, the file

`compute_homology_(parameters)`

created by the program contains all the intermediate and final results. Be aware that this means that calls with the same parameters produce files with the same names and hence old files are overwritten. The intermediate results give the oportunity to abort the computation and continue it some other time, using the parameters `first_diff` and `last_diff` to select certain homology groups.

6.3.1.2. Implementation Details

The computation of the cluster spectral sequence and the homology starts in the main function of the file

```
main_compute_css.cpp
```

The input parameters described above are stored in the struct

```
SessionConfig;
```

which also tests whether the given configuration of parameters is valid, outputting the correct usage to the console if not. Apart from the data members corresponding to the input parameters, the struct `SessionConfig` contains the data member

```
SignConvention sgn_conv;
```

it can set on its own in dependence on the parameters for the coefficients. The `SignConvention` parameter can have three different values, which indicate which signs have to be respected in the computation of the differentials. This way, we avoid sign computations whenever we can. We set the parameter to `no_signs` if we only compute the homology up to sign, which is the case if we use coefficients in $\mathbb{Z}/2\mathbb{Z}$. If we have different coefficients and `m` ≥ 2, the moduli space $\mathfrak{M}_{g,1}^m$ is non-orientable and the sign convention is set to `all_signs`. Otherwise, it equals `no_orientation_sign`.

At the begin of the computation, the constructor of `ClusterSpectralSequenceT` is called with respect to the parameters provided above. Thereby, the bases (see Subsubsection 6.3.3.3) are generated, with basis elements sorted by their cluster number. In particular, printing the E^0-term to screen is readily done.

The main task is determining the first and second page of the cluster spectral sequence. Recall Section 3.3, which discusses the matrix version of the cluster spectral sequence. The

p^{th} transposed transformation matrix of $\partial_{\mathbb{E}}$ is a block matrix of the form

$$\begin{pmatrix} d^1 & d^0 & & & \\ & d^1 & d^0 & & \\ & & d^1 & d^0 & \\ & & & & \ddots \end{pmatrix},$$

if we sort the basis elements by their number of clusters. The modules of the E^1-term are given by

$$\ker(d^0)/\operatorname{im}(d^0)\,,$$

whereas the modules of the E^2-term are given by

$$\ker(d^1|_{\ker(d^0)})/\big(\operatorname{im}(d^0) + \operatorname{im}(d^1|_{\ker(d^0)})\big)\,.$$

Hence, it suffices to apply all row operations induced by the sub-matrices d^0 and proceed with the diagonalization process of the parts of the (altered) sub-matrices d^1 that are in the kernel of the (diagonalized) sub-matrices d^0. In order to save execution time and memory, our program operates on exactly one d^0 and one d^1 sub matrix at a time:

Algorithm 2: Computing E^1 and E^2

```
for p = 1 to 2h do
    for l = 1 to p do
        Construct d^1_{p,l} and apply row operations of d^0_{p,l-1}
        Forget d^0_{p,l-1}
        Generate d^0_{p,l}
        Compute and save kernel and image of d^0_{p,l}
        Print the homological results to the screen
        Save the diagonal of d^0_{p,l} and detect superflous rows of d^1_{p,l}
        Compute and save the kernel and image of d^1_{p,l}
        Print the homological results to the screen
        Forget d^1_{p,l}
Print all three pages of the spectral sequence to the screen.
```

Here, we have $h = 2g + m$ in the parallel case and $h = 2g + m - 1$ in the radial case.

During all computations, the function `compute_css` generates the previously mentioned intermediate results printed out in the console and into the corresponding output file. Furthermore, it measures the duration of the important steps of the computations and also writes them into the console.

6.3.2. The Class Tuple

Recall that we aim to compute the cohomology of the parallel or radial Ehrenfried complex $\mathbb{E}$. A basis for the Ehrenfried complex is given by monotonous cells $\Sigma = (\tau_h \mid \ldots \mid \tau_1)$ satisfiying certain conditions, and the differential for $\mathbb{E}$ can be described by the map $\partial_{\mathbb{E}}$

making the diagram

$$\begin{array}{ccc} \mathbb{E}_p & \xrightarrow{\partial_{\mathbb{E}}} & \mathbb{E}_{p-1} \\ \cong\downarrow\kappa & & \cong\uparrow\pi \\ \mathbb{K}_p & \xrightarrow{\partial_{\mathbb{K}}} & \mathbb{K}_{p-1} \end{array}$$

commute, compare Definition 2.8.8. Hence, the core of the program **kappa** is the class `Tuple`, which represents a tuple of h transpositions $\Sigma = (\tau_h \mid \ldots \mid \tau_1)$ and thus especially the basis elements of $\mathbb{E}$. This class additionally provides several methods which are applied to a basis element during the computation of the differential $\partial_{\mathbb{E}}$.

We are going to give an overview on its data members (Subsubsection 6.3.2.1), the member functions needed to start working with a `Tuple` (Subsubsection 6.3.2.2) and the functions that represent basic properties of a tuple (Subsubsection 6.3.2.3). Afterwards, we explain the class methods computing the orientation sign (Subsubsection 6.3.2.5), the horizontal differential (Subsubsection 6.3.2.4) and the implementation of the maps f and Φ used to compute the isomorphism κ (Subsubsection 6.3.2.6) in detail.

6.3.2.1. Data Members

Since the class `Tuple` is supposed to represent cells $\Sigma = (\tau_h \mid \ldots \mid \tau_1)$ of the Ehrenfried complex $\mathbb{E}$, let us briefly recall what this means. If Σ is a cell of the parallel Ehrenfried complex (compare Definitions 2.3.5, 2.8), it satisfies the following properties:

(i_P) The transpositions τ_i act on the symbols $1, \ldots, p$.

(ii_P) The permutation σ_h has exactly $m + 1$ cycles.

(iii) Each symbol $1, \ldots, p$ is contained in at least one τ_i.

(iv) Σ is monotonous, i.e. $\mathrm{ht}(\tau_h) \geq \ldots \geq \mathrm{ht}(\tau_1)$.

On the other hand, if Σ is a radial cell, it fulfills the same conditions, except for the first two, which are replaced by

(i_R) The transpositions τ_i act on the symbols $0, \ldots, p$,

(ii_R) The permutation σ_h has exactly m cycles.

see also Definitions 2.5.2 and 2.8.8.

Let us now see how the cell Σ is represented by a `Tuple`. The transpositions $\tau_h, \ldots, \tau_1$ belonging to Σ are stored as the data member

```
std::vector< Transposition > rep;
```

where a `Transposition` is defined as a pair of unsigned integers. The unsigned integer `p` is stored as another data member of the class `Tuple`, and there is also a boolean `radial` indicating whether Σ is a radial cell or not (and thus a parallel cell). Depending on this flag, there are other technical parameters to be set, e.g. the minimum symbol that may occur in a transposition, see conditions (i_P) and (i_R).

Our convention for writing a cell $\Sigma = (\tau_h \mid \ldots \mid \tau_1)$ is to store τ_i as `rep[i-1]` for $1 \leq i \leq h$, since by default, a vector starts with the index 0. To make the handling of `Tuples` more intuitive, we offer methods to access the `Transpositions` in a more canonical way, see Subsubsection 6.3.2.2. Another convention is that we always write `Transpositions` like $\tau_i = (a\ b)$ with $a > b$ in order to simplify the source code.

Since it is useful for the computation of the differential, another data member of the class `Tuple` is an unsigned integer `id` indicating the index of a `Tuple` in its basis of the Ehrenfried complex.

6.3.2.2. Class Methods To Get Started

We define two constructors for the class `Tuple`. Firstly, there is a constructor

```
Tuple( size_t h );
```

which initializes `p` with 0 and allocates memory for a `Tuple` of h `Transpositions` that are supposed to be filled later. Secondly, the constructor

```
Tuple( uint32_t symbols, size_t h );
```

sets the data member `p` to be *symbols* and also allocates memory for the h many `Transpositions`.

To create a `Tuple` $\Sigma = (\tau_h \mid \ldots \mid \tau_1)$, one can call one of these constructors, and afterwards initialize for each $i = 1, \ldots, h$ the i^{th} `Transposition` τ_i using the non-const operator

```
Transposition& operator[]( size_t i );
```

It is also possible to use the const respectively non-const version of the method

```
Transposition& at( size_t i );
```

to access the `Transposition` τ_i of the tuple Σ for reading respectively writing.

During the generation of the differential $\partial_{\mathbb{E}}$, we use to mark `Tuples` as degenerate by erasing its data member `rep`. To test whether a `Tuple` is non-degenerate, we hence define

```
operator bool();
```

which returns true if and only if this `Tuple` is non-empty.

Using the methods

```
static void parallel_cell();
```

respectively

```
static void radial_cell();
```

one can mark whether a `Tuple` represents a parallel respectively radial cell.

Furthermore, we define canonical compare operators, overload the `operator«` to print `Tuples` to screen and offer the possibility to save and load `Tuples`.

6.3.2.3. Basic Properties of a Tuple

We provide various class methods for basic calculations with a `Tuple`, e.g. to verify whether a `Tuple` represents an element of the Ehrenfried complex.

Since basis elements of $\mathbb{E}$ are required to be monotonous, we provide a method

```
bool monotonous();
```

to test whether a `Tuple` is monotonous, i. e. whether, for all $1 \leq i < h$, we have $a_i < a_{i+1}$, writing $\tau_i = (a_i, b_i)$ and $\tau_{i+1} = (a_{i+1}, b_{i+1})$ with $a_i > b_i$ and $a_{i+1} > b_{i+1}$.

The class method

```
int32_t norm();
```

returns the norm of the given `Tuple` $\Sigma = (\tau_h \mid \ldots \mid \tau_1)$, i. e. the sum of the norms of all τ_i, $i = 1, \ldots, h$. But since each τ_n is a `Transposition`, the norm of the `Tuple` is simply the number of its transpositions h.

For the computation of the differential, we sometimes want to switch to the homogeneous notation of `Tuples`. Therefore, we need methods

```
Permutation long_cycle();
```

respectively

```
Permutation long_cycle_inv();
```

returning the `Permutation` $\sigma_0 = (1\ 2\ \cdots p-1\ p)$ respectively its inverse, and

```
Permutation sigma_h();
```

returning the `Permutation` $\sigma_h = \tau_h \tau_{h-1} \ldots \tau_1 \sigma_0$. Thereby, a `Permutation` is another class, representing a permutation as a vector storing for each element its image under the permutation.

Since all τ_i are `Transpositions`, we can simplify the computation of σ_h using the following

Algorithm 3: Computing σ_h

Input: A tuple $\Sigma = (\tau_h, \ldots, \tau_1)$ in inhomogeneous notation
Output: The permutation σ_h

1 `Permutation` σ_{inv} := long_cycle_inv()
2 **for** $i = 1$ **to** h **do**
3 Write $\tau_i = (a, b)$
4 Swap the elements $\sigma_{\text{inv}}(a)$ and $\sigma_{\text{inv}}(b)$
5 **for** $j = 1$ **to** p **do**
6 Write $k = \sigma_{\text{inv}}(j)$
7 $\sigma_h(k) := j$
8 **return** σ_h

Proposition 6.3.1. *The given algorithm computes σ_q correctly.*

Proof. In line 1, we initialize the `Permutation` σ_{inv} with σ_0^{-1}. Note that, by definition of σ_i, we have

$$\sigma_i^{-1} = \sigma_{i-1}^{-1} \tau_i = \sigma_{i-1}^{-1}(a, b)$$

for $0 < i \leq h$. Thus, the `Permutation` σ_i^{-1} maps a to $\sigma_{i-1}^{-1}(b)$, b to $\sigma_{i-1}^{-1}(a)$ and behaves like σ_{i-1}^{-1} on all other elements. Hence, for each $i = 1, \ldots, h$, we have $\sigma_{\text{inv}} = \sigma_i^{-1}$ after the i^{th} iteration of the first for loop.

The second for loop computes the inverse of $\sigma_{\text{inv}} = \sigma_h^{-1}$, which is σ_h. □

The algorithm for the computation of σ_h is also used with small adaptions in different parts of the program.

The basis elements of $\mathbb{E}$ are supposed to have a distinguished number of punctures, i.e. number of cycles of σ_h is $m + 1$ for parallel and m for radial cells. Therefore, we give an algorithm to determine the cycle decomposition of a `Permutation`.

Algorithm 4: Cycle Decomposition

Input: A permutation π on a subset of $\{0, \ldots, p\}$
Output: A decomposition of π into disjoint cycles

```
1  i := min{j ∈ {0,...,p}: j belongs to π, but not visited yet}
2  cur := i
3  Initialize a new cycle
4  repeat                                          // Find the cycle containing i
5  |  Mark cur as visited
6  |  prev := cur
7  |  cur := π(prev)
8  |  cycle (prev) := cur
9  until  cur equals i
10 Store the cycle
11 if all symbols in {0,...,p} visited or not belonging to π then
12 |  return the cycle decomposition
13 go to 1
```

Since each element in $\{0, \ldots, p\}$ belonging to the permutation π is considered as *prev* exactly once, we can state

Proposition 6.3.2. *The algorithm to determine the cycle decomposition of a permutation works correctly.*

Combining this with the previous Algorithm 3, we can now define the methods

```
uint32_t num_cycles() const;
```

yielding the number of cycles of σ_h, and

```
bool has_correct_num_cycles(size_t m) const;
```

checking whether the number of cycles fits the requirement of the parallel respectively radial Ehrenfried complex.

Since we need to subdivide the cells of $\mathbb{E}$ according to their numbers of clusters, we introduce the method

```
int32_t Tuple::num_clusters() const;
```

This is another part of our computer program where we use the comfortability of the **boost** library: Let $\Sigma = (\tau_h \mid \ldots \mid \tau_1)$ be a cell represented by a `Tuple`. We construct a graph on

the vertices $0, \dots, p$, where an edge between a and b indicates that there is an i such that $\tau_i = (a, b)$. Then, the number of connected components of this graph equals the number of clusters of Σ, and **boost** offers a graph data structure and an algorithm to compute this directly.

6.3.2.4. The Horizontal Face Operator

In order to construct the Ehrenfried complex $\mathbb{E}$, the computer program has to be able to apply the horizontal differential $\partial'' = \partial_{\mathbb{K}}$ to `Tuples`, compare Definition 2.8.8 and Section 2.6. So recall that, for a cell Σ, this differential is given by the alternating sum

$$\partial''_j(\Sigma) = \sum_{j=0}^{p} (-1)^j \varepsilon_j(\Sigma) d''_j(\Sigma)\,,$$

where $d''_j(\Sigma)$ is the j^{th} horizontal face of Σ, i.e. the cell resulting from Σ by collapsing the j^{th} stripe of the slit domain, and $\varepsilon_j(\Sigma) = \varepsilon''_j(\Sigma)$ is the additional sign introduced by the orientation system. Note that, for parallel cells – but not for radial cells –, the 0^{th} and p^{th} horizontal face is always degenerate.

Here, we will explain our implementation of the face operator d'', and in Subsubsection 6.3.2.5, we will present the orientation sign.

In Proposition 2.3.10, we saw how to express the formula for the j^{th} horizontal face in the inhomogeneous notation, and in Corollary 2.8.12, we saw how to detect the cases when the resulting face is degenerate. These statements result in the following

Algorithm 5: Computing the Horizontal Face

Input: A tuple $\Sigma = (\tau_h, \dots, \tau_1)$ in inhomogeneous notation, a symbol $j \in \{0, \dots, p\}$
Output: The horizontal face $d''_j(\Sigma)$ or the assertion that $d''_j(\Sigma)$ is degenerate

```
for i = 1 to h do
    Write τ_i = (a, b)
    Write k = σ_{i-1}(j)
    if The transpositions τ_i and (j, k) are disjoint then
        τ'_i := τ_i
    else if τ_q = (j, k) or j = k then
        return d''_j(τ) is degenerate
    else
        if k = a or k = b then
            τ'_i := τ_i
        else
            if a ≠ k then
                τ'_i := (a, k)
            else
                τ'_i := (b, k)
Renormalize Σ' = (τ'_h | ... | τ'_1)
return Σ'
```

Using the above mentioned theoretical foundations, we obtain

Proposition 6.3.3. *The above algorithm computes the j^{th} horizontal face of Σ.*

Note that we can apply Algorithm 3 to compute σ_i for $i = 0, \dots, h$. We choose to handle the case that τ_i and (j, k) are disjoint before the degenerate case at first because this is the case that will occure most likely.

The algorithm enables us to define the method

```
Tuple d_hor( uint8_t j );
```

computing the j^{th} horizontal face of this `Tuple`.

6.3.2.5. The Orientation Sign

Recalling the definition of the orientation sign $\varepsilon_j(\Sigma) = \varepsilon''_j(\Sigma)$ introduced by Mehner (see Section 2.6), we immediately obtain the following

Algorithm 6: Computing the Orientation Sign

Input: A tuple $\Sigma = (\tau_h, \dots, \tau_1)$ in inhomogeneous notation
Output: Orientation signs $\varepsilon_j(\Sigma)$ for all $j \in \{0, \dots, p\}$

Decompose σ_h into m resp. $m+1$ disjoint cycles $(\alpha_0)\alpha_1 \dots \alpha_m$
Let a_i be the minimum symbol of the cycle α_i
Sort the cycles α_i such that $a_i < a_{i+1}$ for all i
foreach *cycle* α_i **do**
    if $\alpha_i = a_i$ *is a fixed point* **then**
        Set $\varepsilon_{a_i} = 0$
    Let b be the second minimum cycle of α_i
    Let $k \geq i$ be the minimum integer with $b < a_{k+1}$, or $k = m$, if this does not exist
    Set $\varepsilon_{a_i} = (-1)^{k-i}$
    foreach $c \in \alpha_i$, $c \neq a_i$ **do**
        Set $\varepsilon_c = 1$

Hereby, we again use Algorithm 3 to determine σ_h, and Algorithm 4 to decompose σ_h into disjoint cycles. Note that, in the parallel case, a cell of $\mathbb{E}$ has $m+1$ cycles, while in the radial case, it has m cycles.

Storing the cycle decomposition of σ_h as a map of cycles stored with their smallest element as a key, this algorithm is easily implemented. We obtain the method

```
std::map< uint8_t, int8_t > orientation_sign();
```

returning a map of all orientation signs $\varepsilon_j(\sigma_h)$, stored with $j \in \{1, \dots, p\}$ as a key.

6.3.2.6. Preparations for the Map κ

Having seen how the differential $\partial_{\mathbb{K}}$ is implemented, recall once more that the differential $\partial_{\mathbb{E}}$ of the Ehrenfried complex is given by the diagram

$$\begin{array}{ccc} \mathbb{E}_p & \xrightarrow{\partial_{\mathbb{E}}} & \mathbb{E}_{p-1} \\ \cong \downarrow \kappa & & \cong \uparrow \pi \\ \mathbb{K}_p & \xrightarrow{\partial_{\mathbb{K}}} & \mathbb{K}_{p-1} \end{array} .$$

Note that the projection π onto the monotonous cells can be performed by simply checking whether the `Tuple` is monotonous (see Subsection 6.3.2.3) and marking the `Tuple` as non-valid, if not. It remains to define the isomorphism κ, which is given by

$$\kappa = K_h \circ \ldots \circ K_1$$

with

$$K_q = \sum_{j=1}^{q} (-1)^{q-j} \Phi_j^q$$

and

$$\Phi_j^q = f_j \circ \ldots f_{q-1} .$$

Therefore, the class `Tuple` provides maps

```
bool f( uint32_t j );
```

and

```
bool phi( uint32_t q, uint32_t j );
```

which apply the maps f_j respectively Φ_j^q to this `Tuple` and return true if and only if the resulting `Tuple` is non-degenerate.

The method f is implemented as a huge case distinction concerning the symbols contained in the transpositions τ_j, which is similar to the one in the computation of the horizontal boundary. This provides the opportunity to handle each of the cases in constant time.

The function $\phi(q, j)$ iteratively calls the function f for $j = 1, \ldots, q-1$ according to the definition of Φ_j^q. In each step, we test whether the norm of the `Tuple` decreases, and if so, we abort the computation of Φ to avoid unneccassary computations.

The map κ itself is defined in the class `ClusterSpectralSequence`, compare Subsection 6.3.3.

6.3.3. The Class ClusterSpectralSequence

Having described how basis elements of the Ehrenfried complex $\mathbb{E}$ are represented by our computer program, we will now explain how the cluster spectral sequence associated with $\mathbb{E}$ is realized and how the methods provided by the class `Tuple` (compare Subsection 6.3.2) are combined to compute its differentials. For these purposes, we introduce the class `ClusterSpectralSequence`, which is a template class with the class type of the underlying `ChainComplex` as a template parameter (compare Subsection 6.2.1).

At first, we are going to describe the class CSSBasis in Subsection 6.3.3.1, which represents the basis of a single module of the cluster spectral sequence. Next, we describe the data members of the ClusterSpectralSequence (Subsection 6.3.3.2), which are most importantly a collection of bases of the modules of the Ehrenfried complex and a collection of its differentials. Thereafter, we explain how the bases (see Subsubsection 6.3.3.3) and the differentials (see Subsubsection 6.3.3.4) are generated, and what other methods are provided by the class ClusterSpectralSequence (see Subsubsection 6.3.3.5).

6.3.3.1. CSSBasis

Just like the cluster spectral sequence associated with $\mathbb{E}$ consists of a finite number of modules, our class ClusterSpectralSequence contains a finite number of CSSBases, which are structs representing the bases of these modules.

Thus the only data member of the struct CSSBasis is the basis

```
BasisType basis;
```

Thereby, BasisType is a map storing all Tuples of this basis, sorted by cluster sizes. For each cluster size l, we organize the corresponding Tuples in an `std::unordered_set` with an appropriate hash function that makes it possible to search for basis elements in amortized constant running time.

The struct CSSBasis provides the usual methods for saving and loading as well as the functions

```
uint64_t size( int32_t l ) const;
```

returning the number of basis elements with exactly l clusters and

```
uint64_t total_size() const;
```

returning the total number of basis elements.

Since the computation of the differential (compare Subsubsection 6.3.3.4) requires a unique identification of one basis element among the other basis elements of the same cluster size of one CSSBasis, there is a method

```
int64_t id_of( Tuple& t );
```

returning the unique `id` of the given Tuple `t`. If `t` is not an element of this CSSBasis, we return `-1` to indicate the failure of the function.

The most important method of the struct CSSBasis is the function

```
uint32_t add_basis_element ( Tuple& t );
```

Using the method `num_clusters` of the class Tuple (see Subsubsection 6.3.2.3), it inserts the Tuple `t` into the part of the basis corresponding to its number of clusters and sets the `id` of `t` to the current number of basis elements with exactly l clusters. This means that if one builds up a MonoBasis by successively adding basis elements, all basis elements can be distinguished by their `ids`.

6.3.3.2. Data Members

The class ClusterSpectralSequence represents the cluster spectral sequence assoicated with the Ehrenfried complex. Hence, it contains a collection of CSSBases

```
std::map< uint32_t, CSSBasis > basis_complex;
```

where for each $0 \leq p \leq 2h$, the basis elements of the Ehrenfried complex on the symbols $0, \ldots, p$ are stored, and the data member

```
MatrixComplex diff_complex;
```

where at each time, the differential needed for computations is stored.

Note that MatrixComplex is a template parameter. Depending on the coffficients of the homology one wants to compute, it can be chosen to be ClusterSpectralSequenceQ or ClusterSpectralSequenceZm. For coefficients in the field $\mathbb{F}_2$, we highly recommend to use ClusterSpectralSequenceBool for efficiency reasons. The genus g, the number of punctures m and the number h of transpositions in a basis tuple associated with this MonoComplex are also stored as data members. Furthermore, the data member

```
SignConvention sign_conv;
```

indicates which sign convention (see also Subsubsection 6.3.1.2) is used to compute the homology of this MonoComplex, and the data member

```
size_t num_threads;
```

determines the number of threads using for the construction of the differentials.

6.3.3.3. Generating Bases

The first step to build up a ClusterSpectralSequence is to call the constructor

```
ClusterSpectralSequence( uint32_t genus,
                         uint32_t num_punctures,
                         SignConvention sgn,
                         uint32_t num_working_threads,
                         uint32_t num_remaining_threads );
```

For an explanation of the parameters num_working_threads and num_remaining_threads, see Subsubsection 6.2.6.2. In the constructor, Diagonalizer is configured (compare Subsection 6.2.5), and the bases of all the modules belonging to the MonoComplex are initialized via a recursive method we want to explain now.

Our aim is to enumerate all cells $\Sigma = (\tau_h \mid \ldots \mid \tau_1)$ of bidegree (p, h) for all $0 \leq p \leq 2h$ such that

(i) All τ_i are non-trivial transpositions on the symbols $min, \ldots, p$.

(ii) Each symbol $min, \ldots, p$ is permuted non-trivially by at least one τ_i.

(iii) Σ is monotonous.

Hereby, in the parallel case, min equals 1, and in the radial case, we want to enumerate all cells for $min = 0$ or $min = 1$.

The enumeration of all these cells works recursively. Let $\Sigma = (\tau_k \mid \ldots \mid \tau_1)$ be a cell fulfilling the above conditions, but with bidegree (p, k) with $k < h$. Assume we want to find all possibilities to extend such a cell Σ to a monotonous tuple Σ' of $k+1$ transpositions by inserting a transposition τ_{k+1}, perharps using more symbols. The following cases occur.

(i) We also use the symbols $min, \ldots, p$ for τ_{k+1}. Since Σ' is supposed to be monotonous, τ_{k+1} needs to contain the symbol p. Hence we can set $\tau_{k+1} := (p, i)$ with $i \in \{min, \ldots, p-1\}$ chosen arbitrarily.

(ii) We insert a new row into our parallel slit domain and use the symbols $min, \ldots, p+1$ for Σ'. By monotony, τ_{k+1} has to contain the highest symbol $p+1$. But now there are two possibilities:

a) The new row is inserted as a $(p+1)^{\text{th}}$ row above the old rows. Hence the symbol that is contained in τ_{k+1} apart from $p+1$ is one of the symbols that were already used for the transpositions $\tau_1, \ldots, \tau_k$, and we can set $\tau_{k+1} := (p+1, i)$ with $i \in \{min, \ldots, p\}$ chosen arbitrarily.

b) The new row is inserted as the i^{th} row for some $i \in \{min, \ldots, p\}$ and the indices of the old rows $min, \ldots, p$ are shifted up by one. Note that these indices are also shifted up in the transpositions of Σ. By monotony and since all symbols in $\{min, \ldots, p\}$ have to be covered, the new transposition has to be $\tau_{k+1} := (p+1, i)$, meaning that the symbol $p+1$ is also used by at least one of the transpositions $\tau_1, \ldots, \tau_k$, and that the symbol i is used by τ_{k+1} only.

(iii) We insert two rows into our slit domain, using the symbols $\{min, \ldots, p+2\}$. Thus the symbols used by the new transposition τ_{k+1} do not yet appear in Σ. Therefore τ_{k+1} has to contain the symbol $p+2$ and some other symbol $i \in \{min, \ldots, p+1\}$. Again, the indices of the rows $i+1, \ldots, p$ have to be shifted up by 1 in the transpositions of Σ.

We can use these observations to define the recursive method

```
void gen_bases( uint32_t k, uint32_t p, uint32_t min, Tuple& tuple );
```

This methods gets as input data a monotonous `Tuple` consisting of k transpositions which contain each of the symbols $min, \ldots, p$ at least once, and the minimum symbol the transpositions may contain. Using the above case distinction, it calls itself recursively with the appropriate parameters and stores all the transpositions with h transpositions detected thereby in the corresponding basis, but only if they contain the required number of cycles.

Now we can describe the way the constructor of the `CSS` sets up its `basis_complex`.

Proposition 6.3.4. *We can enumerate all basis elements of the parallel Ehrenfried complex by defining the* `Tuple` $\Sigma = ((2,1))$ *consisting of only one* `Transposition`*, and then calling the recursive function* `gen_bases(1, 2, 1,` Σ`)`*.*

For enumerating all basis elements of the radial Ehrenfried complex, we additionally need to call the recursive function `gen_bases(1, 1, 0,` Σ'`)` *with* $\Sigma' = ((1,0))$*.*

Proof. Note that for a given Σ, the tranpositions arising from the different cases fulfill the above conditions (i) - (iii), and that they are all distinct. If we consider two different `Tuples`, the transpositions arising from the case distinction also cannot coincide since either they have different numbers of transpositions or their starting sequence of transpositions already differs. Especially, we don't enumerate `Tuples` multiple times by the two initial calls in the radial case since the first family of `Tuples` does not contain the symbol 0, and the second family does.

Hence it suffices to show that all monotonous transpositions can be found by our algorithm. By induction on the number of transpositions, we can assume that we have already built up all monotonous tuples with k transpositions. Let $\Sigma' = (\tau_{k+1} \mid \ldots \mid \tau_1)$ be monotonous. Then $\tau_{k+1} = (p+1, i)$ with $i \in \{1, \ldots, p\}$ by monotony. The tuple $\Sigma := (\tau_k \mid \ldots \mid \tau_1)$ is also monotonous, but we might have to shift the indices $i, \ldots, p+1$ down by one if the symbol i is not contained in the transpositions $\tau_1, \ldots, \tau_k$. This yields one of the tuples of k transpositions we have already found. By reverting the process just described, we can rebuild Σ' from Σ, and this case is covered by the above case distinction. □

6.3.3.4. Generating Differentials

In Subsubsection 6.3.1.2, we explained how both the E^1-term and E^2-term are computed. Recalling Chapter 2, the p^{th} differential of the Ehrenfried complex is given by the composition $\pi\partial''_p\kappa$. The member function

```
gen_d0( const int32_t p, const int32_t l );
```

generates the restriction of the p^{th} differential $\partial_{\mathbb{E}}$ to the cells of $\mathbb{E}$ with exactly l clusters. Similarly, the method

```
gen_d1_stage_1( const int32_t p, const int32_t l );
```

generates the restriction of the p^{th} differential $\partial_{\mathbb{E}}$ from the cells with l clusters to the cells with $l-1$ clusters and applies all row operations to this restriction that come from the sub-matrix d^0 from above.

For runtime reasons, we thereby use yet another formula for the map κ.

Proposition 6.3.5. *Let I' be the set of tuples of integers $(t_h, \ldots, t_1)$ such that $0 \leq t_q < q$. Then the map*

$$\{0, \ldots, h! - 1\} \longrightarrow I' \qquad \text{with} \qquad k \longmapsto \left(\left\lfloor \frac{k}{(q-1)!} \right\rfloor \pmod q \right)_q$$

is a bijection.

Proof. We show that

$$(t_h, \ldots, t_1) \longmapsto \sum_{q=2}^{h} t_q \cdot (q-1)!$$

defines an inverse of the above map. Since both sets have the same cardinality, it suffices to show that this map is a right inverse. For a fixed coordinate $q \in \{1, \ldots, h\}$, we compute

$$\sum_{q=2}^{h} t_q \cdot (q-1)! = \sum_{q=r}^{h} t_q \cdot (q-1)! + \sum_{q=2}^{r-1} t_q \cdot (q-1)! \,.$$

Using induction on r, we see that

$$\sum_{q=2}^{r-1} t_q \cdot (q-1)! < (r-1)!\,,$$

since for $r = 1$, the statement is true, and if we assume the statement for $r-1$, we can conclude

$$\begin{aligned}\sum_{q=2}^{r} t_q \cdot (q-1)! &= \sum_{q=2}^{r-1} t_q \cdot (q-1)! + t_r(r-1)! \\ &< (r-1)! + (r-1)(r-1)! \\ &= r!\,.\end{aligned}$$

From this, we get

$$\left\lfloor \frac{\sum_{q=2}^{h} t_q \cdot (q-1)!}{(r-1)!} \right\rfloor = \left\lfloor \sum_{q=r}^{h} t_q \cdot \frac{(q-1)!}{(r-1)!} + \sum_{q=2}^{r-1} t_q \cdot \frac{(q-1)!}{(r-1)!} \right\rfloor = \sum_{q=r}^{h} t_q \cdot \frac{(q-1)!}{(r-1)!}$$

since the left sum is integral and the right sum vanishes after rounding down. Taking the remaining term modulo r, we get t_r as a result since all summands but the r^{th} are zero modulo r. □

6.3.3.5. More Member Functions

We also offer class methods to print the `basis_complex` and the `matrix_complex`, and a method

```
void erase_differential( int32_t p );
```

which deletes the p^{th} differential and releases its memory. This function is defined because we only want to keep a differential in the memory as long as we really need it due to storage limitation.

6.4. Remarks on Compiling

Our software projects were developed and tested on **Debian 7**, **Ubuntu 12.04 LTS** and **Open SUSE 13.1**. If you use a different operating system, your compiler has to support the full C++11 standard. We suggest to use the C++ compiler of the **Gnu Compiler Collection**.

6.4.1. Installing the Required Software

Using an operating system based on **Debian**, it should suffice to install the software and libraries from the official repositories.

```
sudo apt-get install \
    build-essential g++ libboost-all-dev libgmp-dev libbz2-dev
```

We document the source code with the **Doxygen-syntax**. Thus we can generate a documentation using the program **doxygen**. It is installed as follows.

```
sudo apt-get install doxygen doxygen-gui doxygen-latex
```

6.4.2. Building the Projects

Using the provided makefile, the executables are built as follows.

```
make compute_cache
make compute_css
make compute_statistics
make print_basis
```

Moreover, you can create your own executables (with a given name say `my_program`) by creating a corresponding `.cpp` file in the subfolder `./kappa` with the prefix `main_` (e.g. you create `./kappa/main_my_program.cpp`). Calling `make` with the name of your project will create an executable with this name.

6.4.3. More Remarks

Using **doxygen** you can generate a documentation of the source code as follows.

```
make doc
```

The documentation itself can be found in the subdirectory `./doc` in the corresponding project.

The libraries, executables and documentation can be cleaned up as always. The generated results are kept.

```
make clean
```

6.5. Results

As discussed above, our program computes the cluster spectral sequence of a given Ehrenfried complex, i.e. we compute the cohomology of the associated moduli space. In this section, we list the results our computer program provides. Hereby, we distinct the parallel and radial case. We compute the cluster spectral sequence with respect to coefficients R being either the rationals $\mathbb{Q}$ or the field $\mathbb{F}_2$. Given parameters g and m, we provide several tables with entries $\dim_R E^s_{p,l}$ for

(i) s equals 0, 1 or 2,

(ii) p the homological degree and

(iii) l the cluster number.

The rightmost column of each table notes $\dim_R \sum_l E^s_{p,l}$. For $s = 2$, we thus provide the dimensions of the homology of the moduli spaces $\dim_R H_{2h-p}(\mathfrak{M}; R)$, where $h = 2g + m$ in the parallel case and $h = 2g + m - 1$ in the radial case.

6.5.1. The Parallel Case

6.5.1.1. Genus $g = 0$ and Punctures $m = 0, \ldots, 6$

For $g = 0$ and $n = 1$, the moduli space $\mathfrak{M}^m_{g,1}$ is the classifying space of the braid group on m strings. Its homology is understood. Moreover, it is easy to see that degree and cluster number agrees for any cell, so the cluster spectral squence does not give any new insights. We list our computations anyways.

The case $g = 0$, $m = 1$ and $h = 1$ with coefficients in $\mathbb{F}_2$ and $\mathbb{Q}$:

$E^0_{p,l}$ for $\mathbb{F}_2$ and $\mathbb{Q}$			
p \ l	1	2	dim
2	1		1

$E^1_{p,l}$ for $\mathbb{F}_2$ and $\mathbb{Q}$			
p \ l	1	2	dim
2	1		1

$E^2_{p,l}$ for $\mathbb{F}_2$ and $\mathbb{Q}$			
p \ l	1	2	$\dim_R H_{2-p}(\mathfrak{M}^1_{0,1}; R)$
2	1		1

The case $g = 0$, $m = 2$ and $h = 2$ with coefficients in $\mathbb{F}_2$ and $\mathbb{Q}$:

$E^0_{p,l}$ for $\mathbb{F}_2$ and $\mathbb{Q}$			
p \ l	1	2	dim
3	2		2
4		2	2

$E^1_{p,l}$ for $\mathbb{F}_2$ and $\mathbb{Q}$			
p \ l	1	2	dim
3	2		2
4		2	2

	$E^2_{p,l}$ for $\mathbb{F}_2$ and $\mathbb{Q}$		
p \ l	1	2	$\dim_R H_{4-p}(\mathfrak{M}^2_{0,1}; R)$
3	1		1
4		1	1

The case $g = 0$, $m = 3$ and $h = 3$ with coefficients in $\mathbb{F}_2$ and $\mathbb{Q}$:

	$E^0_{p,l}$ for $\mathbb{F}_2$ and $\mathbb{Q}$			
p \ l	1	2	3	dim
4	5			5
5		10		10
6			5	5

	$E^1_{p,l}$ for $\mathbb{F}_2$ and $\mathbb{Q}$			
p \ l	1	2	3	dim
4	5			5
5		10		10
6			5	5

	$E^2_{p,l}$ for $\mathbb{F}_2$ and $\mathbb{Q}$			
p \ l	1	2	3	$\dim_R H_{6-p}(\mathfrak{M}^3_{0,1}; R)$
4	0			0
5		1		1
6			1	1

The case $g = 0$, $m = 4$ and $h = 4$ with coefficients in $\mathbb{F}_2$ and $\mathbb{Q}$:

	$E^0_{p,l}$ for $\mathbb{F}_2$ and $\mathbb{Q}$				
p \ l	1	2	3	4	dim
5	14				14
6		42			42
7			42		42
8				14	14

	$E^1_{p,l}$ for $\mathbb{F}_2$ and $\mathbb{Q}$				
p \ l	1	2	3	4	dim
5	14				14
6		42			42
7			42		42
8				14	14

	$E^2_{p,l}$ for $\mathbb{Q}$				
p \ l	1	2	3	4	$\dim_{\mathbb{Q}} H_{8-p}(\mathfrak{M}^4_{0,1};\mathbb{Q})$
5	0				0
6		0			0
7			1		1
8				1	1

	$E^2_{p,l}$ for $\mathbb{F}_2$				
p \ l	1	2	3	4	$\dim_{\mathbb{F}_2} H_{8-p}(\mathfrak{M}^4_{0,1};\mathbb{F}_2)$
5	1				1
6		1			1
7			1		1
8				1	1

The case $g = 0$, $m = 5$ and $h = 5$ with coefficients in $\mathbb{F}_2$ and $\mathbb{Q}$:

	$E^0_{p,l}$ for $\mathbb{F}_2$ and $\mathbb{Q}$					
p \ l	1	2	3	4	5	dim
6	42					42
7		168				168
8			252			252
9				168		168
10					42	42

	$E^1_{p,l}$ for $\mathbb{F}_2$ and $\mathbb{Q}$					
p \ l	1	2	3	4	5	dim
6	42					42
7		168				168
8			252			252
9				168		168
10					42	42

	$E^2_{p,l}$ for $\mathbb{Q}$					
p \ l	1	2	3	4	5	$\dim_{\mathbb{Q}} H_{10-p}(\mathfrak{M}^5_{0,1};\mathbb{Q})$
6	0					0
7		0				0
8			0			0
9				1		1
10					1	1

	$E^2_{p,l}$ for $\mathbb{F}_2$					
p \ l	1	2	3	4	5	$\dim_{\mathbb{F}_2} H_{10-p}(\mathfrak{M}^5_{0,1};\mathbb{F}_2)$
6	0					0
7		1				1
8			1			1
9				1		1
10					1	1

The case $g = 0$, $m = 6$ and $h = 6$ with coefficients in $\mathbb{F}_2$ and $\mathbb{Q}$:

	$E^0_{p,l}$ for $\mathbb{F}_2$ and $\mathbb{Q}$						
p \ l	1	2	3	4	5	6	dim
7	132						132
8		660					660
9			1320				1320
10				1320			1320
11					660		660
12						132	132

	$E^1_{p,l}$ for $\mathbb{F}_2$ and $\mathbb{Q}$						
p \ l	1	2	3	4	5	6	dim
7	132						132
8		660					660
9			1320				1320
10				1320			1320
11					660		660
12						132	132

	$E^2_{p,l}$ for $\mathbb{Q}$						
p \ l	1	2	3	4	5	6	$\dim_{\mathbb{Q}} H_{12-p}(\mathfrak{M}^6_{0,1};\mathbb{Q})$
7	0						0
8		0					0
9			0				0
10				0			0
11					1		1
12						1	1

	$E^2_{p,l}$ for $\mathbb{F}_2$						
p \ l	1	2	3	4	5	6	$\dim_{\mathbb{F}_2} H_{12-p}(\mathfrak{M}^6_{0,1};\mathbb{F}_2)$
7	0						0
8		1					1
9			2				2
10				1			1
11					1		1
12						1	1

6.5.1.2. Genus $g = 1$ and Punctures $m = 0, \ldots, 6$

The case $g = 1$, $m = 0$ and $h = 2$ with coefficients in $\mathbb{F}_2$ and $\mathbb{Q}$:

	$E^0_{p,l}$ for $\mathbb{F}_2$ and $\mathbb{Q}$		
p \ l	1	2	dim
2	1		1
3	2		2
4		1	1

	$E^1_{p,l}$ for $\mathbb{F}_2$ and $\mathbb{Q}$		
p \ l	1	2	dim
2	0		0
3	1		1
4		1	1

	$E^2_{p,l}$ for $\mathbb{F}_2$ and $\mathbb{Q}$		
p \ l	1	2	$\dim_R H_{4-p}(\mathfrak{M}^0_{1,1}; R)$
2	0		0
3	1		1
4		1	1

The case $g = 1$, $m = 1$ and $h = 3$ with coefficients in $\mathbb{F}_2$ and $\mathbb{Q}$:

	$E^0_{p,l}$ for $\mathbb{F}_2$ and $\mathbb{Q}$			
p \ l	1	2	3	dim
2	1			1
3	12			12
4	25	6		31
5		30		30
6			10	10

	$E^1_{p,l}$ for $\mathbb{Q}$			
p \ l	1	2	3	dim
2	0			0
3	0			0
4	14	0		14
5		24		24
6			10	10

	$E^2_{p,l}$ for $\mathbb{Q}$			
p \ l	1	2	3	$\dim_{\mathbb{Q}} H_{6-p}(\mathfrak{M}^1_{1,1};\mathbb{Q})$
2	0			0
3	0			0
4	0	0		0
5		1		1
6			1	1

	$E^1_{p,l}$ for $\mathbb{F}_2$			
p \ l	1	2	3	dim
2	0			0
3	1			1
4	15	0		15
5		24		24
6			10	10

	$E^2_{p,l}$ for $\mathbb{F}_2$			
p \ l	1	2	3	$\dim_{\mathbb{F}_2} H_{6-p}(\mathfrak{M}^1_{1,1};\mathbb{F}_2)$
2	0			0
3	1			1
4	1	0		1
5		1		1
6			1	1

The case $g = 1$, $m = 2$ and $h = 4$ with coefficients in $\mathbb{F}_2$ and $\mathbb{Q}$:

	$E^0_{p,l}$ for $\mathbb{F}_2$ and $\mathbb{Q}$				
p \ l	1	2	3	4	dim
3	10				10
4	96	4			100
5	210	100			310
6		400	30		430
7			280		280
8				70	70

	$E^1_{p,l}$ for $\mathbb{Q}$				
p \ l	1	2	3	4	dim
3	0				0
4	0	0			0
5	124	0			124
6		304	0		304
7			250		250
8				70	70

	$E^2_{p,l}$ for $\mathbb{Q}$				
p \ l	1	2	3	4	$\dim_{\mathbb{Q}} H_{8-p}(\mathfrak{M}^2_{1,1};\mathbb{Q})$
3	0				0
4	0	0			0
5	0	0			0
6		0	0		0
7			1		1
8				1	1

	$E^1_{p,l}$ for $\mathbb{F}_2$				
p \ l	1	2	3	4	dim
3	0				0
4	3	0			3
5	127	3			130
6		307	0		307
7			250		250
8				70	70

	$E^2_{p,l}$ for $\mathbb{F}_2$				
p \ l	1	2	3	4	$\dim_{\mathbb{F}_2} H_{8-p}(\mathfrak{M}^2_{1,1};\mathbb{F}_2)$
3	0				0
4	1	0			1
5	2	1			3
6		3	0		3
7			2		2
8				1	1

The case $g = 1$, $m = 3$ and $h = 5$ with coefficients in $\mathbb{F}_2$ and $\mathbb{Q}$:

	$E^0_{p,l}$ for $\mathbb{F}_2$ and $\mathbb{Q}$					
p \ l	1	2	3	4	5	dim
4	70					70
5	640	60				700
6	1470	1035	15			2520
7		3850	360			4210
8			4130	140		4270
9				2100		2100
10					420	420

	$E^1_{p,l}$ for $\mathbb{Q}$					
p \ l	1	2	3	4	5	dim
4	0					0
5	1	0				1
6	901	0	0			901
7		2875	0			2875
8			3515	0		3515
9				1960		1960
10					420	420

	$E^2_{p,l}$ for $\mathbb{Q}$					
p \ l	1	2	3	4	5	$\dim_{\mathbb{Q}} H_{10-p}(\mathfrak{M}^3_{1,1};\mathbb{Q})$
4	0					0
5	1	0				1
6	2	0	0			2
7		1	0			1
8			0	0		0
9				1		1
10					1	1

	$E^1_{p,l}$ for $\mathbb{F}_2$					
p \ l	1	2	3	4	5	dim
4	0					0
5	10	0				10
6	910	20	0			930
7		2895	10			3905
8			3525	0		3525
9				1960		1960
10					420	420

	$E^2_{p,l}$ for $\mathbb{F}_2$					
p \ l	1	2	3	4	5	$\dim_{\mathbb{F}_2} H_{10-p}(\mathfrak{M}^3_{1,1};\mathbb{F}_2)$
4	0					0
5	1	0				1
6	2	2	0			4
7		4	1			5
8			3	0		3
9				2		2
10					1	1

The case $g = 1$, $m = 4$ and $h = 6$ with coefficients in $\mathbb{F}_2$:

	$E^0_{p,l}$ for $\mathbb{F}_2$						
p \ l	1	2	3	4	5	6	dim
5	420						420
6	3840	570					4410
7	9240	8526	294				18060
8		30898	7896	56			38850
9			44772	3528			48300
10				34440	630		35070
11					13860		13860
12						2310	2310

	$E^1_{p,l}$ for $\mathbb{F}_2$						
p \ l	1	2	3	4	5	6	dim
5	0						0
6	36	0					36
7	5856	105	0				5961
8		23047	105	0			23152
9			37275	35			37310
10				31003	0		31003
11					13230		13230
12						2310	2310

	$E^2_{p,l}$ for $\mathbb{F}_2$						
p \ l	1	2	3	4	5	6	$\dim_{\mathbb{F}_2} H_{12-p}(\mathfrak{M}^4_{1,1};\mathbb{F}_2)$
5	0						0
6	2	0					2
7	3	2	0				5
8		6	2	0			8
9			7	1			8
10				4	0		4
11					2		2
12						1	1

The case $g = 1$, $m = 5$ and $h = 7$ with coefficients in $\mathbb{F}_2$:

	$E^0_{p,l}$ for $\mathbb{F}_2$							
p \ l	1	2	3	4	5	6	7	dim
6	2310							2310
7	21504	4368						25872
8	54054	61208	3472					118734
9		220500	76608	1344				298452
10			403200	51660	210			455070
11				415800	18480			434280
12					251790	2772		254562
13						84084		84084
14							12012	12012

	$E^1_{p,l}$ for $\mathbb{F}_2$							
p \ l	1	2	3	4	5	6	7	dim
6	0							0
7	129	0						129
8	34989	507	0					35496
9		164167	756	0				164923
10			330820	504	0			331324
11				365988	126			366114
12					233646	0		233646
13						81312		81312
14							12012	12012

	$E^2_{p,l}$ for $\mathbb{F}_2$							
p \ l	1	2	3	4	5	6	7	$\dim_{\mathbb{F}_2} H_{14-p}(\mathfrak{M}^5_{1,1};\mathbb{F}_2)$
6	0							0
7	2	0						2
8	3	4	0					7
9		7	3	0				10
10			8	2	0			10
11				7	1			8
12					4	0		4
13						2		2
14							1	1

The case $g = 1$, $m = 6$ and $h = 8$ with coefficients in $\mathbb{F}_2$: For $p \geq 10$, the differentials of $E_{p,l}$ could not be constructed or diagonalized due to memory and / or time limitations. The first and second page is therefore incomplete.

	$E^0_{p,l}$ for $\mathbb{F}_2$								
p \ l	1	2	3	4	5	6	7	8	dim
7	12012								12012
8	114688	29456							144144
9	300300	400464	31968						732732
10		1448760	634500	18840					2102100
11			3203640	574200	5940				3783780
12				4146780	308880	792			4456452
13					3354780	92664			3447444
14						1681680	12012		1693692
15							480480		480480
16							120120	60060	180180

	$E^1_{p,l}$ for $\mathbb{F}_2$								
p \ l	1	2	3	4	5	6	7	8	dim
7	0								0
8	470	0							470
9	198096	2330	0						200426

⋮

	$E^2_{p,l}$ for $\mathbb{F}_2$								
p \ l	1	2	3	4	5	6	7	8	$\dim_{\mathbb{F}_2} H_{16-p}(\mathfrak{M}^6_{1,1};\mathbb{F}_2)$
7	0								0
8	2	0							2
9	4	5	0						9

⋮

6.5.1.3. Genus $g = 2$ and Punctures $m = 0, 1$

The case $g = 2$, $m = 0$ and $h = 4$ with coefficients in $\mathbb{F}_2$ and $\mathbb{Q}$:

	$E^0_{p,l}$ for $\mathbb{F}_2$ and $\mathbb{Q}$				
p \ l	1	2	3	4	dim
2	1				1
3	18				18
4	78	5			83
5	112	60			172
6		168	15		183
7			98		98
8				21	21

	$E^1_{p,l}$ for $\mathbb{Q}$				
p \ l	1	2	3	4	dim
2	0				0
3	0				0
4	0	0			0
5	51	0			51
6		113	0		113
7			83		83
8				21	21

	$E^2_{p,l}$ for $\mathbb{Q}$				
p \ l	1	2	3	4	$\dim_{\mathbb{Q}} H_{8-p}(\mathfrak{M}^0_{2,1};\mathbb{Q})$
2	0				0
3	0				0
4	0	0			0
5	1	0			1
6		0	0		0
7			0		0
8				1	1

	$E^1_{p,l}$ for $\mathbb{F}_2$				
p \ l	1	2	3	4	dim
2	0				0
3	1				1
4	2	0			2
5	52	0			52
6		113	0		113
7			83		83
8				21	21

	$E^2_{p,l}$ for $\mathbb{F}_2$				
p \ l	1	2	3	4	$\dim_{\mathbb{F}_2} H_{8-p}(\mathfrak{M}^0_{2,1};\mathbb{F}_2)$
2	0				0
3	1				1
4	2	0			2
5	3	0			3
6		2	0		2
7			1		1
8				1	1

The case $g = 2$, $m = 1$ and $h = 5$ with coefficients in $\mathbb{F}_2$ and $\mathbb{Q}$:

	$E^0_{p,l}$ for $\mathbb{F}_2$ and $\mathbb{Q}$					
p \ l	1	2	3	4	5	dim
2	1					1
3	60					60
4	638	12				650
5	2480	380				2860
6	3528	2985	75			6588
7		7238	1470			8708
8			6398	280		6678
9				2772		2772
10					483	483

	$E^1_{p,l}$ for $\mathbb{Q}$					
p \ l	1	2	3	4	5	dim
2	0					0
3	0					0
4	1	0				1
5	1	0				1
6	1627	0	0			1627
7		4621	0			4621
8			5003	0		5003
9				2492		2492
10					483	483

	$E^2_{p,l}$ for $\mathbb{Q}$					
p \ l	1	2	3	4	5	$\dim_{\mathbb{Q}} H_{10-p}(\mathfrak{M}^1_{2,1};\mathbb{Q})$
2	0					0
3	0					0
4	1	0				1
5	1	0				1
6	0	0	0			0
7		2	0			2
8			1	0		1
9				0		0
10					1	1

	$E^1_{p,l}$ for $\mathbb{F}_2$					
p \ l	1	2	3	4	5	dim
2	0					0
3	0					0
4	3	0				3
5	15	3				18
6	1639	20	0			1659
7		4638	5			4643
8			5008			5008
9				2492		2492
10					483	483

	$E^2_{p,l}$ for $\mathbb{F}_2$					
p \ l	1	2	3	4	5	$\dim_{\mathbb{F}_2} H_{10-p}(\mathfrak{M}^1_{2,1};\mathbb{F}_2)$
2	0					0
3	0					0
4	1	0				1
5	2	1				3
6	1	3	0			4
7		4	1			5
8			3	0		3
9				1		1
10					1	1

6.5.1.4. Genus $g = 3$ and Punctures $m = 0, 1$

The case $g = 3$, $m = 0$ and $h = 6$ with coefficients in $\mathbb{F}_2$ and $\mathbb{Q}$:

	$E^0_{p,l}$ for $\mathbb{F}_2$ and $\mathbb{Q}$						
p \ l	1	2	3	4	5	6	dim
2	1						1
3	82						82
4	1212	9					1221
5	7200	440					7640
6	20400	5690	60				26150
7	23760	28980	2016				54756
8		54164	19124	294			73582
9			57424	6552			63976
10				33960	945		34905
11					10890		10890
12						1485	1485

	$E^1_{p,l}$ for $\mathbb{Q}$						
p \ l	1	2	3	4	5	6	dim
2	0						0
3	1						1
4	0	0					0
5	0	0					0
6	1	0					1
7	9429	0	0				9429
8		30443	0	0			30443
9			40256	0			40256
10				27702	0		27702
11					9945		9945
12						1485	1485

	$E^2_{p,l}$ for $\mathbb{Q}$						
p \ l	1	2	3	4	5	6	$\dim_{\mathbb{Q}} H_{12-p}(\mathfrak{M}^0_{3,1};\mathbb{Q})$
2	0						0
3	1						1
4	0	0					0
5	0	0					0
6	1	0					1
7	1	0	0				1
8		0	0	0			0
9			1	0			1
10				1	0		1
11					0		0
12						1	1

	$E^1_{p,l}$ for $\mathbb{F}_2$						
p \ l	1	2	3	4	5	6	dim
2	0						0
3	1						1
4	1	0					1
5	10	0					10
6	33	11					44
7	9452	49	5				9501
8		30481	20	0			30501
9			40271	0			40271
10				27702	0		27702
11					9945		9945
12						1485	1485

	$E^2_{p,l}$ for $\mathbb{F}_2$						
p \ l	1	2	3	4	5	6	$\dim_{\mathbb{F}_2} H_{12-p}(\mathfrak{M}^0_{3,1};\mathbb{F}_2)$
2	0						0
3	1						1
4	1	0					1
5	4	0					4
6	4	1					5
7	1	2	1				4
8		2	2	0			4
9			4	0			4
10				2	0		2
11					0		0
12						1	1

The case $g = 3$, $m = 1$ and $h = 7$ with coefficients in $\mathbb{F}_2$: For $p \geq 7$, the differentials of $E_{p,l}$ could not be constructed or diagonalized due to memory and / or time limitations. The first and second page is therefore incomplete.

	$E^0_{p,l}$ for $\mathbb{F}_2$							
p \ l	1	2	3	4	5	6	7	dim
2	1							1
3	252							252
4	7563	18						7581
5	81360	2010						83370
6	424920	48855	195					473970
7	1141056	469938	13230					1624224
8	1305876	2069844	247898	1540				3625158
9		3593880	1810368	70476				5474724
10			4737360	915390	8715			5661465
11				3702820	258720			3961540
12					1765335	31878		1797213
13						477906		477906
14							56628	56628

	$E^1_{p,l}$ for $\mathbb{F}_2$							
p \ l	1	2	3	4	5	6	7	dim
2	0							0
3	0							0
4	3	0						3
5	8	3						11
6	128	5	0					133

$\vdots$

	$E^2_{p,l}$ for $\mathbb{F}_2$							
p \ l	1	2	3	4	5	6	7	$\dim_{\mathbb{F}_2} H_{14-p}(\mathfrak{M}^1_{3,1};\mathbb{F}_2)$
2	0							0
3	0							0
4	1	0						1
5	5	3						8
6	6	2	0					8

$\vdots$

6.5.2. The Radial Case

Again note that in the radial case, we have $h = 2g + m - 1$. For our techniques to work, we need to require $m > 0$.

6.5.2.1. Genus $g = 0$ and Punctures $m = 1, \ldots, 6$

The case $g = 0$, $m = 1$ and $h = 0$ with coefficients in $\mathbb{F}_2$ and $\mathbb{Q}$:

	$E^0_{p,l}$ for $\mathbb{F}_2$ and $\mathbb{Q}$		
p \ l	1	2	dim
0	1		1

	$E^1_{p,l}$ for $\mathbb{F}_2$ and $\mathbb{Q}$		
p \ l	1	2	dim
0	1		1

	$E^2_{p,l}$ for $\mathbb{F}_2$ and $\mathbb{Q}$		
p \ l	1	2	$\dim_R H_{2-p}(\mathfrak{M}_0(1,1); R)$
0	1		1

The case $g = 0$, $m = 2$ and $h = 1$ with coefficients in $\mathbb{F}_2$ and $\mathbb{Q}$:

	$E^0_{p,l}$ for $\mathbb{F}_2$ and $\mathbb{Q}$		
p \ l	1	2	dim
1	1		1
2		1	1

	$E^1_{p,l}$ for $\mathbb{F}_2$ and $\mathbb{Q}$		
p \ l	1	2	dim
1	1		1
2		1	1

	$E^2_{p,l}$ for $\mathbb{F}_2$ and $\mathbb{Q}$		
p \ l	1	2	$\dim_R H_{2-p}(\mathfrak{M}_0(2,1); R)$
1	1		1
2		1	1

The case $g = 0$, $m = 3$ and $h = 2$ with coefficients in $\mathbb{F}_2$ and $\mathbb{Q}$:

	$E^0_{p,l}$ for $\mathbb{F}_2$ and $\mathbb{Q}$			
p \ l	1	2	3	dim
2	2			2
3		4		4
4			2	2

	$E^1_{p,l}$ for $\mathbb{F}_2$ and $\mathbb{Q}$			
p \ l	1	2	3	dim
2	2			2
3		4		4
4			2	2

	$E^2_{p,l}$ for $\mathbb{F}_2$ and $\mathbb{Q}$			
p \ l	1	2	3	$\dim_R H_{4-p}(\mathfrak{M}_0(3,1); R)$
2				0
3		1		1
4			1	1

The case $g = 0$, $m = 4$ and $h = 3$ with coefficients in $\mathbb{F}_2$ and $\mathbb{Q}$:

	$E^0_{p,l}$ for $\mathbb{F}_2$ and $\mathbb{Q}$				
p \ l	1	2	3	4	dim
3	5				5
4		15			15
5			15		15
6				5	5

	$E^1_{p,l}$ for $\mathbb{F}_2$ and $\mathbb{Q}$				
p \ l	1	2	3	4	dim
3	5				5
4		15			15
5			15		15
6				5	5

	$E^2_{p,l}$ for $\mathbb{Q}$				
p \ l	1	2	3	4	$\dim_{\mathbb{Q}} H_{6-p}(\mathfrak{M}_0(4,1);\mathbb{Q})$
3	0				0
4		0			0
5			1		1
6				1	1

	$E^2_{p,l}$ for $\mathbb{F}_2$				
p \ l	1	2	3	4	$\dim_{\mathbb{F}_2} H_{6-p}(\mathfrak{M}_0(4,1);\mathbb{F}_2)$
3	1				1
4		1			1
5			1		1
6				1	1

The case $g = 0$, $m = 5$ and $h = 4$ with coefficients in $\mathbb{F}_2$ and $\mathbb{Q}$:

	$E^0_{p,l}$ for $\mathbb{F}_2$ and $\mathbb{Q}$					
p \ l	1	2	3	4	5	dim
4	14					14
5		56				56
6			84			84
7				56		56
8					14	14

	$E^1_{p,l}$ for $\mathbb{F}_2$ and $\mathbb{Q}$					
p \ l	1	2	3	4	5	dim
4	14					14
5		56				56
6			84			84
7				56		56
8					14	14

	$E^2_{p,l}$ for $\mathbb{Q}$					
p \ l	1	2	3	4	5	$\dim_{\mathbb{Q}} H_{8-p}(\mathfrak{M}_0(5,1);\mathbb{Q})$
4	0					0
5		0				0
6			0			0
7				1		1
8					1	1

	$E^2_{p,l}$ for $\mathbb{F}_2$					
p \ l	1	2	3	4	5	$\dim_{\mathbb{F}_2} H_{8-p}(\mathfrak{M}_0(5,1);\mathbb{F}_2)$
4	0					0
5		1				1
6			1			1
7				1		1
8					1	1

The case $g = 0$, $m = 6$ and $h = 5$ with coefficients in $\mathbb{F}_2$ and $\mathbb{Q}$:

	$E^0_{p,l}$ for $\mathbb{F}_2$ and $\mathbb{Q}$						
p \ l	1	2	3	4	5	6	dim
5	42						42
6		210					210
7			420				420
8				420			420
9					210		210
10						42	42

	$E^1_{p,l}$ for $\mathbb{F}_2$ and $\mathbb{Q}$						
p \ l	1	2	3	4	5	6	dim
5	42						42
6		210					210
7			420				420
8				420			420
9					210		210
10						42	42

	$E^2_{p,l}$ for $\mathbb{Q}$						
p \ l	1	2	3	4	5	6	$\dim_{\mathbb{Q}} H_{10-p}(\mathfrak{M}_0(6,1);\mathbb{Q})$
5	0						0
6		0					0
7			0				0
8				0			0
9					1		1
10						1	1

	$E^2_{p,l}$ for $\mathbb{F}_2$						
p \ l	1	2	3	4	5	6	$\dim_{\mathbb{F}_2} H_{10-p}(\mathfrak{M}_0(6,1);\mathbb{F}_2)$
5	0						0
6		1					1
7			2				2
8				1			1
9					1		1
10						1	1

The case $g = 0$, $m = 7$ and $h = 6$ with coefficients in $\mathbb{F}_2$ and $\mathbb{Q}$:

	$E^0_{p,l}$ for $\mathbb{F}_2$ and $\mathbb{Q}$							
p \ l	1	2	3	4	5	6	7	dim
6	132							132
7		792						792
8			1980					1980
9				2640				2640
10					1980			1980
11						792		792
12							132	132

	$E^0_{p,l}$ for $\mathbb{F}_2$ and $\mathbb{Q}$							
p \ l	1	2	3	4	5	6	7	dim
6	132							132
7		792						792
8			1980					1980
9				2640				2640
10					1980			1980
11						792		792
12							132	132

	$E^2_{p,l}$ for $\mathbb{Q}$							
p \ l	1	2	3	4	5	6	7	$\dim_{\mathbb{Q}} H_{12-p}(\mathfrak{M}_0(7,1);\mathbb{Q})$
6								
7								
8								
9								
10								
11						1		1
12							1	1

	$E^2_{p,l}$ for $\mathbb{F}_2$							
p \ l	1	2	3	4	5	6	7	$\dim_{\mathbb{F}_2} H_{12-p}(\mathfrak{M}_0(7,1);\mathbb{F}_2)$
6								
7								
8			1					1
9				2				2
10					1			1
11						1		1
12							1	1

The case $g = 0$, $m = 8$ and $h = 7$ with coefficients in $\mathbb{F}_2$ and $\mathbb{Q}$:

	$E^0_{p,l}$ for $\mathbb{F}_2$ and $\mathbb{Q}$								
p \ l	1	2	3	4	5	6	7	8	dim
7	429								429
8		3003							3003
9			9009						9009
10				15015					15015
11					15015				15015
12						9009			9009
13							3003		3003
14								429	429

	$E^1_{p,l}$ for $\mathbb{F}_2$ and $\mathbb{Q}$								
p \ l	1	2	3	4	5	6	7	8	dim
7	429								429
8		3003							3003
9			9009						9009
10				15015					15015
11					15015				15015
12						9009			9009
13							3003		3003
14								429	429

	$E^2_{p,l}$ for $\mathbb{Q}$								
p \ l	1	2	3	4	5	6	7	8	$\dim_{\mathbb{Q}} H_{14-p}(\mathfrak{M}_0(8,1);\mathbb{Q})$
7	0								0
8		0							0
9			0						0
10				0					0
11					0				0
12						0			0
13							1		1
14								1	1

	$E^2_{p,l}$ for $\mathbb{F}_2$								
p \ l	1	2	3	4	5	6	7	8	$\dim_{\mathbb{Q}} H_{14-p}(\mathfrak{M}_0(8,1);\mathbb{Q})$
7	1								1
8		1							1
9			1						1
10				2					2
11					2				2
12						1			1
13							1		1
14								1	1

6.5.2.2. Genus $g = 1$ and Punctures $m = 1, \ldots, 6$

The case $g = 1$, $m = 1$ and $h = 2$ with coefficients in $\mathbb{F}_2$ and $\mathbb{Q}$:

	$E^0_{p,l}$ for $\mathbb{F}_2$ and $\mathbb{Q}$			
p \ l	1	2	3	dim
1	1			1
2	2	1		3
3		3		3
4			1	1

	$E^1_{p,l}$ for $\mathbb{Q}$			
p \ l	1	2	3	dim
1				0
2	1			1
3		2		2
4			1	1

	$E^2_{p,l}$ for $\mathbb{Q}$			
p \ l	1	2	3	$\dim_{\mathbb{Q}} H_{4-p}(\mathfrak{M}_1(1,1);\mathbb{Q})$
1				0
2				0
3		1		1
4			1	1

	$E^1_{p,l}$ for $\mathbb{F}_2$			
p \ l	1	2	3	dim
1	1			1
2	2			2
3		2		2
4			1	1

	$E^2_{p,l}$ for $\mathbb{F}_2$			
p \ l	1	2	3	$\dim_{\mathbb{F}_2} H_{4-p}(\mathfrak{M}_1(1,1);\mathbb{F}_2)$
1	1			1
2	1			1
3		1		1
4			1	1

The case $g = 1$, $m = 2$ and $h = 3$ with coefficients in $\mathbb{F}_2$ and $\mathbb{Q}$:

	$E^0_{p,l}$ for $\mathbb{F}_2$ and $\mathbb{Q}$				
p \ l	1	2	3	4	dim
1	1				1
2	12	1			13
3	25	18			33
4		55	6		61
5			40		40
6				10	10

	$E^1_{p,l}$ for $\mathbb{Q}$				
p \ l	1	2	3	4	dim
1					
2					
3	14				14
4		38			38
5			34		34
6				10	10

	$E^2_{p,l}$ for $\mathbb{Q}$				
p \ l	1	2	3	4	$\dim_{\mathbb{Q}} H_{6-p}(\mathfrak{M}_1(2,1);\mathbb{Q})$
1	0				0
2	0	0			0
3	0	0			0
4		0	0		0
5			1		1
6				1	1

	$E^1_{p,l}$ for $\mathbb{F}_2$				
p \ l	1	2	3	4	dim
1					
2	1				1
3	15	1			16
4		39			39
5			34		34
6				10	10

	$E^2_{p,l}$ for $\mathbb{F}_2$				
p \ l	1	2	3	4	$\dim_{\mathbb{F}_2} H_{6-p}(\mathfrak{M}_1(2,1);\mathbb{F}_2)$
1	0				0
2	1	0			1
3	2	1			3
4		3	0		3
5			2		2
6				1	1

The case $g = 1$, $m = 3$ and $h = 4$ with coefficients in $\mathbb{F}_2$ and $\mathbb{Q}$:

	$E^0_{p,l}$ for $\mathbb{F}_2$ and $\mathbb{Q}$					
p \ l	1	2	3	4	5	dim
2	10					10
3	96	14				110
4	210	196	4			410
5		610	130			740
6			680	30		710
7				350		350
8					70	70

	$E^1_{p,l}$ for $\mathbb{Q}$					
p \ l	1	2	3	4	5	dim
2	0					10
3	1	0				1
4	125	0	0			125
5		428	0			428
6			554	0		554
7				320		320
8					70	70

	$E^2_{p,l}$ for $\mathbb{Q}$					
p \ l	1	2	3	4	5	$\dim_{\mathbb{Q}} H_{8-p}(\mathfrak{M}_1(3,1);\mathbb{Q})$
2	0					0
3	1	0				1
4	2	0	0			2
5		1	0			1
6			0	0		0
7				1		1
8					1	1

	$E^1_{p,l}$ for $\mathbb{F}_2$					
p \ l	1	2	3	4	5	dim
2	0					0
3	3	0				3
4	127	6	0			133
5		434	3			437
6			557	0		557
7				320		320
8					70	70

	$E^2_{p,l}$ for $\mathbb{F}_2$					
p \ l	1	2	3	4	5	$\dim_{\mathbb{F}_2} H_{8-p}(\mathfrak{M}_1(3,1);\mathbb{F}_2)$
2	0					0
3	1	0				1
4	2	2	0			4
5		4	1			5
6			3	0		3
7				2		2
8					1	1

The case $g = 1$, $m = 4$ and $h = 5$ with coefficients in $\mathbb{Q}$ and $\mathbb{F}_2$:

	$E^0_{p,l}$ for $\mathbb{Q}$ and $\mathbb{F}_2$						
p \ l	1	2	3	4	5	6	dim
3	70						70
4	640	130					770
5	1470	1675	75				3220
6		5320	1665	15			7000
7			7980	770			8750
8				6230	140		6370
9					2520		2520
10						420	420

	$E^1_{p,l}$ for $\mathbb{Q}$						
p \ l	1	2	3	4	5	6	dim
3	0						0
4	1	0					1
5	901	1	0				902
6		3776	0	0			3776
7			6390	0			6390
8				5475	0		5475
9					2380		2380
10						420	420

	$E^2_{p,l}$ for $\mathbb{Q}$						
p \ l	1	2	3	4	5	6	$\dim_{\mathbb{Q}} H_{10-p}(\mathfrak{M}_1(4,1);\mathbb{Q})$
3	0						0
4	1	0					1
5	1	1	0				2
6		3	0	0			3
7			2	0			2
8				0	0		0
9					1		1
10						1	1

	$E^1_{p,l}$ for $\mathbb{F}_2$						
p \ l	1	2	3	4	5	6	dim
3	0						0
4	11	0					11
5	911	30	0				941
6		3805	30	0			3835
7			6420	10			6430
8				5485	0		5485
9					2380		2380
10						420	420

	$E^2_{p,l}$ for $\mathbb{F}_2$						
p \ l	1	2	3	4	5	6	$\dim_{\mathbb{F}_2} H_{10-p}(\mathfrak{M}_1(4,1);\mathbb{F}_2)$
3	0						0
4	2	0					2
5	3	2	0				5
6		6	2	0			8
7			7	1			8
8				4	0		4
9					2		2
10						1	1

The case $g = 1$, $m = 5$ and $h = 6$ with coefficients in $\mathbb{Q}$ and $\mathbb{F}_2$: For rational coefficients and $p \geq 9$, the differentials of $E_{p,l}$ could not be constructed or diagonalized due to memory and / or time limitations. The first and second page with rational coefficients is therefore incomplete.

	$E^0_{p,l}$ for $\mathbb{Q}$ and $\mathbb{F}_2$							
p \ l	1	2	3	4	5	6	7	dim
4	420							420
5	3840	990						4830
6	9240	12366	864					22470
7		40138	16422	350				56910
8			75670	11424	56			87150
9				79212	4158			83370
10					48300	630		48930
11						16170		16170
12							2310	2310

	$E^1_{p,l}$ for $\mathbb{Q}$							
p \ l	1	2	3	4	5	6	7	dim
4	0							0
5	2	0						2
6	5822	6	0					5828
7		40138	3	0				40141
8			60115	0	?			60115 + ?

	$E^2_{p,l}$ for $\mathbb{Q}$							
p \ l	1	2	3	4	5	6	7	$\dim_{\mathbb{Q}} H_{12-p}(\mathfrak{M}_1(5,1);\mathbb{Q})$
4	0							0
5	0	0						0
6	0	2	0					2
7		3	1	0				4
8			0	0	?			?

	$E^1_{p,l}$ for $\mathbb{F}_2$							
p \ l	1	2	3	4	5	6	7	dim
4	0							420
5	36	0						4830
6	5856	141	0					22470
7		28903	210	0				56910
8			60322	140	56			87150
9				68278	4158			83370
10					48300	630		48930
11						16170		16170
12							2310	2310

	$E^2_{p,l}$ for $\mathbb{F}_2$							
p \ l	1	2	3	4	5	6	7	$\dim_{\mathbb{Q}} H_{12-p}(\mathfrak{M}_1(5,1);\mathbb{Q})$
4	0							0
5	2	0						2
6	3	4	0					7
7		7	3	0				10
8			8	2	0			10
9				7	1			8
10					4	0		4
11						2		2
12							1	1

The case $g = 1$, $m = 6$ and $h = 7$ with coefficients in $\mathbb{F}_2$:

	$E^0_{p,l}$ for $\mathbb{F}_2$								
p \ l	1	2	3	4	5	6	7	8	dim
5	2310								2310
6	21504	6678							28182
7	54054	82712	7840						144606
8		274554	137816	4816					417186
9			623700	128268	1554				753522
10				819000	70140	210			889350
11					667590	21252			688842
12						335874	2772		338646
13							96096		96096
14							0	12012	12012

	$E^1_{p,l}$ for $\mathbb{F}_2$								
p \ l	1	2	3	4	5	6	7	8	dim
5	0								0
6	129	0							129
7	34989	636	0						35625
8		199156	1263	0					200419
9			494987	1260	0				496247
10				696808	630	0			697438
11					599634	126			599760
12						314958	0		314958
13							93324		93324
14							0	12012	12012

	$E^2_{p,l}$ for $\mathbb{F}_2$								
p \ l	1	2	3	4	5	6	7	8	$\dim_{\mathbb{F}_2} H_{14-p}(\mathfrak{M}_1(6,1);\mathbb{F}_2)$
5	0								0
6	2	0							2
7	4	5	0						9
8		10	5	0					15
9			12	3	0				15
10				11	2	0			13
11					8	1			9
12						4	0		4
13							2		2
14							0	1	1

6.5.2.3. Genus $g = 2$ and Punctures $m = 1, \ldots, 4$

The case $g = 2$, $m = 1$ and $h = 4$ with coefficients in $\mathbb{F}_2$ and $\mathbb{Q}$:

	$E^0_{p,l}$ for $\mathbb{F}_2$ and $\mathbb{Q}$					
p \ l	1	2	3	4	5	dim
1	1					1
2	18	1				19
3	78	23				101
4	112	138	5			255
5		280	75			355
6			266	15		281
7				119		119
8					21	21

	$E^1_{p,l}$ for $\mathbb{F}_2$ and $\mathbb{Q}$					
p \ l	1	2	3	4	5	dim
1	0					0
2	1	0				1
3	1	0				1
4	51	0	0			51
5		164	0			164
6			196	0		196
7				104		104
8					21	21

	$E^2_{p,l}$ for $\mathbb{Q}$					
p \ l	1	2	3	4	5	$\dim_{\mathbb{Q}} H_{8-p}(\mathfrak{M}_2(1,1);\mathbb{Q})$
1	0					0
2	1	0				1
3	1	0				1
4	0	0	0			0
5		2	0			2
6			1	0		1
7				0		0
8					1	1

	$E^1_{p,l}$ for $\mathbb{F}_2$					
p \ l	1	2	3	4	5	dim
1	0					0
2	1	0				1
3	2	1	0			3
4	52	2	0			54
5		165	0			165
6			196	0		196
7				104		104
8					21	21

	$E^2_{p,l}$ for $\mathbb{F}_2$					
p \ l	1	2	3	4	5	$\dim_{\mathbb{F}_2} H_{8-p}(\mathfrak{M}_2(1,1);\mathbb{F}_2)$
1	0					0
2	1	0				1
3	2	1	0			3
4	2	2	0			4
5		5	0			5
6			3	0		3
7				1		1
8					1	1

The case $g = 2$, $m = 2$ and $h = 5$ with coefficients in $\mathbb{F}_2$ and $\mathbb{Q}$:

	$E^0_{p,l}$ for $\mathbb{F}_2$ and $\mathbb{Q}$						
p \ l	1	2	3	4	5	6	dim
1	1						1
2	60	1					61
3	638	72					710
4	2480	1018	12				3510
5	3528	5465	455				9448
6		10766	4455	75			15296
7			13636	1750			15386
8				9170	280		9450
9					3255		3255
10						483	483

	$E^1_{p,l}$ for $\mathbb{Q}$						
p \ l	1	2	3	4	5	6	dim
1	0						0
2	0	0					0
3	0	0					0
4	1	1	0				2
5	1628	1	0				1629
6		6248	0	0			6248
7			9624	0			9624
8				7495	0		7495
9					2975		2975
10						483	483

	$E^2_{p,l}$ for $\mathbb{Q}$						
p \ l	1	2	3	4	5	6	$\dim_{\mathbb{Q}} H_{10-p}(\mathfrak{M}_2(2,1);\mathbb{Q})$
1	0						0
2	0	0					0
3	0	0					0
4	1	1	0				2
5	1	1	0				2
6		1	0	0			1
7			3	0			3
8				1	0		1
9					0		0
10						1	1

	$E^1_{p,l}$ for $\mathbb{F}_2$						
p \ l	1	2	3	4	5	6	dim
1	0						0
2	1	0					1
3	6	0					6
4	19	6	0				25
5	1641	35	3				1679
6		6277	25	0			6302
7			9646	5			9646
8				7500	0		7500
9					2975		2975
10						483	483

	$E^2_{p,l}$ for $\mathbb{F}_2$						
p \ l	1	2	3	4	5	6	$\dim_{\mathbb{F}_2} H_{10-p}(\mathfrak{M}_2(2,1);\mathbb{F}_2)$
1	0						0
2	1	0					1
3	4	0					4
4	7	2	0				9
5	5	5	1				11
6		7	3	0			10
7			8	1			9
8				5	0		5
9					2		2
10						1	1

The case $g = 2$, $m = 3$ and $h = 6$ with coefficients in $\mathbb{F}_2$:

	$E^0_{p,l}$ for $\mathbb{F}_2$							
p \ l	1	2	3	4	5	6	7	dim
2	42							42
3	1296	48						1344
4	11580	1896	6					13482
5	43200	22680	690					66570
6	61908	115230	15510	90				192738
7		224070	125510	5110				354690
8			354774	73640	700			429114
9				318192	23310			341502
10					169470	3150		172620
11						50358		50358
12							6468	6468

	$E^1_{p,l}$ for $\mathbb{F}_2$							
p \ l	1	2	3	4	5	6	7	dim
2	0							0
3	1	0						1
4	14	1	0					15
5	155	34	0					189
6	29176	516	31	0				29725
7		130155	642	10				130807
8			244701	350	0			245051
9				249912	70			249982
10					146930	0		146930
11						47208		47208
12							6468	6468

	$E^2_{p,l}$ for $\mathbb{F}_2$							
p \ l	1	2	3	4	5	6	7	$\dim_{\mathbb{F}_2} H_{12-p}(\mathfrak{M}_2(3,1);\mathbb{F}_2)$
2	0							0
3	1	0						1
4	4	1	0					5
5	8	5	0					13
6	5	12	3	0				20
7		8	9	1				18
8			8	5	0			13
9				9	1			10
10					5	0		5
11						2		2
12							1	1

The case $g = 2$, $m = 4$ and $h = 7$ with coefficients in $\mathbb{F}_2$: For $p \geq 8$, the differentials of $E_{p,l}$ could not be constructed or diagonalized due to memory and / or time limitations. The first and second page is therefore incomplete.

	$E^0_{p,l}$ for $\mathbb{F}_2$								
p \ l	1	2	3	4	5	6	7	8	dim
3	735								735
4	18000	1005							19005
5	149490	31965	300						181755
6	551040	352560	18375	30					922005
7	801801	1739500	326760	4970					2873031
8		3369807	2377900	162750	560				5911017
9			6408591	1860390	44310				8313291
10				7185465	878850	5250			8069565
11					5098170	235620			5333790
12						2269806	27720		2297526
13							582582		582582
14								66066	66066

	$E^1_{p,l}$ for $\mathbb{F}_2$								
p \ l	1	2	3	4	5	6	7	8	dim
3	0								0
4	3	0							3
5	55	6	0						61
6	1426	170	3	0					1599

	$E^2_{p,l}$ for $\mathbb{F}_2$								
p \ l	1	2	3	4	5	6	7	8	$\dim_{\mathbb{F}_2} H_{14-p}(\mathfrak{M}_2(4,1);\mathbb{F}_2)$
3	0								0
4	1	0							1
5	11	2	0						13
6	19	9	1	0					29

6.5.2.4. Genus $g = 3$ and Punctures $m = 1$

The case $g = 3$, $m = 1$ and $h = 6$ with coefficients in $\mathbb{F}_2$:

	$E^0_{p,l}$ for $\mathbb{F}_2$							
p \ l	1	2	3	4	5	6	7	dim
1	1							1
2	82	1						83
3	1212	91						1303
4	7200	1652	9					8861
5	20400	12890	500					33790
6	23760	49380	7706	60				80906
7		77927	48104	2310				128341
8			111588	25676	294			137558
9				91384	7497			98881
10					44850	945		45795
11						12375		12375
12							1485	1485

	$E^1_{p,l}$ for $\mathbb{F}_2$							
p \ l	1	2	3	4	5	6	7	dim
1	0							0
2	1	0						1
3	5	1						6
4	12	1	0					13
5	34	21	0					55
6	9455	82	16	0				9553
7		39933	69	5				40007
8			70752	20	0			70772
9				67973	0			67973
10					37647	0		37647
11						11430		11430
12							1485	1485

	$E^2_{p,l}$ for $\mathbb{F}_2$							
p \ l	1	2	3	4	5	6	7	$\dim_{\mathbb{F}_2} H_{12-p}(\mathfrak{M}_3(1,1);\mathbb{F}_2)$
1	0							0
2	1	0						1
3	5	1						6
4	7	1	0					8
5	7	5	0					12
6	7	6	1	0				14
7		7	2	1				10
8			3	2	0			5
9				4	0			4
10					3	0		3
11						0		0
12							1	1

Appendix

A. The Symmetric Groups $\mathfrak{S}^\Delta$ as Semisimplicial Set

In order to provide a compact notation, we introduce the symmetric groups as semisimplicial set $\mathfrak{S}^\Delta$. The **simplicial category** (which is used to define simplicial sets) is Δ. Its **face maps** are denoted by

$$d_i^\Delta \colon \{0,\dots,n\} \longrightarrow \{0,\dots,n+1\} \qquad \text{i.e.} \qquad d_i^\Delta(c) = \begin{cases} c & c < i \\ c+1 & c \geq i \end{cases},$$

and its **degeneracy maps** by

$$s_i^\Delta \colon \{0,\dots,n+1\} \longrightarrow \{0,\dots,n\} \qquad \text{i.e.} \qquad s_i^\Delta(c) = \begin{cases} c & c \leq i \\ c-1 & c > i \end{cases}.$$

The **semisimplicial category** $\Delta_{semi} \subset \Delta$ is a faithful subcategory. It consists of the same objects, contains all face maps d^Δ and misses all degeneracy maps s^Δ.

Definition A.1. The group of bijections of a set S is the **symmetric group** with respect to S and is denoted by $\mathfrak{S}_S = Aut(S)$. For n a non-negative integer, it is convenient to identify n with $\{0,\dots,n\}$. Consequently, the n^{th} **symmetric group** $\mathfrak{S}_n$ is the group of all bijections of the set $\{0,\dots,n\}$. The subgroup $Aut(\{1,\dots,n\})$ is denoted by $\mathfrak{S}_n^\times$.

Definition A.2. The **support** of a permutation α is the set of non-fixed points, i.e.

$$\operatorname{supp}(\alpha) = \{k \mid \alpha(k) \neq k\}.$$

The **support** of permutations $\alpha_1,\dots,\alpha_n$ is

$$\operatorname{supp}(\alpha_1,\dots,\alpha_n) = \operatorname{supp}(\alpha_1) \cup \dots \cup \operatorname{supp}(\alpha_n)\,.$$

Definition A.3. Let $n > 0$ and $0 \leq i \leq n$. The i^{th} **face**

$$D_i \colon \mathfrak{S}_n \longrightarrow\!\!\!\!\!\rightarrow \mathfrak{S}_{n-1}$$

is defined as follows. Consider a permutation $\alpha \in \mathfrak{S}_n$ and alter it by skipping i, which results in a permutation on $\{0,\dots,n-1\}$ up to renormalization:

$$D_i\alpha = s_i^\Delta \circ \left(\alpha \cdot (i\ \alpha^{-1}(i))\right) \circ d_i^\Delta\,.$$

Remark A.4. Each D_i is a surjective map of sets, but not a homomorphism of groups. The semisimplicial identities

$$D_iD_j = D_{j-1}D_i \qquad \text{for} \qquad i < j$$

are readily verified.

Definition A.5. The symmetric groups define a semisimplicial set $\mathfrak{S}^\Delta$ with $\mathfrak{S}^\Delta_n = \mathfrak{S}_n$ and face maps D_i as above.

Definition A.6. Let $n \geq 0$ and $0 \leq i \leq n$. The i^{th} **pseudo degeneracy**

$$S_i \colon \mathfrak{S}_n \hookrightarrow \mathfrak{S}_{n+1}$$

is defined as follows. Consider a permutation $\alpha \in \mathfrak{S}_n$ and recognize it as permutation on $\{0, \ldots, n+1\}$ via shifting all $j > i$ up by one:

$$(S_i\alpha)(c) = \begin{cases} i & c = i \\ d_i^\Delta \circ \alpha \circ s_i^\Delta & c \neq i \end{cases} .$$

Remark A.7. Each S_i is a monomorphism of groups because $s_i^\Delta d_i^\Delta = \mathrm{id}_{\{0,\ldots,n\}}$

The face and pseudo degeneracy maps fulfill all but one simplicial identity. In particular they do not make $\mathfrak{S}^\Delta$ a simplicial set.

Proposition A.8. *The following identities are fulfilled*

$$\begin{aligned} D_iD_j &= D_{j-1}D_i \qquad \textit{for} \qquad i < j \\ S_iS_j &= S_jS_{i-1} \qquad \textit{for} \qquad i > j \\ D_iS_j &= \begin{cases} S_{j-1}D_i & \textit{for } i < j \\ \mathrm{id} & \textit{for } i = j \\ S_jD_{i-1} & \textit{for } i > j+1 \end{cases} \end{aligned}$$

but

$$D_iS_j \neq \mathrm{id} \qquad \textit{for} \qquad i = j+1 \,.$$

Proof. The identities are readily verified and $(D_{i+1}S_i)(\tau) = 1_{\mathfrak{S}_n}$ holds for any transposition $\tau = (c\ i)$. □

Lemma A.9. *Let π be a permutation on $\pi \in \mathfrak{S}_p$ and $0 \leq j \leq p$. Then we have*

$$N(D_j(\pi)) = \begin{cases} N(\pi) & j \textit{ fix point of } \pi \\ N(\pi) - 1 & \textit{otherwise} \end{cases} ,$$

where N denotes the word length norm.

Proof. Recall that we can express the norm of π as $N(\pi) = p - \mathrm{cyc}(\pi)$, where $\mathrm{cyc}(\pi)$ denotes the number of cycles of π, also considering fixed points as cycles. Now, if j is a fixed point of π, we have

$$\begin{aligned} N(D_j(\pi)) &= (p-1) - \mathrm{cyc}(D_j(\pi)) \\ &= (p-1) - (\mathrm{cyc}(\pi) - 1) \\ &= N(\pi) \end{aligned}$$

since $D_j(\pi)$ consists of the same cycles as π (up to renormalization), except that the fixed point j is not contained in $D_j(\pi)$ anymore. If j is not a fixed point of π, it is removed from its cycle by D_j, but the number of cycles remains the same. Thus, in this case, we have

$$\begin{aligned} N(D_j(\pi)) &= (p-1) - \mathrm{cyc}(D_j(\pi)) \\ &= (p-1) - \mathrm{cyc}(\pi) \\ &= N(\pi) - 1\,. \end{aligned}$$

□

B. A Brief Review on Factorable Groups

Definition B.1. Let $\alpha \in \mathfrak{S}_p$ be a non-trivial permutation. The **height** of α is the largest symbol in the support of α, i.e.

$$\mathrm{ht}(\tau) = \max \mathrm{supp}(\alpha)\,.$$

Definition B.2. Let $G \subset \mathfrak{S}_p$ be the generating set consisting of all transpositions and the trivial permutation $1_{\mathfrak{S}_p}$. The **factorization map** is

$$\eta\colon \mathfrak{S}_p \longrightarrow \mathfrak{S}_p \times G\,, \qquad\qquad \alpha \longmapsto (\overline{\alpha}, \alpha')$$

with

$$\eta(1) = (1,1)$$

and, for $\alpha \neq 1$,

$$\overline{\alpha} = \alpha\alpha' \qquad \text{and} \qquad \alpha' = (c\ \alpha^{-1}(c)) \quad \text{for} \quad c = \mathrm{ht}(\alpha)\,.$$

Remark B.3. For $\alpha \neq 1$, the height of α is permuted non-trivially by α' and a fixed point of $\overline{\alpha}$.

Theorem ([Vis10, Theorem 5.2.1])**.** *The factorization map η makes the symmetric group $\mathfrak{S}_p$ factorable: Denoting the multiplication by $\mu\colon \mathfrak{S}_p \times \mathfrak{S}_p \longrightarrow \mathfrak{S}_p$ in the diagram below, the upper right composition of maps preserves the norm if and only if the lower left composition does. In this case, the diagram commutes.*

$$\begin{array}{ccccccc} \mathfrak{S}_p \times \mathfrak{S}_p & \xrightarrow{\eta \times \mathrm{id}} & \mathfrak{S}_p \times \mathfrak{S}_p \times \mathfrak{S}_p & \xrightarrow{\mathrm{id} \times \mu} & \mathfrak{S}_p \times \mathfrak{S}_p & \xrightarrow{\mathrm{id} \times \eta} & \mathfrak{S}_p \times \mathfrak{S}_p \times \mathfrak{S}_p \\ \downarrow{\scriptstyle \mu} & & & & & & \downarrow{\scriptstyle \mu \times \mathrm{id}} \\ \mathfrak{S}_p & & \xrightarrow{\qquad\qquad\qquad\qquad\qquad\qquad\qquad\qquad\qquad\qquad\qquad\qquad} & & & & \mathfrak{S}_p \times \mathfrak{S}_p \end{array}$$

It is handy to reformulate the above diagram as follows. We start off with 2 strings which represent the left respectively right factor of $\mathfrak{S}_p \times \mathfrak{S}_p$. The composition of maps is now visualised by splitting a string into two parts if η is applied, respectively by joining two strings if μ is applied. We obtain the following Figure.

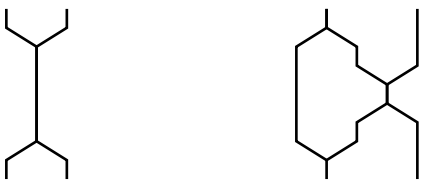

Symbol Index

$\mathbb{1}$	The unit of the little cubes operad $\left(\tilde{C}^k(\mathbb{C})\right)_{k\geq 0}$. – Page 77
$\mathfrak{X}$ or $\mathfrak{X}_j$	The map mueta multiplies two permutations and factors their product via the factorization map η afterwards. – Definition 2.8.4
$\mathfrak{X}^*$ or $\mathfrak{X}_j^*$	The dual of $\mathfrak{X}$ or $\mathfrak{X}_j$ – Definition 2.9.13
$\odot$	The radial composition of surfaces respectively radial slit domains – Definitions 4.6.2 and 4.6.3
$\odot_{\pi_k}$	The radial composition of surfaces respectively radial slit domains w.r.t. a partial pairing π_k – Definitions 4.6.2 and 4.6.3
$\#$	The Pontryagin product – Definition / Corollary 4.1.5
$\sim_{\mathrm{CL}}$	The equivalence relation used to count the clusters of a given cell. – Definition 3.1.1
$\mathbb{A}$	An annulus $\mathbb{A} \subset \mathbb{C}$ in the complex plane
α	The map α adds n new punctures to a parallel cell on $r = n$ levels. – Definition 4.4.2
$(a_h : \ldots : a_0)$	A coboundary trace of a cell Σ. – Definition 2.9.2
$a.\Sigma$	The coboundary of Σ corresponding to a. – Definition 2.9.5
$n\mathbb{A}$	The disjoint union of n annuli in the complex plane. – Page 112
$B_\bullet(\mathfrak{S}_p^\times)$	The bar resolution of the symmertric group. – Page 55
$Bsupp(\Sigma)$	This set is canonically identified with the set of basic coboundary traces of Σ. – Lemma 2.9.21
$Btrace(\Sigma)$	The set of basic coboundary traces of Σ. – Lemma 2.9.21
C_k^+	A (not distinguishable) outgoing boundary curve in a Riemann surface $F \in \mathfrak{M}_g^\bullet(m,n)$. – Section 2.1
C_k^-	The k^{th} incoming boundary curve in a Riemann surface $F \in \mathfrak{M}_g^\bullet(m,n)$. – Section 2.1
$\mathbb{C}$	The complex plane.
$\mathrm{cf}_i(\Sigma)$	The set of all i^{th} cofaces of a given cell Σ – Definition 2.9.1

$\tilde{C}^k(\mathbb{C})$ resp. $C^k(\mathbb{C})$ The ordered respectively unordered configuration space of the complex plane. – Page 77

$\mathcal{C}^+$ The set of outgoing boundary curves in a Riemann surface $F \in \mathfrak{M}_g^\bullet(m,n)$. – Section 2.1

$\mathcal{C}^-$ The set of incoming boundary curves in a Riemann surface $F \in \mathfrak{M}_g^\bullet(m,n)$. – Section 2.1

$\tilde{C}^k(\mathbb{A})$ The ordered configuration space of the annulus $\mathbb{A} \subset \mathbb{C}$. – Page 109

$c(\Sigma)$ The cluster number of a given cell Σ. – Definition 3.1.1

c^+ resp. c^- The arcs of a boundary curve of a surface, which correspond to the top respectively bottom of a slit picture – Page 84

$\partial_{\mathbb{E}}$ The boundary operator of the Ehrenfried complex – Definition 2.8.8

$\partial_{\mathbb{K}}$ The boundary operator of the complex $\mathbb{K}$. – Definition / Theorem 2.8.1

Δ The simplicial category, with face maps d_i^Δ and degeneracy maps s_i^Δ. – Page 203

Δ_{semi} The semisimplicial category with face maps d_i^Δ. – Page 203

$d_i''(\Sigma)$ The i^{th} horizontal face of a parallel cell Σ – Definition 2.3.9

$d_i''(\Sigma)$ The i^{th} horizontal face of a radial cell Σ – Subsection 2.5.3

$d_j'(\Sigma)$ The j^{th} vertical face of a parallel cell Σ – Definition 2.3.8

$d_j'(\Sigma)$ The j^{th} vertical face of a radial cell Σ – Subsection 2.5.3

d_i^Δ The i^{th} simplicial face map. – Page 203

D_i The i^{th} face map of the symmetric groups $\mathfrak{S}^\Delta$. – Definition A.3

$\mathbb{E}$ The Ehrenfried complex associated with (P,P') or (R,R') – Sections 2.1 and 2.8

$\mathbb{E}(h,m)$ The Ehrenfried complex associated with (R,R') for fixed g, n and m. – Section 2.8

$\mathbb{E}(h,m;r_1,\ldots,r_n)$ The Ehrenfried complex associated with (P,P') for fixed g, n, m and $(r_1,\ldots,r_n)$. – Section 2.8

η The factorization map which makes the symmetric groups factorable. – Definition B.2

$E^0_{k,c}(\mathbb{P})$ The cluster spectral sequence of the double complex. – Proposition 3.2.1

$E^0_{p,c}(\mathbb{E})$ The cluster spectral sequence of the Ehrenfried complex. – Proposition 3.2.1

ex	The expansion map – Proposition 2.9.26
F	A topological or Riemann surface.
$F_c\mathbb{E}$	The cluster filtration of the Ehrenfried complex. – Definition 3.1.5
$F_c\mathbb{P}$	The cluster filtration of the double complex $\mathbb{P}$. – Definition 3.1.3
F_pB_q	The norm filtration of the bar resolution of the symmertric group. – Page 55
$\Gamma_g^\bullet(m,n)$	The mapping class group with respect to $\mathfrak{M}_g^\bullet(m,n)$.
$\Gamma_{g,n}^m$	The mapping class group with respect to $\mathfrak{M}_{g,n}^m$.
g	The genus of a surface or a slit domain.
$g(\Sigma)$	The genus of a parallel cell Σ. – Remark 2.3.7
$g(\Sigma)$	The genus of a radial cell Σ. – Remark 2.5.7
$\mathfrak{H}_{g,n}^m[(r_1,\ldots,r_n)]$	The bundle of potential functions over $\mathfrak{M}_{g,n}^m$. – Section 2.2
$\mathfrak{H}_g^\bullet(m,n)$	The bundle of potential functions over $\mathfrak{M}_g^\bullet(m,n)$. – Section 2.4
ht	The height of a permutation, i.e. the largest symbol which is permutated non-trivially. – Definition B.1
$\mathcal{H}$	The Hilbert uniformization. – Sections 2.1, 2.3.4 and 2.5.4
$J.\Sigma = j_1^{\varepsilon_1}.\cdots.j_t^{\varepsilon_t}.\Sigma$	The iterated coboundary of Σ where all j_k are basic coboundary traces. – Definition 2.9.24
j^ϵ	In order to classify the cells of the Ehrenfried complex, we need a more handy notation for basic coboundary traces. – Notation 2.9.22
κ	The homomorphism kappa encodes the base change from $\mathbb{K}_\bullet$ to the Ehrenfried complex. – Definition 2.8.5
κ^*	The dual of κ – Subsection 2.9.2
κ_J^*	The summand $\kappa_J^* = \mathfrak{X}_{j_1}^* \circ \ldots \circ \mathfrak{X}_{j_k}^*$ with $J = (j_1,\ldots,j_k)$. – Definition 2.9.13
κ_I	The summand $\kappa_I = \mathfrak{X}_{i_1} \circ \ldots \circ \mathfrak{X}_{i_k}$ with $I = (i_1,\ldots,i_k)$. – Definition 2.8.10
$\mathbb{K}_\bullet$	The top row of the first page of the spectral sequence associated with the vertical homology of the double complex P/P' respectively R/R'. – Definition / Theorem 2.8.1
$\mathcal{K}_0$	The critical graph of a given potential function u – Page 22
Λ_h^*	Parametrizes the κ^*-squences of length h. – Definition 2.9.13

Λ_h	Parametrizes the κ-squences of length h. – Definition 2.8.10
$\mathfrak{M}_g^{\bullet\bullet}(m,n)$	The moduli space of Riemann surfaces with genus g, m outgoing and n incoming boundary curve, where on each outgoing and incoming boundary curve one point is marked. – Definition 4.6.1
$\mathfrak{M}_{g,n}^m \simeq B\Gamma_{g,n}^m$	The moduli space of Riemann surfaces of genus g with m punctures and n boundary curves.
$\mathfrak{M}_g^{\bullet}(m,n)$	The moduli space of Riemann surfaces with genus g, m outgoing boundary curves and n marked incoming boundary curves.
μ	Either the product in the symmetric group or the product of two slit domains. – Definition 4.1.2
$\mu^{\uparrow\downarrow}$	A selected glueing construction – Subsubsection 4.2.3
$\mu_*^{\uparrow\downarrow}$	A selected homology operation – Definition / Proposition 4.2.4
$\mu^{\uparrow\uparrow}$	A selected glueing construction – Subsubsection 4.2.2
$\mu_*^{\uparrow\uparrow}$	A selected homology operation – Definition / Proposition 4.2.3
μ^{cs}	A selected glueing construction – Subsubsection 4.2.4
μ_*^{cs}	A selected homology operation – Definition / Proposition 4.2.11
$\multimap\!\bullet\!\multimap$	Radial multiplication map – Definition 4.5.1
m	The number of punctures respectively outgoing boundary curves of a surface or slit domain.
$m(\Sigma)$	The number of punctures of a parallel cell Σ. – Definition 2.3.6
$m(\Sigma)$	The number of punctures of a radial cell Σ. – Definition 2.5.4
$\mathcal{N}[\mathfrak{S}_p^\times]$	The spectral sequence associated with the norm filtration called norm complex – Page 55
$\mathrm{ncyc}(\Sigma)$	The number of cycles of a parallel cell Σ. – Definition 2.3.6
$\mathrm{ncyc}(\Sigma)$	The number of cycles of a radial cell Σ. – Definition 2.5.4
n	The number of (incomming) boundary curves of a surface of slit domain.
$N(\Sigma)$	The norm of a parallel cell Σ. – Definition 2.3.6
$N(\Sigma)$	The norm of a radial cell Σ. – Definition 2.5.4
$n(\Sigma)$	The number of boundaries of a parallel cell Σ. – Definition 2.3.6
$n(\Sigma)$	The number of boundaries of a radial cell Σ. – Definition 2.5.4

$\mathcal{O}$ Orientation system of the manifold $\mathfrak{H}^m_{g,n}[(r_1,\ldots,r_n)]$ or $\mathfrak{H}^\bullet_g(m,n)$. – Section 2.6

$\otimes$ The natural map $\otimes\colon H_p(B;R)\otimes H_q(F;R)\longrightarrow H_{p+q}(X;R)$ being the homology cross product for trivial bundles. – Definition 4.3.1

(P,P') The parallel slit complex. – Sections 2.1 and 2.3

$[p]=\{\underline{0}_1,\underline{1}_1,\ldots,\underline{p}_1,\ldots,\underline{0}_r,\underline{1}_r,\ldots,\underline{p}_r\}$ A partition of p into r levels. – Definition 2.3.1

$\mathcal{P}=\{P_1,\ldots,P_m\}$ The set of punctures in a Riemann surface $F\in\mathfrak{M}^m_{g,n}$. – Section 2.1

$\mathcal{P}=\{P_1,\ldots,P_n\}$ The set of marked points on the n incoming boundary curves in a Riemann surface $F\in\mathfrak{M}^\bullet_g(m,n)$. – Section 2.1

$\mathcal{P}ow$ The power set operator – Proposition 2.9.26

$\mathfrak{Par}$ A shorthand for $\mathfrak{Par}=\coprod_{g,m,(r_1,\ldots,r_n)}\mathfrak{Par}^m_{g,n}[(r_1,\ldots,r_n)]$. – Page 89

$\mathfrak{Par}_1$ A shorthand for $\coprod_{g,m}\mathfrak{Par}^m_{g,1}$. – Page 77

$\mathfrak{Par}_n[(r_1,\ldots,r_n)]$ A shorthand for $\mathfrak{Par}_n[(r_1,\ldots,r_n)]=\coprod_{g,m}\mathfrak{Par}^m_{g,n}[(r_1,\ldots,r_n)]$. – Page 87

$\mathfrak{Par}^m_{g,n}$ A shorthand for $\mathfrak{Par}^m_{g,n}[(1)]$. – Page 77

$\mathfrak{Par}^m_{g,n}[(r_1,\ldots,r_n)]$ The space of parallel slit domains. – Sections 2.1 and 2.3

$\mathbb{P}_{\bullet,\bullet}$ The abbriviation $\mathbb{P}_{\bullet,\bullet}(h,m,;r_1,\ldots,r_n)=(P/P')_{\bullet,\bullet}$ with $P_{\bullet,\bullet}=P_{\bullet,\bullet}(h,m,;r_1,\ldots,r_n)$. – Page 73

$\mathrm{punc}(\Sigma)$ The symbols of the m cycles of Σ corresponding to the punctures. – Definition 4.3.5

$\mathcal{Q}=(Q_1,\ldots,Q_n)$ The enumerated points at which the non-vanishing tangent vectors $\mathcal{X}$ are attached. – Section 2.1

Q_0 and Q_1 Dyer–Lashof operations of degree 0 and 1 – Definition 4.1.9

(R,R') The radial slit complex. – Sections 2.1 and 2.5

$\mathfrak{Rad}_g(m,n)$ The space of radial slit domains. – Sections 2.1 and 2.5

$\mathfrak{Rad}(n)$ A shorthand for $\mathfrak{Rad}(n)=\coprod_{g,m}\mathfrak{Rad}_g(m,n)$. – Page 109

$\mathfrak{Rad}^{\bullet\bullet}_g(m,n)$ The space of radial slit domains with marked points also on the outgoing boundary curves. – Definition 4.6.1

$\Re$ The real part of a complex valued function.

R^Σ The set of relevant κ^*-sequences. – Definition 2.9.17

$\mathbb{S}^k$ The k-dimensional sphere.

$\mathcal{S}$	The set of stagnation points of a given potential function u – Page 22
$\Sigma = (\sigma_q, \ldots, \sigma_0)$	A parallel cell written in homogeneous notation – Definition 2.3.2
$\Sigma = (\sigma_q, \ldots, \sigma_0)$	A radial cell written in homogeneous notation – Definition 2.5.1
$\Sigma = (\tau_q \mid \ldots \mid \tau_1)$	A parallel cell written in inhomogeneous notation – Definition 2.3.5
$\Sigma = (\tau_q \mid \ldots \mid \tau_1)$	A radial cell written in inhomogeneous notation – 2.5.3
$\mathrm{supp}(\alpha)$	The support of a permutation α. – Definition A.2
$\mathfrak{S}^{\Delta}$	The symmetric groups $\mathfrak{S}^{\Delta}$. – Definition A.5
$\mathfrak{S}_n$	The n^{th} symmetric group is $\mathfrak{S}_n = Aut(\{0, \ldots, n\})$. – Definition A.1
$\mathfrak{S}_n^{\times}$	A shorthand for $\mathfrak{S}_n^{\times} = Aut(\{1, \ldots, n\}) \subset \mathfrak{S}_n$. – Definition A.1
S	A critical point of a given potential function u – Page 22
s_i^{Δ}	The i^{th} simplicial degeneracy map. – Page 203
S_i	The i^{th} pseudo degeneracy map of the symmetric groups $\mathfrak{S}^{\Delta}$. – Definition A.6
$(\tilde{\vartheta}_E)_*$	The homology operation induced by $\tilde{\vartheta}_E$. – Definition 4.3.4
$(\tilde{\vartheta}_F)_*$	The homology operation induced by $\tilde{\vartheta}_F$. – Definition 4.3.3
$(\tilde{\vartheta}_T)_*$	The homology operation induced by $\tilde{\vartheta}_T$. – Definition 4.3.2
θ	Equips $\left(\tilde{C}^k(\mathbb{C})\right)_{k\geq 0}$ with the structure of a little cubes operad. – Page 77
$Thin^m_{g,n}[(r_1, \ldots, r_n)]$	The set of thin cells – Definition 2.9.25
$\tilde{\vartheta}$	The action of the little cubes operad. – Theorem 4.1.1
$\tilde{\vartheta}_*$	The homology operation induced by $\tilde{\vartheta}$ – Definition 4.1.3
$\tilde{\vartheta}_F$	A map inserting a pair of slits. – Page 94
$\tilde{\vartheta}_T$	A map inserting a pair of slits. – Page 95
$\tilde{\vartheta}_T$	A map inserting a pair of slits. – Page 93
ϑ	The action of the little cubes operad by the equivariant action of the symmetric group. – Theorem 4.1.1
$T(\Sigma)$	The homology operation T of Σ in terms of the dual Ehrenfried complex. – Definition 4.3.7
$T_i(\Sigma)$	The set of all i^{th} coboundary traces of a given cell Σ. – Definition 2.9.2
tr	The transfer map. – Page 93

u	A potential function defined on a Riemann surface. – Page 22
$\tilde{v}_0$ and $\tilde{v}_1$	The selected generators of $H_0(\tilde{C}^2)$ and $H_1(\tilde{C}^2)$ – Definition 4.1.4
$\mathbb{V}$	The so-called Visy complex. – Page 56
$\tilde{w}_0$ and $\tilde{w}_1$	The selected chains in $\tilde{C}^2$ which map to the selected generators of $H_0(C^2(\mathbb{C}))$ and $H_1(C^2(\mathbb{C}))$ – Definition 4.1.8
$\mathcal{X} = (X_1, \ldots, X_n)$	The enumerated non-vanishing tangent vectors. – Section 2.1

Index

basin, 23

cell
  basic expansion of a cell, 68
  connected cell, 30
  degenerate, 33, 43
  expansion of a cell, 70
  genus of a parallel cell, 31
  genus of a radial cell, 43
  horizontal face of a parallel cell, 32
  horizontal face of a radial cell, 43
  inner parallel cell, 28
  inner radial cell, 39
  monotonous cell, 56
  non-degenerate, 33, 43
  norm of a parallal cell, 30
  norm of a radial cell, 41
  number of boundaries of a parallel cell, 30
  number of boundaries of a radial cell, 41
  number of cycles of a parallel cell, 30
  number of cycles of a radial cell, 41
  number of punctures of a parallel cell, 30
  number of punctures of a radial cell, 41
  parallel cell in homogeneous notation, 28
  parallel cell in inhomogeneous notation, 30
  radial cell in homogeneous notation, 39
  set of thin cells, 70
  thin cell, 70
  vertical face of a parallel cell, 31
  vertical face of a radial cell, 43
cluster
  cluster filtration of the double complex, 74
  cluster filtration of the Ehrenfried complex, 74
  cluster number, 73
  cluster spectral sequence, 75
  index cluster, 73
coboundary
  basic coboundary trace, 68
  coboundary of a cell, 61
  coboundary trace, 61
  set of coboundaries, 61
  set of coboundary traces, 61
configuration space, 77
connected sum of parallel slit domains, 90
critical edge, 23
critical graph, 23

factorization map, 205
fibre bundle
  q-dimensional fibre bundle, 92

Hilbert uniformization, 20

inhomogeneous notation, 41

kappa, 56
  irrelevent kappa star sequence, 66
  kappa sequence, 57
  kappa star sequence, 65
  relevant kappa star sequence, 66

levels
  ascendingly ordered levels, 28

mueta, 56

norm complex, 55
norm filtration, 55

operad, 77
    little cubes operad, 77
operation
    Browder operation, 81
operations
    Dyer–Lashof operations, 81
orientation
    with respect to a coefficient ring, 92
orientation system, 44

parallel slit complex, 33, 43
partition into levels, 28, 37
Pontryagin product, 80
potential function, 22

radial cell in homogeneous notation, 39
radial cell in inhomogeneous notation, 41
radial composition, 104, 105
radial composition w.r.t. a partial pairing, 107
radial multiplication, 100
radial slit annulus, 39
radial slit picture, 37

simplicial
    semisimplicial category, 203
    simplicial category, 203
    simplicial degeneracy map, 203
    simplicial face map, 203
stagnation point, 22
    set of stagnation points, 22
symbols of a puncture, 96
symmetric group, 203
    bar resolution of the symmetric group, 55
    degeneracy map, 204
    face map, 203
    height of a permutation, 205
    support of permutations, 203
    symmetric groups as semisimplicial set, 204

transfer, 93

Bibliography

[ABE08] Jochen Abhau, Carl-Friedrich Bödigheimer, and Ralf Ehrenfried. "Homology of the mapping class group $\Gamma_{2,1}$ for surfaces of genus 2 with a boundary curve". In: *The Zieschang Gedenkschrift*. Vol. 14. Geometry and Topology Monographs. Geometry and Topology Publications, 2008, pp. 1–25.

[Abh05] Jochen Abhau. "Die Homologie von Modulräumen Riemannscher Flächen – Berechnungen für $g \leq 2$". Diplomarbeit. Rheinische Friedrich-Wilhelms-Universität Bonn, 2005.

[Aus03] Matthew Austern. *A Proposal to Add Hash Tables to the Standard Library (revision 4)*. Accessed: 2014-02-15. Apr. 2003.

[Beu14] Sven Beuchler. Personal communication. Feb. 2014.

[BL14] Bruno Benedetti and Frank H. Lutz. "Random Discrete Morse Theory and a New Library of Triangulations". In: *Experimental Mathematics* 23.1 (2014), pp. 66–94.

[Böd03] Carl-Friedrich Bödigheimer. "The moduli space of Riemann surfaces with boundary". In: *Preprint* (2003).

[Böd06] Carl-Friedrich Bödigheimer. "Configuration models for moduli spaces of Riemann surfaces with boundary". In: *Abhandlungen aus dem Mathematischen Seminar der Universität Hamburg* 76 (2006), pp. 191–233.

[Böd14] Carl-Friedrich Bödigheimer. Personal communication. 2013-2014.

[Böd90a] Carl-Friedrich Bödigheimer. "On the topology of moduli spaces of Riemann surfaces. Part I : Hilbert Uniformization". In: *Mathematica Gottingensis* (1990).

[Böd90b] Carl-Friedrich Bödigheimer. "On the topology of moduli spaces of Riemann surfaces. Part II: Homology Operations". In: *Mathematica Gottingensis* (1990).

[boost] Beman G. Dawes et al. *boost C++ libraries*. 1998 - 2013.

[Bro82] Kenneth S. Brown. *Cohomology of Groups*. Springer, Nov. 1982.

[BT01] Carl-Friedrich Bödigheimer and Ulrike Tillmann. "Stripping and splitting decorated mapping class groups". In: *Cohomological Methods in Homotopy Theory*. Vol. 196. Progress in Mathematics. Birkhäuser Basel, 2001, pp. 47–57.

[CLM76] Frederick R. Cohen, Thomas J. Lada, and J. Peter May. *The homology of iterated loop spaces*. Lecture Notes in Mathematics Vol. 533. Springer-Verlag, Berlin-New York, 1976, pp. vii+490.

[Cou77] Richard Courant. *Dirichlet's principle, conformal mapping, and minimal surfaces*. With an appendix by M. Schiffer, Reprint of the 1950 original. Springer-Verlag, New York-Heidelberg, 1977, pp. xi+332.

[DL62] Eldon Dyer and Richard K. Lashof. “Homology of iterated loop spaces”. In: *American Journal of Mathematics* 84 (1962), pp. 35–88.

[Ehr97] Ralf Ehrenfried. “Die Homologie der Modulräume berandeter Riemannscher Flächen von kleinem Geschlecht”. Dissertation. Rheinische Friedrich-Wilhelms-Universität Bonn, 1997.

[For02] Robin Forman. “A User’s Guide to Discrete Morse Theory”. In: *Séminaire Lotharingien de Combinatoire* 48 (2002), pp. 225–241.

[GL81] Alan George and Joseph W.H. Liu. *Computer Solutions of Large Sparse Positive Definite Systems*. Prentice Hall, 1981.

[GMP] Torbjörn Granlund et al. *GNU multiple precision arithmetic library*. 1991 - 2013.

[God07] Véronique Godin. “The unstable integral homology of the mapping class groups of a surface with boundary”. In: *Mathematische Annalen* 337.1 (2007), pp. 15–60.

[Har85] John L. Harer. “Stability of the homology of the mapping class groups of orientable surfaces”. In: *Annals of Mathematics. Second Series* 121.2 (1985), pp. 215–249.

[Har91] John L. Harer. “The third homology group of the moduli space of curves”. In: *Duke Mathematical Journal* 63.1 (1991), pp. 25–55.

[Hes12] Alexander Hess. “Factorable Monoids: Resolutions and Homology via Discrete Morse Theory”. Dissertation. Rheinische Friedrich-Wilhelms-Universität Bonn, 2012.

[Hil09] David Hilbert. *Zur Theorie der konformen Abbildung*. Nachrichten von der Königlichen Gesellschaft der Wissenschaften und der Georg-Augusts-Universität zu Göttingen, 1909, pp. 314–323.

[Jäg03] Gerold Jäger. “Parallel Algorithm for Computing the Smith Normal Form of Large Matrices.” In: vol. 2840. Lecture Notes in Computer Science. Springer, 2003, pp. 170–179.

[Jos12] Nicolai M. Josuttis. *The C++ Standard Library: A Tutorial and Reference*. 2nd ed. Addison-Wesley Professional, Apr. 2012.

[JP06] Michael Joswig and Marc E. Pfetsch. “Computing Optimal Morse Matchings.” In: *SIAM Journal on Discrete Mathematics* 20.1 (2006), pp. 11–25.

[JW09] Gerold Jäger and Clemens Wagner. “Efficient parallelization of Hermite and Smith normal form algorithms”. In: *Parallel Computing. Systems & Applications* 35.6 (2009), pp. 345–357.

[KM00] Mustafa Korkmaz and John D. McCarthy. “Surface mapping class groups are ultrahopfian”. In: *Mathematical Proceedings of the Cambridge Philosophical Society* 129.1 (2000), pp. 35–53.

[Koc91] Helmut Koch. *Introduction to Classical Mathematics I: From the Quadratic Reciprocity Law to the Uniformization Theorem*. Springer, 1991.

[KS03] Mustafa Korkmaz and András I. Stipsicz. “The second homology groups of mapping class groups of oriented surfaces”. In: *Mathematical Proceedings of the Cambridge Philosophical Society* 134.3 (2003), pp. 479–489.

[May72] J. Peter May. *The geometry of iterated loop spaces*. Lectures Notes in Mathematics Vol. 271. Springer-Verlag, Berlin-New York, 1972, pp. viii+175.

[Meh11] Stefan Mehner. “Homologieberechnungen von Modulräumen Riemannscher Flächen durch diskrete Morse-Theorie”. Diplomarbeit. Rheinische Friedrich-Wilhelms-Universität Bonn, 2011.

[MP12] J. Peter May and Kate Ponto. *More Concise Algebraic Topology: Localization, Completion, and Model Categories*. University of Chicago Press, Feb. 2012.

[Mum67] David Mumford. “Abelian quotients of the Teichmüller modular group”. In: *Journal d'Analyse Mathématique* 18 (1967), pp. 227–244.

[MW07] Ib Madsen and Michael Weiss. “The stable moduli space of Riemann surfaces: Mumford's conjecture”. In: *Annals of Mathematics. Second Series* 165.3 (2007), pp. 843–941.

[Pow78] Jerome Powell. “Two theorems on the mapping class group of a surface”. In: *Proceedings of the American Mathematical Society* 68.3 (1978), pp. 347–350.

[Sak12] Takuya Sakasai. “Lagrangian mapping class groups from a group homological point of view”. In: *Algebraic & Geometric Topology* 12.1 (2012), pp. 267–291.

[Spa94] Edwin H. Spanier. *Algebraic Topology*. Springer, Dec. 1994.

[Str13] Bjarne Stroustrup. *The C++ Programming Language, 4th Edition*. 4th ed. Addison-Wesley Professional, May 2013.

[Tsu59] Masatsugu Tsuji. *Potential theory in modern function theory*. 1959.

[Ver98] Vladimir V. Vershinin. “Homology of braid groups and their generalizations”. In: *Knot theory*. Vol. 42. Banach Center Publications. Polish Academy of Sciences, 1998, pp. 421–446.

[Vis10] Balázs Visy. “Factorable Groups and their Homology”. Dissertation. Rheinische Friedrich-Wilhelms-Universität Bonn, 2010.

[Wah08] Nathalie Wahl. “Homological stability for the mapping class groups of non-orientable surfaces”. In: *Inventiones Mathematicae* 171.2 (2008), pp. 389–424.

[Wah12] Nathalie Wahl. “Homological stability for mapping class groups of surfaces”. In: *Handbook of Moduli: Volume III* 3 (2012), pp. 547–583.

[Wah13] Nathalie Wahl. “The Mumford conjecture, Madsen-Weiss and homological stability for mapping class groups of surfaces”. In: *Moduli spaces of Riemann surfaces*. Vol. 20. IAS/Park City Mathematics Series. American Mathematical Society; IAS/Park City Mathematics Institute, 2013, pp. 109–138.

[Wan11] Rui Wang. “Homology Computations for Mapping Class Groups, in particular for $\Gamma^0_{3,1}$”. Dissertation. Rheinische Friedrich-Wilhelms-Universität Bonn, 2011.

[Wei95] Charles A. Weibel. *An Introduction to Homological Algebra*. Cambridge University Press, Oct. 1995.